

Since the total energy is $E_k + mc^2 = 10.511 \text{ MeV}$, we have, from the magnitude of the energy/momentum four-vector (Equation 2-31),

$$\begin{aligned} pc &= \sqrt{E^2 - (mc^2)^2} = \sqrt{(10.511)^2 - (0.511)^2} \\ &= 10.50 \text{ MeV} \end{aligned}$$

The exact calculation then gives $p = 10.50 \text{ MeV}/c$. The high-energy or extreme relativistic approximation $p \approx E/c = 10.50 \text{ MeV}$ is in good agreement with the exact result. If we use Equation 2-34, we obtain for the speed $u/c = pc/E = 10.50 \text{ MeV}/10.51 \text{ MeV} = 0.999$. On the other hand, the approximation of Equation 2-40 gives

$$\frac{u}{c} \approx 1 - \frac{1}{2}\left(\frac{1}{\gamma}\right)^2 = 1 - \frac{1}{2}\left(\frac{1}{20.57}\right)^2 = 0.999$$

2. For the proton, the total energy is $E_k + mc^2 = 10 \text{ MeV} + 938.3 \text{ MeV} = 948.3 \text{ MeV}$. From Equation 2-39 we obtain $\gamma = 1 + E_k/mc^2 = 1 + 10/938.3 = 1.01$. Equation 2-31 gives for the momentum

$$\begin{aligned} pc &= \sqrt{E^2 - (mc^2)^2} = \sqrt{(948.3)^2 - (938.3)^2} \\ p &= 137.4 \text{ MeV}/c \end{aligned}$$

The nonrelativistic approximation gives

$$E_k \approx \frac{1}{2}mu^2 = \frac{(mu)^2}{2m} \approx \frac{p^2}{2m} = \frac{p^2c^2}{2mc^2}$$

or

$$\begin{aligned} pc &\approx \sqrt{2mc^2E_k} = \sqrt{(2)(938.3)(10)} \\ p &= 137.0 \text{ MeV}/c \end{aligned}$$

The speed can be determined from Equation 2-34 exactly or from $p = mu$ approximately. From Equation 2-34 we obtain

$$\frac{u}{c} = \frac{pc}{E} = \frac{137.4}{948.3} = 0.1449$$

From $p \approx mu$, the nonrelativistic expression for p , we obtain

$$\frac{u}{c} \approx \frac{pc}{mc^2} = \frac{137.0}{938.3} = 0.1460$$

2-5 General Relativity

The generalization of relativity to noninertial reference frames by Einstein in 1916 is known as the *general theory of relativity*. This theory is much more difficult mathematically than the special theory of relativity, and there are fewer situations in which it can be tested. Nevertheless, its importance in the areas of astrophysics and cosmology and the need to take account of its predictions in the design of such things as global navigation systems¹³ calls for its inclusion here. A full description of the general theory uses tensor analysis at a quite sophisticated level, well beyond the scope of this book,

The sensitivity of modern electronic devices is so exceptional that general relativistic effects are included in the design of such systems as the Global Positioning System.

so we will be limited to qualitative or, in some instances, semiquantitative discussions. An additional purpose to the discussion that follows is to give you something that few people will ever have, namely, an acquaintance with one of the most remarkable of all scientific accomplishments and a bit of a feel for the man who did it.

Einstein's development of the general theory of relativity was not motivated by any experimental enigma. Instead, it grew out of his desire to include the descriptions of *all* natural phenomena within the framework of the special theory. By 1907 he realized that he could accomplish that goal with the single exception of the law of gravitation. About that exception he said,¹⁴

I felt a deep desire to understand the reason behind this [exception].

The “reason” came to him, as he said later, while he was sitting in a chair in the patent office in Bern. He described it like this:¹⁵

Then there occurred to me the happiest thought of my life, in the following form. The gravitational field has only a relative existence in a way similar to the electric field generated by electromagnetic induction. Because for an observer falling freely from the roof of a house there exists—at least in his immediate surroundings—no gravitational field [Einstein's italics]. . . . The observer then has the right to interpret his state as “at rest.”

Out of this “happy thought” grew the *principle of equivalence* that became Einstein’s fundamental postulate for general relativity.

Principle of Equivalence

The basis of the general theory of relativity is what we may call Einstein’s third postulate, the principle of equivalence, which states:

A homogeneous gravitational field is completely equivalent to a uniformly accelerated reference frame.

This principle arises in a somewhat different form in Newtonian mechanics because of the apparent identity of gravitational and inertial mass. In a uniform gravitational field, all objects fall with the same acceleration g independent of their mass because the gravitational force is proportional to the (gravitational) mass while the acceleration varies inversely with the (inertial) mass. That is, the mass m in

$$\mathbf{F} = m\mathbf{a} \quad (\text{inertial } m)$$

and that in

$$\mathbf{F} = \frac{GMm}{r^2}\hat{\mathbf{r}} \quad (\text{gravitational } m)$$

appear to be identical in classical mechanics, although classical theory provides no explanation for this equality. For example, near Earth’s surface, $F_G = GMm/r^2 = m_{\text{grav}}g = m_{\text{inertial}}a = F$. Recent experiments have shown that $m_{\text{inertial}} = m_{\text{grav}}$ to better than one part in 10^{12} .

To understand what the equivalence principle means, consider a compartment in space far away from any matter and undergoing uniform acceleration \mathbf{a} as shown in Figure 2-15a. If people in the compartment drop objects, they fall to the “floor” with acceleration $\mathbf{g} = -\mathbf{a}$. If they stand on a spring scale, it will read their “weight” of magnitude ma . No mechanics experiment can be performed *within* the compartment

FÉUE WHI

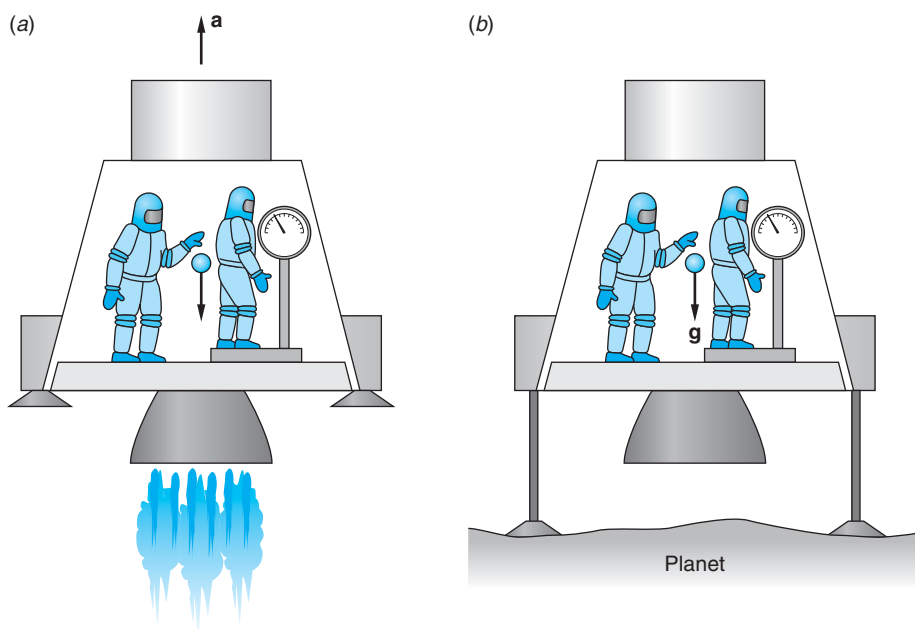


Figure 2-15 Results from experiments in a uniformly accelerated reference frame (a) cannot be distinguished from those in a uniform gravitational field (b) if the acceleration \mathbf{a} and gravitational field \mathbf{g} have the same magnitude.

that will distinguish whether the compartment is actually accelerating in space or is at rest (or moving with uniform velocity) in the presence of a uniform gravitational field $\mathbf{g} = -\mathbf{a}$.

Einstein broadened the principle of equivalence to apply to *all* physical experiments, not just to mechanics. In effect, he assumed that there is no experiment of any kind that can distinguish uniformly accelerated motion from the presence of a gravitational field. A direct consequence of the principle is that $m_{\text{inertial}} = m_{\text{grav}}$ is a requirement, not a coincidence. The principle of equivalence extends Einstein's first postulate, the principle of relativity, to *all* reference frames, non-inertial (i.e., accelerated) as well as inertial. It follows that there is no absolute acceleration of a reference frame. Acceleration, like velocity, is only relative.

Question

6. For his 76th (and last) birthday Einstein received a present designed to demonstrate the principle of equivalence. It is shown in Figure 2-16. The object is, starting with the ball hanging down as shown to put the ball into the cup with a method that works every time (as opposed to random shaking). How would you do it? (Note: When it was given to Einstein, he was delighted and did the experiment correctly immediately.)

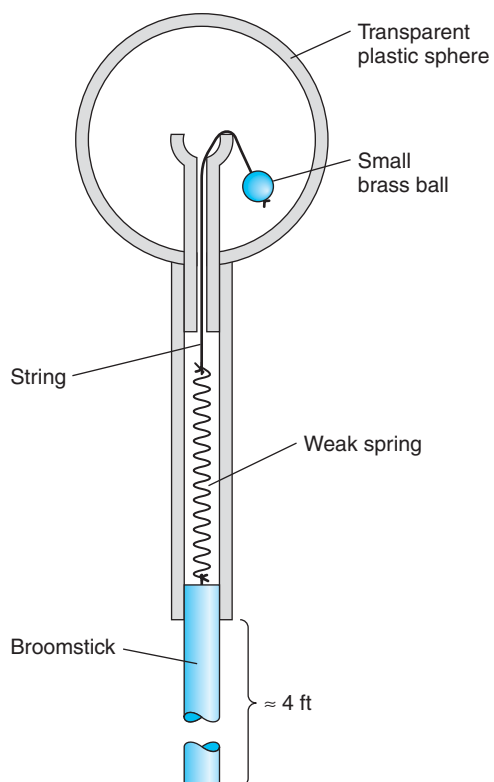


Figure 2-16 Principle of equivalence demonstrator given to Einstein by E. M. Rogers. The object is to put the hanging brass ball into the cup by a technique that always works. The spring is weak, too weak to pull the ball in as it stands, and is stretched even when the ball is in the cup. The transparent sphere, about 10 cm in diameter, does not open. [From A. P. French, *Albert Einstein: A Centenary Volume*, Harvard University Press, Cambridge, Mass. (1979).]

Some Predictions of General Relativity

In his first paper on general relativity, in 1916, Einstein was able to explain quantitatively a discrepancy of long standing between the measured and (classically) computed values of the advance of the perihelion of Mercury's orbit, about 43 arc seconds/century. It was the first success of the new theory. A second prediction, the bending of light in a gravitational field, would seem to be more difficult to measure owing to the very small effect. However, it was accurately confirmed less than five years later when Arthur Eddington measured the deflection of starlight passing near the limb of the Sun during a total solar eclipse. The theory also predicts the slowing of light itself and the slowing of clocks—i.e., frequencies—in gravitational fields, both effects of considerable importance to the determination of astronomical distances and stellar recession rates. The predicted slowing of clocks, called gravitational redshift, was demonstrated by Pound and co-workers in 1960 in Earth's gravitational field using the ultrasensitive frequency measuring technique of the Mössbauer effect (see Chapter 11). The slowing of light was conclusively measured in 1971 by Shapiro and co-workers using radar signals reflected from several planets. Two of these experimental tests of relativity's predictions, bending of light and gravitational redshift, are discussed in the Exploring sections that follow. The perihelion of Mercury's orbit and the delay of light are discussed in More sections on the book's Web page. Many other predictions of general relativity are subjects of active current research. Two of these, black holes and gravity waves, are discussed briefly in the concluding paragraphs of this chapter.



EXPLORING

Deflection of Light in a Gravitational Field

This relativistic effect results in gravitational lenses in the cosmos that focus light from extremely distant galaxies, greatly improving their visibility in telescopes, both on Earth and in orbit.

With the advent of special relativity, several features of the Newtonian law of gravitation $F_G = GMm/r^2$ became conceptually troublesome. One of these was the implication from the relativistic concept of mass-energy equivalence that even particles with zero rest mass should exhibit properties such as weight and inertia, thought of classically as masslike; classical theory does not include such particles. According to the equivalence principle, however, light, too, would experience the gravitational force. Indeed, the deflection of a light beam passing through the gravitational field near a large mass was one of the first consequences of the equivalence principle to be tested experimentally.

To see why a deflection of light would be expected, consider Figure 2-17, which shows a beam of light entering an accelerating compartment. Successive positions of the compartment are shown at equal time intervals. Because the compartment is accelerating, the distance it moves in each time interval increases with time. The path of the beam of light, as observed from inside the compartment, is therefore a parabola. But according to the equivalence principle, there is no way to distinguish between an accelerating compartment and one with uniform velocity in a uniform gravitational field. We conclude, therefore, that a beam of light will accelerate in a gravitational field as do objects with rest mass. For example, near the surface of Earth light will fall with acceleration 9.8 m/s^2 . This is difficult to observe because of the enormous speed of light. For example, in a distance of 3000 km, which takes about 0.01 second to cover, a beam of light should fall about 0.5 mm. Einstein pointed out that the deflection of a light beam in a gravitational field might be observed when light from a distant star passes close to the Sun.¹⁶ The deflection, or bending, is computed as follows.

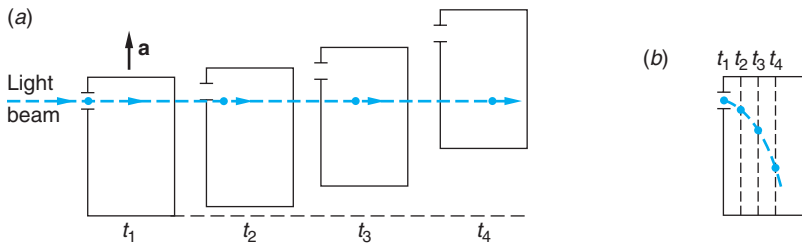


Figure 2-17 (a) Light beam moving in a straight line through a compartment that is undergoing uniform acceleration. The position of the light beam is shown at equally spaced times t_1, t_2, t_3, t_4 . (b) In the reference frame of the compartment, the light travels in a parabolic path, as would a ball were it projected horizontally. Note that in both (a) and (b) the vertical displacements are greatly exaggerated for emphasis.

Rewriting the spacetime interval Δs (Equation 2-32) in differential form and converting the space Cartesian coordinates to polar coordinates (in two dimensions, since the deflection occurs in a plane) yields

$$ds^2 = c^2 dt^2 - (dr^2 + r^2 d\theta^2) \quad 2-42$$

Einstein showed that this expression is slightly modified in the presence of a (spherical, nonrotating) mass M to become

$$ds^2 = \gamma(r)^2 c^2 dt^2 - dr^2/\gamma(r)^2 - r^2 d\theta^2 \quad 2-43$$

where $\gamma(r) = (1 - 2GM/c^2r)^{1/2}$, with G = universal gravitational constant and r = distance from the mass M . The factor $\gamma(r)$ is roughly analogous to the γ of special relativity. In the following Exploring section on gravitational redshift, we will describe how $\gamma(r)$ arises. For now, $\gamma(r)$ can be thought of as correcting for *gravitational time dilation* (the first term on the right of Equation 2-43) and *gravitational length contraction* (the second term).

This situation is illustrated in Figure 2-18, which shows the light from a distant star just grazing the edge of the Sun. The gravitational deflection of light (with mass $\gamma m = E/c^2$) can be treated as a refraction of the light. The speed of light is reduced to $\gamma(r)c$ in the vicinity of the mass M since $\gamma(r) < 1$ (see Equation 2-43), thus bending the wave fronts, and hence the beam, toward M . This is analogous to the deflection of starlight toward Earth's surface as a result of the changing density—hence index of refraction—of the atmosphere. By integrating Equation 2-43 over the entire trajectory of the light beam (recall that $ds = 0$ for light) as it passes by M , the total deflection α is found to be¹⁷

$$\alpha = 4GM/c^2R \quad 2-44$$

where R = distance of closest approach of the beam to the center of M . For a beam just grazing the Sun, $R = R_\odot$ = solar radius = 6.96×10^8 m. Substituting the values for G and the solar mass ($M = 1.99 \times 10^{30}$ kg) yields $\alpha = 1.75$ arc second.¹⁸

Ordinarily, of course, the brightness of the Sun prevents astronomers (or anyone else) from seeing stars close to the limbs (edges) of the Sun, except during a total eclipse. Einstein completed the calculation of α in 1915, and in 1919 expeditions were organized by Eddington¹⁹ at two points along the line of totality of a solar eclipse, both of which were successful in making measurements of α for several stars and testing the predicted $1/R_\odot$ dependence of α . The measured values of α for grazing beams at the two sites were:

At Sobral (South America): $\alpha = 1.98 \pm 0.12$ arc seconds

At Principe Island (Africa): $\alpha = 1.61 \pm 0.30$ arc seconds

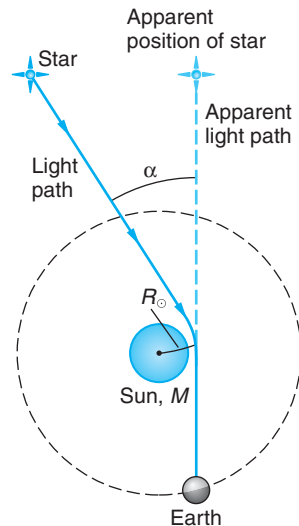


Figure 2-18 Deflection (greatly exaggerated) of a beam of starlight due to the gravitational attraction of the Sun.

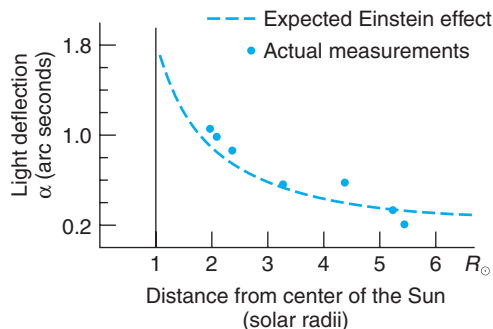


Figure 2-19 The deflection angle α depends on the distance of closest approach R_{\odot} according to Equation 2-44. Shown here is a sample of the data for 7 of the 13 stars measured by the Eddington expeditions. The agreement with the relativistic prediction is apparent.

their average agreeing with the general relativistic prediction to within about 2 percent. Figure 2-19 illustrates the agreement of the $1/R_{\odot}$ dependence with Equation 2-44. (Einstein learned of the successful measurements via a telegram from H. A. Lorentz.) Since 1919, many measurements of α have been made during eclipses. Since the development of radio telescopes, which are not blinded by sunlight and hence don't require a total eclipse, many more measurements have been made. The latest data agree with the deflection predicted by general relativity to within about 0.1 percent.

The gravitational deflection of light is being put to use by modern astronomers via the phenomenon of *gravitational lensing* to help in the study of galaxies and other large masses in space. Light from very distant galaxies passing near or through other galaxies or clusters of galaxies between the source and Earth can be bent so as to reach Earth in much the same way that light from an object on a bench in the laboratory can be refracted by a glass lens and thus reach the eye of an observer. An intervening galaxy or cluster of galaxies can thus produce images of the distant source, even ones magnified and distorted, just as the glass lens can. Figure 2-20a will serve as a reminder of a refracting lens in the laboratory, while Figure 2-20b illustrates the corresponding action

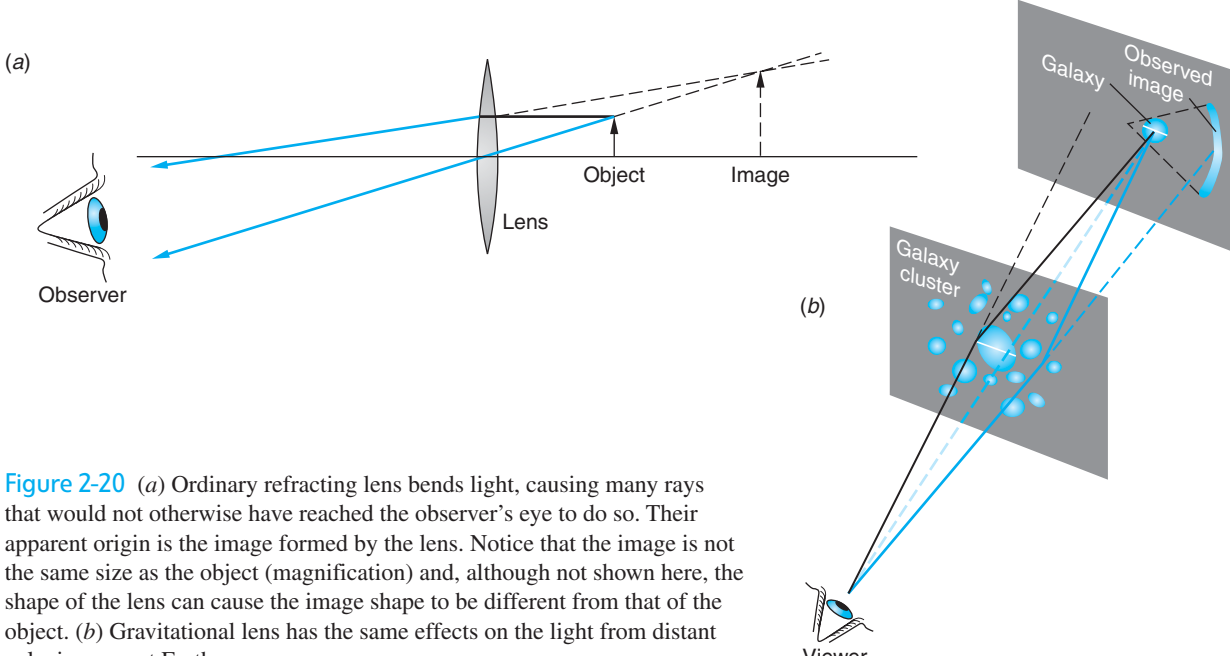


Figure 2-20 (a) Ordinary refracting lens bends light, causing many rays that would not otherwise have reached the observer's eye to do so. Their apparent origin is the image formed by the lens. Notice that the image is not the same size as the object (magnification) and, although not shown here, the shape of the lens can cause the image shape to be different from that of the object. (b) Gravitational lens has the same effects on the light from distant galaxies seen at Earth.

of a gravitational lens. The accompanying photograph shows the images of several distant galaxies drawn out into arcs by the lens effect of the cluster of galaxies in the center. The first confirmed discovery of images formed by a gravitational lens, the double image of the quasar QSO 0957, was made in 1979 by D. Walsh and his co-workers. Since then, astronomers have found many such images. Their discovery and interpretation is currently an active area of research. Gravitational lensing was recently used to help image the first apparent findings of dark matter in this cosmos. (See Chapter 13.)



EXPLORING Gravitational Redshift

A second prediction of general relativity concerns the rates of clocks and the frequencies of light in a gravitational field. As a specific case that illustrates the gravitational redshift as a direct consequence of the equivalence principle, suppose we consider two identical light sources (A and A') and detectors (B and B') located in identical spaceships (S and S') as illustrated in Figure 2-21. The spaceship S' in Figure 2-21b is located far from any mass. At time $t = 0$, S' begins to accelerate, and simultaneously an atom in the source A' emits a light pulse of its characteristic frequency f_0 . During the time $t (= h/c)$ for the light to travel from A' to B' , B' acquires a speed $v = at = gh/c$, and the detector B' , receding from the original location of A' , measures the frequency of the incoming light to be *redshifted* by a fractional amount $(f_0 - f)/f_0 \approx \beta$ for $v \ll c$. (See Section 1-5.) Thus,

$$(f_0 - f)/f_0 = \Delta f/f \approx \beta = v/c = gh/c^2 \quad 2-45$$

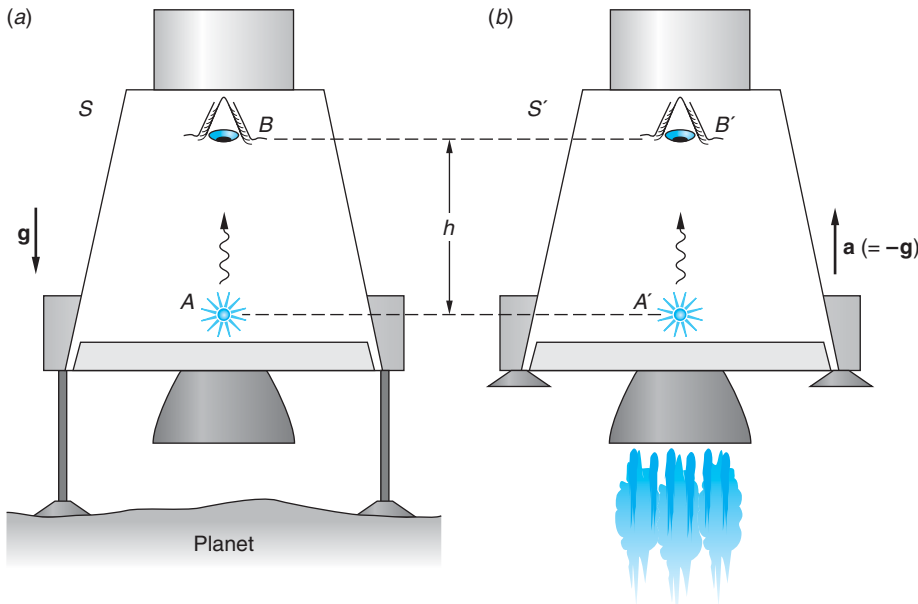


Figure 2-21 (a) System S is at rest in the gravitational field of the planet. (b) Spaceship S' , far from any mass, accelerates with $\mathbf{a} = -\mathbf{g}$.

Notice that the right side of Equation 2-45 is equal to the gravitational potential (i.e., the gravitational potential energy per unit mass) $\Delta\phi = gh$ between A and B , divided by c^2 . According to the equivalence principle, the detector at B in S must also measure the frequency of the arriving light to be f , even though S is at rest on the planet and, therefore, the shift cannot be due to the Doppler effect! Since the vibrating atom that produced the light pulse at A can be considered to be a clock and since no “cycles” of the vibration are lost on the pulse’s trip from A to B , the observer at B must conclude that the clock at A runs slow, compared with an identical clock (or an identical atom) located at B . Since A is at the lowest potential, the observer concludes that *clocks run more slowly the lower the gravitational potential*. This shift of clock rates to lower frequencies, hence longer wavelengths, in lower gravitational potentials is the *gravitational redshift*.

In the more general case of a spherical, nonrotating mass M , the change in gravitational potential between the surface at some distance R from the center and a point at infinity is given by

$$\Delta\phi = \int_R^\infty \frac{GM}{r^2} dr = GM(-1/r) \Big|_R^\infty = \frac{GM}{R} \quad 2-46$$

and the factor by which gravity shifts the light frequency is found from

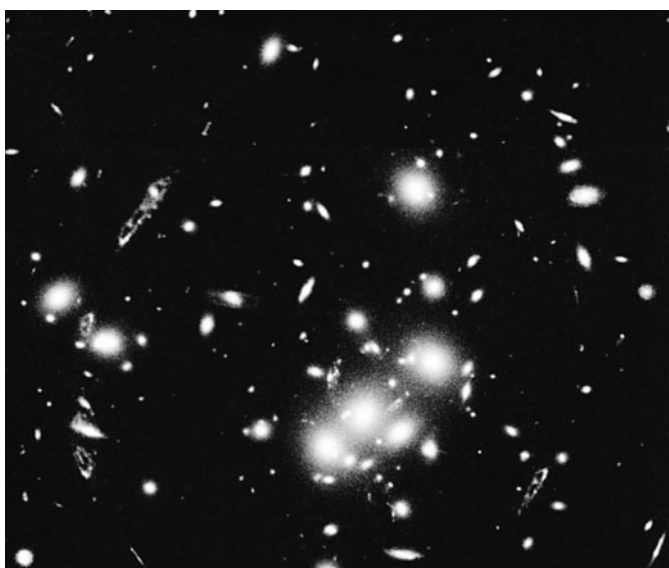
$$\Delta f/f_0 = (f_0 - f)/f_0 = GM/c^2 R$$

or

$$f/f_0 = 1 - GM/c^2 R \quad (\text{gravitational redshift}) \quad 2-47$$

Notice that if the light is moving the other way, i.e., from high to low gravitational potential, the limits of integration in Equation 2-46 are reversed and Equation 2-47 becomes

$$f/f_0 = 1 + GM/c^2 R \quad (\text{gravitational blueshift}) \quad 2-48$$



Images of distant galaxies are drawn out into arcs by the massive cluster of galaxies Abell 2218, whose enormous gravitational field acts as a lens to magnify, brighten, and distort the images. Abell 2218 is about 2 billion $c \cdot y$ from Earth. The arcs in this January 2000 Hubble Space Telescope photograph are images of galaxies 10 to 20 billion $c \cdot y$ away. [NASA, A. Fruchter; ERO Team.]

Analyzing the frequency of starlight for gravitational effects is exceptionally difficult because several shifts are present. For example, the light is gravitationally redshifted as it leaves the star and blueshifted as it arrives at Earth. The blueshift near Earth is negligibly small with current measuring technology; however, the redshift due to the receding of nearby stars and distant galaxies from us as a part of the general expansion of the universe is typically much larger than gravitational effects and, together with thermal frequency broadening in the stellar atmospheres, results in large uncertainties in measurements. Thus, it is quite remarkable that the relativistic prediction of Equation 2-48 has been tested in the relatively small gravitational field of Earth. R. V. Pound and his co-workers,²⁰ first in 1960 and then again in 1964 with improved precision, measured the shift in the frequency of 14.4-keV gamma rays emitted by ^{57}Fe falling through a height h of only 22.5 m. Using the Mössbauer effect, an extremely sensitive frequency shift measuring technique developed in 1968, Pound's measurements agreed with the predicted fractional blueshift $gh/c^2 = 2.45 \times 10^{-15}$ to within 1 percent. Equations 2-47 and 2-48 have been tested a number of times since then—using atomic clocks carried on aircraft, as described in Section 1-4, and, in 1980, by R. F. C. Vessot and his co-workers using a precision microwave transmitter carried to 10,000 km from Earth by a space probe. The results of these tests, too, agree with the relativistically predicted frequency shift, the latter to 1 part in 14,000.

Question

7. The frequency f in Equation 2-47 can be shifted to zero by an appropriate value of M/R . What would be the corresponding value of R for a star with the mass of the Sun? Speculate on the significance of this result.

More



The inability of Newtonian gravitational theory to correctly account for the observed rate at which the major axis of Mercury's orbit precessed about the Sun was a troubling problem, pointing as it did to some subtle failure of the theory. Einstein's first paper on general relativity, the *Perihelion of Mercury's Orbit*, quantitatively explained the advance of Mercury's orbit, setting the stage for general relativity to supplant the old Newtonian theory. A clear description of the relativistic explanation is on the home page: www.whfreeman.com/tiplermodernphysics5e. See also Equations 2-49 through 2-51 here, as well as Figure 2-22 and Table 2-2.

More



General relativity includes a gravitational interaction for particles with zero rest mass, such as photons, which are excluded in Newtonian theory. One consequence is the prediction of a *Delay of Light in a Gravitational Field*. This phenomenon and its subsequent observation are described qualitatively on the home page: www.whfreeman.com/tiplermodernphysics5e. See also Equation 2-52 here, as well as Figures 2-23 and 2-24.

Black Holes Black holes were first predicted by J. R. Oppenheimer and H. Snyder in 1939. According to the general theory of relativity, if the density of an object such as a star is great enough, the gravitational attraction will be so large that nothing can escape

from its surface, not even light or other electromagnetic radiation. It is as if space itself were being drawn inward faster than light could move outward through it. A remarkable property of such an object is that nothing that happens inside it can be communicated to the outside world. This occurs when the gravitational potential at the surface of the mass M becomes so large that the frequency of radiation emitted at the surface is redshifted to zero. From Equation 2-47 we see that the frequency will be zero when the radius of the mass has the critical value $R_G = GM/c^2$. This result is a consequence of the principle of equivalence, but Equation 2-47 is a $v \ll c$ approximation. A precise derivation of the critical value of the radius R_G , called the *Schwarzschild radius*, yields

$$R_G = \frac{2MG}{c^2} \quad 2-53$$

For an object with mass equal to that of our Sun to be a black hole, its radius would be about 3 km. A large number of black holes have been identified by astronomers in recent years, one of them in the center of the Milky Way. (See Chapter 13.)

An interesting historical note is that Equation 2-53 was first derived by nineteenth-century French physicist Pierre Laplace using Newtonian mechanics to compute the escape velocity v_e from a planet of mass M before anyone had ever heard of Einstein or black holes. The result, derived in first-year physics courses by setting the kinetic energy of the escaping object equal to the gravitational potential energy at the surface of the planet (or star), is

$$v_e = \sqrt{\frac{2GM}{r}}$$

Setting $v_e = c$ gives Equation 2-53. Laplace obtained the correct result by making two fundamental errors that just happened to cancel each other!

Gravitational Waves Einstein's formulation of general relativity in 1916 explicitly predicted the existence of gravitational radiation. He showed that, just as accelerated electric charges generate time-dependent electromagnetic fields in space—i.e., electromagnetic waves—accelerated masses would create time-dependent gravitational fields in space—i.e., *gravitational waves*—that propagate from their source at the speed of light. The gravitational waves are propagating ripples, or distortions of spacetime. Figure 2-25 illustrates gravitational radiation emitted by two merging black holes distorting the otherwise flat “fabric” of spacetime.

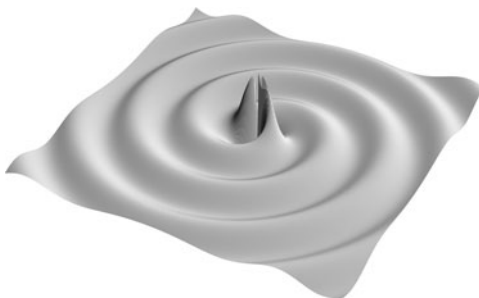


Figure 2-25 Gravitational waves, intense ripples in the fabric of spacetime, are expected to be generated by a merging binary system of neutron stars or black holes. The amplitude decreases with distance due to the $1/R$ falloff and because waves farther from the source were emitted at an earlier time, when the emission was weaker.

[Courtesy of Patrick Brady.]

The best experimental evidence that exists so far in support of the gravitational wave prediction is indirect. In 1974 R. A. Hulse and J. H. Taylor²⁴ discovered the first binary pulsar, i.e., a pair of neutron stars orbiting each other, one of which was emitting periodic flashes of electromagnetic radiation (pulses). In an exquisitely precise experiment they showed that the gradual decrease in the orbital period of the pair was in good agreement with the general relativistic prediction for the rate of loss of gravitational energy via the emission of gravitational waves.

Experiments are currently under way in several countries to directly detect gravitational waves arriving at Earth. One of the most promising is LIGO (*Laser Interferometer Gravitational-Wave Observatory*), a pair of large Michelson interferometers with Fabry-Perot cavities at the Livingston Observatory in Louisiana and the

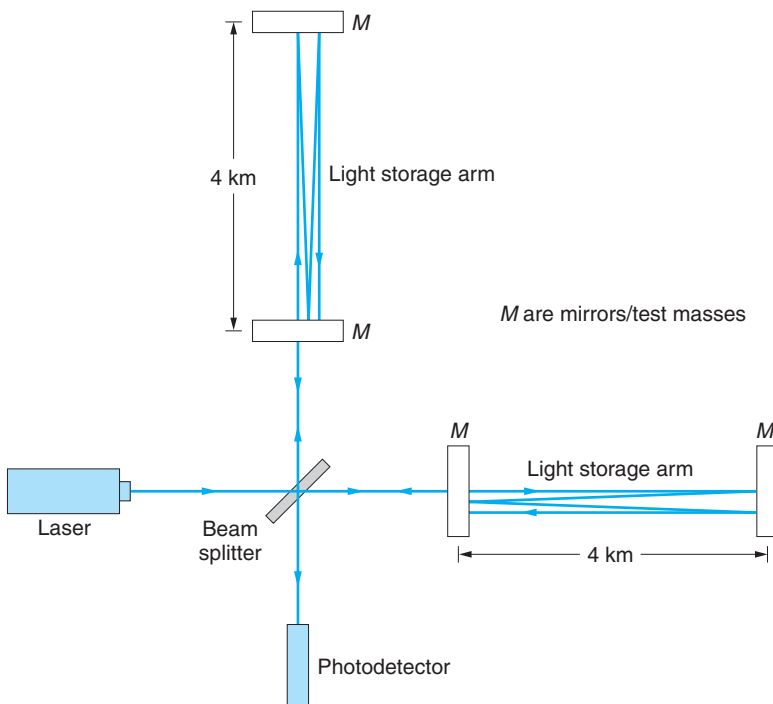


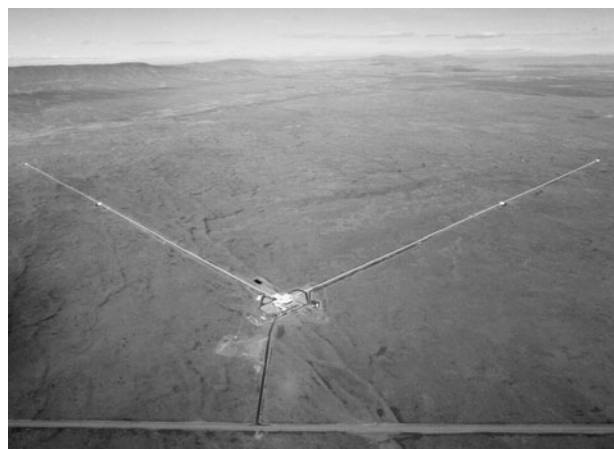
Figure 2-26 The LIGO detectors are equal-arm Michelson interferometers. The mirrors, each 25 cm in diameter by 10 cm thick and isolated from Earth's motions, are also the test masses of the gravitational wave detector. Arrival of a gravitational wave would change the length of each arm by about the diameter of an atomic nucleus and result in light signal at the photodetector.

Hanford Observatory 3002 km away in Washington, operating in coincidence. Figure 2-26 illustrates one of the LIGO interferometers. Each arm is 4 km long. The laser beams are reflected back and forth in the cavities, making about 75 round trips along each arm and recombining at the photodetector, making the effective lengths of the arms about 400 km. (A half-size but equally sensitive instrument using Fabry-Perot cavities is also housed at the Hanford Observatory.) The arrival of a gravitational wave would stretch one arm of the interferometer by about 1/1000 of the diameter of a proton and squeeze the other arm by the same minuscule amount! Nonetheless, that tiny change in the lengths is sufficient to change very slightly the relative phase of the recombining laser beams and produce a signal at the detector. The two LIGO interferometers must record the event within 10 ms of each other for the signal to be interpreted as a gravitational wave, that being the travel time between the two observatories for a gravitational wave moving at speed c . LIGO completed its two-year, low-sensitivity initial operational phase and went online in mid-2002. By 2005 LIGO had completed two science runs that included observations on 28 pulsars. (See Chapter 13.) At this writing a third science run with improved sensitivity is under way, operating jointly with GEO 600, a similar gravitational wave interferometer in Germany. A third gravitational wave observatory, Virgo, in Italy, is currently being commissioned and will soon join the search. These instruments are by far the most sensitive scientific instruments ever built. So far, none of the half-dozen or so experiments under way around the world has detected a gravitational wave.²⁵

An enormous amount remains to be learned about the predictions and implications of general relativity—not just about such things as black holes and gravity waves, but also, for example, about gravity and spacetime in the very early universe,

This application of
Michelson's interferometer
may well lead to the first
direct detection of "ripples"
or waves in spacetime.

Aerial view of the LIGO gravitational wave interferometer near Hanford, Washington. Each of the two arms is 4 km long. [CalTech/LIGO.]



when forces were unified and the constituents were closely packed. These and other fascinating matters are investigated more specifically in the areas of astrophysics and cosmology (Chapter 13) and particle physics (Chapter 12), fields of research linked by general relativity, perhaps the grandest of Einstein's great scientific achievements.

Question

8. Speculate on what the two errors made by Laplace in deriving Equation 2-53 might have been.

Summary

| TOPIC | RELEVANT EQUATIONS AND REMARKS | |
|--|---|------|
| 1. Relativistic momentum | $\mathbf{p} = \gamma m\mathbf{u}$ | 2-7 |
| | The relativistic momentum is conserved and approaches $m\mathbf{u}$ for $v \ll c$. $\gamma = (1 - u^2/c^2)^{-1/2}$ in Equation 2-7, where u = particle speed in S . | |
| 2. Relativistic energy | $E = \gamma mc^2$ | 2-10 |
| Total energy | The relativistic total energy is conserved. | |
| Kinetic energy | $E_k = \gamma mc^2 - mc^2$ | 2-9 |
| | mc^2 is the rest energy. $\gamma = (1 - u^2/c^2)^{-1/2}$ in Equations 2-9 and 2-10. | |
| 3. Lorentz transformation for E and \mathbf{p} . | $p'_x = \gamma(p_x - vE/c^2)$ $p'_y = p_y$ $E' = \gamma(E - vp_x)$ $p'_z = p_z$ | 2-16 |
| | where v = relative speed of the systems and $\gamma = (1 - v^2/c^2)^{-1/2}$ | |
| 4. Mass/energy conversion | Whenever additional energy ΔE in any form is stored in an object, the rest mass of the object is increased by $\Delta m = \Delta E/c^2$. | |
| 5. Invariant mass | $(mc^2) = E^2 - (pc)^2$ | 2-32 |
| | The energy and momentum of any system combine to form an invariant four-vector whose magnitude is the rest energy of the mass m . | |

| TOPIC | RELEVANT EQUATIONS AND REMARKS |
|------------------------|---|
| 6. Force in relativity | The force $\mathbf{F} = m\mathbf{a}$ is not invariant in relativity. Relativistic force is defined as $\mathbf{F} = \frac{d\mathbf{p}}{dt} = \frac{d(\gamma m\mathbf{u})}{dt} \quad 2-8$ |
| 7. General relativity | Principle of equivalence A homogeneous gravitational field is completely equivalent to a uniformly accelerated reference frame. |

General References

The following general references are written at a level appropriate for readers of this book.

- Bohm, D., *The Special Theory of Relativity*, W. A. Benjamin, New York, 1965.
- French, A. P., *Albert Einstein: A Centenary Volume*. Harvard University Press, Cambridge, Mass., 1979. An excellent collection of contributions from many people about Einstein's life and work.
- Lorentz, H. A., A. Einstein, H. Minkowski, and W. Weyl, *The Principle of Relativity: A Collection of Original Memoirs on the Special and General Theory of Relativity* (trans. W. Perrett and J. B. Jeffery), Dover, New York, 1923. Two of Einstein's papers reprinted here are of interest in connection with this chapter: "On the Electrodynamics of Moving Bodies" [*Annalen der Physik*, **17** (1905)], and "Does the Inertia of a Body Depend upon Its Energy Content?" [*Annalen der Physik*, **17** (1905)].
- Ohanian, H. C., *Special Relativity: A Modern Introduction*, Physics Curriculum & Instruction, 2001.
- Pais, A., *Subtle Is the Lord . . .*, Oxford University Press, Oxford, 1982.
- Resnick, R., *Introduction to Relativity*, Wiley, New York, 1968.
- Resnick, R., and D. Halliday, *Basic Concepts in Relativity and Early Quantum Theory*, 2d ed., Macmillan, New York, 1992.
- Rosser, W. G. V., *The Theory of Relativity*, Butterworth, London, 1964.
- Taylor, E. F., and J. A. Wheeler, *Spacetime Physics*, 2d ed., W. H. Freeman and Co., 1992. A good book with many examples, problems, and diagrams.

Notes

1. This *Gedankenexperiment* (thought experiment) is based on one first suggested by G. N. Lewis and R. C. Tolman, *Philosophical Magazine*, **18**, 510, (1909).
2. You can see that this is so by rotating Figure 2-1a through 180° in its own plane; it then matches Figure 2-1b exactly.
3. C. G. Adler, *American Journal of Physics*, **55**, 739 (1987).
4. This idea grew out of the results of the measurements of masses in chemical reactions in the nineteenth century, which, within the limits of experimental uncertainties of the time, were always observed to conserve mass. The conservation of energy had a similar origin in the experiments of James Joule (1818–1889) as interpreted by Hermann von Helmholtz (1821–1894). This is not an unusual way for conservation laws to originate; they still do it this way.
5. The approximation of Equation 2-10 used in this discussion was, of course, not developed from Newton's equations. The rest energy mc^2 has no classical counterpart.
6. "Facilitates" means that we don't have to make frequent unit conversions or carry along large powers of 10 with nearly every factor in many calculations. However, a word of caution is in order. Always remember that the eV is *not* a basic SI unit. When making calculations whose results are to be in SI units, don't forget to convert the eV!
7. A. Einstein, *Annalen der Physik*, **17**, 1905.
8. Strictly speaking, the time component should be written $i c \Delta t$, where $i = (-1)^{1/2}$. The i is the origin of the minus sign in the spacetime interval, as well as in Equation 2-32 for the energy/momentum four-vector and other four-vectors in both special and general relativity. Its inclusion was a contribution of Hermann Minkowski (1864–1909), a Russian-German mathematician who developed the geometric interpretation of relativity and who was one of Einstein's professors at Zurich. Consideration of the four-dimensional geometry is beyond the scope of our discussions, so we will not be concerned with the i .

- 9.** Other conservation laws must also be satisfied, e.g., electric charge, angular momentum.
- 10.** The positron is a particle with the same mass as an ordinary electron but with a positive electric charge of the same magnitude as that carried by the electron. It and other antiparticles will be discussed in Chapters 11 and 12.
- 11.** Since electrons are thought to be point particles, i.e., they have no space dimensions, it isn't clear what it means to "hit" an electron. Think of it as the photon close to the electron's location, hence within its strong electric field.
- 12.** Such a system is called a *polyelectron*. It is analogous to an ionized hydrogen molecule much as positronium is analogous to a hydrogen atom. (See Figure 2-12 caption.)
- 13.** Satellite navigation systems, e.g., the Global Positioning System, are now so precise that the minute corrections arising primarily from the general relativistic time dilation must be taken into account by the system's programs.
- 14.** From Einstein's lecture in Kyoto in late 1922. See A. Pais, *Subtle Is the Lord . . .* (Oxford: Oxford University Pres, 1982).
- 15.** From an unpublished paper now in the collection of the Pierpont Morgan Library in New York. See Pais (1982).
- 16.** Einstein inquired of the astronomer George Hale (after whom the 5-m telescope on Palomar Mountain is named) in 1913 whether such minute deflections could be measured near the Sun. The answer was no, but a corrected calculation two years later doubled the predicted deflection and brought detection to within the realm of possibility.
- 17.** This is not a simple integration. See, e.g., Adler et al., *Introduction to General Relativity* (New York: McGraw-Hill, 1963).

18. Both Newtonian mechanics and special relativity predict half this value. The particle-scattering formula used in Chapter 4 to obtain Equation 4-3, applied to the gravitational deflection of a photon of mass $h\nu/c^2$ by the solar mass M_\odot at impact parameter b equal to the solar radius R_\odot , shows how this value arises.

19. A copy of Einstein's work (he was then in Berlin) was smuggled out of Germany to Eddington in England so that he could plan the project. Germany and England were then at war. Arthur S. Eddington was at the time director of the prestigious Cambridge Observatory. British authorities approved the eclipse expeditions to avoid the embarrassment of putting such a distinguished scientist as Eddington, a conscientious objector, into a wartime internment camp.

20. See, e.g., R. V. Pound and G. A. Rebka, Jr., *Physical Review Letters*, **4**, 337 (1960).

21. These values are relative to the fixed stars.

22. A. Einstein, "The Foundation of the General Theory of Relativity," *Annalen der Physik*, **49**, 769 (1916).

23. I. I. Shapiro et al., *Physical Review Letters*, **26**, 1132 (1971).

24. R. A. Hulse and J. H. Taylor, *Astrophysical Journal*, **195**, L51 (1975).

25. Gravity wave detectors outside the U.S. are the TAMA 300 (Japan), GEO600 (Germany), and Virgo (Italy). NASA and the European Space Agency are designing a space-based gravity-wave detector, LISA, that will have arms 5 million kilometers long. The three satellites that LISA will comprise are scheduled for launch in 2011.

Problems

Level I

Section 2-1 Relativistic Momentum and Section 2-2 Relativistic Energy

- 2-1.** Show that $p_{yA} = -p_{yB}$, where p_{yA} and p_{yB} are the relativistic momenta and speeds of the balls in Figure 2-1, given by

$$p_{yA} = \frac{mu_0}{\sqrt{1 - u_0^2/c^2}} \quad p_{yB} = \frac{mu_{yB}}{\sqrt{1 - (u_{xB}^2 + u_{yB}^2)/c^2}}$$

$$u_{yB} = -u_0 \sqrt{1 - v^2/c^2} \quad u_{xB} = v$$

- 2-2.** Show that $d(\gamma mu) = m(1 - u^2/c^2)^{-3/2} du$.

- 2-3.** An electron of rest energy $mc^2 = 0.511$ MeV moves with respect to the laboratory at speed $u = 0.6c$. Find (a) γ , (b) p in units of MeV/ c , (c) E , and (d) E_k .

- 2-4.** How much energy would be required to accelerate a particle of mass m from rest to a speed of (a) 0.5 c , (b) 0.9 c , and (c) 0.99 c ? Express your answers as multiples of the rest energy.

- 2-5.** Two 1-kg masses are separated by a spring of negligible mass. They are pushed together, compressing the spring. If the work done in compressing the spring is 10 J, find the change in mass of the system in kilograms. Does the mass increase or decrease?

2-6. At what value of u/c does the measured mass of a particle exceed its rest mass by (a) 10%, (b) a factor of 5, and (c) a factor of 20?

2-7. A cosmic ray proton is moving at such a speed that it can travel from the Moon to Earth in 1.5 s. (a) At what fraction of the speed of light is the proton moving? (b) What is its kinetic energy? (c) What value would be measured for its mass by an observer in Earth's reference frame? (d) What percent error is made in the kinetic energy by using the classical relation? (The Earth-Moon distance is 3.8×10^5 km. Ignore Earth's rotation.)

2-8. How much work must be done on a proton to increase its speed from (a) $0.15c$ to $0.16c$? (b) $0.85c$ to $0.86c$? (c) $0.95c$ to $0.96c$? Notice that the change in the speed is the same in each case.

2-9. The Relativistic Heavy Ion Collider (RHIC) at Brookhaven is colliding fully ionized gold (Au) nuclei accelerated to an energy of 200 GeV per nucleon. Each Au nucleus contains 197 nucleons. (a) What is the speed of each Au nucleus just before collision? (b) What is the momentum of each at that instant? (c) What energy and momentum would be measured for one of the Au nuclei by an observer in the rest system of the other Au nucleus?

2-10. (a) Compute the rest energy of 1 g of dirt. (b) If you could convert this energy entirely into electrical energy and sell it for 10 cents per kilowatt-hour, how much money would you get? (c) If you could power a 100-W lightbulb with the energy, for how long could you keep the bulb lit?

2-11. An electron with rest energy of 0.511 MeV moves with speed $u = 0.2c$. Find its total energy, kinetic energy, and momentum.

2-12. A proton with rest energy of 938 MeV has a total energy of 1400 MeV. (a) What is its speed? (b) What is its momentum?

2-13. The orbital speed of the Sun relative to the center of the Milky Way is about 250 km/s. By what fraction do the relativistic and Newtonian values differ for (a) the Sun's momentum and (b) the Sun's kinetic energy?

2-14. An electron in a hydrogen atom has a speed about the proton of 2.2×10^6 m/s. (a) By what percent do the relativistic and Newtonian values of E_k differ? (b) By what percent do the momentum values differ?

2-15. Suppose that you seal an ordinary 60-W lightbulb and a suitable battery inside a transparent enclosure and suspend the system from a very sensitive balance. (a) Compute the change in the mass of the system if the lamp is on continuously for one year at full power. (b) What difference, if any, would it make if the inner surface of the container were a perfect reflector?

Section 2-3 Mass/Energy Conversion and Binding Energy

2-16. Use Appendix A and Table 2-1 to find how much energy is needed to remove one proton from a ${}^4\text{He}$ atom, leaving a ${}^3\text{H}$ atom plus a proton and an electron.

2-17. Use Appendix A and Table 2-1 to find how much energy is required to remove one of the neutrons from a ${}^3\text{H}$ atom to yield a ${}^2\text{H}$ atom plus a neutron.

2-18. The energy released when sodium and chlorine combine to form NaCl is 4.2 eV. (a) What is the increase in mass (in unified mass units) when a molecule of NaCl is dissociated into an atom of Na and an atom of Cl? (b) What percentage of error is made in neglecting this mass difference? (The mass of Na is about 23 u and that of Cl is about 35.5 u.)

2-19. In a nuclear fusion reaction two ${}^2\text{H}$ atoms are combined to produce one ${}^4\text{He}$. (a) Calculate the decrease in rest mass in unified mass units. (b) How much energy is released in this reaction? (c) How many such reactions must take place per second to produce 1 W of power?

2-20. An elementary particle of mass M completely absorbs a photon, after which its mass is $1.01M$. (a) What was the energy of the incoming photon? (b) Why is that energy greater than $0.01Mc^2$?

2-21. When a beam of high-energy protons collides with protons at rest in the laboratory (e.g., in a container of water or liquid hydrogen), neutral pions (π^0) are produced by the reaction $p + p \rightarrow p + p + \pi^0$. Compute the threshold energy of the protons in the beam for this reaction to occur. (See Table 2-1 and Example 2-11.)

2-22. The energy released in the fission of a ^{235}U nucleus is about 200 MeV. How much rest mass (in kg) is converted to energy in this fission?

2-23. The temperature of the Sun's core is about 1.5×10^7 K. Assuming the core to consist of atomic hydrogen gas and recalling that temperature measures the average kinetic energy of the atoms, compute (a) the thermal energy of 1 kg of the gas and (b) the mass associated with this energy ($\bar{E}_k = 3kT/2$, where k is the Boltzmann constant; see Chapter 3).

Section 2-4 Invariant Mass

2-24. Compute the force exerted on the palm of your hand by the beam from a 1.0-W flashlight (a) if your hand absorbs the light, and (b) if the light reflects from your hand. What would be the mass of a particle that exerts that same force in each case if you hold it at Earth's surface?

2-25. An electron-positron pair combined as positronium is at rest in the laboratory. The pair annihilate, producing a pair of photons (gamma rays) moving in opposite directions in the lab. Show that the invariant rest energy of the gamma rays is equal to that of the electron pair.

2-26. Show that Equation 2-31 can be written $E = mc^2(1 + p^2/m^2c^2)^{1/2}$ and use the binomial expansion to show that, when pc is much less than mc^2 , $E \approx mc^2 + p^2/2m$.

2-27. An electron of rest energy 0.511 MeV has a total energy of 5 MeV. (a) Find its momentum in units of MeV/c. (b) Find u/c .

2-28. Make a sketch of the total energy of an electron E as a function of its momentum p . (See Equations 2-36 and 2-39 for the behavior of E at large and small values of p .)

2-29. What is the speed of a particle that is observed to have momentum 500 MeV/c and energy 1746 MeV? What is the particle's mass (in MeV/c^2)?

2-30. An electron of total energy 4.0 MeV moves perpendicular to a uniform magnetic field along a circular path whose radius is 4.2 cm. (a) What is the strength of the magnetic field B ? (b) By what factor does γm exceed m ?

2-31. A proton is bent into a circular path of radius 2 m by a magnetic field of 0.5 T. (a) What is the momentum of the proton? (b) What is its kinetic energy?

Section 2-5 General Relativity

2-32. Compute the deflection angle α for light from a distant star that would, according to general relativity, be measured by an observer on the Moon as the light grazes the edge of Earth.

2-33. A set of twins work in the Sears Tower, a very tall office building in Chicago. One works on the top floor and the other works in the basement. Considering general relativity, which twin will age more slowly? (a) They will age at the same rate. (b) The twin who works on the top floor will age more slowly. (c) The twin who works in the basement will age more slowly. (d) It depends on the building's speed. (e) None of the previous choices is correct.

2-34. Jupiter makes 8.43 orbits/century and exhibits an orbital eccentricity $\epsilon = 0.048$. Jupiter is 5.2 AU from the Sun (see footnote for Table 2-2 in the More section) and has a mass 318 times the Earth's 5.98×10^{24} kg. What does general relativity predict for the rate of precession of Jupiter's perihelion? (It has not yet been measured.) (The astronomical unit AU = the mean Earth-Sun distance = 1.50×10^{11} m.)

2-35. A synchronous satellite "parked" in orbit over the equator is used to relay microwave transmissions between stations on the ground. To what frequency must the satellite's receiver be tuned if the frequency of the transmission from Earth is exactly 9.375 GHz? (Ignore all Doppler effects.)

2-36. A particular distant star is found to be $92 c \cdot y$ from Earth. On a direct line between us and the star and $35 c \cdot y$ from the distant star is a dense white dwarf star with a mass equal to 3 times the Sun's mass M_\odot and a radius of 104 km. Deflection of the light beam from the distant star by the white dwarf causes us to see it as a pair of circular arcs like those shown in Figure 2-20(b). Find the angle 2α formed by the lines of sight to the two arcs.

Level II

2-37. A clock is placed on a satellite that orbits Earth with a period of 90 min at an altitude of 300 km. By what time interval will this clock differ from an identical clock on Earth after 1 year? (Include both special and general relativistic effects.)

2-38. Referring to Example 2-11, find the total energy E' as measured in S' where $p' = 0$.

2-39. In the Stanford linear collider, small bundles of electrons and positrons are fired at each other. In the laboratory's frame of reference, each bundle is about 1 cm long and 10 μm in diameter. In the collision region, each particle has energy of 50 GeV, and the electrons and positrons are moving in opposite directions. (a) How long and how wide is each bundle in its own reference frame? (b) What must be the minimum proper length of the accelerator for a bundle to have both its ends simultaneously in the accelerator in its own reference frame? (The actual length of the accelerator is less than 1000 m.) (c) What is the length of a positron bundle in the reference frame of the electron bundle? (d) What are the momentum and energy of the electrons in the rest frame of the positrons?

2-40. The rest energy of a proton is about 938 MeV. If its kinetic energy is also 938 MeV, find (a) its momentum and (b) its speed.

2-41. A spaceship of mass 10^6 kg is coasting through space when suddenly it becomes necessary to accelerate. The ship ejects 10^3 kg of fuel in a very short time at a speed of $c/2$ relative to the ship. (a) Neglecting any change in the rest mass of the system, calculate the speed of the ship in the frame in which it was initially at rest. (b) Calculate the speed of the ship using classical Newtonian mechanics. (c) Use your results from (a) to estimate the change in the rest mass of the system.

2-42. A clock (or a light-emitting atom) located at Earth's equator moves at about 463 m/s relative to one located at the pole. The equator clock is also about 21 km farther from the center of Earth than the pole clock due to Earth's equatorial bulge. For an inertial reference frame centered on Earth, compute the time dilation effect for each clock as seen by an observer at the other clock. Show that the effects nearly cancel and that, as a result, the clocks read very close to the same time. (Assume that g is constant over the 21 km of the equatorial bulge.)

2-43. Professor Spenditt, oblivious to economics and politics, proposes the construction of a circular proton accelerator around Earth's circumference using bending magnets that provide a magnetic field of 1.5 T. (a) What would be the kinetic energy of protons orbiting in this field in a circle of radius R_E ? (b) What would be the period of rotation of these protons?

2-44. In ancient Egypt the annual flood of the Nile was predicted by the rise of Sirius (the Dog Star). Sirius is one of a binary pair whose companion is a white dwarf. Orbital analysis of the pair indicates that the dwarf's mass is 2×10^{30} kg (i.e., about one solar mass). Comparison of spectral lines emitted by the white dwarf with those emitted by the same element on Earth shows a fractional frequency shift of 7×10^{-4} . Assuming this to be due to a gravitational redshift, compute the density of the white dwarf. (For comparison, the Sun's density is 1409 kg/m³.)

2-45. Show that the creation of an electron-positron pair (or any particle-antiparticle pair, for that matter) by a single photon is not possible in isolation, i.e., that additional mass (or radiation) must be present. (*Hint:* Use the conservation laws.)

2-46. With inertial systems S and S' arranged with their corresponding axes parallel and S' moving in the $+x$ direction, it was apparent that the Lorentz transformation for y and z would be $y' = y$ and $z' = z$. The transformations for the y and z components of the momentum are not so apparent, however. Show that, as stated in Equations 2-16 and 2-17, $p'_y = p_y$ and $p'_z = p_z$.

Level III

2-47. Two identical particles of rest mass m are each moving toward the other with speed u in frame S . The particles collide inelastically with a spring that locks shut (see Figure 2-9) and come to rest in S , and their initial kinetic energy is transformed into potential energy. In this problem you are going to show that the conservation of momentum in reference frame S' , in which one of the particles is initially at rest, requires that the total rest mass of the system after the collision be $2m/(1 - u^2/c^2)^{1/2}$. (a) Show that the speed of the particle not at rest in frame S' is

$$u' = \frac{2u}{1 + u^2/c^2}$$

and use this result to show that

$$\sqrt{1 - \frac{u'^2}{c^2}} = \frac{1 - u^2/c^2}{1 + u^2/c^2}$$

(b) Show that the initial momentum in frame S' is $p' = 2mu/(1 - u^2/c^2)$. (c) After the collision, the composite particle moves with speed u in S' (since it is at rest in S). Write the total momentum after the collision in terms of the final rest mass M , and show that the conservation of momentum implies that $M = 2m/(1 - u^2/c^2)^{1/2}$. (d) Show that the total energy is conserved in each reference frame.

2-48. An antiproton \bar{p} has the same rest energy as a proton. It is created in the reaction $p + p \rightarrow p + p + p + \bar{p}$. In an experiment, protons at rest in the laboratory are bombarded with protons of kinetic energy E_k , which must be great enough so that kinetic energy equal to $2mc^2$ can be converted into the rest energy of the two particles. In the frame of the laboratory, the total kinetic energy cannot be converted into rest energy because of conservation of momentum. However, in the zero-momentum reference frame in which the two initial protons are moving toward each other with equal speed u , the total kinetic energy can be converted into rest energy. (a) Find the speed of each proton u such that the total kinetic energy in the zero-momentum frame is $2mc^2$. (b) Transform to the laboratory's frame in which one proton is at rest, and find the speed u' of the other proton. (c) Show that the kinetic energy of the moving proton in the laboratory's frame is $E_k = 6mc^2$.

2-49. In a simple thought experiment, Einstein showed that there is mass associated with electromagnetic radiation. Consider a box of length L and mass M resting on a frictionless surface. At the left wall of the box is a light source that emits radiation of energy E , which is absorbed at the right wall of the box. According to classical electromagnetic theory, this radiation carries momentum of magnitude $p = E/c$. (a) Find the recoil velocity of the box such that momentum is conserved when the light is emitted. (Since p is small and M is large, you may use classical mechanics.) (b) When the light is absorbed at the right wall of the box, the box stops, so the total momentum remains zero. If we neglect the very small velocity of the box, the time it takes for the radiation to travel across the box is $\Delta t = L/c$. Find the distance moved by the box in this time. (c) Show that if the center of mass of the system is to remain at the same place, the radiation must carry mass $m = E/c^2$.

2-50. A pion spontaneously decays into a muon and a muon antineutrino according to (among other processes) $\pi^- \rightarrow \mu^- + \bar{\nu}_\mu$. Recent experimental evidence indicates that the mass m of the $\bar{\nu}_\mu$ is no larger than about $190 \text{ keV}/c^2$ and may be as small as zero. Assuming that the pion decays at rest in the laboratory, compute the energies and momenta of the muon and muon antineutrino (a) if the mass of the antineutrino were zero and (b) if its mass were $190 \text{ keV}/c^2$. The mass of the pion is $139.56755 \text{ MeV}/c^2$ and the mass of the muon is $105.65839 \text{ MeV}/c^2$. (See Chapters 11 and 12 for more on the neutrino mass.)

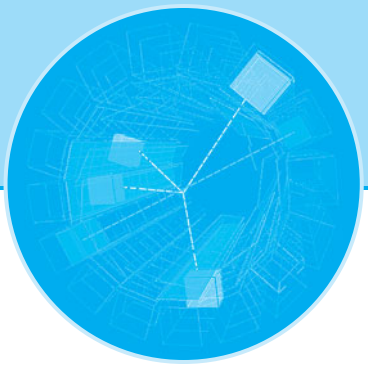
2-51. Use Equation 2-47 to obtain the gravitational redshift in terms of the wavelength λ . Use that result to determine the shift in wavelength of light emitted by a white dwarf star at 720.0 nm . Assume the white dwarf has the same mass as the Sun ($1.99 \times 10^{30} \text{ kg}$) but a radius equal to only 1 percent of the solar radius R_\odot ($R_\odot = 6.96 \times 10^8 \text{ m}$).

2-52. For a particle moving in the xy plane of S , show that the y' component of the acceleration is given by

$$a'_y = \frac{a_y}{\gamma^2(1 - u_x v/c^2)^2} + \frac{a_x u_y v/c^2}{\gamma^2(1 - u_x v/c^2)^3}$$

2-53. Consider an object of mass m at rest in S acted upon by a force F with components F_x and F_y . System S' moves with instantaneous velocity v in the $+x$ direction. Defining the force with Equation 2-8 and using the Lorentz velocity transformation, show that (a) $F'_x = F_x$ and (b) $F'_y = F_y/\gamma$. (Hint: See Problem 2-52.)

2-54. An unstable particle of mass M decays into two identical particles, each of mass m . Obtain an expression for the velocities of the two decay particles in the lab frame (a) if M is at rest in the lab and (b) if M has total energy $4mc^2$ when it decays and the decay particles move along the direction of M .



Quantization of Charge, Light, and Energy

The idea that all matter is composed of tiny particles, or atoms, dates to the speculations of the Greek philosopher Democritus¹ and his teacher Leucippus in about 450 B.C. However, little attempt was made to correlate such speculations with observations of the physical world until the seventeenth century. Pierre Gassendi, in the mid-seventeenth century, and Robert Hooke, somewhat later, attempted to explain states of matter and the transitions between them with a model of tiny, indestructible solid objects flying in all directions. But it was Avogadro's hypothesis, advanced in 1811, that all gases at a given temperature contain the same number of molecules per unit volume, that led to great success in the interpretation of chemical reactions and to development of kinetic theory in about 1900. Avogadro's hypothesis made possible quantitative understanding of many bulk properties of matter and led to general (though not unanimous) acceptance of the molecular theory of matter. Thus, matter is not continuous, as it appears, but is *quantized* (i.e., discrete) on the microscopic scale. Scientists of the day understood that the small size of the atom prevented the discreteness of matter from being readily observable.

In this chapter, we will study how three additional great quantization discoveries were made: (1) electric charge, (2) light energy, and (3) energy of oscillating mechanical systems. The quantization of electric charge was not particularly surprising to scientists in 1900; it was quite analogous to the quantization of mass. However, the quantization of light energy and mechanical energy, which are of central importance in modern physics, were revolutionary ideas.

3-1 Quantization of Electric Charge

Early Measurements of e and e/m

The first estimates of the order of magnitude of the electric charges found in atoms were obtained from Faraday's law. The work of Michael Faraday (1791–1867) in the early to mid-1800s stands out even today for its vision, experimental ingenuity, and thoroughness. The story of this self-educated blacksmith's son who rose from errand boy and

| | |
|-------------------------------------|-----|
| 3-1 Quantization of Electric Charge | 115 |
| 3-2 Blackbody Radiation | 119 |
| 3-3 The Photoelectric Effect | 127 |
| 3-4 X Rays and the Compton Effect | 133 |

bookbinder's apprentice to become the director of the distinguished Royal Institution of London and the foremost experimental investigator of his time is a fascinating one. One aspect of his work concerned the study of the conduction of electricity in weakly conducting solutions. His discovery that the same quantity of electricity, F , now called the *faraday* and equal to about 96,500 C, always decomposes one gram-ionic weight, that is, Avogadro's number N_A , of monovalent ions leads to the reasonable conclusion that each monovalent ion carries the same electric charge, e , and therefore

$$F = N_A e \quad \text{3-1}$$

Equation 3-1 is called Faraday's law of electrolysis. While F was readily measurable, neither N_A nor e could be experimentally determined at the time. Faraday was aware of this but could not determine either quantity. Even so, it seemed logical to expect that electric charge, like matter, was not continuous, but consisted of particles of some discrete minimum charge. In 1874, G. J. Stoney² used an estimate of N_A from kinetic theory to compute the value of e from Equation 3-1 to be about 10^{-20} C; however, direct measurement of the value of e had to await an ingenious experiment conducted by R. A. Millikan a third of a century later.

Meanwhile, Pieter Zeeman, in 1896, obtained the first evidence for the existence of atomic particles with a specific charge-to-mass ratio by looking at the changes in the discrete *spectral lines* emitted by atoms when they were placed in a strong magnetic field. He discovered that the individual spectral lines split into three very closely spaced lines of slightly different frequencies when the atoms were placed in the magnetic field. (This phenomenon is called the *Zeeman effect* and will be discussed further in Chapter 7.) Classical electromagnetic theory relates the slight differences in the frequencies of adjacent lines to the charge-to-mass ratio of the oscillating charges producing the light.

 From his measurements of the splitting, Zeeman calculated q/m to be about 1.6×10^{11} C/kg, which compares favorably with the presently accepted value, 1.759×10^{11} C/kg (see Appendix D). From the polarization of the spectral lines, Zeeman concluded that the oscillating particles were negatively charged.

Discovery of the Electron: J. J. Thomson's Experiment

The year following Zeeman's work, J. J. Thomson³ measured the q/m value for the so-called cathode rays that were produced in electrical discharges in gases and pointed out that, if their charge was Faraday's charge e as determined by Stoney, then their mass was only a small fraction of the mass of a hydrogen atom. Two years earlier J. Perrin had collected cathode rays on an electrometer and found them to carry a negative electric charge.⁴ Thus, with his measurement of q/m for the cathode rays, Thomson had, in fact, discovered the *electron*. That direct measurement of e/m of electrons by J. J. Thomson in 1897, a little over a century ago, can be justly considered to mark the beginning of our understanding of atomic structure.

 **Measurement of e/m** When a uniform magnetic field of strength B is established perpendicular to the direction of motion of charged particles, the particles move in a circular path. The radius R of the path can be obtained from Newton's second law by setting the magnetic force quB equal to the mass m times the centripetal acceleration u^2/R , where u is the speed of the particles:

$$quB = \frac{mu^2}{R} \quad \text{or} \quad R = \frac{mu}{qB} \quad \text{and} \quad \frac{q}{m} = \frac{u}{RB} \quad \text{3-2}$$

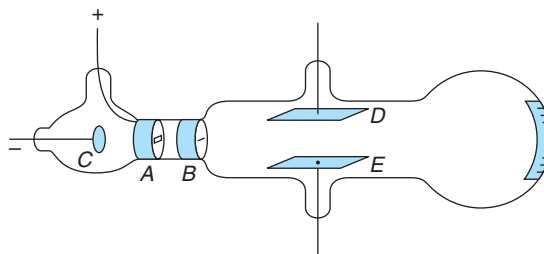


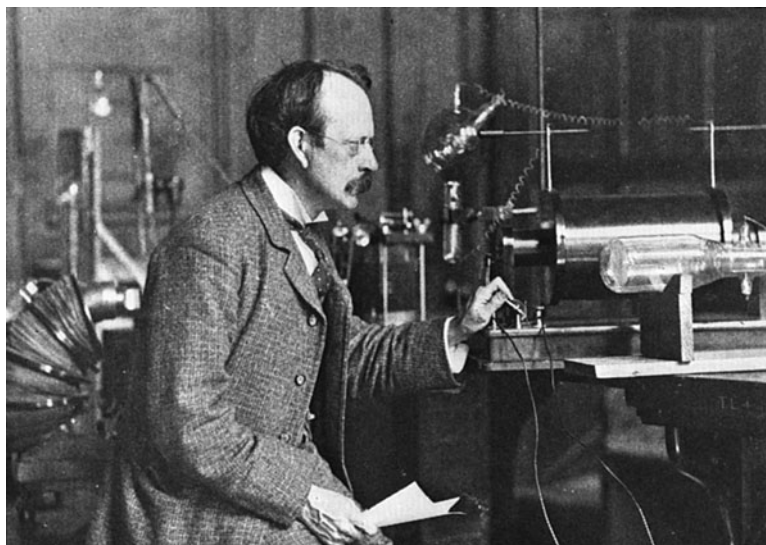
Figure 3-1 J. J. Thomson's tube for measuring e/m . Electrons from the cathode C pass through the slits at A and B and strike a phosphorescent screen. The beam can be deflected by an electric field between the plates D and E or by a magnetic field (not shown) whose direction is perpendicular to the electric field between D and E . From the deflections measured on a scale on the tube at the screen, e/m can be determined. [From J. J. Thomson, "Cathode Rays," *Philosophical Magazine* (5), **44**, 293 (1897).]

Thomson performed two e/m experiments of somewhat different designs. The second, more reproducible of the two has become known as the *J. J. Thomson experiment* (Figure 3-1). In this experiment he adjusted perpendicular B and \mathcal{E} fields so that the particles were undeflected. This allowed him to determine the speed of the electrons by equating the magnitudes of the magnetic and electric forces and then to compute $e/m (\equiv q/m)$ from Equation 3-2:

$$quB = q\mathcal{E} \quad \text{or} \quad u = \frac{\mathcal{E}}{B} \quad \text{3-3}$$

Thomson's experiment was remarkable in that he measured e/m for a subatomic particle using only a voltmeter, an ammeter, and a measuring rod, obtaining the result $0.7 \times 10^{11} \text{ C/kg}$. Present-day particle physicists routinely use the modern equivalent of Thomson's experiment to measure the momenta of elementary particles.

Thomson's technique for controlling the direction of the electron beam with "crossed" electric and magnetic fields was subsequently applied in the development of cathode ray tubes used in oscilloscopes and the picture tubes of television receivers.



J. J. Thomson in his laboratory. He is facing the screen end of an e/m tube; an older cathode ray tube is visible in front of his left shoulder. [Courtesy of Cavendish Laboratory.]

Thomson repeated the experiment with different gases in the tube and different metals for cathodes and always obtained the same value for e/m within his experimental uncertainty, thus showing that these particles are common to all metals. The agreement of these results with Zeeman's led to the unmistakable conclusion that these particles—called *corpuscles* by Thomson and later called *electrons* by Lorentz—which have one unit of negative charge e and a mass about 2000 times less than the mass of the lightest known atom were constituents of *all* atoms.

Questions

1. One advantage of Thomson's evidence over others' (such as Faraday's or Zeeman's) was its directness. Another was that it was not just a statistical inference. How does the Thomson experiment show that e/m is the same for a large number of the particles?
2. Thomson noted that his values for e/m were about 2000 times larger than those for the lightest known ion, that of hydrogen. Could he tell from his data whether this was the result of the electron having either a greater charge or a smaller mass than the hydrogen ion?

Measuring the Electric Charge: Millikan's Experiment

The fact that Thomson's e/m measurements always yielded the same results regardless of the materials used for the cathodes or the kind of gas in the tube was a persuasive argument that the electrons all carried one unit e of negative electric charge. Thomson initiated a series of experiments to determine the value of e . The first of these experiments, which turned out to be very difficult to do with high precision, was carried out by his student J. S. E. Townsend. The idea was simple: a small (but visible) cloud of identical water droplets, each carrying a single charge e , was observed to drift downward in response to the gravitational force. The total charge on the cloud $Q = Ne$ was measured, as were the mass of the cloud and the radius of a single drop. Finding the radius allowed calculation of N , the total number of drops in the cloud, and, hence, the value of e .

The accuracy of Thomson's method was limited by the uncertain rate of evaporation of the cloud. In addition, the assumption that each droplet contained a single charge could not be verified. R. A. Millikan tried to eliminate the evaporation problem by using a field strong enough to hold the top surface of the cloud stationary so that he could observe the rate of evaporation and correct for it. That, too, turned out to be very difficult, but then he made a discovery of enormous importance, one that allowed him to measure directly the charge of a single electron! Millikan described his discovery in the following words:

It was not found possible to balance the cloud as had been originally planned, but it was found possible to do something much better: namely, to hold individual charged drops suspended by the field for periods varying from 30 to 60 seconds. I have never actually timed drops which lasted more than 45 seconds, although I have several times observed drops which in my judgment lasted considerably longer than this. The drops which it was found possible to balance by an electric field always carried multiple charges, and the difficulty experienced in balancing such drops was less than had been anticipated.⁵

The discovery that he could see individual droplets and that droplets suspended in a vertical electric field sometimes suddenly moved upward or downward, evidently because they had picked up a positive or negative ion, led to the possibility of observing the charge of a single ion. In 1909, Millikan began a series of experiments that not only showed that charges occurred in integer multiples of an elementary unit e , but measured the value of e to about 1 part in 1000. To eliminate evaporation, he used oil drops sprayed into dry air between the plates of a capacitor (Figure 3-2). These drops were already charged by the spraying process, i.e., by friction in the spray nozzle, and during the course of the observation they picked up or lost additional charges. By switching the direction of the electric field between the plates, a drop could be moved up or down and observed for several hours. When the charge on a drop changed, the velocity of the drop with the field “on” changed also. Assuming only that the terminal velocity of the drop was proportional to the force acting on it (this assumption was carefully checked experimentally), Millikan’s oil drop experiment⁶ gave conclusive evidence that electric charges always occur in integer multiples of a fundamental unit e , whose value he determined to be $1.601 \times 10^{-19} \text{ C}$. The currently accepted value⁷ is $1.60217653 \times 10^{-19} \text{ C}$. An expanded discussion of Millikan’s experiment is included in the Classical Concept Review.

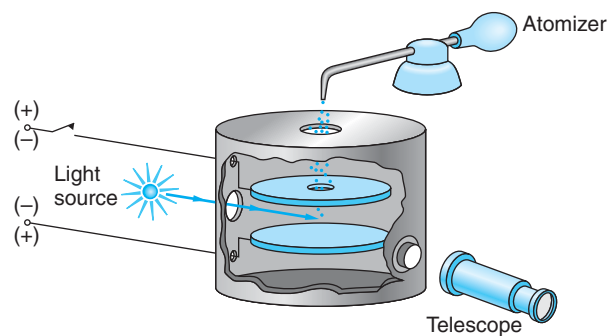


Figure 3-2 Schematic diagram of Millikan’s oil drop experiment. The drops are sprayed from an atomizer and pick up a static charge, a few falling through the hole in the top plate. Their fall due to gravity and their rise due to the electric field between the capacitor plates can be observed with the telescope. From measurements of the rise and fall times, the electric charge on a drop can be calculated. The charge on a drop could be changed by exposure to x rays from a source (not shown) mounted opposite the light source.

integers multiples of a fundamental unit e , whose value he determined to be $1.601 \times 10^{-19} \text{ C}$. The currently accepted value⁷ is $1.60217653 \times 10^{-19} \text{ C}$.

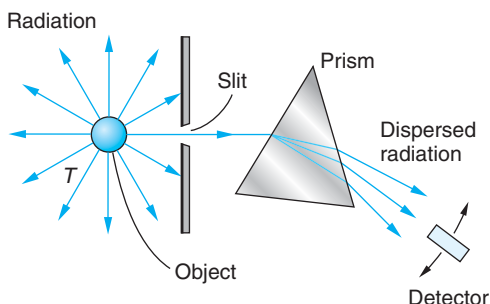


3-2 Blackbody Radiation

The first clue to the quantum nature of radiation came from the study of thermal radiation emitted by opaque bodies. When radiation falls on a opaque body, part of it is reflected and the rest is absorbed. Light-colored bodies reflect most of the visible radiation incident on them, whereas dark bodies absorb most of it. The absorption part of the process can be described briefly as follows. The radiation absorbed by the body increases the kinetic energy of the constituent atoms, which oscillate about their equilibrium positions. Since the average translational kinetic energy of the atoms determines the temperature of the body, the absorbed energy causes the temperature to rise. However, the atoms contain charges (the electrons), and they are accelerated by the oscillations. Consequently, as required by electromagnetic theory, the atoms emit electromagnetic radiation, which reduces the kinetic energy of the oscillations and tends to reduce the temperature. When the rate of absorption equals the rate of emission, the temperature is constant, and we say that the body is in thermal equilibrium with its surroundings. A good absorber of radiation is therefore also a good emitter.

The electromagnetic radiation emitted under these circumstances is called *thermal radiation*. At ordinary temperatures (below about 600°C) the thermal radiation emitted by a body is not visible; most of the energy is concentrated in wavelengths much longer than those of visible light. As a body is heated, the quantity of thermal radiation emitted increases, and the energy radiated extends to shorter and shorter wavelengths. At about $600^\circ\text{--}700^\circ\text{C}$ there is enough energy in the visible spectrum so that the body glows and becomes a dull red, and at higher temperatures it becomes bright red or even “white hot.”

Figure 3-3 Radiation emitted by the object at temperature T that passes through the slit is dispersed according to its wavelengths. The prism shown would be an appropriate device for that part of the emitted radiation in the visible region. In other spectral regions other types of devices or wavelength-sensitive detectors would be used.



A body that absorbs *all* radiation incident on it is called an *ideal blackbody*. In 1879 Josef Stefan found an empirical relation between the power radiated by an ideal blackbody and the temperature:

$$R = \sigma T^4 \quad 3-4$$

where R is the power radiated per unit area, T is the absolute temperature, and $\sigma = 5.6703 \times 10^{-8} \text{ W/m}^2\text{K}^4$ is a constant called Stefan's constant. This result was also derived on the basis of classical thermodynamics by Ludwig Boltzmann about five years later, and Equation 3-4 is now called the Stefan-Boltzmann law. Note that the power per unit area radiated by a blackbody depends only on the temperature and not on any other characteristic of the object, such as its color or the material of which it is composed. Note, too, that R tells us the *rate* at which energy is emitted by the object. For example, doubling the absolute temperature of an object, e.g., a star, increases the energy flow out of the object by a factor of $2^4 = 16$. An object at room temperature (300°C) will double the rate at which it radiates energy as a result of a temperature increase of only 57°C . Thus, the Stefan-Boltzmann law has an enormous effect on the establishment of thermal equilibrium in physical systems.

Objects that are not ideal blackbodies radiate energy per unit area at a rate less than that of a blackbody at the same temperature. For those objects the rate does depend on properties in addition to the temperature, such as color and the composition of the surface. The effects of those dependencies are combined into a factor called the *emissivity* ϵ which multiplies the right side of Equation 3-4. The values of ϵ , which is itself temperature dependent, are always less than unity.

Like the total radiated power R , the *spectral distribution* of the radiation emitted by a blackbody is found empirically to depend *only* on the absolute temperature T . The spectral distribution is determined experimentally as illustrated schematically in Figure 3-3. With $R(\lambda) d\lambda$ the power emitted per unit area with wavelength between λ and $\lambda + d\lambda$, Figure 3-4 shows the measured spectral distribution function $R(\lambda)$ versus λ for several values of T ranging from 1000 K to 6000 K.

The $R(\lambda)$ curves in Figure 3-4 are quite remarkable in several respects. One is that the wavelength at which the distribution has its maximum value varies inversely with the temperature:

$$\lambda_m \propto \frac{1}{T}$$

or

$$\lambda_m T = \text{constant} = 2.898 \times 10^{-3} \text{ m} \cdot \text{K} \quad 3-5$$

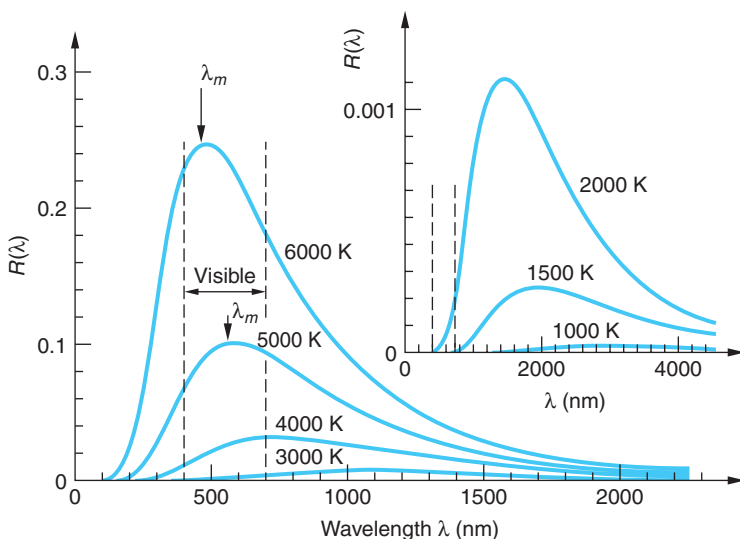


Figure 3-4 Spectral distribution function $R(\lambda)$ measured at different temperatures. The $R(\lambda)$ axis is in arbitrary units for comparison only. Notice the range of λ in the visible spectrum. The Sun emits radiation very close to that of a blackbody at 5800 K. λ_m is indicated for the 5000-K and 6000-K curves.

This result is known as Wien's displacement law. It was obtained by Wien in 1893. Examples 3-1 and 3-2 illustrate its application.

EXAMPLE 3-1 How Big Is a Star? Measurement of the wavelength at which the spectral distribution $R(\lambda)$ from a certain star is maximum indicates that the star's surface temperature is 3000 K. If the star is also found to radiate 100 times the power P_\odot radiated by the Sun, how big is the star? (The symbol $\odot = \text{Sun}$.) The Sun's surface temperature is 5800 K.

SOLUTION

If the Sun and the star both radiate as blackbodies (astronomers nearly always make that assumption, based on, among other things, the fact that the solar spectrum is very nearly that of an ideal blackbody), their surface temperatures from Equation 3-5 are 5800 K and 3000 K, respectively. Measurement also indicates that $P_{\text{star}} = 100 P_\odot$. Thus, from Equation 3-4 we have

$$R_{\text{star}} = \frac{P_{\text{star}}}{(\text{area})_{\text{star}}} = \frac{100 P_\odot}{4\pi r_{\text{star}}^2} = \sigma T_{\text{star}}^4$$

and

$$R_\odot = \frac{P_\odot}{(\text{area})_\odot} = \frac{P_\odot}{4\pi r_\odot^2} = \sigma T_\odot^4$$

So we have

$$\begin{aligned} r_{\text{star}}^2 &= 100 r_\odot^2 \left(\frac{T_\odot}{T_{\text{star}}} \right)^4 \\ r_{\text{star}} &= 10 r_\odot \left(\frac{T_\odot}{T_{\text{star}}} \right)^2 = 10 \left(\frac{5800}{3000} \right)^2 r_\odot \\ r_{\text{star}} &= 37.4 r_\odot \end{aligned}$$

Since $r_\odot = 6.96 \times 10^8$ m, this star has a radius of about 2.6×10^{10} m, or about half the radius of the orbit of Mercury. This star is a red giant (see Chapter 13).

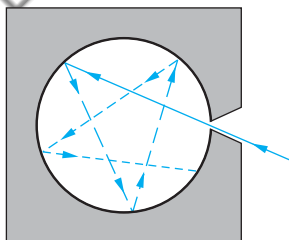


Figure 3-5 A small hole in the wall of a cavity approximating an ideal blackbody. Radiation entering the hole has little chance of leaving before it is completely absorbed within the cavity.

Rayleigh-Jeans Equation

The calculation of the distribution function $R(\lambda)$ involves the calculation of the energy density of electromagnetic waves in a cavity. Materials such as black velvet or lamp-black come close to being ideal blackbodies, but the best practical realization of an ideal blackbody is a small hole leading into a cavity (such as a keyhole in a closet door; Figure 3-5). Radiation incident on the hole has little chance of being reflected back out of the hole before it is absorbed by the walls of the cavity. The power radiated *out* of the hole is proportional to the total energy density U (the energy per unit volume of the radiation in the cavity). The proportionality constant can be shown to be $c/4$, where c is the speed of light.⁸

$$R = \frac{1}{4}cU \quad \text{3-6}$$

Similarly, the spectral distribution of the power emitted from the hole is proportional to the spectral distribution of the energy density in the cavity. If $u(\lambda) d\lambda$ is the fraction of the energy per unit volume in the cavity in the range $d\lambda$, then $u(\lambda)$ and $R(\lambda)$ are related by

$$R(\lambda) = \frac{1}{4}cu(\lambda) \quad \text{3-7}$$

The energy density distribution function $u(\lambda)$ can be calculated from classical physics in a straightforward way. The method involves finding the number of modes of oscillation of the electromagnetic field in the cavity with wavelengths in the interval $d\lambda$ and multiplying by the average energy per mode. The result is that the number of modes of oscillation per unit volume, $n(\lambda)$, is independent of the shape of the cavity and is given by



$$n(\lambda) = 8\pi\lambda^{-4} \quad \text{3-8}$$

According to classical kinetic theory, the average energy per mode of oscillation is kT , the same as for a one-dimensional harmonic oscillator, where k is the Boltzmann constant. Classical theory thus predicts for the energy density distribution function

$$u(\lambda) = kT n(\lambda) = 8\pi kT \lambda^{-4} \quad \text{3-9}$$

This prediction, initially derived by Lord Rayleigh,⁹ is called the *Rayleigh-Jeans equation*. It is illustrated in Figure 3-6.

At very long wavelengths the Rayleigh-Jeans equation agrees with the experimentally determined spectral distribution, but at short wavelengths this equation predicts that $u(\lambda)$ becomes large, approaching infinity as $\lambda \rightarrow 0$, whereas experiment shows (see Figure 3-4) that the distribution actually approaches zero as $\lambda \rightarrow 0$. This enormous disagreement between the experimental measurement of $u(\lambda)$ and the prediction of the fundamental laws of classical physics at short wavelengths was called the *ultraviolet catastrophe*. The word *catastrophe* was not used lightly; Equation 3-9 implies that

$$\int_0^\infty u(\lambda) d\lambda \longrightarrow \infty \quad \text{3-10}$$

That is, every object would have an infinite energy density, which observation assures us is not true.

Planck's Law

In 1900 the German physicist Max Planck¹⁰ announced that by making somewhat strange assumptions, he could derive a function $u(\lambda)$ that agreed with the experimental data. He first found an empirical function that fit the data and then searched for a way to modify the usual calculation so as to predict his empirical formula. We can see the type of modification needed if we note that, for any cavity, the shorter the wavelength, the more standing waves (modes) will be possible. Therefore, as $\lambda \rightarrow 0$ the number of modes of oscillation approaches infinity, as evidenced in Equation 3-8. In order for the energy density distribution function $u(\lambda)$ to approach zero, we expect the average energy per mode to depend on the wavelength λ and approach zero as λ approaches zero, rather than be equal to the value kT predicted by classical theory.

Parenthetically, we should note that those working on the ultraviolet catastrophe at the time—and there were many besides Planck—had no a priori way of knowing whether the number of modes $n(\lambda)$ or the average energy per mode kT (or both) was the source of the problem. Both were correct classically. Many attempts were made to rederive each so as to solve the problem. As it turned out, it was the average energy per mode (that is, kinetic theory) that was at fault.

Classically, the electromagnetic waves in the cavity are produced by accelerated electric charges in the walls of the cavity vibrating as simple harmonic oscillators. Recall that the radiation emitted by such an oscillator has the same frequency as the oscillation itself. The average energy for a one-dimensional simple harmonic oscillator is calculated classically from the energy distribution function, which in turn is found from the Maxwell-Boltzmann distribution function. That energy distribution function has the form (see Chapter 8)

$$f(E) = Ae^{-E/kT} \quad 3-11$$

where A is a constant and $f(E)$ is the fraction of the oscillators with energy equal to E . The average energy \bar{E} is then found, as is any weighted average, from

$$\bar{E} = \int_0^{\infty} E f(E) dE = \int_0^{\infty} EAe^{-E/kT} dE \quad 3-12$$

with the result $\bar{E} = kT$, as was used by Rayleigh and others.

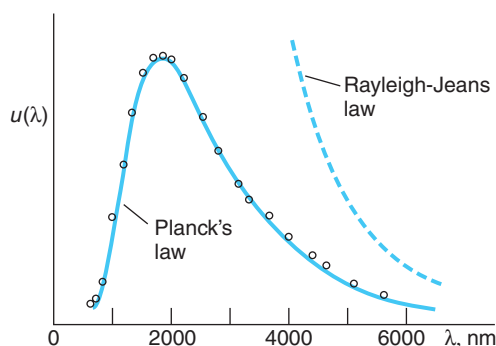


Figure 3-6 Comparison of Planck's law and the Rayleigh-Jeans equation with experimental data at $T = 1600$ K obtained by W. W. Coblenz in about 1915. The $u(\lambda)$ axis is linear. [Adapted from F. K. Richmyer, E. H. Kennard, and J. N. Cooper, *Introduction to Modern Physics*, 6th ed., McGraw-Hill, New York (1969), by permission.]

Planck found that he could derive his empirical formula by calculating the average energy \bar{E} assuming that the energy of the oscillating charges, and hence the radiation that they emitted, was a discrete variable; i.e., that it could take on only the values $0, \epsilon, 2\epsilon, \dots, n\epsilon$ where n is an integer; and further, that E was proportional to the frequency of the oscillators and, hence, to that of the radiation. Planck therefore wrote the energy as

$$E_n = n\epsilon = nhf \quad n = 0, 1, 2, \dots \quad 3-13$$

where the proportionality constant h is now called *Planck's constant*. The Maxwell-Boltzmann distribution (Equation 3-11) then becomes

$$f_n = Ae^{-E_n/kT} = Ae^{-n\epsilon/kT} \quad 3-14$$

where A is determined by the normalization condition that the sum of all fractions f_n must, of course, equal 1, i.e.,

$$\sum_{n=0}^{\infty} f_n = A \sum_{n=0}^{\infty} e^{-n\epsilon/kT} = 1 \quad 3-15$$

The average energy of an oscillator is then given by the discrete-sum equivalent of Equation 3-12:

$$\bar{E} = \sum_{n=0}^{\infty} E_n f_n = \sum_{n=0}^{\infty} E_n Ae^{-E_n/kT} \quad 3-16$$

Calculating the sums in Equations 3-15 and 3-16 (see Problem 3-58) yields the result

$$\bar{E} = \frac{\epsilon}{e^{\epsilon/kT} - 1} = \frac{hf}{e^{hf/kT} - 1} = \frac{hc/\lambda}{e^{hc/\lambda kT} - 1} \quad 3-17$$

Multiplying this result by the number of oscillators per unit volume in the interval $d\lambda$ given by Equation 3-8, we obtain for the energy density distribution function of the radiation in the cavity

$$u(\lambda) = \frac{8\pi hc\lambda^{-5}}{e^{hc/\lambda kT} - 1} \quad 3-18$$

This function, called *Planck's law*, is sketched in Figure 3-6. It is clear from the figure that the result fits the data quite well.

For very large λ , the exponential in Equation 3-18 can be expanded using $e^x \approx 1 + x + \dots$ for $x \ll 1$, where $x = hc/\lambda kT$. Then

$$e^{hc/\lambda kT} - 1 \approx \frac{hc}{\lambda kT}$$

and

$$u(\lambda) \rightarrow 8\pi\lambda^{-4}kT$$

which is the Rayleigh-Jeans formula. For short wavelengths, we can neglect the 1 in the denominator of Equation 3-18, and we have

$$u(\lambda) \rightarrow 8\pi hc\lambda^{-5}e^{-hc/\lambda kT} \rightarrow 0$$

as $\lambda \rightarrow 0$. The value of the constant in Wein's displacement law also follows from Planck's law, as you will show in Problem 3-23.

The value of Planck's constant, h , can be determined by fitting the function given by Equation 3-18 to the experimental data, although direct measurement (see Section 3-3) is better but more difficult. The presently accepted value is

$$h = 6.626 \times 10^{-34} \text{ J} \cdot \text{s} = 4.136 \times 10^{-15} \text{ eV} \cdot \text{s} \quad \text{3-19}$$

Planck tried at length to reconcile his treatment with classical physics but was unable to do so. The fundamental importance of the quantization assumption implied by Equation 3-13 was suspected by Planck and others but was not generally appreciated until 1905. In that year Einstein applied the same ideas to explain the photoelectric effect and suggested that, rather than being merely a mysterious property of the oscillators in the cavity walls and blackbody radiation, quantization was a fundamental characteristic of light energy.

EXAMPLE 3-2 Peak of the Solar Spectrum The surface temperature of the Sun is about 5800 K, and measurements of the Sun's spectral distribution show that it radiates very nearly like a blackbody, deviating mainly at very short wavelengths. Assuming that the Sun radiates like an ideal blackbody, at what wavelength does the peak of the solar spectrum occur?

SOLUTION

1. The wavelength at the peak, or maximum intensity, of an ideal blackbody is given by Equation 3-5:

$$\lambda_m T = \text{constant} = 2.898 \times 10^{-3} \text{ m} \cdot \text{K}$$

2. Rearranging and substituting the Sun's surface temperature yield

$$\begin{aligned} \lambda_m &= (2.898 \times 10^{-3} \text{ m} \cdot \text{K})/T = \frac{2.898 \times 10^{-3} \text{ m} \cdot \text{K}}{5800 \text{ K}} \\ &= \frac{2.898 \times 10^6 \text{ nm} \cdot \text{K}}{5800 \text{ K}} = 499.7 \text{ nm} \end{aligned}$$

where $1 \text{ nm} = 10^{-9} \text{ m}$.

Remarks: This value is near the middle of the visible spectrum.

The electromagnetic spectrum emitted by incandescent bulbs is a common example of blackbody radiation, the amount of visible light being dependent on the temperature of the filament. Another application is the pyrometer, a device that measures the temperature of a glowing object, such as molten metal in a steel mill.

EXAMPLE 3-3 Average Energy of an Oscillator What is the average energy \bar{E} of an oscillator that has a frequency given by $hf = kT$ according to Planck's calculation?

SOLUTION

$$\bar{E} = \frac{\epsilon}{e^{\epsilon/kT} - 1} = \frac{kT}{e^1 - 1} = 0.582 kT$$

Remarks: Recall that according to classical theory, $\bar{E} = kT$ regardless of the frequency.

EXAMPLE 3-4 Stefan-Boltzmann from Planck Show that the total energy density in a blackbody cavity is proportional to T^4 in accordance with the Stefan-Boltzmann law.

SOLUTION

The total energy density is obtained from the distribution function (Equation 3-18) by integrating over all wavelengths:

$$U = \int_0^\infty u(\lambda) d\lambda = \int_0^\infty \frac{8\pi hc\lambda^{-5}}{e^{hc/\lambda kT} - 1} d\lambda$$

Define the dimensionless variable $x = hc/\lambda kT$. Then $dx = -(hc/\lambda^2 kT) d\lambda$ or $d\lambda = -\lambda^2(kT/hc) dx$. Then

$$U = - \int_0^\infty \frac{8\pi hc\lambda^{-3}}{e^x - 1} \left(\frac{kT}{hc} \right) dx = 8\pi hc \left(\frac{kT}{hc} \right)^4 \int_0^\infty \frac{x^3}{e^x - 1} dx$$

Since the integral is now dimensionless, this shows that U is proportional to T^4 . The value of the integral can be obtained from tables; it is $\pi^4/15$. Then $U = (8\pi^5 k^4 / 15 h^3 c^3) T^4$. This result can be combined with Equations 3-4 and 3-6 to express Stefan's constant in terms of π , k , h , and c (see Problem 3-13).

A dramatic example of an application of Planck's law on the current frontier of physics is in tests of the Big Bang theory of the formation and present expansion of the universe. Current cosmological theory holds that the universe originated in an extremely high-temperature explosion of space, one consequence of which was to fill the infant universe with radiation whose spectral distribution must surely have been that of an ideal blackbody. Since that time, the universe has expanded to its present size and cooled to its present temperature T_{now} . However, it should still be filled with radiation whose spectral distribution should be that characteristic of a blackbody at T_{now} .

In 1965, Arno Penzias and Robert Wilson discovered radiation of wavelength 7.35 cm reaching Earth with the same intensity from all directions in space. It was soon recognized that this radiation could be a remnant of the Big Bang fireball, and measurements were subsequently made at other wavelengths in order to construct an experimental energy density $u(\lambda)$ versus λ graph. The most recent data from the Cosmic Background Explorer (COBE) satellite, shown in Figure 3-7, and by the

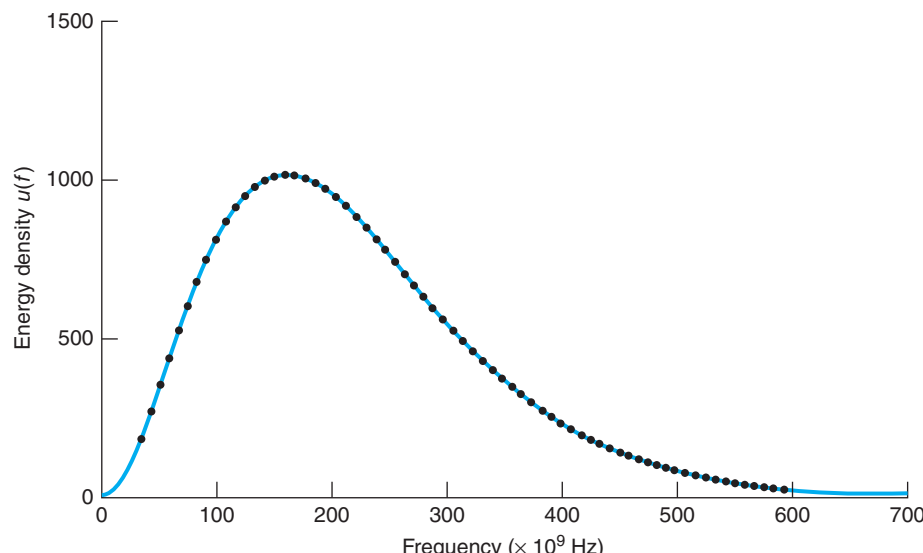


Figure 3-7 The energy density spectral distribution of the cosmic microwave background radiation. The solid line is Planck's law with $T = 2.725$ K. These measurements (the black dots) were made by the COBE satellite.

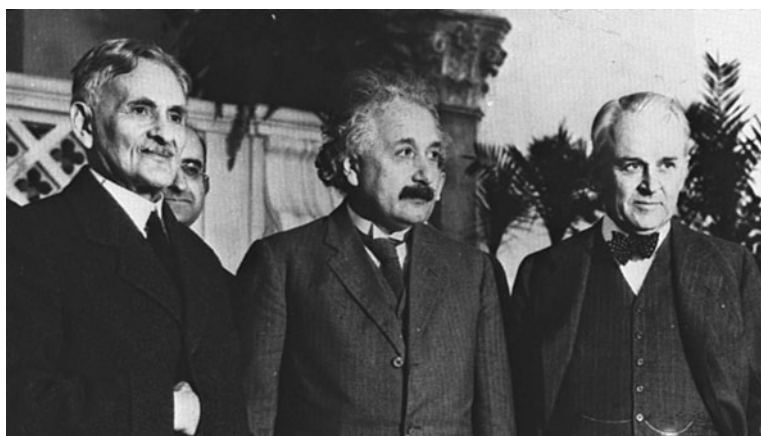
Wilkinson Microwave Anisotropy Probe (WMAP) have established the temperature of the background radiation field at 2.725 ± 0.001 K. The excellent agreement of the data with Planck's equation, indeed, the best fit that has ever been measured, is considered to be very strong support for the Big Bang theory (see Chapter 13).

3-3 The Photoelectric Effect

It is one of the ironies in the history of science that in the famous experiment of Heinrich Hertz¹¹ in 1887, in which he produced and detected electromagnetic waves, thus confirming Maxwell's wave theory of light, he also discovered the photoelectric effect, which led directly to the particle description of light. Hertz was using a spark gap in a tuned circuit to generate the waves and another similar circuit to detect them. He noticed accidentally that when the light from the generating gap was shielded from the receiving gap, the receiving gap had to be made shorter in order for the spark to jump the gap. Light from any spark that fell on the terminals of the gap facilitated the passage of the sparks. He described the discovery with these words:

In a series of experiments on the effects of resonance between very rapid electric oscillations that I had carried out and recently published, two electric sparks were produced by the same discharge of an induction coil, and therefore simultaneously. One of these sparks, spark *B*, was the discharge spark of the induction coil, and served to excite the primary oscillation. I occasionally enclosed spark *B* in a dark case so as to make observations more easily, and in so doing I observed that the maximum spark length became decidedly smaller inside the case than it was before.¹²

The unexpected discovery of the photoelectric effect annoyed Hertz because it interfered with his primary research, but he recognized its importance immediately and interrupted his other work for six months in order to study it in detail. His results, published later that year, were then extended by others. It was found that negative particles were emitted from a clean surface when exposed to light. P. Lenard in 1900 deflected them in a magnetic field and found that they had a charge-to-mass ratio of the same magnitude as that measured by Thomson for cathode rays: the particles being emitted were electrons.



Albert A. Michelson, Albert Einstein, and Robert A. Millikan at a meeting in Pasadena, California, in 1931. [AP/Wide World Photos.]

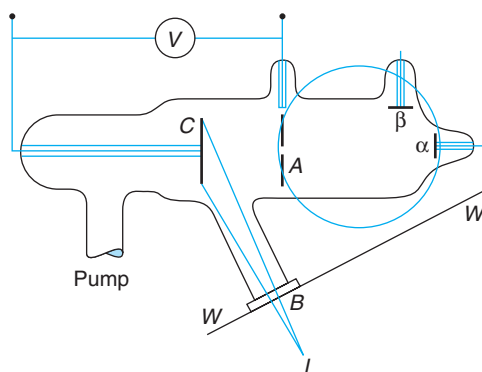


Figure 3-8 Schematic diagram of the apparatus used by P. Lenard to demonstrate the photoelectric effect and to show that the particles emitted in the process were electrons. Light from the source L strikes the cathode C . Photoelectrons going through the hole in anode A are recorded by the electrometer connected to α . A magnetic field, indicated by the circular pole piece, could deflect the particles to a second electrometer connected to β , making possible the establishment of the sign of the charges and their e/m ratio. [P. Lenard, *Annalen der Physik*, 2, 359 (1900).]

Figure 3-8 shows a schematic diagram of the basic apparatus used by Lenard. When light L is incident on a clean metal surface (cathode C), electrons are emitted. If some of these electrons that reach the anode A pass through the small hole, a current results in the external electrometer circuit connected to α . The number of the emitted electrons reaching the anode can be increased or decreased by making the anode positive or negative with respect to the cathode. Letting V be the potential difference between the cathode and anode, Figure 3-9a shows the current versus V for two values of the intensity of light incident on the cathode. When V is positive, the electrons are attracted to the anode. At sufficiently large V all the emitted electrons reach the anode and the current reaches its maximum value. Lenard observed that the maximum current was proportional to the light intensity, an expected result since doubling the energy per unit time incident on the cathode should double the number of electrons emitted. Intensities too low to provide the electrons with the energy necessary to escape from the metal should result in no emission of electrons. However, in contrast with the classical expectation, there was no minimum intensity below which the current was absent. When V is negative, the electrons are repelled from the anode. Then only electrons with initial kinetic energy $mv^2/2$ greater than $e|V|$ can reach the anode. From Figure 3-9a we see that if V is less than $-V_0$, no electrons reach the anode. The potential V_0 is called the *stopping potential*. It is related to the maximum kinetic energy of the emitted electrons by

$$\left(\frac{1}{2}mv^2 \right) = eV_0 \quad 3-20$$

The experimental result, illustrated by Figure 3-9a, that V_0 is independent of the incident light intensity was surprising. Apparently, increasing the rate of energy falling on the cathode does not increase the maximum kinetic energy of the emitted electrons, contrary to classical expectations. In 1905 Einstein offered an explanation of this result in a remarkable paper in the same volume of *Annalen der Physik* that contained his papers on special relativity and Brownian motion.

FÉUE WHI

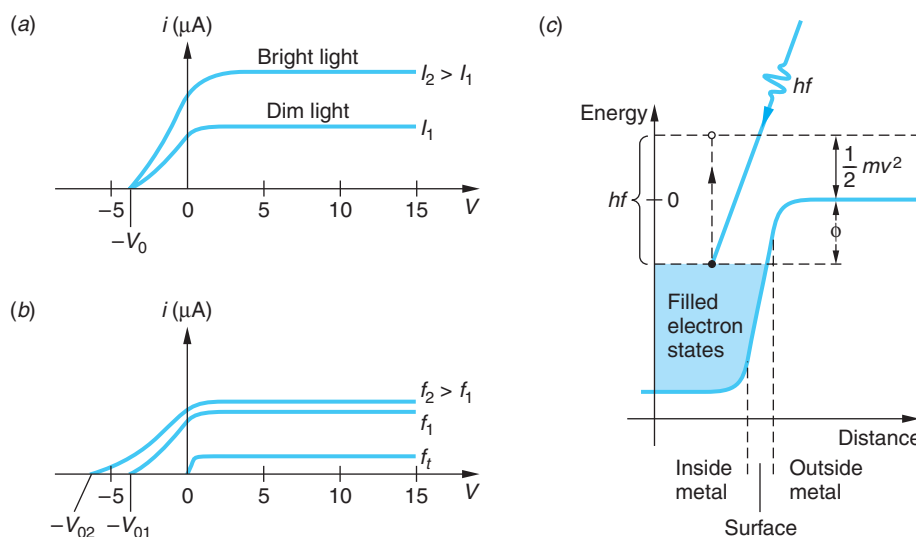


Figure 3-9 (a) Photocurrent i versus anode voltage V for light of frequency f with two intensities I_1 and I_2 , where $I_2 > I_1$. The stopping voltage V_0 is the same for both. (b) For constant I , Einstein's explanation of the photoelectric effect indicates that the magnitude of the stopping voltage should be greater for f_2 than f_1 , as observed, and that there should be a threshold frequency f_t below which no photoelectrons were seen, also in agreement with experiment. (c) Electron potential energy curve across the metal surface. An electron with the highest energy in the metal absorbs a photon of energy hf . Conservation of energy requires that its kinetic energy after leaving the surface be $hf - \phi$.

Einstein assumed that the *energy quantization used by Planck in solving the blackbody radiation problem was, in fact, a universal characteristic of light*. Rather than being distributed evenly in the space through which it propagated, light energy consisted of discrete quanta, each of energy hf . When one of these quanta, called a *photon*, penetrates the surface of the cathode, all of its energy may be absorbed completely by a single electron. If ϕ is the energy necessary to remove an electron from the surface (ϕ is called the *work function* and is a characteristic of the metal), the maximum kinetic energy of an electron leaving the surface will be $hf - \phi$ as a consequence of energy conservation; see Figure 3-9c. (Some electrons will have less than this amount because of energy lost in traversing the metal.) Thus, the stopping potential should be given by

$$eV_0 = \left(\frac{1}{2}mv^2 \right)_{\max} = hf - \phi \quad 3-21$$

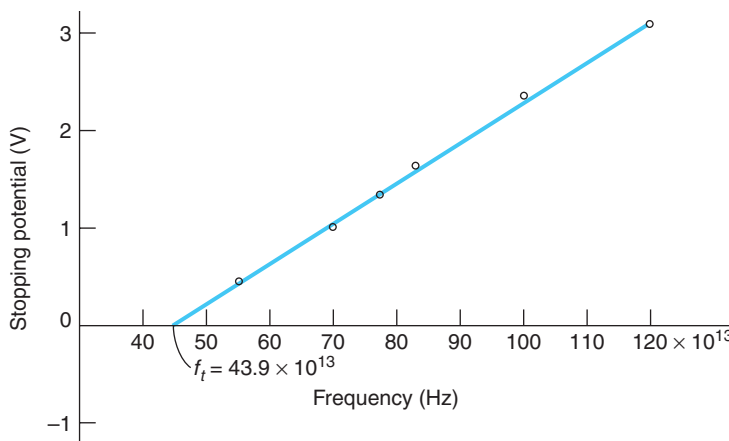
Equation 3-21 is referred to as the photoelectric effect equation. As Einstein noted,

If the derived formula is correct, then V_0 , when represented in Cartesian coordinates as a function of the frequency of the incident light, must be a straight line whose slope is independent of the nature of the emitting substance.¹³

As can be seen from Equation 3-21, the slope of V_0 versus f should equal h/e . At the time of this prediction there was no evidence that Planck's constant had anything to do with the photoelectric effect. There was also no evidence for the dependence of

Among the many applications of the photoelectric effect is the photomultiplier, a device that makes possible the accurate measurement of the energy of the light absorbed by a photosensitive surface. The SNO and Kamiokande neutrino observatories (see Chapter 12) use thousands of photomultipliers. Hundreds more are being deployed inside the Antarctic ice cap in the Ice Cube particle physics experiment.

Figure 3-10 Millikan's data for stopping potential versus frequency for the photoelectric effect. The data fall on a straight line with slope h/e , as predicted by Einstein a decade before the experiment. The intercept on the stopping potential axis is $-\phi/e$. [R. A. Millikan, *Physical Review*, 7, 362 (1915).]



the stopping potential V_0 on the frequency. Careful experiments by Millikan, reported in 1914 and in more detail in 1916, showed that Equation 3-21 was correct and that measurements of h from it agreed with the value obtained by Planck. A plot taken from this work is shown in Figure 3-10.

The minimum, or threshold, frequency for the photoelectric effect, labeled f_t in this plot and in Figure 3-9b, and the corresponding threshold wavelength λ_t are related to the work function ϕ by setting $V_0 = 0$ in Equation 3-21:

$$\phi = hf_t = \frac{hc}{\lambda_t} \quad \text{3-22}$$

Photons of frequencies lower than f_t (and therefore having wavelengths greater than λ_t) do not have enough energy to eject an electron from the metal. Work functions for metals are typically on the order of a few electron volts. The work functions for several elements are given in Table 3-1.

Table 3-1 Photoelectric work functions

| Element | Work function (eV) |
|---------|--------------------|
| Na | 2.28 |
| C | 4.81 |
| Cd | 4.07 |
| Al | 4.08 |
| Ag | 4.73 |
| Pt | 6.35 |
| Mg | 3.68 |
| Ni | 5.01 |
| Se | 5.11 |
| Pb | 4.14 |

EXAMPLE 3-5 Photoelectric Effect in Potassium The threshold frequency of potassium is 558 nm. What is the work function for potassium? What is the stopping potential when light of 400 nm is incident on potassium?

SOLUTION

- Both questions can be answered with the aid of Equation 3-21:

$$eV_0 = \left(\frac{1}{2} mv^2 \right)_{\max} = hf - \phi$$

$$V_0 = \frac{hf}{e} - \frac{\phi}{e}$$

- At the threshold wavelength the photoelectrons have just enough energy to overcome the work function barrier, so $\left(\frac{1}{2} mv^2 \right)_{\max} = 0$, hence $V_0 = 0$, and

$$\frac{\phi}{e} = \frac{hf_{te}}{e} = \frac{hc}{e\lambda_t}$$

$$= \frac{1240 \text{ eV} \cdot \text{nm}}{558 \text{ nm}} = 2.22 \text{ eV}$$

- When 400-nm light is used, V_0 is given by Equation 3-21:

$$V_0 = \frac{hf}{e} - \frac{\phi}{e} = \frac{hc}{e\lambda} - \frac{\phi}{e}$$

$$= \frac{1240 \text{ eV} \cdot \text{nm}}{400 \text{ nm}} - 2.22 \text{ eV}$$

$$= 3.10 \text{ eV} - 2.22 \text{ eV} = 0.88 \text{ V}$$

Another interesting feature of the photoelectric effect that is contrary to classical physics but is easily explained by the photon hypothesis is the lack of any time lag between the turning on of the light source and the appearance of photoelectrons. Classically, the incident energy is distributed uniformly over the illuminated surface; the time required for an area the size of an atom to acquire enough energy to allow the emission of an electron can be calculated from the intensity (power per unit area) of the incident radiation. Experimentally, the incident intensity can be adjusted so that the calculated time lag is several minutes or even hours. But no time lag is ever observed. The photon explanation of this result is that although the rate at which photons are incident on the metal is very small when the intensity is low, *each* photon has enough energy to eject an electron, and there is some chance that a photon will be absorbed immediately. The classical calculation gives the correct *average* number of photons absorbed per unit time.

EXAMPLE 3-6 Classical Time Lag Light of wavelength 400 nm and intensity 10^{-2} W/m^2 is incident on potassium. Estimate the time lag for the emission of photoelectrons expected classically.

SOLUTION

According to Example 3-5, the work function for potassium is 2.22 eV. If we assume $r = 10^{-10} \text{ m}$ to be the typical radius of an atom, the total energy falling on the atom in time t is

$$E = (10^{-2} \text{ W/m}^2)(\pi r^2)t = (10^{-2} \text{ W/m}^2)(\pi 10^{-20} \text{ m}^2)t$$

$$= (3.14 \times 10^{-22} \text{ J/s})t$$

Setting this energy equal to 2.22 eV gives

$$(3.14 \times 10^{-22} \text{ J/s})t = (2.22 \text{ eV})(1.60 \times 10^{-19} \text{ J/eV})$$

$$t = \frac{(2.22 \text{ eV})(1.60 \times 10^{-19} \text{ J/eV})}{(3.14 \times 10^{-22} \text{ J/s})} = 1.13 \times 10^3 \text{ s} = 18.8 \text{ min}$$

According to the classical prediction, no atom would be expected to emit an electron until 18.8 min after the light source was turned on. According to the photon model of light, each photon has enough energy to eject an electron immediately. Because of the low intensity, there are few photons incident per second, so the chance of any particular atom absorbing a photon and emitting an electron in any given time interval is small. However, there are so many atoms in the cathode that some emit electrons immediately.

EXAMPLE 3-7 Incident Photon Intensity In Example 3-6, how many photons are incident per second per square meter?

SOLUTION

The energy of each photon is

$$\begin{aligned} E = hf &= hc/\lambda = (1240 \text{ eV} \cdot \text{nm})/(400 \text{ nm}) = (3.10 \text{ eV})(1.60 \times 10^{-19} \text{ J/eV}) \\ &= 4.96 \times 10^{-19} \text{ J} \end{aligned}$$

Since the incident intensity is $10^{-2} \text{ W/m}^2 = 10^{-2} \text{ J/s} \cdot \text{m}^2$, the number of photons per second per square meter is

$$\begin{aligned} N &= \frac{10^{-2} \text{ J/s} \cdot \text{m}^2}{4.96 \times 10^{-19} \text{ J/photon}} \\ &= 2.02 \times 10^{16} \text{ photons/s} \cdot \text{m}^2 \end{aligned}$$

This is, of course, a lot of photons, not a few; however, the number n per atom at the surface is quite small. $n = 2.02 \times 10^{16} \text{ photons/s} \cdot \text{m}^2 \times \pi(10^{-10})^2 \text{ m}^2/\text{atom} = 6.3 \times 10^{-4} \text{ photons/s} \cdot \text{atom}$, or about 1 photon for every 1000 atoms.

Questions

3. How is the result that the maximum photoelectric current is proportional to the intensity explained in the photon model of light?
4. What experimental features of the photoelectric effect can be explained by classical physics? What features cannot?

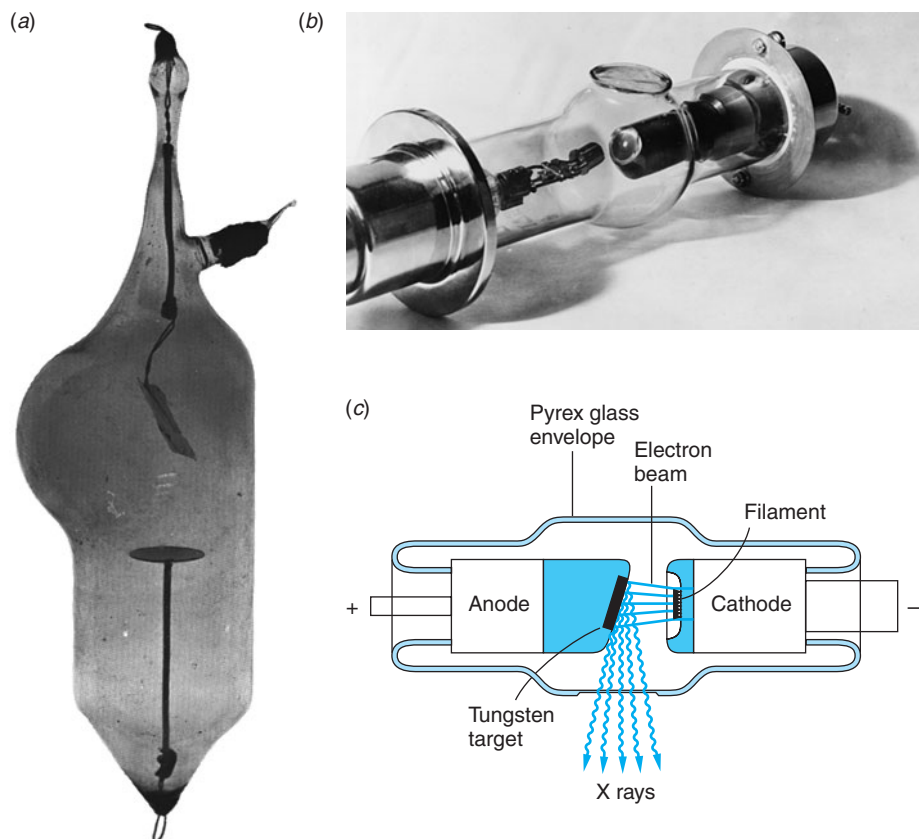
The photoemission of electrons has developed into a significant technique for investigating the detailed structure of molecules and solids, making possible discoveries far beyond anything that Hertz may have imagined. The use of x-ray sources (see Section 3-4) and precision detectors has made possible precise determination of valence electron configurations in chemical compounds, leading to detailed understanding of chemical bonding and the differences between the bulk and surface atoms of solids. Photoelectric-effect microscopes will show the chemical situation of each element in a specimen, a prospect of intriguing and crucial importance in molecular biology and microelectronics. And they are all based on a discovery that annoyed Hertz—at first.

3-4 X Rays and the Compton Effect

Further evidence of the correctness of the photon concept was furnished by Arthur H. Compton, who measured the scattering of x rays by free electrons and, by his analysis of the data, resolved the last lingering doubts regarding special relativity (see Chapter 1). Before we examine Compton scattering in detail, we will briefly describe some of the early work with x rays since it provides a good conceptual understanding of x-ray spectra and scattering.

X Rays

The German physicist Wilhelm K. Roentgen discovered x rays in 1895 when he was working with a cathode-ray tube. Coming five years before Planck's explanation of the blackbody emission spectrum, Roentgen's discovery turned out to be the first significant development in quantum physics. He found that "rays" originating from the point where the cathode rays (electrons) hit the glass tube, or a target within the tube, could pass through materials opaque to light and activate a fluorescent screen or photographic film. He investigated this phenomenon extensively and found that all materials are transparent to these rays to some degree and that the transparency decreases with increasing density. This fact led to the medical use of x rays within months after the publication of Roentgen's first paper.¹⁴



(a) Early x-ray tube. [Courtesy of Cavendish Laboratory.] (b) X-ray tubes became more compact over time. This tube was a design typical of the mid-twentieth century. [Courtesy of Schenectady Museum, Hall of Electrical History, Schenectady, NY.] (c) Diagram of the components of a modern x-ray tube. Design technology has advanced enormously, enabling very high operating voltages, beam currents, and x-ray intensities, but essential elements of the tubes remain unchanged.

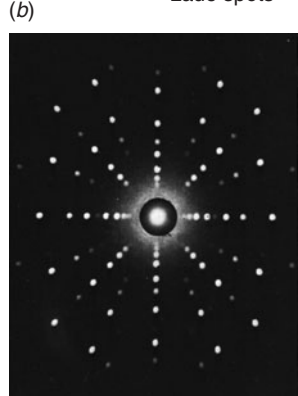
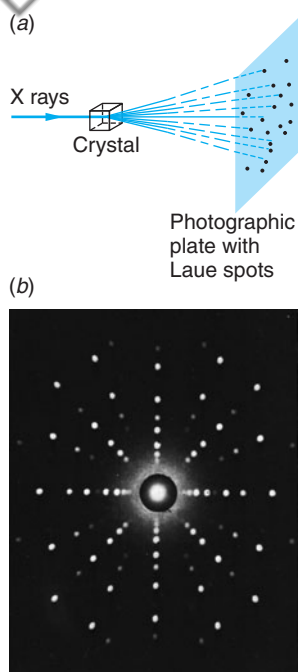


Figure 3-11 (a) Schematic sketch of a Laue experiment. The crystal acts as a three-dimensional grating, which diffracts the x-ray beam and produces a regular array of spots, called a *Laue pattern*, on photographic film or an x-ray-sensitive charge-coupled device (CCD) detector. (b) Laue x-ray diffraction pattern using a niobium boride crystal and 20-keV molybdenum x rays. [General Electric Company.]



An x ray of Mrs. Roentgen's hand taken by Roentgen shortly after his discovery.

Roentgen was unable to deflect these rays in a magnetic field, nor was he able to observe refraction or the interference phenomena associated with waves. He thus gave the rays the somewhat mysterious name of x rays. Since classical electromagnetic theory predicts that accelerated charges will radiate electromagnetic waves, it is natural to expect that x rays are electromagnetic waves produced by the acceleration of the electrons when they are deflected and stopped by the atoms of a target. Such radiation is called *bremssstrahlung*, German for “braking radiation.” The slight diffraction broadening of an x-ray beam after passing through slits a few thousandths of a millimeter wide indicated the wavelength of x rays to be of the order of 10^{-10} m = 0.1 nm. In 1912 Max von Laue suggested that since the wavelengths of x rays were of the same order of magnitude as the spacing of atoms in a crystal, the regular array of atoms in a crystal might act as a three-dimensional grating for the diffraction of x rays. Experiments (Figure 3-11) soon confirmed that x rays are a form of electromagnetic radiation with wavelengths in the range of about 0.01 to 0.10 nm and that atoms in crystals are arranged in regular arrays.

W. L. Bragg, in 1912, proposed a simple and convenient way of analyzing the diffraction of x rays by crystals.¹⁵ He examined the interference of x rays due to scattering from various sets of parallel planes of atoms, now called *Bragg planes*. Two sets of Bragg planes are illustrated in Figure 3-12 for NaCl, which has a cubic structure called *face-centered cubic*. Consider Figure 3-13. Waves scattered from the two successive atoms within a plane will be in phase and thus interfere constructively, independent of the wavelength, if the scattering angle equals the incident angle. (This condition is the same as for reflection.) Waves scattered at equal angles from atoms in two

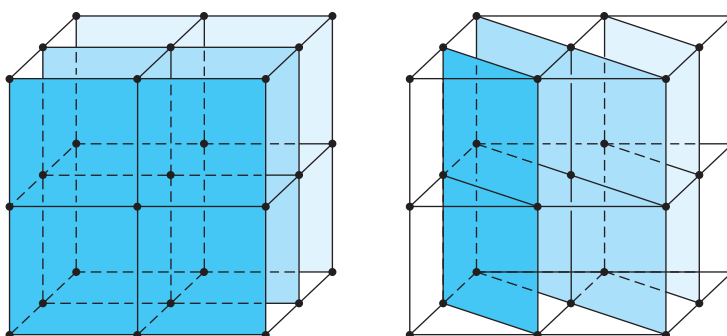


Figure 3-12 A crystal of NaCl showing two sets of Bragg planes.

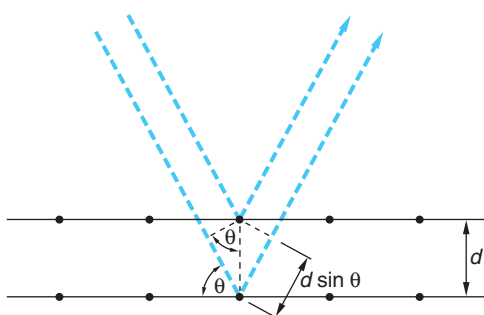


Figure 3-13 Bragg scattering from two successive planes. The waves from the two atoms shown have a path length difference of $2d \sin \theta$. They will be in phase if the Bragg condition $2d \sin \theta = m\lambda$ is met.

different planes will be in phase (constructive interference) only if the difference in path length is an integral number of wavelengths. From Figure 3-13 we see that this condition is satisfied if

$$2d \sin \theta = m\lambda \quad \text{where } m = \text{an integer} \quad 3-23$$

Equation 3-23 is called the *Bragg condition*.

Measurements of the spectral distribution of the intensity of x rays as a function of the wavelength using an experimental arrangement such as that shown in Figure 3-14 produces the x-ray spectrum and, for classical physics, some surprises. Figure 3-15a shows two typical x-ray spectra produced by accelerating electrons through two voltages V and bombarding a tungsten target mounted on the anode of the tube. In this figure $I(\lambda)$ is the intensity emitted within the wavelength interval $d\lambda$ for each value of λ . Figure 3-15b shows the short wavelength lines produced with a molybdenum target and 35-keV electrons. Three features of the spectra are of immediate interest, only one of which could be explained by classical physics. (1) The spectrum consists of a series of sharp lines, called the *characteristic spectrum*, superimposed on (2) the continuous

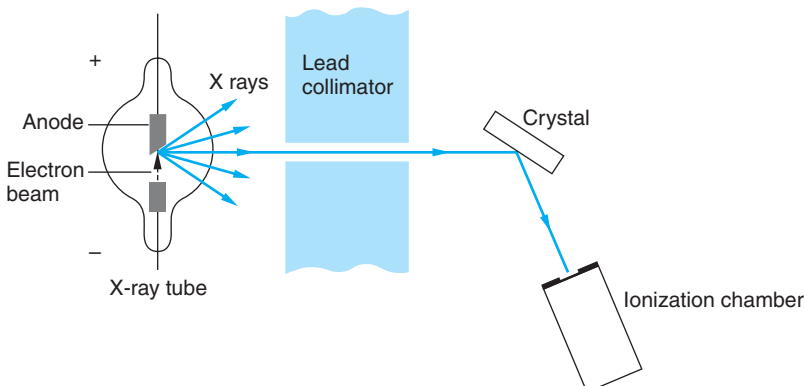


Figure 3-14 Schematic diagram of a Bragg crystal spectrometer. A collimated x-ray beam is incident on a crystal and scattered into an ionization chamber. The crystal and ionization chamber can be rotated to keep the angles of incidence and scattering equal as both are varied. By measuring the ionization in the chamber as a function of angle, the spectrum of the x rays can be determined using the Bragg condition $2d \sin \theta = m\lambda$, where d is the separation of the Bragg planes in the crystal. If the wavelength λ is known, the spacing d can be determined.

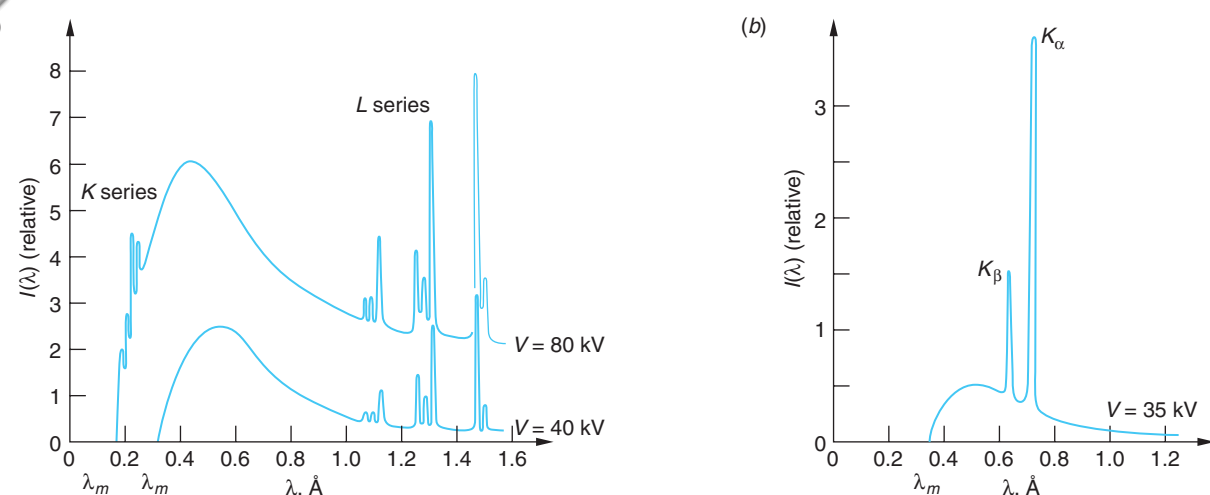


Figure 3-15 (a) X-ray spectra from tungsten at two accelerating voltages and (b) from molybdenum at one. The names of the line series (K and L) are historical and explained in Chapter 4. The L -series lines for molybdenum (not shown) are at about 0.5 nm. The cutoff wavelength λ_m is independent of the target element and is related to the voltage on the x-ray tube V by $\lambda_m = hc/eV$. The wavelengths of the lines are characteristic of the element.

bremsstrahlung spectrum. The line spectrum is characteristic of the target material and varies from element to element. (3) The continuous spectrum has a sharp cutoff wavelength, λ_m , which is independent of the target material but depends on the energy of the bombarding electrons. If the voltage on the x-ray tube is V volts, the cutoff wavelength is found empirically to be given by

$$\lambda_m = \frac{1.24 \times 10^3}{V} \text{ nm} \quad 3-24$$

Equation 3-24 is called the *Duane-Hunt rule*, after its discoverers. It was pointed out rather quickly by Einstein that x-ray production by electron bombardment was an inverse photoelectric effect and that Equation 3-21 should apply. The Duane-Hunt λ_m simply corresponds to a photon with the maximum energy of the electrons, that is, the photon emitted when the electron losses all of its kinetic energy in a single collision. Since the kinetic energy of the electrons in an x-ray tube is 20,000 eV or higher, the work function ϕ (a few eV) is negligible by comparison. That is, Equation 3-21 becomes $eV \approx hf = hc/\lambda_m$ or $\lambda_m = hc/eV = 1.2407 \times 10^{-6} V^{-1} \text{ m} = 1.24 \times 10^3 V^{-1} \text{ nm}$. Thus, the Duane-Hunt rule is explained by Planck's quantum hypothesis. (Notice that the value of λ_m can be used to determine h/e .)

The continuous spectrum was understood as the result of the acceleration (i.e., “braking”) of the bombarding electrons in the strong electric fields of the target atoms. Maxwell's equation predicted the continuous radiation. The real problem for classical physics was the sharp lines. The wavelengths of the sharp lines were a function of the target element, the set for each element being always the same. But the sharp lines never appeared if V was such that λ_m was larger than the particular line, as can be seen from Figure 3-15a, where the shortest-wavelength group disappears when V is reduced from 80 keV to 40 keV so that λ_m becomes larger. The origin of the sharp lines was a mystery that had to await the discovery of the nuclear atom. We will explain them in Chapter 4.

Well-known applications of x rays are medical and dental x rays (both diagnostic and treatment) and industrial x-ray inspection of welds and castings. Perhaps not so well known is the use of x rays in determining the structure of crystals, identifying black holes in the cosmos, and “seeing” the folded shapes of proteins in biological materials.

Compton Effect

It had been observed that scattered x rays were “softer” than those in the incident beam, that is, were absorbed more readily. Compton¹⁶ pointed out that if the scattering process were considered a “collision” between a photon of energy hf_1 (and momentum hf_1/c) and an electron, the recoiling electron would absorb part of the incident photon’s energy. The energy hf_2 of the scattered photon would therefore be less than the incident one and thus of lower frequency f_2 and momentum hf_2/c . (The fact that electromagnetic radiation of energy E carried momentum E/c was known from classical theory and from the experiments of Nichols and Hull in 1903. This relation is also consistent with the relativistic expression $E^2 = p^2c^2 + (mc^2)^2$ for a particle with zero rest energy.) Compton applied the laws of conservation of momentum and energy in their relativistic form (see Chapter 2) to the collision of a photon with an isolated electron to obtain the change in the wavelength $\lambda_2 - \lambda_1$ of the photon as a function of the scattering angle θ . The result, called *Compton’s equation* and derived in a More section on the home page, is

$$\lambda_2 - \lambda_1 = \frac{h}{mc}(1 - \cos \theta) \quad 3-25$$

The change in wavelength is thus predicted to be independent of the original wavelength. The quantity h/mc has the dimensions of length and is called the *Compton wavelength of the electron*. Its value is

$$\lambda_c = \frac{h}{mc} = \frac{hc}{mc^2} = \frac{1.24 \times 10^3 \text{ eV} \cdot \text{nm}}{5.11 \times 10^5 \text{ eV}} = 0.00243 \text{ nm}$$

Because $\lambda_2 - \lambda_1$ is small, it is difficult to observe unless λ_1 is very small so that the fractional change $(\lambda_2 - \lambda_1)/\lambda_1$ is appreciable. For this reason the Compton effect is generally only observed for x rays and gamma radiation.

Compton verified his result experimentally using the characteristic x-ray line of wavelength 0.0711 nm from molybdenum for the incident monochromatic photons and scattering these photons from electrons in graphite. The wavelength of the scattered photons was measured using a Bragg crystal spectrometer. His experimental arrangement is shown in Figure 3-16; Figure 3-17 shows his results. The first peak at

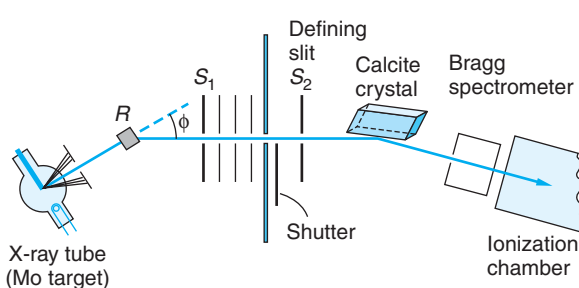


Figure 3-16 Schematic sketch of Compton’s apparatus. X rays from the tube strike the carbon block R and are scattered into a Bragg-type crystal spectrometer. In this diagram, the scattering angle is 30° . The beam was defined by slits S_1 and S_2 . Although the entire spectrum is being scattered by R , the spectrometer scanned the region around the K_α line of molybdenum.

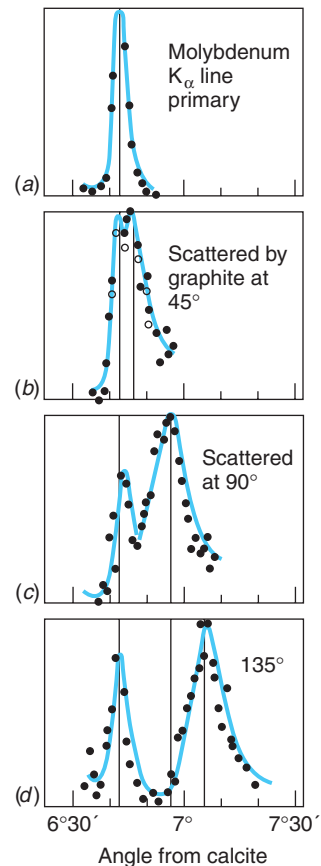


Figure 3-17 Intensity versus wavelength for Compton scattering at several angles. The left peak in each case results from photons of the original wavelength that are scattered by tightly bound electrons, which have an effective mass equal to that of the atom. The separation in wavelength of the peaks is given by Equation 3-25. The horizontal scale used by the Compton “angle from calcite” refers to the calcite analyzing crystal in Figure 3-16.

Arthur Compton. After discovering the Compton effect, he became a world traveler seeking an explanation for cosmic rays. He ultimately showed that their intensity varied with latitude, indicating an interaction with Earth's magnetic field, and thus proved that they are charged particles. [Courtesy of American Institute of Physics, Niels Bohr Library.]



each scattering angle corresponds to scattering with no shift in the wavelength due to scattering by the inner electrons of carbon. Since these are tightly bound to the atom, it is the entire atom that recoils rather than the individual electrons. The expected shift in this case is given by Equation 3-25, with m being the mass of the atom, which is about 10^4 times that of the electron; thus, this shift is negligible. The variation of $\Delta\lambda = \lambda_2 - \lambda_1$ with θ was found to be that predicted by Equation 3-25.

We have seen in this section and the preceding two sections that the interaction of electromagnetic radiation with matter is a discrete interaction that occurs at the atomic level. It is perhaps curious that after so many years of debate about the nature of light, we now find that we must have both a particle (i.e., quantum) theory to describe in detail the energy exchange between electromagnetic radiation and matter and a wave theory to describe the interference and diffraction of electromagnetic radiation. We will discuss this so-called wave-particle duality in more detail in Chapter 5.



More

Derivation of Compton's Equation, applying conservation of energy and momentum to the relativistic collision of a photon and an electron, is included on the home page: www.whfreeman.com/tiplermodernphysics5e. See also Equations 3-26 and 3-27 and Figure 3-18 here.

Questions

5. Why is it extremely difficult to observe the Compton effect using visible light?
6. Why is the Compton effect unimportant in the transmission of television and radio waves? How many Compton scatterings would a typical FM signal have before its wavelengths were shifted by 0.01 percent?

EXAMPLE 3-8 X Rays from TV The acceleration voltage of the electrons in a typical television picture tube is 25 keV. What is the minimum wavelength x ray produced when these electrons strike the inner front surface of the tube?

SOLUTION

From Equation 3-24, we have

$$\lambda_m = \frac{1.24 \times 10^3}{V} \text{ nm} = \frac{1.24 \times 10^3}{25,000} = 0.050 \text{ nm}$$

These x rays penetrate matter very effectively. Manufacturers provide essential shields to protect against the hazard.

EXAMPLE 3-9 Compton Effect In a particular Compton scattering experiment it is found that the incident wavelength λ_1 is shifted by 1.5 percent when the scattering angle $\theta = 120^\circ$. (a) What is the value of λ_1 ? (b) What will be the wavelength λ_2 of the shifted photon when the scattering angle is 75° ?

SOLUTION

- For question (a), the value of λ_1 is found from Equation 3-25:

$$\begin{aligned}\lambda_2 - \lambda_1 &= \Delta\lambda = \frac{h}{mc}(1 - \cos\theta) \\ &= 0.00243(1 - \cos 120^\circ)\end{aligned}$$

- That the scattered wavelength λ_2 is shifted by 1.5 percent from λ_1 means that

$$\frac{\Delta\lambda}{\lambda_1} = 0.015$$

- Combining these yields:

$$\begin{aligned}\lambda_1 &= \frac{\Delta\lambda}{0.015} = \frac{0.00243(1 - \cos 120)}{0.015} \\ &= 0.243 \text{ nm}\end{aligned}$$

- Question (b) is also solved with the aid of Equation 3-25, rearranged as

$$\lambda_2 = \lambda_1 + 0.00243(1 - \cos\theta)$$

- Substituting $\theta = 75^\circ$ and λ_1 from above yields

$$\begin{aligned}\lambda_2 &= 0.243 + 0.00243(1 - \cos 75) \\ &= 0.243 + 0.002 \\ &= 0.245 \text{ nm}\end{aligned}$$

A Final Comment

In this chapter, together with Section 2-4 of the previous chapter, we have introduced and discussed at some length the three primary ways by which photons interact with matter: (1) the photoelectric effect, (2) the Compton effect, and (3) pair production. As we proceed with our explorations of modern physics throughout the remainder of the book, we will have many occasions to apply what we have learned here to aid in our understanding of myriad phenomena, ranging from atomic structure to the fusion “furnaces” of stars.

Summary

| TOPIC | RELEVANT EQUATIONS AND REMARKS | |
|------------------------------------|--|------|
| 1. J. J. Thomson's experiment | Thomson's measurements with cathode rays showed that the same particle (the electron), with e/m about 2000 times that of ionized hydrogen, exists in all elements. | |
| 2. Quantization of electric charge | $e = 1.60217653 \times 10^{-19} \text{ C}$ | |
| 3. Blackbody radiation | | |
| Stefan-Boltzmann law | $R = \sigma T^4$ | 3-4 |
| Wein's displacement law | $\lambda_m T = 2.898 \times 10^{-3} \text{ m} \cdot \text{K}$ | 3-5 |
| Planck's radiation law | $u(\lambda) = \frac{8\pi hc\lambda^{-5}}{e^{hc/\lambda kT} - 1}$ | 3-18 |
| Planck's constant | $h = 6.626 \times 10^{-34} \text{ J} \cdot \text{s}$ | 3-19 |
| 4. Photoelectric effect | $eV_0 = hf - \phi$ | 3-21 |
| 5. Compton effect | $\lambda_2 - \lambda_1 = \frac{h}{mc}(1 - \cos\theta)$ | 3-25 |
| 6. Photon-matter interaction | The (1) photoelectric effect, (2) Compton effect, and (3) pair production are the three ways of interaction. | |

General References

The following general references are written at a level appropriate for readers of this book.

Millikan, R. A., *Electrons (+ and -) Protons, Photons, Neutrons, Mesotrons, and Cosmic Rays*, 2d ed., University of Chicago Press, Chicago, 1947. This book on modern physics by one of the great experimentalists of his time contains fascinating, detailed descriptions of Millikan's oil drop experiment and his verification of the Einstein photoelectric-effect equation.

Mohr, P. J., and B. N. Taylor, "The Fundamental Physical Constants," *Physics Today* (August 2004). Also available at <http://www.physicstoday.org/guide/fundcont.html>.

Richtmyer, F. K., E. H. Kennard, and J. N. Cooper, *Introduction to Modern Physics*, 6th ed., McGraw-Hill, New York, 1969. This excellent text was originally published in 1928, intended as a survey course for graduate students.

Shamos, M. H. (ed.), *Great Experiments in Physics*, Holt, Rinehart, and Winston, New York, 1962. This book contains 25 original papers and extensive editorial comment.

Of particular interest for this chapter are papers by Faraday, Hertz, Roentgen, J. J. Thomson, Einstein (photo electric effect), Millikan, Planck, and Compton.

Thomson, G. P., *J. J. Thomson, Discoverer of the Electron*, Doubleday/Anchor, Garden City, NY, 1964. An interesting study of J. J. Thomson by his son, also a physicist.

Virtual Laboratory (PEARL), Physics Academic Software, North Carolina State University, Raleigh, 1996. Computer simulation software allows the user to analyze blackbody radiation emitted over a wide range of temperatures and investigate the Compton effect in detail.

Weart, S. R., *Selected Papers of Great American Physicists*, American Institute of Physics, New York, 1976. The bi-centennial commemorative volume of the American Physical Society.

Notes

1. Democritus (about 470 B.C. to about 380 B.C.). Among his other modern-sounding ideas were the suggestions that the Milky Way is a vast conglomeration of stars and that the Moon, like Earth, has mountains and valleys.
2. G. J. Stoney (1826–1911). An Irish physicist who first called the fundamental unit of charge the electron. After Thomson discovered the particle that carried the charge, the name was transferred from the quantity of charge to the particle itself by Lorentz.
3. Joseph J. Thomson (1856–1940). English physicist and director for more than 30 years of the Cavendish Laboratory, the first laboratory in the world established expressly for research in physics. He was awarded the Nobel Prize in 1906 for his work on the electron. Seven of his research assistants also won Nobel Prizes.
4. Much early confusion existed about the nature of cathode rays due to the failure of Heinrich Hertz in 1883 to observe any deflection of the rays in an electric field. The failure was later found to be the result of ionization of the gas in the tube; the ions quickly neutralized the charges on the deflecting plates so that there was actually no electric field between the plates. With better vacuum technology in 1897, Thomson was able to work at lower pressure and observe electrostatic deflection.
5. R. A. Millikan, *Philosophical Magazine* (6), **19**, 209 (1910). Millikan, who held the first physics Ph.D. awarded by Columbia University, was one of the most accomplished experimentalists of his time. He received the Nobel Prize in 1923 for the measurement of the electron's charge. Also among his many contributions, he coined the phrase *cosmic rays* to describe radiation produced in outer space.
6. R. A. Millikan, *Physical Review*, **32**, 349 (1911).
7. Mohr, P. J., and B. N. Taylor, "The Fundamental Physical Constants," *Physics Today* (August 2004).
8. See pp. 135–137 of F. K. Richtmyer, E. H. Kennard, and J. N. Cooper (1969).
9. John W. S. Rayleigh (1842–1919). English physicist, almost invariably referred to by the title he inherited from his father. He was Maxwell's successor and Thomson's predecessor as director of the Cavendish Laboratory.
10. Max K. E. L. Planck (1858–1947). Most of his career was spent at the University of Berlin. In his later years his renown in the world of science was probably second only to that of Einstein.
11. Heinrich R. Hertz (1857–1894), German physicist, student of Helmholtz. He was the discoverer of electromagnetic "radio" waves, later developed for practical communication by Marconi.
12. H. Hertz, *Annalen der Physik*, **31**, 983 (1887).
13. A. Einstein, *Annalen der Physik*, **17**, 144 (1905).
14. A translation of this paper can be found in E. C. Watson, *American Journal of Physics*, **13**, 284 (1945), and in Shamos (1962). Roentgen (1845–1923) was honored in 1901 with the first Nobel Prize in Physics for his discovery of x rays.
15. William Lawrence Bragg (1890–1971), Australian-English physicist. An infant prodigy, his work on x-ray diffraction performed with his father, William Henry Bragg (1862–1942), earned for them both the Nobel Prize in Physics in 1915, the only father-son team to be so honored thus far. In 1938 W. L. Bragg became director of the Cavendish Laboratory, succeeding Rutherford.
16. Arthur H. Compton (1892–1962), American physicist. It was Compton who suggested the name *photon* for the light quantum. His discovery and explanation of the Compton effect earned him a share of the Nobel Prize in Physics in 1927.

Problems

Level I

Section 3-1 Quantization of Electric Charge

3-1. A beam of charged particles consisting of protons, electrons, deuterons, and singly ionized helium atoms and H_2 molecules all pass through a velocity selector, all emerging with speeds of 2.5×10^6 m/s. The beam then enters a region of uniform magnetic field $B = 0.40$ T directed perpendicular to their velocity. Compute the radius of curvature of the path of each type of particle.

3-2. Consider Thomson's experiment with the electric field turned "off." If the electrons enter a region of uniform magnetic field B and length l , show that the electrons are deflected through an angle $\theta \approx e\ell B/mu\ell$ for small values of θ . (Assume that the electrons are moving at non-relativistic speeds.)

3-3. Equation 3-3 suggests how a velocity selector for particles or mixtures of different particles all having the same charge can be made. Suppose you wish to make a velocity selector that allows undeflected passage for electrons whose kinetic energy is 5.0×10^4 eV. The electric field available to you is 2.0×10^5 V/m. What magnetic field will be needed?

3-4. A cosmic ray proton approaches Earth vertically at the equator, where the horizontal component of Earth's magnetic field is 3.5×10^{-5} T. If the proton is moving at 3.0×10^6 m/s, what is the ratio of the magnetic force to the gravitational force on the proton?

3-5. An electron of kinetic energy 45 keV moves in a circular orbit perpendicular to a magnetic field of 0.325 T. (a) Compute the radius of the orbit. (b) Find the period and frequency of the motion.

3-6. If electrons have kinetic energy of 2000 eV, find (a) their speed, (b) the time needed to traverse a distance of 5 cm between plates D and E in Figure 3-1, and (c) the vertical component of their velocity after passing between the plates if the electric field is 3.33×10^3 V/m.

3-7. In J. J. Thomson's first method (see Problem 3-44), the heat capacity of the beam stopper was about 5×10^{-3} cal/ $^{\circ}$ C and the temperature increase was about 2° C. How many 2000-eV electrons struck the beam stopper?

3-8. On drop #16, Millikan measured the following total charges, among others, at different times:

$$\begin{array}{lll} 25.41 \times 10^{-19} \text{ C} & 17.47 \times 10^{-19} \text{ C} & 12.70 \times 10^{-19} \text{ C} \\ 20.64 \times 10^{-19} \text{ C} & 19.06 \times 10^{-19} \text{ C} & 14.29 \times 10^{-19} \text{ C} \end{array}$$

What value of the fundamental quantized charge e do these numbers imply?

3-9. Show that the electric field needed to make the rise time of the oil drop equal to its field-free fall time is $\mathcal{E} = 2mg/q$.

3-10. One variation of the Millikan oil drop apparatus arranges the electric field horizontally, rather than vertically, giving charged droplets acceleration in the horizontal direction. The result is that the droplet falls in a straight line that makes an angle θ with the vertical. Show that

$$\sin \theta = q\mathcal{E}/bv'_t$$

where v'_t is the terminal speed along the angled path.

3-11. A charged oil droplet falls 5.0 mm in 20.0 s at terminal speed in the absence of an electric field. The specific gravity of air is 1.35×10^{-3} and that of oil is 0.75. The viscosity of air is 1.80×10^{-5} N · s/m². (a) What are the mass and radius of the drop? (b) If the droplet carries two units of electric charge and is in an electric field of 2.5×10^5 V/m, what is the ratio of the electric force to the gravitational force on the droplet?

Section 3-2 Blackbody Radiation

3-12. Find λ_m for blackbody radiation at (a) $T = 3$ K, (b) $T = 300$ K, and (c) $T = 3000$ K.

3-13. Use the result of Example 3-4 and Equations 3-4 and 3-6 to express Stefan's constant in terms of h , c , and k . Using the known values of these constants, calculate Stefan's constant.

3-14. Show that Planck's law, Equation 3-18, expressed in terms of the frequency f , is

$$u(f) = \frac{8\pi f^2}{c^3} \frac{hf}{e^{hf/kT} - 1}$$

3-15. As noted in the chapter, the cosmic microwave background radiation fits the Planck equation for a blackbody at 2.7 K. (a) What is the wavelength at the maximum intensity of the spectrum of the background radiation? (b) What is the frequency of the radiation at the maximum? (c) What is the total power incident on Earth from the background radiation?

3-16. Find the temperature of a blackbody if its spectrum has its peak at (a) $\lambda_m = 700$ nm (visible), (b) $\lambda_m = 3$ cm (microwave region), and (c) $\lambda_m = 3$ m (FM radio waves).

3-17. If the absolute temperature of a blackbody is doubled, by what factor is the total emitted power increased?

3-18. Calculate the average energy \bar{E} per mode of oscillation for (a) a long wavelength $\lambda = 10 hc/kT$, (b) a short wavelength $\lambda = 0.1 hc/kT$, and compare your results with the classical prediction kT (see Equation 3-9). (The classical value comes from the equipartition theorem discussed in Chapter 8.)

3-19. A particular radiating cavity has the maximum of its spectra distribution of radiated power at a wavelength of $27.0 \mu\text{m}$ (in the infrared region of the spectrum). The temperature is then changed so that the total power radiated by the cavity doubles. (a) Compute the new temperature. (b) At what wavelength does the new spectral distribution have its maximum value?

3-20. A certain very bright star has an effective surface temperature of 20,000 K. (a) Assuming that it radiates as a blackbody, what is the wavelength at which $u(\lambda)$ is maximum? (b) In what part of the electromagnetic spectrum does the maximum lie?

3-21. The energy reaching Earth from the Sun at the top of the atmosphere is $1.36 \times 10^3 \text{ W/m}^2$, called the *solar constant*. Assuming that Earth radiates like a blackbody at uniform temperature, what do you conclude is the equilibrium temperature of Earth?

3-22. A 40-W incandescent bulb radiates from a tungsten filament operating at 3300 K. Assuming that the bulb radiates like a blackbody, (a) what are the frequency f_m and the wavelength λ_m at the maximum of the spectral distribution? (b) If f_m is a good approximation of the average frequency of the photons emitted by the bulb, about how many photons is the bulb radiating per second? (c) If you are looking at the bulb from 5 m away, how many photons enter your eye per second? (The diameter of your pupil is about 5.0 mm.)

3-23. Use Planck's law, Equation 3-18, to derive the constant in Wein's law, Equation 3-5.

Section 3-3 The Photoelectric Effect

3-24. The wavelengths of visible light range from about 380 nm to about 750 nm. (a) What is the range of photon energies (in eV) in visible light? (b) A typical FM radio station's broadcast frequency is about 100 MHz. What is the energy of an FM photon of the frequency?

3-25. The orbiting space shuttle moves around Earth well above 99 percent of the atmosphere, yet it still accumulates an electric charge on its skin due, in part, to the loss of electrons caused by the photoelectric effect with sunlight. Suppose the skin of the shuttle is coated with Ni, which has a relatively large work function $\phi = 4.87 \text{ eV}$ at the temperatures encountered in orbit. (a) What is the maximum wavelength in the solar spectrum that can result in the emission of photoelectrons from the shuttle's skin? (b) What is the maximum fraction of the total power falling on the shuttle that could potentially produce photoelectrons?

3-26. The work function for cesium is 1.9 eV, the lowest of any metal. (a) Find the threshold frequency and wavelength for the photoelectric effect. Find the stopping potential if the wavelength of the incident light is (b) 300 nm and (c) 400 nm.

3-27. (a) If 5 percent of the power of a 100-W bulb is radiated in the visible spectrum, how many visible photons are radiated per second? (b) If the bulb is a point source radiating equally in all directions, what is the flux of photons (number per unit time per unit area) at a distance of 2 m?

3-28. The work function of molybdenum is 4.22 eV. (a) What is the threshold frequency for the photoelectric effect in molybdenum? (b) Will yellow light of wavelength 560 nm cause ejection of photoelectrons from molybdenum? Prove your answer.

3-29. The NaCl molecule has a bond energy of 4.26 eV; that is, this energy must be supplied in order to dissociate the molecule into neutral Na and Cl atoms (see Chapter 9). (a) What are the minimum frequency and maximum wavelength of the photon necessary to dissociate the molecule? (b) In what part of the electromagnetic spectrum is this photon?

3-30. A photoelectric experiment with cesium yields stopping potentials for $\lambda = 435.8 \text{ nm}$ and $\lambda = 546.1 \text{ nm}$ to be 0.95 V and 0.38 V, respectively. Using these data only, find the threshold frequency and work function for cesium and the value of h .

3-31. Under optimum conditions, the eye will perceive a flash if about 60 photons arrive at the cornea. How much energy is this in joules if the wavelength of the light is 550 nm?

3-32. The longest wavelength of light that will cause emission of electrons from cesium is 653 nm. (a) Compute the work function for cesium. (b) If light of 300 nm (ultraviolet) were to shine on cesium, what would be the energy of the ejected electrons?

Section 3-4 X Rays and the Compton Effect

3-33. Use Compton's equation (Equation 3-25) to compute the value of $\Delta\lambda$ in Figure 3-17d. To what percent shift in the wavelength does this correspond?

3-34. X-ray tubes currently used by dentists often have accelerating voltages of 80 kV. What is the minimum wavelength of the x rays they produce?

3-35. Find the momentum of a photon in eV/c and in $\text{kg} \cdot \text{m/s}$ if the wavelength is (a) 400 nm, (b) 1 Å = 0.1 nm, (c) 3 cm, and (d) 2 nm.

3-36. Gamma rays emitted by radioactive nuclei also exhibit measurable Compton scattering. Suppose a 0.511-MeV photon from a positron-electron annihilation scatters at 110° from a free electron. What are the energies of the scattered photon and the recoiling electron? Relative to the initial direction of the 0.511-MeV photon, what is the direction of the recoiling electron's velocity vector?

3-37. The wavelength of Compton-scattered photons is measured at $\theta = 90^\circ$. If $\Delta\lambda/\lambda$ is to be 1 percent, what should the wavelength of the incident photon be?

3-38. Compton used photons of wavelength 0.0711 nm. (a) What is the energy of these photons? (b) What is the wavelength of the photons scattered at $\theta = 180^\circ$? (c) What is the energy of the photons scattered at $\theta = 180^\circ$? (d) What is the recoil energy of the electrons if $\theta = 180^\circ$?

3-39. Compute $\Delta\lambda$ for photons scattered at 120° from (a) free protons, (b) free electrons, and (c) N_2 molecules in air.

3-40. Compton's equation (Equation 3-25) indicates that a graph of λ_2 versus $(1 - \cos\theta)$ should be a straight line whose slope h/mc allows a determination of h . Given that the wavelength of λ_1 in Figure 3-17 is 0.0711 nm, compute λ_2 for each scattering angle in the figure and graph the results versus $(1 - \cos\theta)$. What is the slope of the line?

3-41. (a) Compute the Compton wavelength of an electron and a proton. (b) What is the energy of a photon whose wavelength is equal to the Compton wavelength of (1) the electron and (2) the proton?

Level II

3-42. When light of wavelength 450 nm is incident on potassium, photoelectrons with stopping potential of 0.52 V are emitted. If the wavelength of the incident light is changed to 300 nm, the stopping potential is 1.90 V. Using *only* these numbers together with the values of the speed of light and the electron charge, (a) find the work function of potassium and (b) compute a value for Planck's constant.

3-43. Assuming that the difference between Thomson's calculated e/m in his second experiment (Figure 3-19) and the currently accepted value was due entirely to his neglecting the horizontal component of Earth's magnetic field outside the deflection plates, what value for that component does the difference imply? (Thomson's data: $B = 5.5 \times 10^{-4}$ T, $E = 1.5 \times 10^4$ V/m, $x_1 = 5$ cm, $y_2/x_2 = 8/110$.)

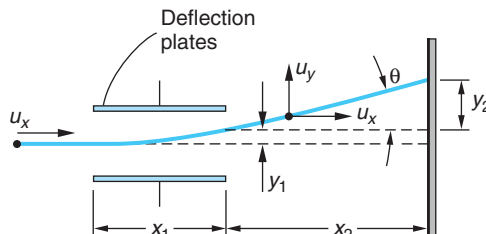


Figure 3-19 Deflection of the electron beam in Thomson's apparatus. The deflection plates are D and E in Figure 3-1. Deflection is shown with magnetic field off and the top plate positive. The magnetic field is applied perpendicular to the plane of the diagram and directed into the page.

3-44. In his first e/m experiment, Thomson determined the speed of electrons accelerated through a potential ΔV by collecting them in an insulated beam stopper and measuring both the total collected charge Q and the temperature rise ΔT of the beam stopper. (a) Show that with those measurements he could obtain an expression for e/m in terms of the speed of the electrons and the directly measured quantities. (b) Show that the expression obtained in (a) together with the result of Problem 3-2 enabled Thomson to compute e/m in terms of directly measured quantities.

3-45. Data for stopping potential versus wavelength for the photoelectric effect using sodium are

| λ , nm | 200 | 300 | 400 | 500 | 600 |
|----------------|------|------|------|------|------|
| V_0 , V | 4.20 | 2.06 | 1.05 | 0.41 | 0.03 |

Plot these data in such a way as to be able to obtain (a) the work function, (b) the threshold frequency, and (c) the ratio h/e .

3-46. Prove that the photoelectric effect cannot occur with a completely free electron, i.e., one not bound to an atom. (*Hint:* Consider the reference frame in which the total momentum of the electron and the incident photon is zero.)

3-47. When a beam of monochromatic x rays is incident on a particular NaCl crystal, Bragg reflection in the first order (i.e., with $m = 1$) occurs at $\theta = 20^\circ$. The value of $d = 0.28$ nm. What is the minimum voltage at which the x-ray tube can be operating?

3-48. A 100-W beam of light is shone onto a blackbody of mass 2×10^{-3} kg for 10^4 s. The blackbody is initially at rest in a frictionless space. (a) Compute the total energy and momentum absorbed by the blackbody from the light beam, (b) calculate the blackbody's velocity at the end of the period of illumination, and (c) compute the final kinetic energy of the blackbody. Why is the latter less than the total energy of the absorbed photons?

3-49. Show that the maximum kinetic energy E_k , called the Compton edge, that a recoiling electron can carry away from a Compton scattering event is given by

$$E_k = \frac{hf}{1 + mc^2/2hf} = \frac{2E_\gamma^2}{2E_\gamma + mc^2}$$

3-50. The x-ray spectrometer on board a satellite measures the wavelength at the maximum intensity emitted by a particular star to be $\lambda_m = 82.8$ nm. Assuming that the star radiates like a blackbody, (a) compute the star's surface temperature. (b) What is the ratio of the intensity radiated at $\lambda = 70$ nm and at $\lambda = 100$ nm to that radiated at λ_m ?

3-51. Determine the fraction of the energy radiated by the Sun in the visible region of the spectrum (350 nm to 700 nm). Assume that the Sun's surface temperature is 5800 K.

3-52. Millikan's data for the photoelectric effect in lithium are shown in the table:

| Incident λ (nm) | 253.5 | 312.5 | 365.0 | 404.7 | 433.9 |
|----------------------------|-------|-------|-------|-------|-------|
| Stopping voltage V_0 (V) | 2.57 | 1.67 | 1.09 | 0.73 | 0.55 |

(a) Graph the data and determine the work function for lithium. (b) Find the value of Planck's constant directly from the graph in (a). (c) The work function for lead is 4.14 eV. Which, if any, of the wavelengths in the table would not cause emission of photoelectrons from lead?

Level III

3-53. This problem is to derive the Wein displacement law, Equation 3-5. (a) Show that the energy density distribution function can be written $u = C\lambda^{-5}(e^{a/\lambda} - 1)^{-1}$, where C is a constant and $a = hc/kT$. (b) Show that the value of λ for which $du/d\lambda = 0$ satisfies the equation $5\lambda(1 - e^{-a/\lambda}) = a$. (c) This equation can be solved with a calculator by the trial-and-error method. Try $\lambda = \alpha a$ for various values of α until λ/a is determined to four significant figures. (d) Show that your solution in (c) implies $\lambda_m T = \text{constant}$ and calculate the value of the constant.

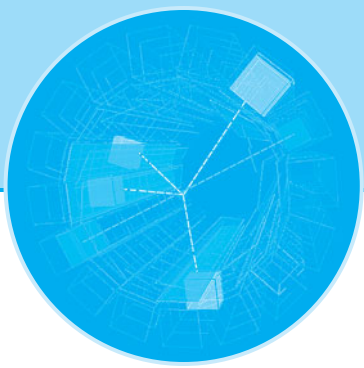
3-54. This problem is one of estimating the time lag (expected classically, but not observed) for the photoelectric effect. Assume that a point light source emits 1 W = 1 J/s of light energy. (a) Assuming uniform radiation in all directions, find the light intensity in eV/s \cdot m² at a distance of 1 m from the light source. (b) Assuming some reasonable size for an atom, find the energy per unit time incident on the atom for this intensity. (c) If the work function is 2 eV, how long does it take for this much energy to be absorbed, assuming that all of the energy hitting the atom is absorbed?

3-55. A photon can be absorbed by a system that can have internal energy. Assume that a 15-MeV photon is absorbed by a carbon nucleus initially at rest. The recoil momentum of the carbon nucleus must be $15 \text{ MeV}/c$. (a) Calculate the kinetic energy of the carbon nucleus. What is the internal energy of the nucleus? (b) The carbon nucleus comes to rest and then loses its internal energy by emitting a photon. What is the energy of the photon?

3-56. The maximum kinetic energy given to the electron in a Compton scattering event plays a role in the measurement of gamma-ray spectra using scintillation detectors. The maximum is referred to as the *Compton edge*. Suppose that the Compton edge in a particular experiment is found to be 520 keV. What were the wavelength and energy of the incident gamma rays?

3-57. An electron accelerated to 50 keV in an x-ray tube has two successive collisions in being brought to rest in the target, emitting two bremsstrahlung photons in the process. The second photon emitted has a wavelength 0.095 nm longer than the first. (a) What are the wavelengths of the two photons? (b) What was the energy of the electron after emission of the first photon?

3-58. Derive Equation 3-17 from Equations 3-15 and 3-16.

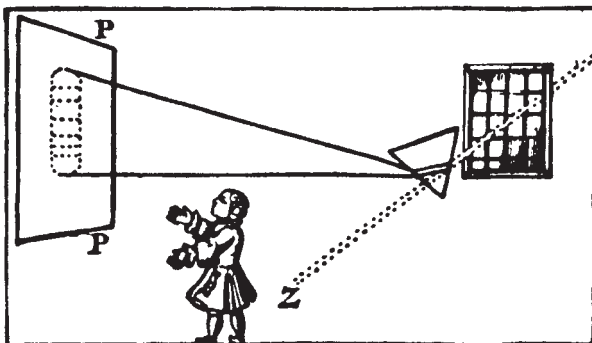


The Nuclear Atom

Among his many experiments, Newton found that sunlight passing through a small opening in a window shutter could be refracted by a glass prism so that it would fall on a screen. The white sunlight thus refracted was spread into a rainbow-colored band—a spectrum. He had discovered *dispersion*, and his experimental arrangement was the prototype of the modern *spectroscope* (Figure 4-1a). When, 150 years later, Fraunhofer¹ dispersed sunlight using an experimental setup similar to that shown in Figure 4-1b to test prisms made of glasses that he had developed, he found that the solar spectrum was crossed by more than 600 narrow, or sharp, dark lines.² Soon after, a number of scientists observed sharp *bright* lines in the spectra of light emitted by flames, arcs, and sparks. *Spectroscopy* quickly became an important area of research.

It soon became clear that chemical elements and compounds emit three general types of spectra. *Continuous* spectra, emitted mainly by incandescent solids, show no lines at all, bright or dark, in spectrosopes of the highest possible resolving power. *Band* spectra consist of very closely packed groups of lines that appear to be continuous in instruments of low resolving power. These are emitted when small pieces of solid materials are placed in the source flame or electrodes. The *line* spectra mentioned above arise when the source contains unbound chemical elements. The lines and bands turned out to be characteristic of individual elements and chemical compounds when excited under specific conditions. Indeed, the spectra could be (and are today) used as a highly sensitive test for the presence of elements and compounds.

| | |
|--|------------|
| 4-1 Atomic Spectra | 148 |
| 4-2 Rutherford's Nuclear Model | 150 |
| 4-3 The Bohr Model of the Hydrogen Atom | 159 |
| 4-4 X-Ray Spectra | 169 |
| 4-5 The Franck-Hertz Experiment | 174 |



Voltaire's depiction of Newton's discovery of dispersion. [*Elémens de la Philosophie de Newton*, Amsterdam, 1738.]

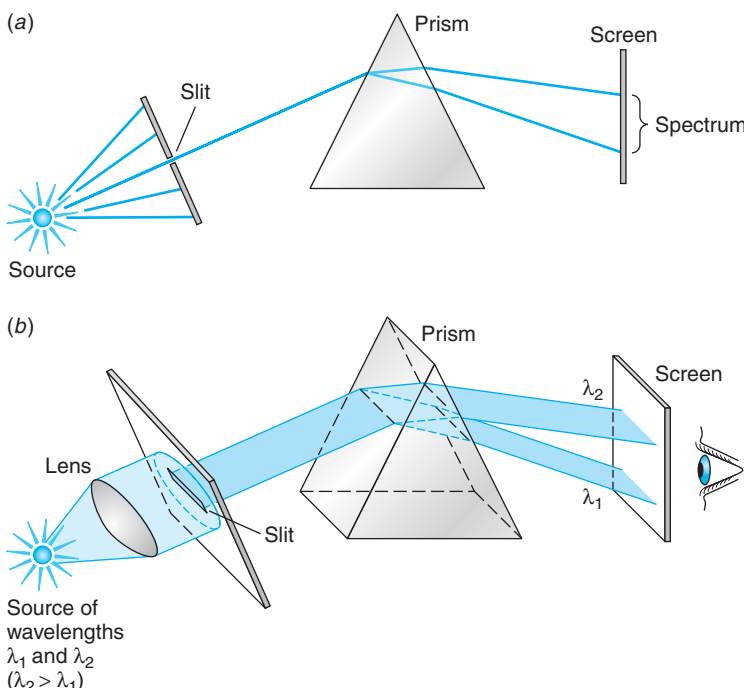


Figure 4-1 (a) Light from the source passes through a small hole or a narrow slit before falling on the prism. The purpose of the slit is to ensure that all the incident light strikes the prism face at the same angle so that the dispersion by the prism causes the various frequencies that may be present to strike the screen at different places with minimum overlap. (b) The source emits only two wavelengths, $\lambda_2 > \lambda_1$. The source is located at the focal point of the lens so that parallel light passes through the narrow slit, projecting a narrow line onto the face of the prism. Ordinary dispersion in the prism bends the shorter wavelength through the larger total angle, separating the two wavelengths at the screen. In this arrangement each wavelength appears on the screen (or on film replacing the screen) as a narrow line, which is an image of the slit. Such a spectrum was dubbed a “line spectrum” for that reason. Prisms have been almost entirely replaced in modern spectrosopes by diffraction gratings, which have much higher resolving power.

Line spectra raised an enormous theoretical problem: although classical physics could account for the existence of a continuous spectrum (if not its detailed shape, as we saw with blackbodies), it could in no way explain *why* sharp lines and bands should exist. Explaining the origin of the sharp lines and accounting for the primary features of the spectrum of hydrogen, the simplest element, was a major success of the so-called old quantum theory begun by Planck and Einstein and will be the main topic in this chapter. Full explanation of the lines and bands requires the later, more sophisticated quantum theory, which we will begin studying in Chapter 5.

4-1 Atomic Spectra

The characteristic radiation emitted by atoms of individual elements in a flame or in a gas excited by an electrical discharge was the subject of vigorous study during the late nineteenth and early twentieth centuries. When viewed or photographed through a spectroscope, this radiation appears as a set of discrete lines, each of a particular

color or wavelength; the positions and intensities of the lines are characteristic of the element. The wavelengths of these lines could be determined with great precision, and much effort went into finding and interpreting regularities in the spectra. A major breakthrough was made in 1885 by a Swiss schoolteacher, Johann Balmer, who found that the lines in the visible and near ultraviolet spectrum of hydrogen could be represented by the empirical formula

$$\lambda_n = 364.6 \frac{n^2}{n^2 - 4} \text{ nm}$$

4-1

The uniqueness of the line spectra of the elements has enabled astronomers to determine the composition of stars, chemists to identify unknown compounds, and theme parks and entertainers to have laser shows.

where n is a variable integer that takes on the values $n = 3, 4, 5, \dots$. Figure 4-2a shows the set of spectral lines of hydrogen (now known as the *Balmer series*) whose wavelengths are given by Balmer's formula. For example, the wavelength of the H_α line could be found by letting $n = 3$ in Equation 4-1 (try it!), and other integers each predicted a line that was found in the spectrum. Balmer suggested that his formula might be a special case of a more-general expression applicable to the spectra of other elements when ionized to a single electron, i.e., hydrogen-like elements.

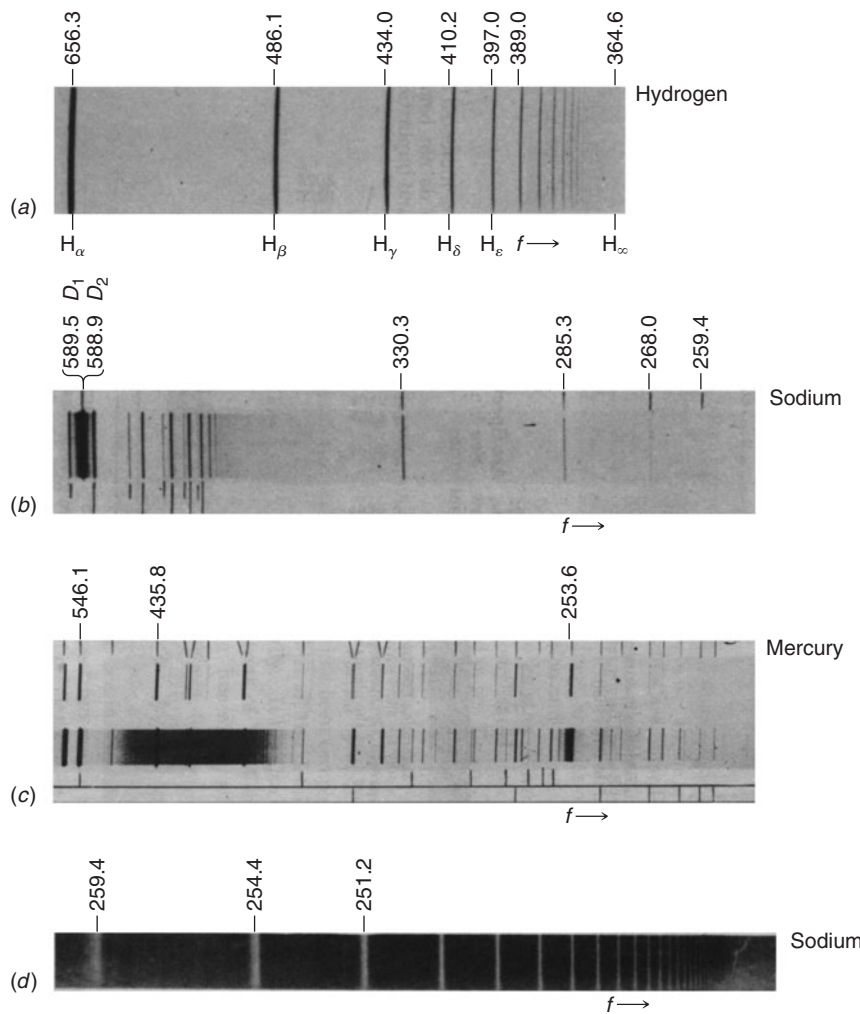


Figure 4-2 (a) Emission line spectrum of hydrogen in the visible and near ultraviolet. The lines appear dark because the spectrum was photographed; hence, the bright lines are exposed (dark) areas on the film. The names of the first five lines are shown, as is the point beyond which no lines appear, H_∞ , called the *limit* of the series. (b) Part of the emission spectrum of sodium. The two very close bright lines at 589 nm are the D_1 and D_2 lines. They are the principal radiation from sodium street lighting. (c) Part of the emission spectrum of mercury. (d) Part of the dark line (absorption) spectrum of sodium. White light shining through sodium vapor is absorbed at certain wavelengths, resulting in no exposure of the film at those points. Note that the line at 259.4 nm is visible here in both the bright and dark line spectra. Note, too, that frequency increases toward the right, wavelength toward the left in the four spectra shown.

Such an expression, found independently by J. R. Rydberg and W. Ritz and thus called the *Rydberg-Ritz formula*, gives the reciprocal wavelength³ as

$$\frac{1}{\lambda_{mn}} = R \left(\frac{1}{m^2} - \frac{1}{n^2} \right) \quad \text{for } n > m \quad 4-2$$

where m and n are integers and R , the *Rydberg constant*, is the same for all series of spectral lines of the same element and varies only slightly, and in a regular way, from element to element. For hydrogen, the value of R is $R_H = 1.096776 \times 10^7 \text{ m}^{-1}$. For very heavy elements, R approaches the value of $R_\infty = 1.097373 \times 10^7 \text{ m}^{-1}$. Such empirical expressions were successful in predicting other series of spectral lines, such as other hydrogen lines outside the visible region.

EXAMPLE 4-1 Hydrogen Spectral Series The hydrogen Balmer series reciprocal wavelengths are those given by Equation 4-2, with $m = 2$ and $n = 3, 4, 5, \dots$. For example, the first line of the series, H_α, would be for $m = 2, n = 3$:

$$\frac{1}{\lambda_{23}} = R \left(\frac{1}{2^2} - \frac{1}{3^2} \right) = \frac{5}{36} R = 1.523 \times 10^6 \text{ m}^{-1}$$

or

$$\lambda_{23} = 656.5 \text{ nm}$$

Other series of hydrogen spectral lines were found for $m = 1$ (by Theodore Lyman) and $m = 3$ (by Friedrich Paschen). Compute the wavelengths of the first lines of the Lyman and Paschen series.

SOLUTION

For the Lyman series ($m = 1$), the first line is for $m = 1, n = 2$:

$$\frac{1}{\lambda_{12}} = R \left(\frac{1}{1^2} - \frac{1}{2^2} \right) = \frac{3}{4} R = 8.22 \times 10^6 \text{ m}^{-1}$$

$$\lambda_{12} = 121.6 \text{ nm} \quad (\text{in the ultraviolet})$$

For the Paschen series ($m = 3$), the first line is for $m = 3, n = 4$:

$$\frac{1}{\lambda_{34}} = R \left(\frac{1}{3^2} - \frac{1}{4^2} \right) = \frac{7}{144} R = 5.332 \times 10^5 \text{ m}^{-1}$$

$$\lambda_{34} = 1876 \text{ nm} \quad (\text{in the infrared})$$

All of the lines predicted by the Rydberg-Ritz formula for the Lyman and Paschen series are found experimentally. Note that no lines are predicted to lie beyond $\lambda_\infty = 1/R = 91.2 \text{ nm}$ for the Lyman series and $\lambda_\infty = 9/R = 820.6 \text{ nm}$ for the Paschen series and none are found by experiments.

4-2 Rutherford's Nuclear Model

Many attempts were made to construct a model of the atom that yielded the Balmer and Rydberg-Ritz formulas. It was known that an atom was about 10^{-10} m in diameter (see Problem 4-6), that it contained electrons much lighter than the atom (see Section 3-1), and that it was electrically neutral. The most popular model was J. J. Thomson's model, already quite successful in explaining chemical reactions. Thomson

FÉUE WHI

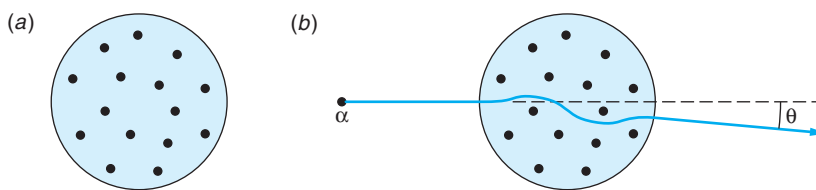


Figure 4-3 Thomson's model of the atom: (a) A sphere of positive charge with electrons embedded in it so that the net charge would normally be zero. The atom shown would have been phosphorus. (b) An α particle scattered by such an atom would have a scattering angle θ much smaller than 1° .

attempted various models consisting of electrons embedded in a fluid that contained most of the mass of the atom and had enough positive charge to make the atom electrically neutral. (See Figure 4-3a.) He then searched for configurations that were stable and had normal modes of vibration corresponding to the known frequencies of the spectral lines. One difficulty with all such models was that electrostatic forces alone cannot produce stable equilibrium. Thus, the charges were required to move and, if they stayed within the atom, to accelerate; however, the acceleration would result in continuous emission of radiation, which is not observed. Despite elaborate mathematical calculations, Thomson was unable to obtain from his model a set of frequencies of vibration that corresponded with the frequencies of observed spectra.

The Thomson model of the atom was replaced by one based on the results of a set of experiments conducted by Ernest Rutherford⁴ and his students H. W. Geiger and E. Marsden. Rutherford was investigating radioactivity and had shown that the radiations from uranium consisted of at least two types, which he labeled α and β . He showed, by an experiment similar to that of Thomson, that q/m for the α was half that of the proton. Suspecting that the α particles were doubly ionized helium, Rutherford and his co-workers in a classic experiment let a radioactive substance α decay in a previously evacuated chamber; then, by spectroscopy, they detected the spectral lines of ordinary helium gas in the chamber. Realizing that this energetic, massive α particle would make an excellent probe for “feeling about” within the interiors of other atoms, Rutherford began a series of experiments with this purpose.



Hans Geiger and Ernest Rutherford in their Manchester Laboratory. [Courtesy of University of Manchester.]

In these latter experiments, a narrow beam of α particles fell on a zinc sulfide screen, which emitted visible light scintillations when struck (Figure 4-4). The distribution of scintillations on the screen was observed when various thin metal foils were placed between it and the source. Most of the α particles were either undeflected or

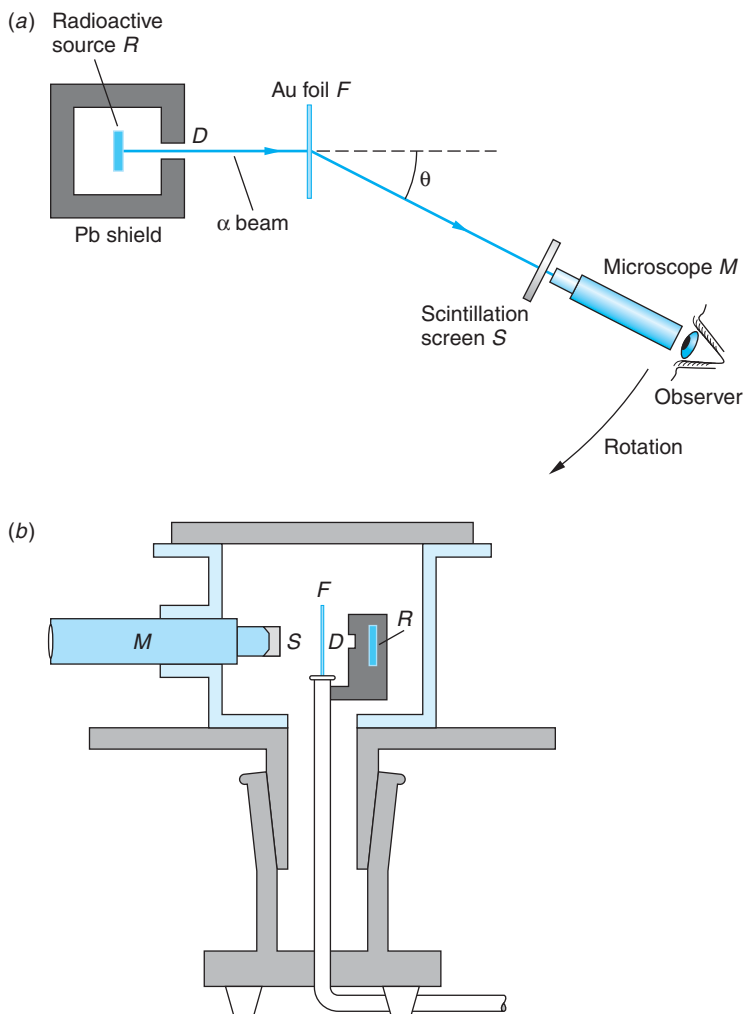


Figure 4-4 Schematic diagram of the apparatus used by Geiger and Marsden to test Rutherford's atomic model. (a) The beam of α particles is defined by the small hole D in the shield surrounding the radioactive source R of ^{214}Bi (called RaC in Rutherford's day). The α beam strikes an ultrathin gold foil F (about 2000 atoms thick), and the α particles are individually scattered through various angles. Those scattering at the angle θ shown strike a small screen S coated with a scintillator, i.e., a material that emits tiny flashes of light (scintillations) when struck by an α particle. The scintillations were viewed by the observer through a small microscope M . The scintillation screen-microscope combination could be rotated about the center of the foil. The region traversed by the α beam is evacuated. The experiment consisted of counting the number of scintillations as a function of θ . (b) A diagram of the actual apparatus as it appeared in Geiger and Marsden's paper describing the results. The letter key is the same as in (a). [Part (b) from H. Geiger and E. Marsden, *Philosophical Review*, 25, 507 (1913).]

deflected through very small angles of the order of 1° . Quite unexpectedly, however, a few α particles were deflected through angles as large as 90° or more. If the atom consisted of a positively charged sphere of radius 10^{-10} m, containing electrons as in the Thomson model, only a very small deflection could result from a single encounter between an α particle and an atom, even if the α particle penetrated into the atom. Indeed, calculations showed that the Thomson atomic model could not possibly account for the number of large-angle scatterings that Rutherford saw. The unexpected scatterings at large angles were described by Rutherford with these words:

It was quite the most incredible event that ever happened to me in my life. It was as incredible as if you fired a 15-inch shell at a piece of tissue paper and it came back and hit you.

Rutherford's Scattering Theory and the Nuclear Atom

The question is, then, Why would one obtain the large-angle scattering that Rutherford saw? The trouble with the Thomson atom is that it is too “soft”—the maximum force experienced by the α is too weak to give a large deflection. If the positive charge of the atom is concentrated in a more compact region, however, a much larger force will occur at near impacts. Rutherford concluded that the large-angle scattering obtained experimentally could result only from a single encounter of the α particle with a massive charge confined to a volume much smaller than that of the whole atom. Assuming this “nucleus” to be a point charge, he calculated the expected angular distribution for the scattered α particles. His predictions of the dependence of scattering probability on angle, nuclear charge, and kinetic energy were completely verified in a series of experiments carried out in his laboratory by Geiger and Marsden.

We will not go through Rutherford's derivation in detail, but merely outline the assumptions and conclusions. Figure 4-5 shows the geometry of an α particle being scattered by a nucleus, which we take to be a point charge Q at the origin. Initially, the α particle approaches with speed v along a line a distance b from a parallel line COA through the origin. The force on the α particle is $F = kq_\alpha Q/r^2$, given by

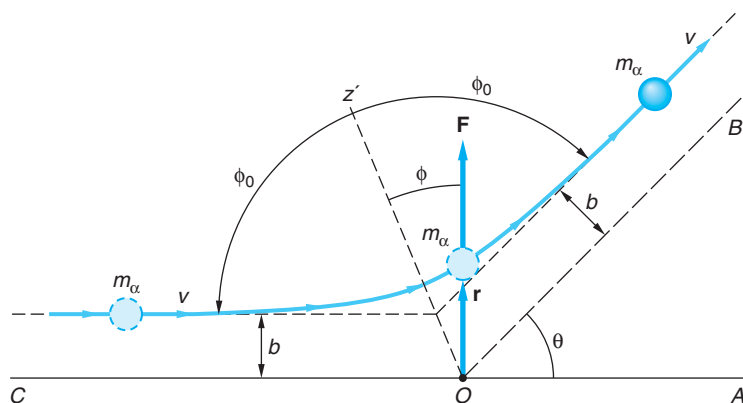


Figure 4-5 Rutherford scattering geometry. The nucleus is assumed to be a point charge Q at the origin O . At any distance r the α particle experiences a repulsive force $kq_\alpha Q/r^2$. The α particle travels along a hyperbolic path that is initially parallel to line COA a distance b from it and finally parallel to line OB , which makes an angle θ with OA . The scattering angle θ can be related to the impact parameter b by classical mechanics.

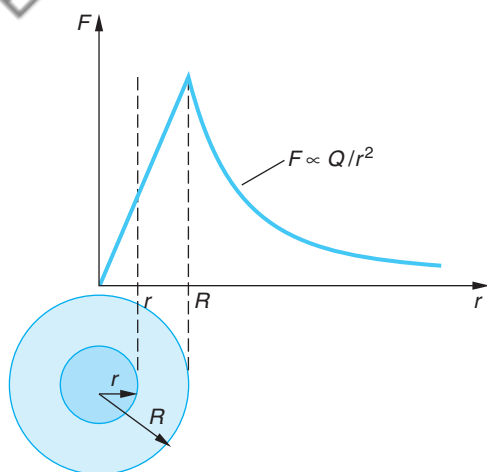


Figure 4-6 Force on a point charge versus distance r from the center of a uniformly charged sphere of radius R . Outside the sphere the force is proportional to Q/r^2 , where Q is the total charge. Inside the sphere, the force is proportional to $q'/r^2 = QrR/R^3$, where $q' = Q(r/R)^3$ is the charge within a sphere of radius r . The maximum force occurs at $r = R$.

The particle-scattering technique devised by Rutherford to “look” at atoms now has wide application throughout physics. Scattering of high-energy electrons from protons and neutrons provided our first experimental hint of the existence of quarks. Rutherford back-scattering spectroscopy is widely used as a highly sensitive surface analysis technique.

Coulomb’s law (Figure 4-6). After scattering, when the α particle is again far from the nucleus, it is moving with the same speed v parallel to the line OB , which makes an angle θ with line COA . (Since the potential energy is again zero, the final speed must be equal to the initial speed by conservation of energy, assuming, as Rutherford did, that the massive nucleus remains fixed during the scattering.) The distance b is called the *impact parameter* and the angle θ , the *scattering angle*. The path of the α particle can be shown to be a hyperbola, and the scattering angle θ can be related to the impact parameter b from the laws of classical mechanics. The result is

$$b = \frac{kq_\alpha Q}{m_\alpha v^2} \cot \frac{\theta}{2} \quad 4-3$$

Of course, it is not possible to choose or know the impact parameter for any particular α particle, but when one recalls the values of the cotangent between 0° and 90° , all such particles with impact parameters less than or equal to a particular b will be scattered through an angle θ greater than or equal to that given by Equation 4-3; i.e., the smaller the impact parameter, the larger the scattering angle (Figure 4-7). Let the intensity of the incident α particle beam be I_0 particles per second per unit area. The number per second scattered by one nucleus through angles greater than θ equals the number per second that have impact parameters less than $b(\theta)$. This number is $\pi b^2 I_0$.

The quantity πb^2 , which has the dimensions of an area, is called the *cross section* σ for scattering through angles greater than θ . The cross section σ is thus defined as the number scattered per nucleus per unit time divided by the incident intensity.

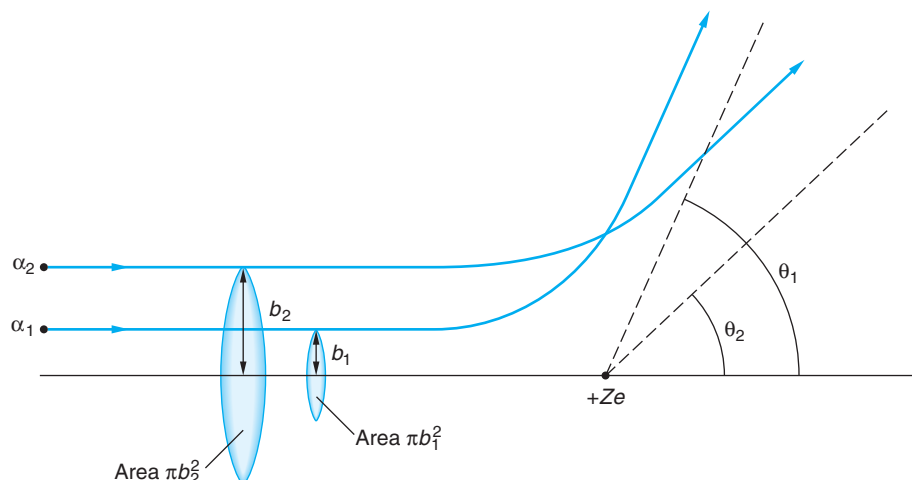


Figure 4-7 Two α particles with equal kinetic energies approach the positive charge $Q = +Ze$ with impact parameters b_1 and b_2 , where $b_1 < b_2$. According to Equation 4-3, the angle θ_1 through which α_1 is scattered will be larger than θ_2 . In general, all α particles with impact parameters smaller than a particular value of b will have scattering angles larger than the corresponding value of θ from Equation 4-3. The area πb^2 is called the cross section for scattering with angles greater than θ .

The total number of particles scattered per second is obtained by multiplying $\pi b^2 I_0$ by the number of nuclei in the scattering foil (this assumes the foil to be thin enough to make the chance of overlap negligible). Let n be the number of nuclei per unit volume:

$$n = \frac{\rho(\text{g/cm}^3)N_A(\text{atoms/mol})}{M(\text{g/mol})} = \frac{\rho N_A}{M} \frac{\text{atoms}}{\text{cm}^3} \quad 4-4$$

For a foil of thickness t , the total number of nuclei “seen” by the beam is nAt , where A is the area of the beam (Figure 4-8). The total number scattered per second through angles greater than θ is thus $\pi b^2 I_0 n t A$. If we divide this by the number of α particles incident per second $I_0 A$, we get the fraction f scattered through angles greater than θ :

$$f = \pi b^2 n t \quad 4-5$$

EXAMPLE 4-2 Scattered Fraction f Calculate the fraction of an incident beam of α particles of kinetic energy 5 MeV that Geiger and Marsden expected to see for $\theta \geq 90^\circ$ from a gold foil ($Z = 79$) 10^{-6} m thick.

SOLUTION

1. The fraction f is related to the impact parameter b , the number density of nuclei n , and the thickness t by Equation 4-5:
 2. The particle density n is given by Equation 4-4:
 3. The impact parameter b is related to θ by Equation 4-3:
 4. Substituting these into Equation 4-5 yields f :
- $$\begin{aligned} f &= \pi b^2 n t \\ n &= \frac{\rho N_A}{M} = \frac{(19.3 \text{ g/cm}^3)(6.02 \times 10^{23} \text{ atoms/mol})}{197 \text{ gm/mol}} \\ &= 5.90 \times 10^{22} \text{ atoms/cm}^3 = 5.90 \times 10^{28} \text{ atoms/m}^3 \\ b &= \frac{k q_\alpha Q}{m_\alpha v^2} \cot \frac{\theta}{2} = \frac{(2)(79)ke^2}{2K_\alpha} \cot \frac{90^\circ}{2} \\ &= \frac{(2)(79)(1.44 \text{ eV} \cdot \text{nm})}{(2)(5 \times 10^6 \text{ eV})} = 2.28 \times 10^{-5} \text{ nm} \\ &= 2.28 \times 10^{-14} \text{ m} \\ f &= \pi(2.28 \times 10^{-14} \text{ m})^2 \left(5.9 \times 10^{28} \frac{\text{atoms}}{\text{m}^3} \right) (10^{-6} \text{ m}) \\ &= 9.6 \times 10^{-5} \approx 10^{-4} \end{aligned}$$

Remarks: This outcome is in good agreement with Geiger and Marsden's measurement of about 1 in 8000 in their first trial. Thus, the nuclear model is in good agreement with their results.

On the strength of the good agreement between the nuclear atomic model and the measured fraction of the incident α particles scattered at angles $\theta \geq 90^\circ$, Rutherford derived an expression, based on the nuclear model, for the number of α particles ΔN that would be scattered at any angle θ . That number, which also depends on the atomic

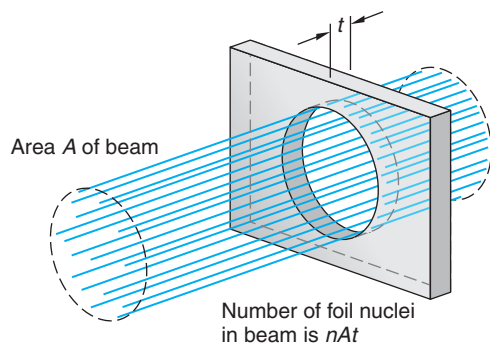


Figure 4-8 The total number of nuclei of foil atoms in the area covered by the beam is nAt , where n is the number of foil atoms per unit volume, A is the area of the beam, and t is the thickness of the foil.

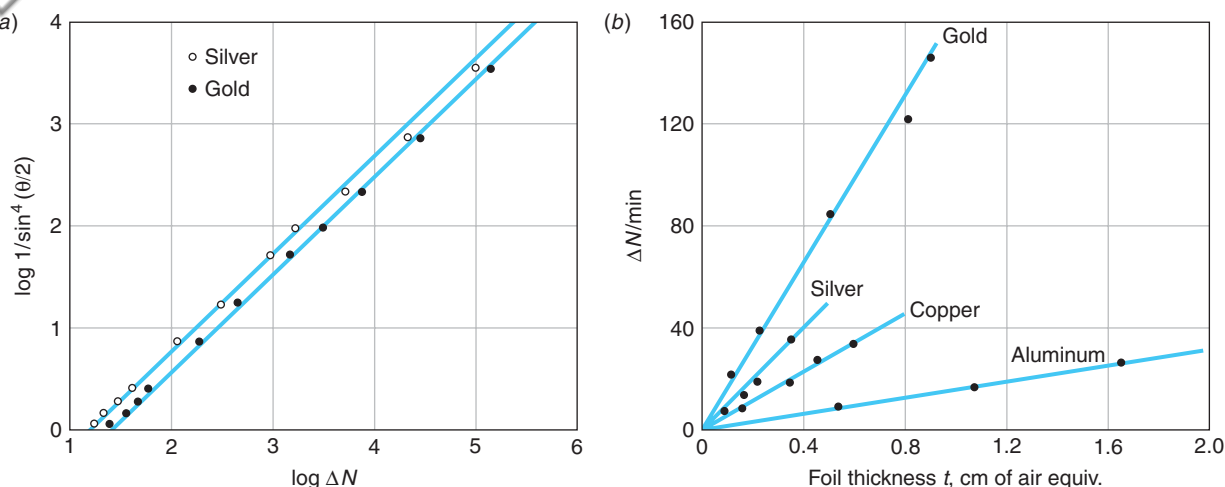


Figure 4-9 (a) Geiger and Marsden's data for α scattering from thin gold and silver foils. The graph is a log-log plot to show the data over several orders of magnitude. Note that scattering angle increases downward along the vertical axis. (b) Geiger and Marsden also measured the dependence of ΔN on t predicted by Equation 4-6 for foils made from a wide range of elements, this being an equally critical test. Results for four of the elements used are shown.

number Z and thickness t of the scattering foil, on the intensity I_0 of the incident α particles and their kinetic energy E_k , and on the geometry of the detector (A_{sc} is the detector area and r is the foil-detector distance), is given by

$$\Delta N = \left(\frac{I_0 A_{sc} n t}{r^2} \right) \left(\frac{k Z e^2}{2 E_k} \right)^2 \frac{1}{\sin^4 \frac{\theta}{2}} \quad 4-6$$

Within the uncertainties of their experiments, which involved visually observing several hundred thousand α particles, Geiger and Marsden verified every one of the predictions of Rutherford's formula over four orders of magnitude of ΔN . The excellent agreement of their data with Equation 4-6 firmly established the nuclear atomic model as the correct basis for further studies of atomic and nuclear phenomena. (See Figure 4-9.)



More

Rutherford's derivation of Equation 4-6 was based on his atomic model and the well-known Coulomb scattering process of charged particles. *Rutherford's Prediction and Geiger and Marsden's Results* are described on the home page: www.whfreeman.com/tiplermodernphysics5e. See also Equations 4-7 through 4-10 here, as well as Figures 4-10 through 4-12.

The Size of the Nucleus

The fact that the force law is shown to be correct, confirming Rutherford's model, does not imply that the nucleus is a mathematical point charge, however. The force law would be the same even if the nucleus were a ball of charge of some radius R_0 as long as the α particle did not penetrate the ball. (See Figures 4-6 and 4-13.) For a given scattering angle, the distance of closest approach of the α particle to the nucleus can be calculated from the geometry of the collision. For the largest angle, near 180° , the collision is nearly "head-on." The corresponding distance of closest approach r_d is thus an experimental

upper limit on the size of the target nucleus. We can calculate the distance of closest approach for a head-on collision r_d by noting that conservation of energy requires the potential energy at this distance to equal the original kinetic energy:

$$(V + E_k)_{\text{large } r} = (V + E_k)_{r_d}$$

$$\left(0 + \frac{1}{2}m_\alpha v^2\right)_{\text{large } r} = \left(\frac{kq_\alpha Q}{r_d} + 0\right)_{r_d}$$

$$\frac{1}{2}m_\alpha v^2 = \frac{kq_\alpha Q}{r_d}$$

or

$$r_d = \frac{kq_\alpha Q}{\frac{1}{2}m_\alpha v^2} \quad 4-11$$

For the case of 7.7-MeV α particles, the distance of closest approach for a head-on collision is

$$r_d = \frac{(2)(79)(1.44 \text{ eV} \cdot \text{nm})}{7.7 \times 10^6 \text{ eV}} = 3 \times 10^{-5} \text{ nm} = 3 \times 10^{-14} \text{ m}$$

For other collisions, the distance of closest approach is somewhat greater, but for α particles scattered at large angles it is of the same order of magnitude. The excellent agreement of Geiger and Marsden's data at large angles with the prediction of Equation 4-6 thus indicates that the radius of the gold nucleus is no larger than about 3×10^{-14} m. If higher-energy particles could be used, the distance of closest approach would be smaller, and as the energy of the α particles increased, we might expect that eventually the particles would penetrate the nucleus. Since, in that event, the force law is no longer $F = kq_\alpha Q/r^2$, the data would not agree with the point-nucleus calculation. Rutherford did not have higher-energy α particles available, but he could reduce the distance of closest approach by using targets of lower atomic numbers.⁹ For the case of aluminum, with $Z = 13$, when the most energetic α particles that he had available (7.7 MeV from ^{214}Bi) scattered at large angles, they did not follow the predictions of Equation 4-6. However, when the kinetic energy of the particles was reduced by passing the beam through thin mica sheets of various thicknesses, the data again followed the prediction of Equation 4-6. Rutherford's data are shown in Figure 4-14. The value of r_d (calculated from Equation 4-11) at which the data begin to deviate from the prediction can be thought of as the surface of the nucleus. From these data, Rutherford estimated the radius of the aluminum nucleus to be about 1.0×10^{-14} m. (The radius of the Al nucleus is actually about 3.6×10^{-15} m. See Chapter 11.)

A unit of length convenient for describing nuclear sizes is the fermi, or femtometer (fm), defined as $1 \text{ fm} = 10^{-15} \text{ m}$. As we will see in Chapter 11, the nuclear radius varies from about 1 to 10 fm from the lightest to the heaviest atoms.

EXAMPLE 4-3 Rutherford Scattering at Angle θ In a particular experiment, α particles from ^{226}Ra are scattered at $\theta = 45^\circ$ from a silver foil and 450 particles are counted each minute at the scintillation detector. If everything is kept the same except that the detector is moved to observe particles scattered at 90° , how many will be counted per minute?

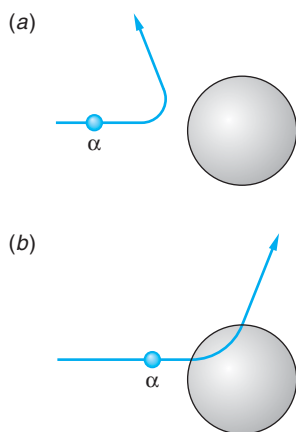


Figure 4-13 (a) If the α particle does not penetrate the nuclear charge, the nucleus can be considered a point charge located at the center. (b) If the particle has enough energy to penetrate the nucleus, the Rutherford scattering law does not hold but would require modification to account for that portion of the nuclear charge “behind” the penetrating α particle.

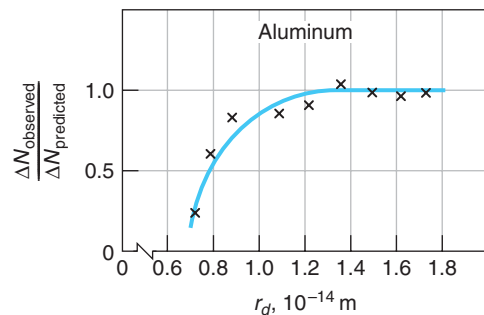


Figure 4-14 Data from Rutherford's group showing observed α scattering at a large fixed angle versus values of r_d computed from Equation 4-11 for various kinetic energies.

SOLUTION

Using Equation 4-6, we have that $\Delta N = 450$ when $\theta = 45^\circ$, but we don't have any of the other parameters available. Letting all of the quantities in the parenthesis equal a constant C , we have that

$$\Delta N = 450 = C \sin^{-4} \frac{45^\circ}{2}$$

or

$$C = 450 \sin^4 \left(\frac{45^\circ}{2} \right)$$

When the detector is moved to $\theta = 90^\circ$, the value of C is unchanged, so

$$\begin{aligned}\Delta N &= C \sin^{-4} \left(\frac{90^\circ}{2} \right) = 450 \sin^4 \left(\frac{45^\circ}{2} \right) \sin^{-4} \left(\frac{90^\circ}{2} \right) \\ &= 38.6 \approx 39 \text{ particles/min}\end{aligned}$$

EXAMPLE 4-4 Alpha Scattering A beam of α particles with $E_k = 6.0 \text{ MeV}$ impinges on a silver foil $1.0 \mu\text{m}$ thick. The beam current is 1.0 nA . How many α particles will be counted by a small scintillation detector of area equal to 5 mm^2 located 2.0 cm from the foil at an angle of 75° ? (For silver $Z = 47$, $\rho = 10.5 \text{ gm/cm}^3$, and $M = 108$.)

SOLUTION

1. The number counted ΔN is given by Equation 4-6:
$$\Delta N = \left(\frac{I_0 A_{sc} n t}{r^2} \right) \left(\frac{k Z e^2}{2 E_k} \right)^2 \frac{1}{\sin^4 \frac{\theta}{2}}$$
2. Since each α particle has $q_\alpha = 2e$, I_0 is:
$$I_0 = (1.0 \times 10^{-9} \text{ A})(2 \times 1.60 \times 10^{-19} \text{ C}/\alpha)^{-1} = 3.12 \times 10^9 \text{ } \alpha/\text{s}$$
3. The kinetic energy of each α is
$$E_k = (6.0 \text{ MeV})(1.60 \times 10^{-13} \text{ J/MeV}) = 9.60 \times 10^{-13} \text{ J}$$
4. For silver, n is given by
$$\begin{aligned}n &= \rho N_A / M \\ &= \frac{(10.5 \text{ g/cm}^3)(6.02 \times 10^{23} \text{ atoms/mol})}{108 \text{ g/mol}} \\ &= 5.85 \times 10^{22} \text{ atoms/cm}^3 = 5.85 \times 10^{28} \text{ atoms/m}^3\end{aligned}$$
5. Substituting the given values and computed results into Equation 4-6 gives ΔN :
$$\begin{aligned}\Delta N &= \frac{(3.12 \times 10^9 \text{ } \alpha/\text{s})(5 \times 10^{-6} \text{ m}^2)(5.85 \times 10^{28} \text{ atoms/m}^3)(10^{-6} \text{ m})}{(2 \times 10^{-2})^2 \sin^4 (75^\circ/2)} \\ &\quad \times \left[\frac{(9 \times 10^9)(47)(1.60 \times 10^{-19})^2}{(2)(9.60 \times 10^{-13})} \right]^2 \\ &= 528 \text{ } \alpha/\text{s}\end{aligned}$$

EXAMPLE 4-5 Radius of the Au Nucleus The radius of the gold (Au) nucleus has been measured by high-energy electron scattering as 6.6 fm . What kinetic energy α particles would Rutherford have needed so that for 180° scattering, the α particle would just reach the nuclear surface before reversing direction?

SOLUTION

From Equation 4-11, we have

$$\frac{1}{2}mv^2 = \frac{kq_\alpha Q}{r_d} = \frac{(9 \times 10^9)(2)(79)(1.60 \times 10^{-19})^2}{6.6 \times 10^{-15}} \\ = 5.52 \times 10^{-12} \text{ J} = 34.5 \text{ MeV}$$

Alpha particles of such energy are not emitted by naturally radioactive materials and so were not accessible to Rutherford. Thus, he could not have performed an experiment for Au equivalent to that for Al illustrated by Figure 4-14.

Questions

1. Why can't the impact parameter for a particular α particle be chosen?
2. Why is it necessary to use a very thin target foil?
3. Why could Rutherford place a lower limit on the radius of the Al nucleus but not on the Au nucleus?
4. How could you use the data in Figure 4-9a to determine the charge on a silver nucleus relative to that on a gold nucleus?
5. How would you expect the data (not the curve) to change in Figure 4-9 if the foil were so thick that an appreciable number of gold nuclei were hidden from the beam by being in the "shadow" of the other gold nuclei?

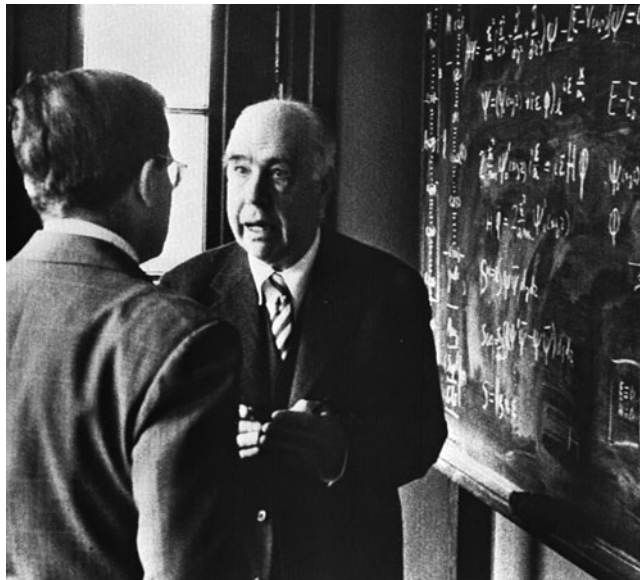
4-3 The Bohr Model of the Hydrogen Atom

In 1913, the Danish physicist Niels H. D. Bohr¹⁰ proposed a model of the hydrogen atom that combined the work of Planck, Einstein, and Rutherford and was remarkably successful in predicting the observed spectrum of hydrogen. The Rutherford model assigned charge and mass to the nucleus but was silent regarding the distribution of the charge and mass of the electrons. Bohr, who had been working in Rutherford's laboratory during the experiments of Geiger and Marsden, made the assumption that the electron in the hydrogen atom moved in an orbit about the positive nucleus, bound by the electrostatic attraction of the nucleus. Classical mechanics allows circular or elliptical orbits in this system, just as in the case of the planets orbiting the Sun. For simplicity, Bohr chose to consider circular orbits.

Such a model is mechanically stable because the Coulomb potential $V = -kZe^2/r$ provides the centripetal force

$$F = \frac{kZe^2}{r^2} = \frac{mv^2}{r} \quad 4-12$$

necessary for the electron to move in a circle of radius r at speed v , but it is electrically unstable because the electron is always accelerating toward the center of the circle.



Niels Bohr explains a point in front of the blackboard (1956).
[American Institute of Physics, Niels Bohr Library, Margrethe Bohr Collection.]

The laws of electrodynamics predict that such an accelerating charge will radiate light of frequency f equal to that of the periodic motion, which in this case is the frequency of revolution. Thus, classically,

$$f = \frac{v}{2\pi r} = \left(\frac{kZe^2}{rm} \right)^{1/2} \frac{1}{2\pi r} = \left(\frac{kZe^2}{4\pi^2 m} \right)^{1/2} \frac{1}{r^{3/2}} \sim \frac{1}{r^{3/2}} \quad 4-13$$

The total energy of the electron is the sum of the kinetic and the potential energies:

$$E = \frac{1}{2}mv^2 + \left(-\frac{kZe^2}{r} \right)$$

From Equation 4-12, we see that $\frac{1}{2}mv^2 = kZe^2/2r$ (a result that holds for circular motion in any inverse-square force field), so the total energy can be written as

$$E = \frac{kZe^2}{2r} - \frac{kZe^2}{r} = -\frac{kZe^2}{2r} \sim -\frac{1}{r} \quad 4-14$$

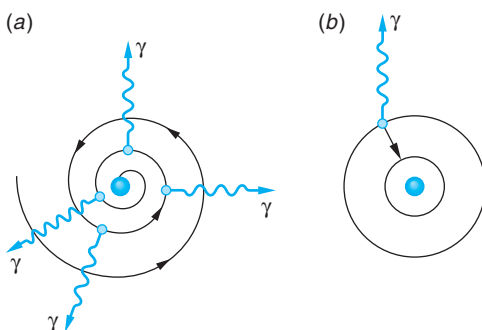


Figure 4-15 (a) In the classical orbital model, the electron orbits about the nucleus and spirals into the center because of the energy radiated. (b) In the Bohr model, the electron orbits without radiating until it jumps to another allowed radius of lower energy, at which time radiation is emitted.

Thus, classical physics predicts that, as energy is lost to radiation, the electron's orbit will become smaller and smaller while the frequency of the emitted radiation will become higher and higher, further increasing the rate at which energy is lost and ending when the electron reaches the nucleus. (See Figure 4-15a.) The time required for the electron to spiral into the nucleus can be calculated from classical mechanics and electrodynamics; it turns out to be less than a microsecond. Thus, at first sight, this model predicts that the atom will radiate a continuous spectrum (since the frequency of revolution changes continuously as the electron spirals in) and will collapse after a very short time, a result that fortunately does not occur. Unless excited by some external means, atoms do not radiate at all, and when excited atoms do radiate, a line spectrum is emitted, not a continuous one.

Bohr "solved" these formidable difficulties with two decidedly nonclassical postulates. His first postulate was that *electrons could move in certain orbits without radiating*. He called these orbits *stationary states*. His second postulate was to assume that *the atom radiates when the electron makes a transition from one stationary state to another* (Figure 4-15b) and that the frequency f of the emitted radiation is not the frequency of motion in either stable orbit but is related to the energies of the orbits by Planck's theory

$$hf = E_i - E_f \quad 4-15$$

where h is Planck's constant and E_i and E_f are the energies of the initial and final states. The second assumption, which is equivalent to that of energy conservation with the emission of a photon, is crucial because it deviated from classical theory, which requires the frequency of radiation to be that of the motion of the charged particle. Equation 4-15 is referred to as the *Bohr frequency condition*.

In order to determine the energies of the allowed, nonradiating orbits, Bohr made a third assumption, now known as the *correspondence principle*, which had profound implications:

In the limit of large orbits and large energies, quantum calculations must agree with classical calculations.

Thus, the correspondence principle says that whatever modifications of classical physics are made to describe matter at the submicroscopic level, when the results are extended to the macroscopic world, they must agree with those from the classical laws of physics that have been so abundantly verified in the everyday world. While Bohr's detailed model of the hydrogen atom has been supplanted by modern quantum theory, which we will discuss in later chapters, his frequency condition (Equation 4-15) and the correspondence principle remain as essential features of the new theory.

In his first paper,¹¹ in 1913, Bohr pointed out that his results implied that the angular momentum of the electron in the hydrogen atom can take on only values that are integral multiples of Planck's constant divided by 2π , in agreement with a discovery made a year earlier by J. W. Nicholson. That is, *angular momentum is quantized; it can assume only the values $nh/2\pi$, where n is an integer*. Rather than follow the intricacies of Bohr's derivation, we will use the fundamental conclusion of angular momentum quantization to find his expression for the observed spectra. The development that follows applies not only to hydrogen, but to any atom of nuclear charge $+Ze$ with a single orbital electron—e.g., singly ionized helium He^+ or doubly ionized lithium Li^{2+} .

If the nuclear charge is $+Ze$ and the electron charge $-e$, we have noted (Equation 4-12) that the centripetal force necessary to move the electron in a circular orbit is provided by the Coulomb force kZe^2/r^2 . Solving Equation 4-12 for the speed of the orbiting electron yields

$$v = \left(\frac{kZe^2}{mr} \right)^{1/2} \quad 4-16$$

Bohr's quantization of the angular momentum L is

$$L = mvr = \frac{nh}{2\pi} = n\hbar \quad n = 1, 2, 3, \dots \quad 4-17$$

where the integer n is called a *quantum number* and $\hbar = h/2\pi$. (The constant \hbar , read “h-bar,” is often more convenient to use than h itself, just as the angular frequency $\omega = 2\pi f$ is often more convenient than the frequency f .) Combining Equations 4-16 and 4-17 allows us to write for the circular orbits

$$r = \frac{nh}{mv} = \frac{n\hbar}{m} \left(\frac{rm}{kZe^2} \right)^{1/2}$$

Squaring this relation gives

$$r^2 = \frac{n^2\hbar^2}{m^2} \left(\frac{rm}{kZe^2} \right)$$

and canceling common quantities yields

$$r_n = \frac{n^2\hbar^2}{mkZe^2} = \frac{n^2a_0}{Z} \quad 4-18$$

where

$$a_0 = \frac{\hbar^2}{mke^2} = 0.529 \text{ \AA} = 0.0529 \text{ nm} \quad 4-19$$

is called the *Bohr radius*. The Å, a unit commonly used in the early days of spectroscopy, equals 10^{-10} m or 10^{-1} nm. Thus, we find that the stationary orbits of Bohr's first postulate have quantized radii, denoted in Equation 4-18 by the subscript on r_n .

Notice that the Bohr radius a_0 for hydrogen ($Z = 1$) corresponds to the orbit radius with $n = 1$, the smallest Bohr orbit possible for the electron in a hydrogen atom. Since $r_n \sim Z^{-1}$, the Bohr orbits for single-electron atoms with $Z > 1$ are closer to the nucleus than the corresponding ones for hydrogen.

The total energy of the electron (Equation 4-14) then becomes, upon substitution of r_n from Equation 4-18,

$$\begin{aligned} E_n &= -\frac{kZe^2}{2r_n} = -\frac{kZe^2}{2} \left(\frac{mkZe^2}{n^2\hbar^2} \right) \\ E_n &= -\frac{mk^2Z^2e^4}{2\hbar^2n^2} = -E_0 \frac{Z^2}{n^2} \quad n = 1, 2, 3, \dots \end{aligned} \quad 4-20$$

where $E_0 = mk^2e^4/2\hbar^2$. Thus, the energy of the electron is also quantized; i.e., the stationary states correspond to specific values of the total energy. This means that energies E_i and E_f that appear in the frequency condition of Bohr's second postulate must be from the allowed set E_n , and Equation 4-15 becomes

$$hf = E_{n_i} - E_{n_f} = -E_0 \frac{Z^2}{n_i^2} - \left(-E_0 \frac{Z^2}{n_f^2} \right)$$

or

$$f = \frac{E_0 Z^2}{h} \left(\frac{1}{n_f^2} - \frac{1}{n_i^2} \right) \quad 4-21$$

which can be written in the form of the Rydberg-Ritz equation (Equation 4-2) by substituting $f = c/\lambda$ and dividing by c to obtain

$$\frac{1}{\lambda} = \frac{E_0 Z^2}{hc} \left(\frac{1}{n_f^2} - \frac{1}{n_i^2} \right)$$

or

$$\frac{1}{\lambda} = Z^2 R \left(\frac{1}{n_f^2} - \frac{1}{n_i^2} \right) \quad 4-22$$

where

$$R = \frac{E_0}{hc} = \frac{mk^2e^4}{4\pi c\hbar^3} \quad 4-23$$

is Bohr's prediction for the value of the Rydberg constant.

Using the values of m , e , c , and \hbar known in 1913, Bohr calculated R and found his result to agree (within the limits of uncertainties of the constants) with the value obtained from spectroscopy, $1.097 \times 10^7 \text{ m}^{-1}$. Bohr noted in his original paper that this equation might be valuable in determining the best values for the constants e , m , and \hbar because of the extreme precision possible in measuring R . This has indeed turned out to be the case.

The possible values of the energy of the hydrogen atom predicted by Bohr's model are given by Equation 4-20 with $Z = 1$:

$$E_n = -\frac{mk^2e^4}{2\hbar^2n^2} = -\frac{E_0}{n^2} \quad 4-24$$

where

$$E_0 = \frac{mk^2e^4}{2\hbar^2} = 2.18 \times 10^{-18} \text{ J} = 13.6 \text{ eV}$$

is the magnitude of E_n with $n = 1$. $E_1 (= -E_0)$ is called the *ground state*. It is convenient to plot these allowed energies of the stationary states as in Figure 4-16. Such a plot is called an *energy-level diagram*. Various series of transitions between the stationary states are indicated in this diagram by vertical arrows drawn between the levels. The frequency of light emitted in one of these transitions is the energy difference divided by h according to Bohr's frequency condition, Equation 4-15. The energy required to remove the electron from the atom, 13.6 eV, is called the *ionization energy*, or *binding energy*, of the electron.

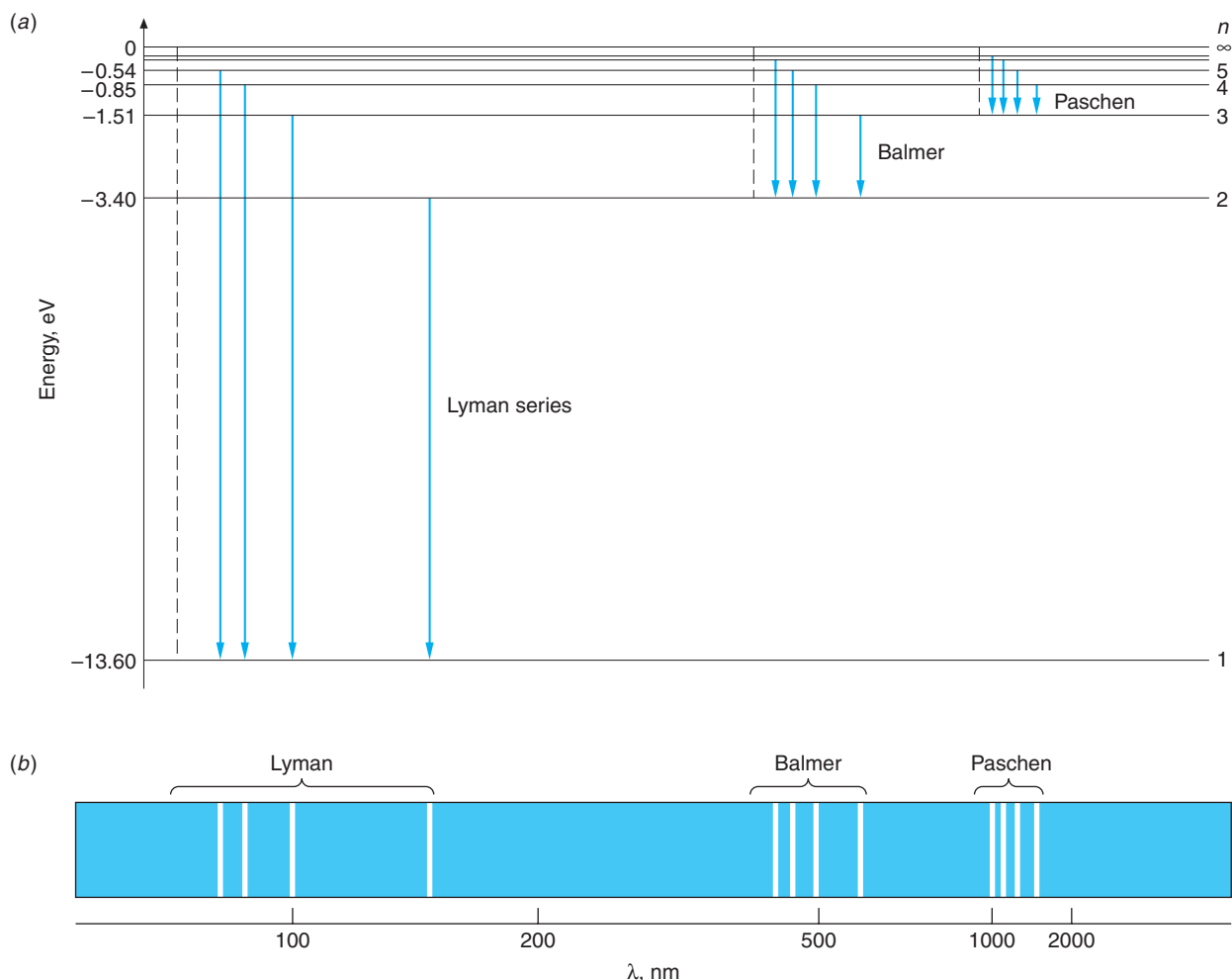


Figure 4-16 Energy-level diagram for hydrogen showing the seven lowest stationary states and the four lowest energy transitions each for the Lyman, Balmer, and Paschen series. There are an infinite number of levels. Their energies are given by $E_n = -13.6/n^2$ eV, where n is an integer. The dashed line shown for each series is the *series limit*, corresponding to the energy that would be radiated by an electron at rest far from the nucleus ($n \rightarrow \infty$) in a transition to the state with $n = n_f$ for that series. The horizontal spacing between the transitions shown for each series is proportional to the wavelength spacing between the lines of the spectrum. (b) The spectral lines corresponding to the transitions shown for the three series. Notice the regularities within each series, particularly the short-wavelength limit and the successively smaller separation between adjacent lines as the limit is approached. The wavelength scale in the diagram is not linear.

A bit different sort of application, the Bohr/Rutherford model of the nuclear atom and electron orbits is the picture that, for millions of people, provides their link to the world of the atom and subatomic phenomena.

At the time Bohr's paper was published, there were two spectral series known for hydrogen: the Balmer series, corresponding to $n_f = 2$, $n_i = 3, 4, 5, \dots$, and a series named after its discoverer, Paschen (1908), corresponding to $n_f = 3$, $n_i = 4, 5, 6, \dots$. Equation 4-22 indicates that other series should exist for different values of n_f . In 1916 Lyman found the series corresponding to $n_f = 1$, and in 1922 and 1924 F. S. Brackett and A. H. Pfund, respectively, found series corresponding to $n_f = 4$ and $n_f = 5$. As can be easily determined by computing the wavelengths for these series, only the Balmer series lies primarily in the visible portion of the electromagnetic spectrum. The Lyman series is in the ultraviolet, the others in the infrared.

EXAMPLE 4-6 Wavelength of the H_{β} Line Compute the wavelength of the H_{β} spectral line, i.e., the second line of the Balmer series predicted by Bohr's model. The H_{β} line is emitted in the transition from $n_i = 4$ to $n_f = 2$.

SOLUTION

1. *Method 1:* The wavelength is given by Equation 4-22 with $Z = 1$:

$$\frac{1}{\lambda} = R \left(\frac{1}{n_f^2} - \frac{1}{n_i^2} \right)$$

2. Substituting $R = 1.097 \times 10^7 \text{ m}^{-1}$ and the values of n_i and n_f :

$$\frac{1}{\lambda} = (1.097 \times 10^7 \text{ m}^{-1}) \left(\frac{1}{2^2} - \frac{1}{4^2} \right)$$

or

$$\lambda = 4.86 \times 10^{-7} = 486 \text{ nm}$$

3. *Method 2:* The wavelength may also be computed from Equation 4-15:

$$hf = hc/\lambda = E_i - E_f$$

or

$$\frac{1}{\lambda} = \frac{1}{hc}(E_i - E_f)$$

4. The values of E_i and E_f are given by Equation 4-24:

$$E_i = -\left(\frac{13.6 \text{ eV}}{n_i^2}\right) = -\left(\frac{13.6 \text{ eV}}{4^2}\right) = -0.85 \text{ eV}$$

$$E_f = -\left(\frac{13.6 \text{ eV}}{n_f^2}\right) = -\left(\frac{13.6 \text{ eV}}{2^2}\right) = -3.4 \text{ eV}$$

5. Substituting these into Equation 4-15 yields

$$\begin{aligned} \frac{1}{\lambda} &= \frac{[-0.85 \text{ eV} - (-3.4 \text{ eV})](1.60 \times 10^{-19} \text{ J/eV})}{(6.63 \times 10^{-34} \text{ J} \cdot \text{s})(3.00 \times 10^8 \text{ m/s})} \\ &= 2.051 \times 10^6 \text{ m}^{-1} \end{aligned}$$

or

$$\lambda = 4.87 \times 10^{-7} \text{ m} = 487 \text{ nm}$$

Remarks: The difference in the two results is due to rounding of the Rydberg constant to three decimal places.

Reduced Mass Correction

The assumption by Bohr that the nucleus is fixed is equivalent to the assumption that it has infinite mass. In fact, the Rydberg constant in Equation 4-23 is normally written a R_∞ , as we will do henceforth. If the nucleus has mass M , its kinetic energy will be $\frac{1}{2}Mv^2 = p^2/2M$, where $p = Mv$ is the momentum. If we assume that the total momentum of the atom is zero, conservation of momentum requires that the momenta of the nucleus and electron be equal in magnitude. The total kinetic energy is then

$$E_k = \frac{p^2}{2M} + \frac{p^2}{2m} = \frac{M+m}{2mM} p^2 = \frac{p^2}{2\mu}$$

where

$$\mu = \frac{mM}{m+M} = \frac{m}{1+m/M} \quad 4-25$$

This is slightly different from the kinetic energy of the electron because μ , called the *reduced mass*, is slightly different from the electron mass. The results derived above for a nucleus of infinite mass can be applied directly for the case of a nucleus of mass M if we replace the electron mass in the equations by reduced mass μ , defined by Equation 4-25. (The validity of this procedure is proved in most intermediate and advanced mechanics books.) The Rydberg constant (Equation 4-23) is then written

$$R = \frac{\mu k^2 e^4}{4\pi c \hbar^3} = \frac{mk^2 e^4}{4\pi c \hbar^3} \left(\frac{1}{1+m/M} \right) = R_\infty \left(\frac{1}{1+m/M} \right) \quad 4-26$$

This correction amounts to only 1 part in 2000 for the case of hydrogen and to even less for other nuclei; however, the predicted variation in the Rydberg constant from atom to atom is precisely that which is observed. For example, the spectrum of a singly ionized helium atom, which has one remaining electron, is just that predicted by Equation 4-22 and 4-26 with $Z = 2$ and the proper helium mass. The current value for the Rydberg constant R_∞ from precision spectroscopic measurements¹² is

$$R_\infty = 1.0973732 \times 10^7 \text{ m}^{-1} = 1.0973732 \times 10^{-2} \text{ nm}^{-1} \quad 4-27$$

Urey¹³ used the reduced mass correction to the spectral lines of the Balmer series to discover (in 1931) a second form of hydrogen whose atoms had twice the mass of ordinary hydrogen. The heavy form was called *deuterium*. The two forms, atoms with the same Z but different masses, are called *isotopes*.

EXAMPLE 4-7 Rydberg Constants for H and He⁺ Compute the Rydberg constants for H and He⁺ applying the reduced mass correction. ($m = 9.1094 \times 10^{-31}$ kg, $m_p = 1.6726 \times 10^{-27}$ kg, $m_\alpha = 5.0078 \times 10^{-27}$ kg)

SOLUTION

For hydrogen:

$$R_H = R_\infty \left(\frac{1}{1+m/M_H} \right) = R_\infty \left(\frac{1}{1+9.1094 \times 10^{-31}/1.6726 \times 10^{-27}} \right) \\ = 1.09677 \times 10^7 \text{ m}^{-1}$$

For helium: Since M in the reduced mass correction is the mass of the nucleus, for this calculation we use M equal to the α particle mass.

$$\begin{aligned} R_{\text{He}} &= R_{\infty} \left(\frac{1}{1 + m/M_{\text{H}}} \right) = R_{\infty} \left(\frac{1}{1 + 9.1094 \times 10^{-31}/5.0078 \times 10^{-27}} \right) \\ &= 1.09752 \times 10^7 \text{ m}^{-1} \end{aligned}$$

Thus, the two Rydberg constants differ by about 0.04 percent.

Correspondence Principle

According to the correspondence principle, which applies also to modern quantum mechanics, when the energy levels are closely spaced, quantization should have little effect; classical and quantum calculations should give the same results. From the energy-level diagram of Figure 4-16, we see that the energy levels are close together when the quantum number n is large. This leads us to a slightly different statement of Bohr's correspondence principle: *In the region of very large quantum numbers (n in this case) quantum calculation and classical calculation must yield the same results.* To see that the Bohr model of the hydrogen atom does indeed obey the correspondence principle, let us compare the frequency of a transition between level $n_i = n$ and level $n_f = n - 1$ for large n with the classical frequency, which is the frequency of revolution of the electron. From Equation 4-22 we have

$$f = \frac{c}{\lambda} = \frac{Z^2 mk^2 e^4}{4\pi\hbar^3} \left[\frac{1}{(n-1)^2} - \frac{1}{n^2} \right] = \frac{Z^2 mk^2 e^4}{4\pi\hbar^3} \frac{2n-1}{n^2(n-1)^2}$$

For large n we can neglect the ones subtracted from n and $2n$ to obtain

$$f = \frac{Z^2 mk^2 e^4}{4\pi\hbar^3} \frac{2}{n^3} = \frac{Z^2 mk^2 e^4}{2\pi\hbar^3 n^3} \quad \text{4-28}$$

The classical frequency of revolution of the electron is (see Equation 4-13)

$$f_{\text{rev}} = \frac{v}{2\pi r}$$

Using $v = n\hbar/mr$ from Equation 4-17 and $r = n^2\hbar^2/mkZe^2$ from Equation 4-18, we obtain

$$\begin{aligned} f_{\text{rev}} &= \frac{(n\hbar/mr)}{2\pi r} = \frac{n\hbar}{2\pi mr^2} = \frac{n\hbar}{2\pi m(n^2\hbar^2/mkZe^2)^2} \\ f_{\text{rev}} &= \frac{m^2 k^2 Z^2 e^4 n \hbar}{2\pi m n^4 \hbar^4} = \frac{mk^2 Z^2 e^4}{2\pi \hbar^3 n^3} \end{aligned} \quad \text{4-29}$$

which is the same as Equation 4-28.

Fine Structure Constant

The demonstration of the correspondence principle for large n in the preceding paragraph was for $\Delta n = n_i - n_f = 1$; however, we have seen (see Figure 4-16) that transitions occur in the hydrogen atom for $\Delta n \geq 1$ when n is small, and such transitions should occur for large n too. If we allow $\Delta n = 2, 3, \dots$ for large values of n , then the frequencies of the emitted radiation would be, according to Bohr's model, integer multiples of the frequency given in Equation 4-28. In that event, Equations 4-28 and 4-29 would not agree. This disagreement can be avoided by allowing elliptical orbits.¹⁴ A result of Newtonian mechanics, familiar from planetary motion, is that in an inverse-square force

field, the energy of an orbiting particle depends only on the major axis of the ellipse and not on its eccentricity. There is consequently no change in the energy at all unless the force differs from inverse square or unless Newtonian mechanics is modified. A. Sommerfeld considered the effect of special relativity on the mass of the electron in the Bohr model in an effort to explain the observed *fine structure* of the hydrogen spectral lines.¹⁵ Since the relativistic corrections should be of the order of v^2/c^2 (see Chapter 2), it is likely that a highly eccentric orbit would have a larger correction because v becomes greater as the electron moves nearer the nucleus. The Sommerfeld calculations are quite complicated, but we can estimate the order of magnitude of the effect of special relativity by calculating v/c for the first Bohr orbit in hydrogen. For $n = 1$, we have from Equation 4-17 that $mvr_1 = \hbar$. Then, using $r_1 = a_0 = \hbar^2/mke^2$, we have

$$v = \frac{\hbar}{mr_1} = \frac{\hbar}{m(\hbar^2/mke^2)} = \frac{ke^2}{\hbar}$$

and

$$\frac{v}{c} = \frac{ke^2}{\hbar c} = \frac{1.44 \text{ eV} \cdot \text{nm}}{197.3 \text{ eV} \cdot \text{nm}} \approx \frac{1}{137} = \alpha \quad 4-30$$

where we have used another convenient combination

$$\hbar c = \frac{1.24 \times 10^3 \text{ eV} \cdot \text{nm}}{2\pi} = 197.3 \text{ eV} \cdot \text{nm} \quad 4-31$$

The dimensionless quantity $ke^2/\hbar c = \alpha$ is called the *fine-structure constant* because of its first appearance in Sommerfeld's theory, but as we will see, it has much more fundamental importance.

Though v^2/c^2 is very small, an effect of this magnitude is observable. In Sommerfeld's theory, the fine structure of the hydrogen spectrum is explained in the following way. For each allowed circular orbit of radius r_n and energy E_n , a set of n elliptical orbits is possible of equal major axes but different eccentricities. Since the velocity of a particle in an elliptical orbit depends on the eccentricity, so then will the mass and momentum, and therefore the different ellipses for a given n will have slightly different energies. Thus, the energy radiated when the electron changes orbit depends slightly on the eccentricities of the initial and final orbits as well as on their major axes. The splitting of the energy levels for a given n is called *fine-structure splitting*, and its value turns out to be of the order of $v^2/c^2 = \alpha^2$, just as Sommerfeld predicted. However, the agreement of Sommerfeld's prediction with the observed fine-structure splitting was quite accidental and led to considerable confusion in the early days of quantum theory. Although he had used the relativistic mass and momentum, he computed the energy using classical mechanics, leading to a correction much larger than that actually due only to relativistic effects. As we will see in Chapter 7, fine structure is associated with a completely nonclassical property of the electron called *spin*.

A lasting contribution of Sommerfeld's effort was the introduction of the fine-structure constant $\alpha = ke^2/\hbar c \approx 1/137$. With it we can write the Bohr radius a_0 and the quantized energies of the Bohr model in a particularly elegant form. Equations 4-24 and 4-19 for hydrogen become

$$E_n = -\frac{mk^2e^4}{2\hbar^2n^2}\frac{c^2}{c^2} = -\frac{mc^2}{2}\alpha^2\frac{1}{n^2} \quad 4-32$$

$$a_0 = \frac{\hbar^2}{mke^2}\frac{c}{c} = \frac{\hbar}{mc}\frac{1}{\alpha} \quad 4-33$$



Since α is a dimensionless number formed of universal constants, *all* observers will measure the same value for it and find that energies and dimensions of atomic systems are proportional to α^2 and $1/\alpha$, respectively. We will return to the implications of this intriguing fact later in the book.



EXPLORING Giant Atoms

Giant atoms called *Rydberg atoms*, long understood to be a theoretical possibility and first detected in interstellar space in 1965, are now being produced and studied in the laboratory. Rydberg atoms are huge! They are atoms that have one of the valence electrons in a state with a very large quantum number n . (See Figure 4-17.) Notice in Equation 4-18 that the radius of the electron orbit $r_n = n^2 a_0 / Z \propto n^2$ and n can be any positive integer, so the diameter of a hydrogen atom (or any other atom, for that matter) could be very large, a millimeter or even a meter! What keeps such giant atoms from being common is that the energy difference between adjacent allowed energy states is extremely small when n is large and the allowed states are very near the $E_\infty = 0$ level where ionization occurs, because $E_n \propto 1/n^2$. For example, if $n = 1000$, the diameter of a hydrogen atom would be $r_{1000} = 0.1$ mm, but both E_{1000} and the difference in energy $\Delta E = E_{1001} - E_{1000}$ are about 10^{-5} eV! This energy is far below the average energy of thermal motion at ordinary temperatures (about 0.025 eV), so random collisions would quickly ionize an atom whose electron happened to get excited to a level with n equal to 20 or so with r still only about 10^{-8} m.

The advent of precisely tunable dye lasers in the 1970s made it possible to nudge electrons carefully into orbits with larger and larger n values. The largest Rydberg atoms made so far, typically using sodium or potassium, are 10,000 times the diameter of ordinary atoms, about 20 μm across or the size of a fine grain of sand, and exist for several milliseconds inside vacuum chambers. For hydrogen, this corresponds to quantum number $n \approx 600$. An electron moving so far from the nucleus is bound by a minuscule force. It also moves rather slowly since the classical period of $T = 1/f \propto n^3$ and follows an elliptical orbit. These characteristics of very large n orbits provide several intriguing possibilities. For example, very small electric fields might be studied, making possible the tracking of chemical reactions that proceed too quickly to be followed otherwise. More dramatic is the possibility of directly testing Bohr's correspondence principle by directly observing the slow (since $v \propto 1/n$) movement of the electron around the large n orbits—the transition from quantum mechanics to classical mechanics. Computer simulations of the classical motion of a Rydberg electron “wave” (see Chapter 5) in orbit around a nucleus are aiding the design of experiments to observe the correspondence principle.

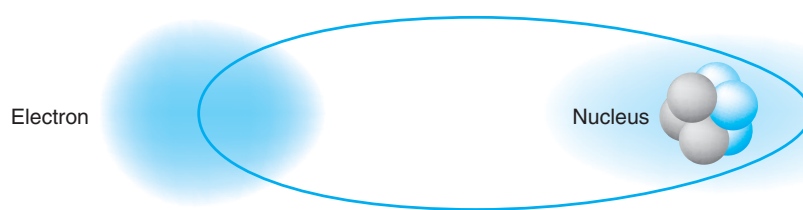


Figure 4-17 A lithium ($Z = 3$) Rydberg atom. The outer electron occupies a small volume and follows a nearly classical orbit with a large value of n . The two inner electrons are not shown.

Questions

6. If the electron moves in an orbit of greater radius, does its total energy increase or decrease? Does its kinetic energy increase or decrease?
7. What is the energy of the shortest-wavelength photon that can be emitted by the hydrogen atom?
8. How would you characterize the motion and location of an electron with $E = 0$ and $n \rightarrow \infty$ in Figure 4-16?

4-4 X-Ray Spectra

The extension of the Bohr theory to atoms more complicated than hydrogen proved difficult. Quantitative calculations of the energy levels of atoms of more than one electron could not be made from the model, even for helium, the next element in the periodic table. However, experiments by H. Moseley in 1913 and J. Franck and G. Hertz in 1914 strongly supported the general Bohr-Rutherford picture of the atom as a positively charged core surrounded by electrons that moved in quantized energy states relatively far from the core. Moseley's analysis of x-ray spectra will be discussed in this section, and the Franck-Hertz measurement of the transmission of electrons through gases will be discussed in the chapter's concluding section.

Using the methods of crystal spectrometry that had just been developed by W. H. Bragg and W. L. Bragg, Moseley¹⁶ measured the wavelengths of the characteristic x-ray line spectra for about 40 different target elements. (Typical x-ray spectra are shown in Figure 3-15.) He noted that the x-ray line spectra varied in a regular way from element to element, unlike the irregular variations of optical spectra. He surmised that this regular variation occurred because characteristic x-ray spectra were due to transitions involving the innermost electrons of the atoms. (See Figure 4-18.) Because the inner electrons are



Henry G.-J. Moseley.
[Courtesy of University of Manchester.]

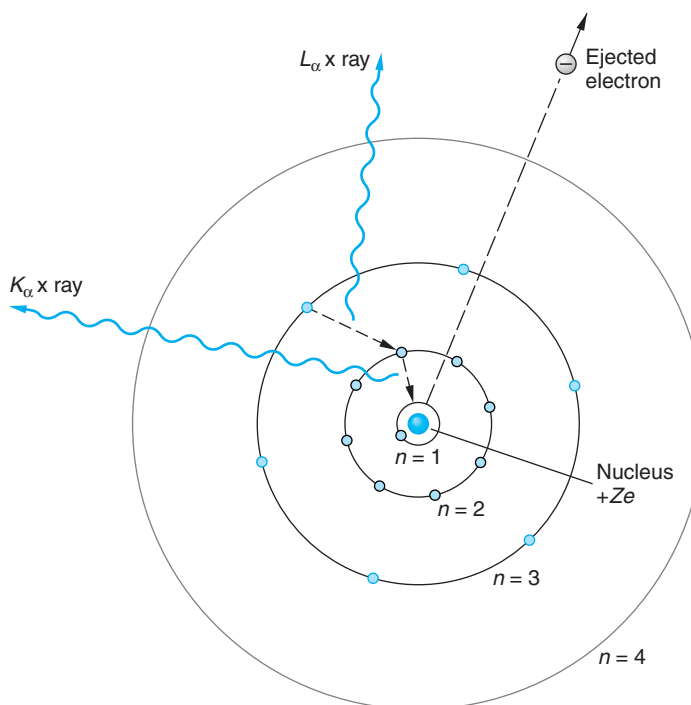


Figure 4-18 A stylized picture of the Bohr circular orbits for $n = 1, 2, 3$, and 4 . The radii $r_n \sim n^2$. In a high- Z element (elements with $Z \geq 12$ emit x rays), electrons are distributed over all the orbits shown. If an electron in the $n = 1$ orbit is knocked from the atom, e.g., by being hit by a fast electron accelerated by the voltage across an x-ray tube, the vacancy thus produced is filled by an electron of higher energy (i.e., $n = 2$ or higher). The difference in energy between the two orbits is emitted as a photon, according to the Bohr frequency condition, whose wavelength will be in the x-ray region of the spectrum if Z is large enough.

shielded from the outermost electrons by those in intermediate orbits, their energies do not depend on the complex interactions of the outer electrons, which are responsible for the complicated optical spectra. Furthermore, the inner electrons are well shielded from the interatomic forces that are responsible for the binding of atoms in solids.

According to the Bohr theory (published earlier the same year, 1913), the energy of an electron in the first Bohr orbit is proportional to the square of the nuclear charge (see Equation 4-20). Moseley reasoned that the energy, and therefore the frequency, of a characteristic x-ray photon should vary as the square of the atomic number of the target element. He therefore plotted the square root of the frequency of a particular characteristic line in the x-ray spectrum of various target elements versus the atomic number Z of the element. Such a plot, now called a *Moseley plot*, is shown in Figure 4-19.

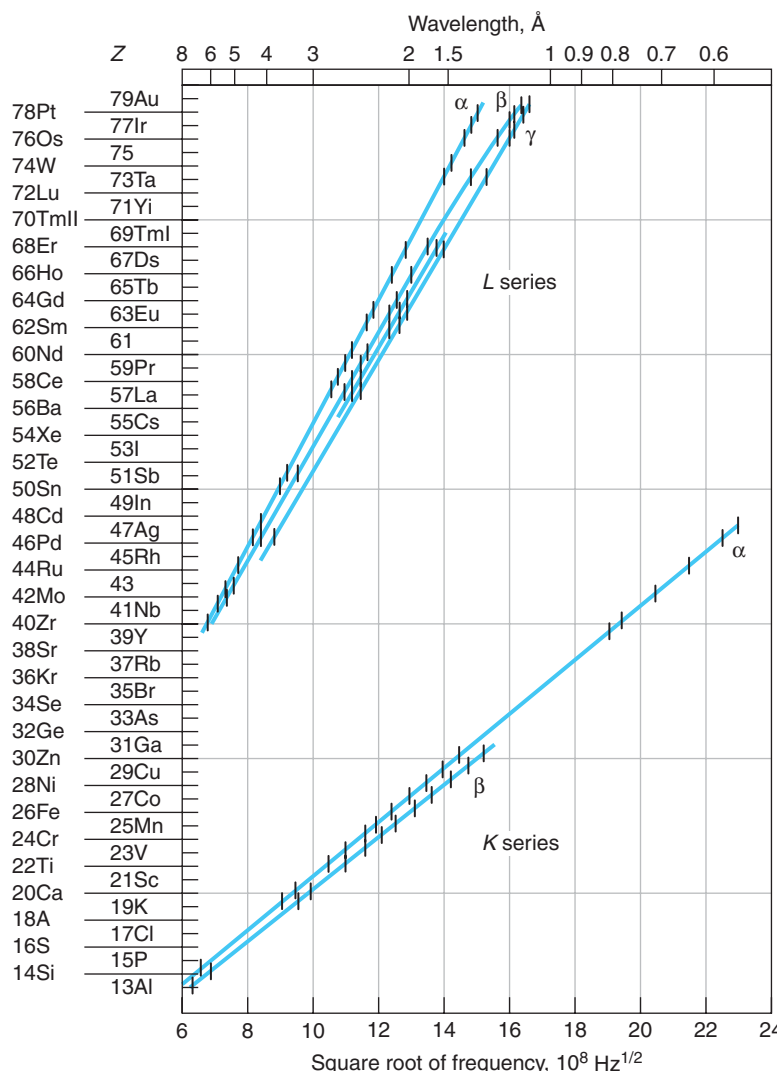


Figure 4-19 Moseley's plots of the square root of frequency versus Z for characteristic x rays. When an atom is bombarded by high-energy electrons, an inner atomic electron is sometimes knocked out, leaving a vacancy in the inner shell. The K -series x rays are produced by atomic transitions to vacancies in the $n = 1$ (K) shell, whereas the L series is produced by transitions to the vacancies in the $n = 2$ (L) shell. [From H. Moseley, *Philosophical Magazine* (6), 27, 713 (1914).]

These curves can be fitted by the empirical equation

$$f^{1/2} = A_n(Z - b) \quad 4-34$$

where A_n and b are constants for each characteristic x-ray line. One family of lines, called the *K series*, has $b = 1$ and slightly different values of A_n for each line in the graph. The other family shown in Figure 4-19, called the *L series*,¹⁷ could be fitted by Equation 4-34 with $b = 7.4$.

If the bombarding electron in the x-ray tube causes ejection of an electron from the innermost orbit ($n = 1$) in a target atom completely out of the atom, photons will be emitted corresponding to transitions of electrons in other orbits ($n = 2, 3, \dots$) to fill the vacancy in the $n = 1$ orbit. (See Figure 4-18.) (Since these lines are called the *K series*, the $n = 1$ orbit came to be called the *K shell*.) The lowest-frequency line corresponds to the lowest-energy transition ($n = 2 \rightarrow n = 1$). This line is called the K_{α} line. The transition $n = 3 \rightarrow n = 1$ is called the K_{β} line. It is of higher energy, and hence higher frequency, than the K_{α} line. A vacancy created in the $n = 2$ orbit by emission of a K_{α} x ray may then be filled by an electron of higher energy, e.g., one in the $n = 3$ orbit, resulting in the emission of a line in the *L series*, and so on. The multiple *L* lines in the Moseley plot (Figure 4-19) are due in part to the fact that there turn out to be small differences in the energies of electrons with a given n that are not predicted by the Bohr model. Moseley's work gave the first indication of these differences, but the explanation will have to await our discussion of more advanced quantum theory in Chapter 7.

Using the Bohr relation for a one-electron atom (Equation 4-21) with $n_f = 1$ and using $(Z - 1)$ in place of Z , we obtain for the frequencies of the *K* series

$$f = \frac{mk^2e^4}{4\pi\hbar^3}(Z - 1)^2 \left(\frac{1}{l^2} - \frac{1}{n^2} \right) = cR_{\infty}(Z - 1)^2 \left(1 - \frac{1}{n^2} \right) \quad 4-35$$

where R_{∞} is the Rydberg constant. Comparing this with Equation 4-34, we see that A_n is given by

$$A_n^2 = cR_{\infty} \left(1 - \frac{1}{n^2} \right) \quad 4-36$$

The wavelengths of the lines in the *K* series are then given by

$$\lambda = \frac{c}{f} = \frac{c}{A_n^2(Z - 1)^2} = \frac{1}{R_{\infty}(Z - 1)^2 \left(1 - \frac{1}{n^2} \right)} \quad 4-37$$

EXAMPLE 4-8 K_{α} for Molybdenum Calculate the wavelength of the K_{α} line of molybdenum ($Z = 42$), and compare the result with the value $\lambda = 0.0721$ nm measured by Moseley and with the spectrum in Figure 3-15b.

SOLUTION

Using $n = 2$, $R_{\infty} = 1.097 \times 10^7 \text{ m}^{-1}$, and $Z = 42$, we obtain

$$\lambda = \left[(1.097 \times 10^7 \text{ m}^{-1})(41)^2 \left(1 - \frac{1}{4} \right) \right]^{-1} = 7.23 \times 10^{-11} \text{ m} = 0.0723 \text{ nm}$$

This value is within 0.3 percent of Moseley's measurement and agrees well with that in Figure 3-15b.

The fact that f is proportional to $(Z - 1)^2$ rather than to Z is explained by the partial shielding of the nuclear charge by the other electron remaining in the K shell as “seen” by electrons in the $n = 2$ (L) shell.¹⁸ Using this reasoning, Moseley concluded that, since $b = 7.4$ for the L series, these lines involved electrons farther from the nucleus, which “saw” the nuclear charge shielded by more inner electrons. Assuming that the L series was due to transitions to the $n = 2$ shell, we see that the frequencies for this series are given by

$$f = cR_{\infty} \left(\frac{1}{2^2} - \frac{1}{n^2} \right) (Z - 7.4)^2 \quad 4-38$$

where $n = 3, 4, 5, \dots$

Before Moseley’s work, the atomic number was merely the place number of the element in Mendeleev’s periodic table of the elements arranged by weight. The experiments of Geiger and Marsden showed that the nuclear charge was approximately $A/2$, while x-ray scattering experiments by C. G. Barkla showed that the number of electrons in an atom was also approximately $A/2$. These two experiments are consistent since the atom as a whole must be electrically neutral. However, several discrepancies were found in the periodic table as arranged by weight. For example, the 18th element in order of weight is potassium (39.102), and the 19th is argon (39.948). Arrangement by weight, however, puts potassium in the column with the inert gases and argon with the active metals, the reverse of their known chemical properties. Moseley showed that for these elements to fall on the line $f^{1/2}$ versus Z , argon had to have $Z = 18$ and potassium $Z = 19$. Arranging the elements by the Z number obtained from the Moseley plot rather than by weight, gave a periodic chart in complete agreement with the chemical properties. Moseley also pointed out that there were gaps in the periodic table at $Z = 43, 61$, and 75 , indicating the presence of undiscovered elements. All have subsequently been found. Figure 4-20 illustrates the discovery of promethium ($Z = 61$).

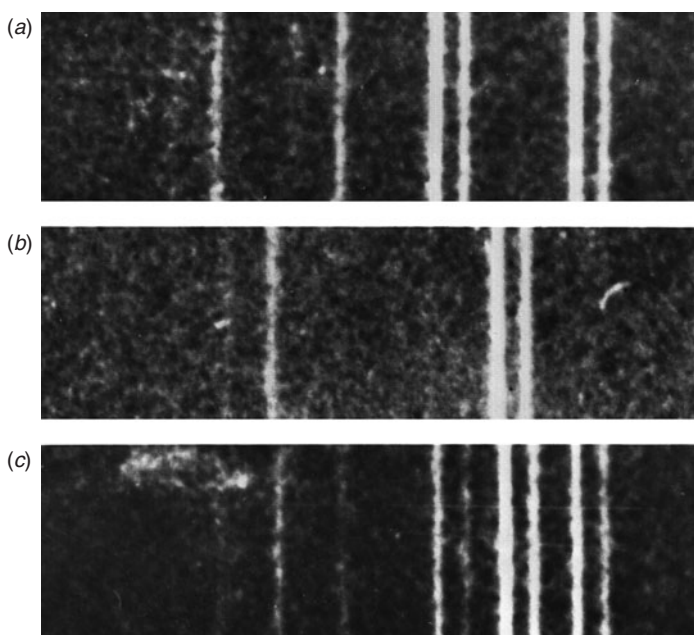


Figure 4-20 Characteristic x-ray spectra. (a) Part of the spectra of neodymium ($Z = 60$) and samarium ($Z = 62$). The two pairs of bright lines are the K_{α} and K_{β} lines. (b) Part of the spectrum of the artificially synthesized element promethium ($Z = 61$). This element was first positively identified in 1945 at the Clinton Laboratory (now Oak Ridge). Its K_{α} and K_{β} lines fall between those of neodymium and samarium, just as Moseley predicted. (c) Part of the spectra of all three of the elements neodymium, promethium, and samarium. [Courtesy of J. A. Swartout, Oak Ridge National Laboratory.]

Auger Electrons

The process of producing x rays necessarily results in the ionization of the atom since an inner electron is ejected. The vacancy created is filled by an outer electron, producing the x rays studied by Moseley. In 1923 Pierre Auger discovered that, as an alternative to x-ray emission, the atom may eject a third electron from a higher-energy outer shell via a radiationless process called the *Auger effect*. In the Auger (pronounced oh-zhay) process, the energy difference $\Delta E = E_2 - E_1$ that could have resulted in the emission of a K_α x ray is removed from the atom by the third electron, e.g., one in the $n = 3$ shell. Since the magnitude of $E_3 < \Delta E$, the $n = 3$ electron would leave the atom with a characteristic kinetic energy $\Delta E - |E_3|$, which is determined by the stationary-state energies of the particular atom.¹⁹ Thus, each element has a characteristic Auger electron spectrum. (See Figure 4-21a.) Measurement of the Auger electrons provides a simple and highly sensitive tool for identifying impurities on clean surfaces in electron microscope systems and investigating electron energy shifts associated with molecular bonding. (See Figure 4-21b.)

Question

9. Why did Moseley plot $f^{1/2}$ versus Z rather than f versus Z ?

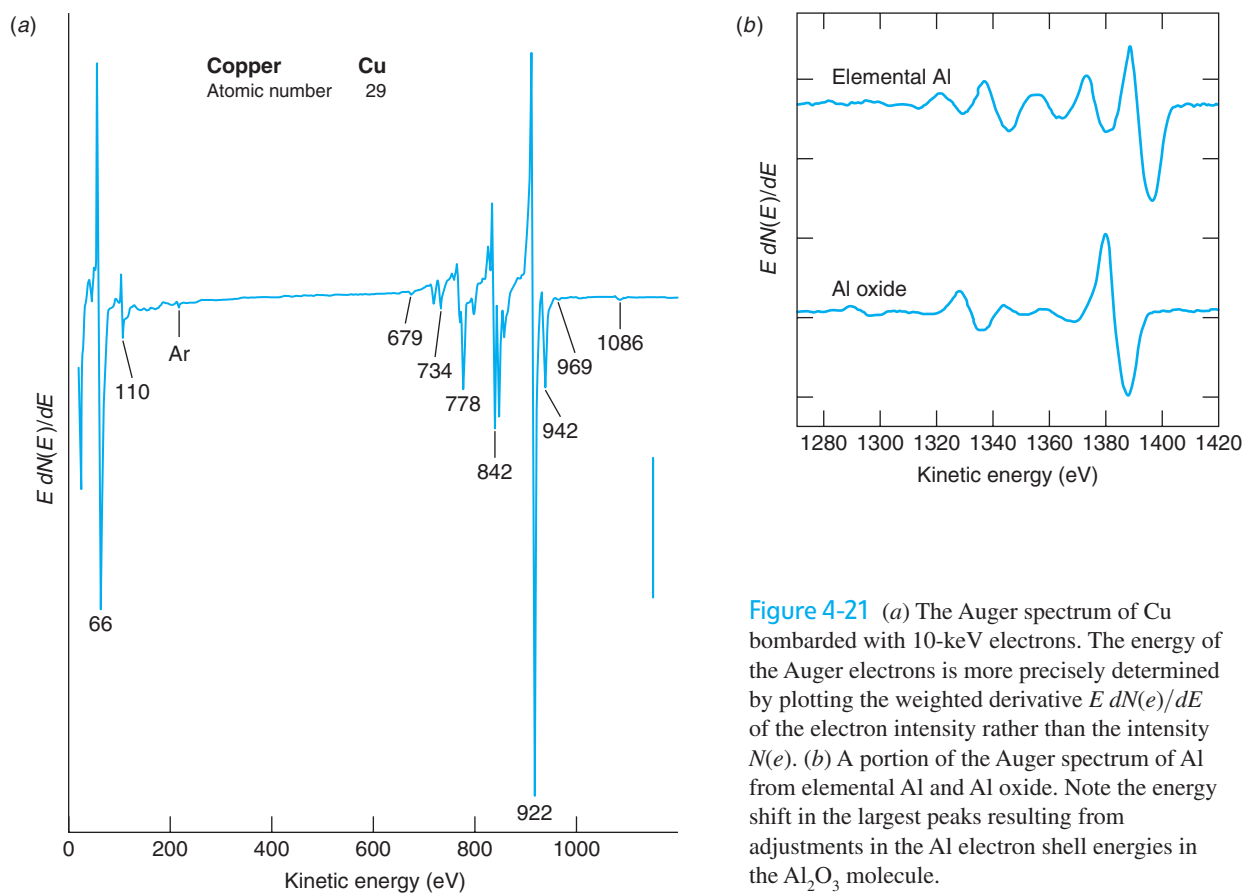


Figure 4-21 (a) The Auger spectrum of Cu bombarded with 10-keV electrons. The energy of the Auger electrons is more precisely determined by plotting the weighted derivative $E dN(e)/dE$ of the electron intensity rather than the intensity $N(e)$. (b) A portion of the Auger spectrum of Al from elemental Al and Al oxide. Note the energy shift in the largest peaks resulting from adjustments in the Al electron shell energies in the Al_2O_3 molecule.

4-5 The Franck-Hertz Experiment

We conclude this chapter with discussion of an important experiment that provided strong support for the quantization of atomic energies, thus helping to pave the way for modern quantum mechanics. While investigating the inelastic scattering of electrons, J. Franck and G. Hertz²⁰ made a discovery that confirmed by *direct measurement* Bohr's hypothesis of energy quantization in atoms. First done in 1914, it is now a standard undergraduate laboratory experiment. Figure 4-22a is a schematic diagram of the apparatus. A small heater heats the cathode. Electrons are ejected from the heated cathode and accelerated toward a grid, which is at a positive potential V_0 relative to the cathode. Some electrons pass through the grid and reach the plate P , which is at a slightly lower potential $V_p = V_0 - \Delta V$. The tube is filled with a low-pressure gas of the element being investigated (mercury vapor, in Franck and Hertz's experiment). The experiment involves measuring the plate current as a function of V_0 . As V_0 is increased from 0, the current increases until a critical value (about 4.9 V for Hg) is reached, at which point the current suddenly decreases. As V_0 is increased further, the current rises again.

The explanation of this result is a bit easier to visualize if we think for the moment of a tube filled with hydrogen atoms instead of mercury. (See Figure 4-22b.) Electrons accelerated by V_0 that collide with hydrogen electrons cannot transfer energy to the latter unless they have acquired kinetic energy $eV_0 = E_2 - E_1 = 10.2$ eV since the hydrogen electron according to Bohr's model cannot occupy states with energies intermediate between E_1 and E_2 . Such a collision will thus be elastic; i.e., the incident electron's kinetic energy will be unchanged by the collision, and thus it can overcome the potential ΔV and contribute to the current I . However, if $eV_0 \geq 10.2$ eV,

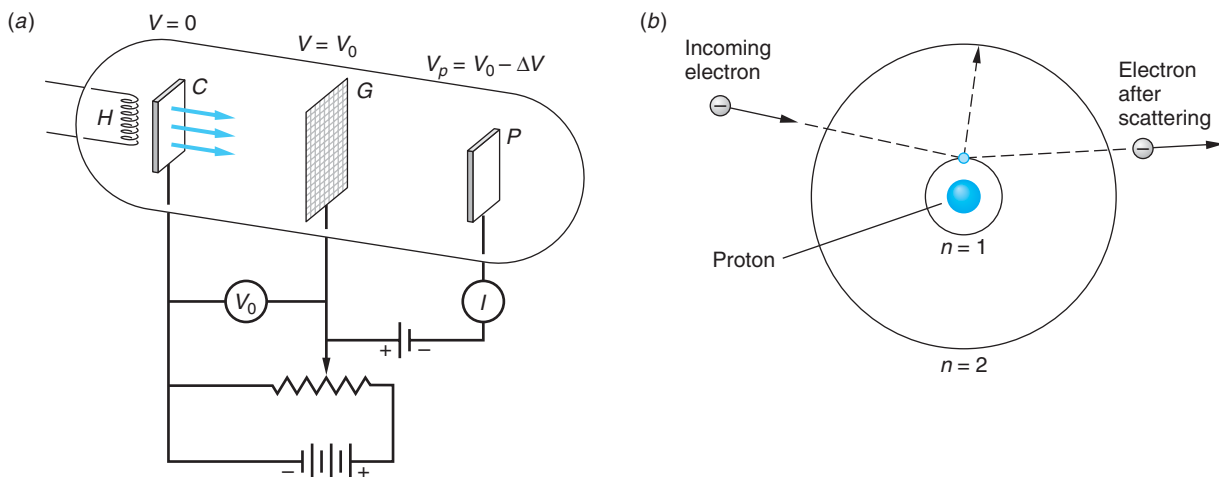


Figure 4-22 (a) Schematic diagram of the Franck-Hertz experiment. Electrons ejected from the heated cathode C at zero potential are drawn to the positive grid G . Those passing through the holes in the grid can reach the plate P and thereby contribute to the current I if they have sufficient kinetic energy to overcome the small back potential ΔV . The tube contains a low-pressure gas of the element being studied. (b) Results for hydrogen. If the incoming electron does not have sufficient energy to transfer $\Delta E = E_2 - E_1$ to the hydrogen electron in the $n = 1$ orbit (ground state), then the scattering will be elastic. If the incoming electron does have at least ΔE kinetic energy, then an inelastic collision can occur in which ΔE is transferred to the $n = 1$ electron, moving it to the $n = 2$ orbit. The excited electron will typically return to the ground state very quickly, emitting a photon of energy ΔE .

then the incoming electron can transfer 10.2 eV to the hydrogen electron in the *ground state* ($n = 1$ orbit), putting it into the $n = 2$ orbit (called the *first excited state*). The incoming electron's energy is thus reduced by 10.2 eV; it has been inelastically scattered. With insufficient energy to overcome the small retarding potential ΔV , the incoming electrons can no longer contribute to the plate current I , and I drops sharply.

The situation with Hg in the tube is more complicated since Hg has 80 electrons. Although Bohr's theory cannot predict their individual energies, we still expect the energy to be quantized with a ground state, first excited state, and so on, for the atom. Thus, the explanation of the observed 4.9-V critical potential for Hg is that the first excited state is about 4.9 eV above the lowest level (ground state). Electrons with energy less than this cannot lose energy to the Hg atoms, but electrons with energy greater than 4.9 eV can have inelastic collisions and lose 4.9 eV. If this happens near the grid, these electrons cannot gain enough energy to overcome the small back voltage ΔV and reach the plate; the current therefore decreases. If this explanation is correct, the Hg atoms that are excited to an energy level of 4.9 eV above the ground state should return to the ground state by emitting light of wavelength

$$\lambda = \frac{c}{f} = \frac{hc}{hf} = \frac{hc}{eV_0} = 253 \text{ nm}$$

There is indeed a line of this wavelength in the mercury spectrum. When the tube is viewed with a spectroscope, this line is seen when V_0 is greater than 4.9 eV, while no lines are seen when V_0 is less than this amount. For further increases in V_0 , additional sharp decreases in the current are observed, corresponding either to excitation of other levels in Hg (e.g., the second excited state of Hg is at 6.7 eV above the ground state) or to multiple excitations of the first excited state, i.e., due to an electron losing 4.9 eV more than once. In the usual setup, multiple excitations of the first level are observed and dips are seen every 4.9 V.²¹ The probability of observing such multiple first-level excitations, or excitations of other levels, depends on the detailed variation of the potential of the tube. For example, a second decrease in the current at $V_0 = 2 \times 4.9 = 9.8$ V results when electrons have inelastic collisions with Hg atoms about halfway between the cathode and grid (see Figure 4-22a). They are reaccelerated, reaching 4.9 eV again in the vicinity of the grid. A plot of the data of Franck and Hertz is shown in Figure 4-23.

The Franck-Hertz experiment was an important confirmation of the idea that discrete optical spectra were due to the existence in atoms of discrete energy levels that could be excited by nonoptical methods. It is particularly gratifying to be able to detect the existence of discrete energy levels directly by measurements using only voltmeters and ammeters.

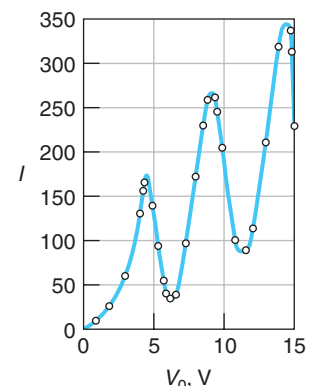
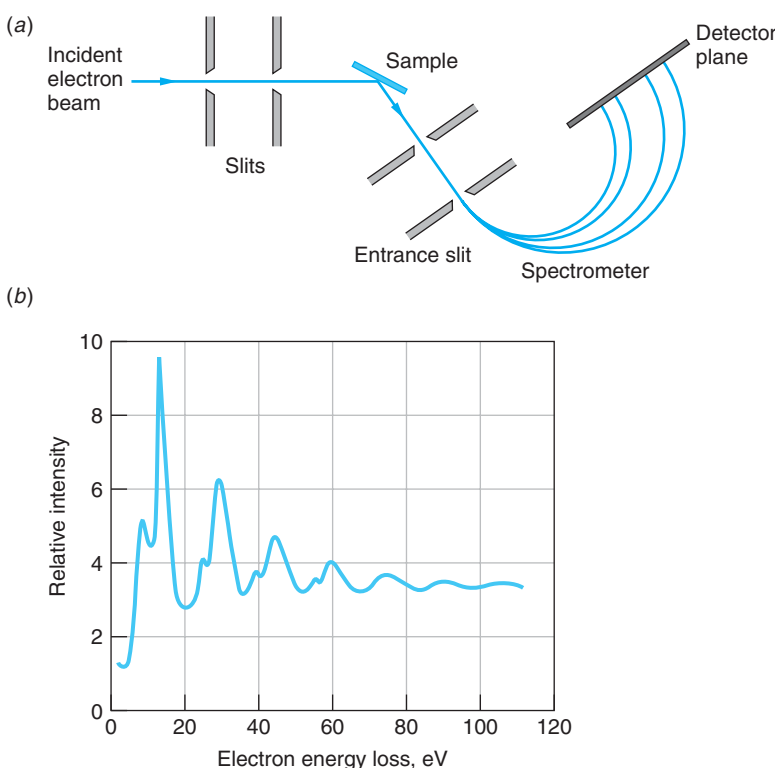


Figure 4-23 Current versus accelerating voltage in the Franck-Hertz experiment. The current decreases because many electrons lose energy due to inelastic collisions with mercury atoms in the tube and therefore cannot overcome the small back potential indicated in Figure 4-21a. The regular spacing of the peaks in this curve indicates that only a certain quantity of energy, 4.9 eV, can be lost to the mercury atoms. This interpretation is confirmed by the observation of radiation of photon energy 4.9 eV emitted by the mercury atoms, when V_0 is greater than this energy. [From J. Franck and G. Hertz, *Verband Deutscher Physikalischer Gesellschaften*, **16**, 457 (1914).]

Electron Energy Loss Spectroscopy

The Franck-Hertz experiment was the precursor of a highly sensitive technique for measuring the quantized energy states of atoms in both gases and solids. The technique, called *electron energy loss spectroscopy (EELS)*, is particularly useful in solids, where it makes possible measurement of the energy of certain types of lattice vibrations and other processes. It works like this. Suppose that the electrons in an incident beam all have energy E_{inc} . They collide with the atoms of a material, causing them to undergo some process (e.g., vibration, lattice rearrangement, electron excitation) that requires energy E_l . Then, if a beam electron initiates a single such process, it will exit the material with energy $E_{\text{inc}} - E_l$ —i.e., it has been inelastically scattered.

Figure 4-24 Energy-loss spectrum measurement. (a) A well-defined electron beam impinges upon the sample. Electrons inelastically scattered at a convenient angle enter the slit of the magnetic spectrometer, whose B field is directed out of the paper, and turn through radii R determined by their energy $E_{\text{inc}} - E_1$ via Equation 3-2 written in the form $R = [2m(E_{\text{inc}} - E_1)]^{1/2}/eB$. (b) An energy-loss spectrum for a thin Al film. [From C. J. Powell and J. B. Swan, *Physical Review*, **115**, 869 (1954).]



The exit energy can be measured very accurately with, e.g., a magnetic spectrometer designed for electrons.²² Figure 4-24a illustrates a typical experimental arrangement for measuring an energy-loss spectrum.

As an example of its application, if an incident beam of electrons with $E_{\text{inc}} = 2$ keV is reflected from a thin Al film, the scattered electron energies measured in the magnetic spectrometer result in the energy-loss spectrum shown in Figure 4-24b, which directly represents the quantized energy levels of the target material. The loss peaks in this particular spectrum are due to the excitation of harmonic vibrations in the thin film sample, as well as some surface vibrations. The technique is also used to measure the vibrational energies of impurity atoms that may be absorbed on the surface and, with higher incident electron energies, to measure energy losses at the atomic inner levels, thus yielding information about bonding and other characteristics of absorbed atoms. Inelastic scattering techniques, including those using particles in addition to electrons, provide very powerful means for probing the energy structure of atomic, molecular, and nuclear systems. We will have occasion to refer to them many times throughout the rest of the book.



More

Here and in Chapter 3 we have discussed many phenomena that were “explained” by various ad hoc quantum assumptions. A *Critique of Bohr Theory and the “Old Quantum Mechanics”* contrasts some of its successes with some of its failures on the Web page: whfreeman.com/modphysics5e.

FÉUE WHU

Summary

TOPIC

RELEVANT EQUATIONS AND REMARKS

1. Atomic spectra

$$\frac{1}{\lambda_{mn}} = R \left(\frac{1}{m^2} - \frac{1}{n^2} \right) \quad n > m \quad 4-2$$

This empirical equation computes the correct wavelengths of observed spectral lines. The Rydberg constant R varies in a regular way from element to element.

2. Rutherford scattering

Impact parameter $b = \frac{kq_\alpha Q}{m_\alpha v^2} \cot \frac{\theta}{2}$ 4-3

Scattered fraction $f = \pi b^2 nt$ 4-5

for a scattering foil with n nuclei/unit volume and thickness t

Number of scattered alphas observed $\Delta N = \left(\frac{I_0 A_{sc} nt}{r^2} \right) \left(\frac{kZe^2}{2E_k} \right)^2 \frac{1}{\sin^4 \frac{\theta}{2}}$ 4-6

Size of nucleus $r_d = \frac{kq_\alpha Q}{\frac{1}{2} m_\alpha v^2}$ 4-11

3. Bohr model

- Bohr's postulates
- Electrons occupy only certain nonradiating, stable, circular orbits selected by quantization of the angular momentum L .

$$L = mvr = \frac{n\hbar}{2\pi} = n\hbar \quad \text{for integer } n \quad 4-17$$

- Radiation of frequency f occurs when the electron jumps from an allowed orbit of energy E_i to one of lower energy E_f . f is given by the frequency condition

$$hf = E_i - E_f \quad 4-15$$

Correspondence principle

In the region of very large quantum numbers classical and quantum calculations must yield the same results.

Bohr radius $a_0 = \frac{\hbar^2}{mk^2e^2} = \frac{\hbar}{mc\alpha} = 0.0529 \text{ nm}$ 4-19

Allowed energies $E_n = -\frac{Z^2 E_0}{n^2} \quad \text{for } n = 1, 2, 3, \dots$ 4-20

where $E_0 = mk^2e^2/2\hbar^2 = 13.6 \text{ eV}$

Reduced mass $\mu = \frac{mM}{m + M}$ 4-25

Fine-structure constant $\alpha = \frac{ke^2}{\hbar c} \approx 1/137$ 4-30

| TOPIC | RELEVANT EQUATIONS AND REMARKS | |
|--------------------------------------|---|------|
| 4. X-ray spectra Moseley equation | $f^{1/2} = A_n(Z - b)$ | 4-34 |
| 5. Franck-Hertz experiment | Supported Bohr's theory by verifying the quantization of atomic energies in absorption. | |

General References

The following general references are written at a level appropriate for the readers of this book.

Boorse, H., and L. Motz (eds.), *The World of the Atom*, Basic Books, New York, 1966. This two-volume, 1873-page work is a collection of original papers, translated and edited. Much of the work referred to in this chapter and throughout this book can be found in these volumes.

Cline, B., *The Questioners: Physicists and the Quantum Theory*, Thomas Y. Crowell, New York, 1965.

Gamow, G., *Thirty Years That Shook Physics: The Story of the Quantum Theory*, Doubleday, Garden City, NY, 1965.

Herzberg, G., *Atomic Spectra and Atomic Structure*, Dover Publications, New York, 1944. This is without doubt one of the all-time classics of atomic physics.

Melissinos, A., and J. Napolitano, *Experiments in Modern Physics*, 2d ed., Academic Press, New York, 2003. Many of the classic experiments that are now undergraduate laboratory experiments are described in detail in this text.

Mohr, P. J., and B. N. Taylor, "The Fundamental Physical Constants," *Physics Today* (August 2004). Also available at <http://physicstoday.org/guide/fundcont.html>.

Shamos, M. H. (ed.), *Great Experiments in Physics*, Holt, Rinehart & Winston, New York, 1962.

Virtual Laboratory (PEARL), Physics Academic Software, North Carolina State University, Raleigh, 1996. Includes an interactive model of the Bohr atom.

Virtual Spectroscope, Physics Academic Software, North Carolina State University, Raleigh, 2003. Several sources can be viewed with a spectroscope to display the corresponding spectral lines.

Visual Quantum Mechanics, Kansas State University, Manhattan, 1996. The atomic spectra component of this software provides an interactive construction of the energy levels for several elements, including hydrogen and helium.

Notes

1. Joseph von Fraunhofer (1787–1826), German physicist. Although he was not the first to see the dark lines in the solar spectrum that bear his name (Wollaston had seen seven, 12 years earlier), he systematically measured their wavelengths, named the prominent ones, and showed that they always occurred at the same wavelength even if the sunlight were reflected from the moon or a planet.

2. To date, more than 10,000 Fraunhofer lines have been found in the solar spectrum.

3. Although experimentalists preferred to express their measurements in terms of wavelengths, it had been shown that the many empirical formulas being constructed to explain the observed regularities in the line spectra could be expressed in simpler form if the reciprocal wavelength, called the *wave number* and equal to the number of waves per unit length, was used instead. Since $c = f\lambda$, this was equivalent to expressing the formulas in terms of the frequency.

4. Ernest Rutherford (1871–1937), English physicist, an exceptional experimentalist and a student of J. J. Thomson. He was an early researcher in the field of radioactivity and received the Nobel Prize in 1908 for his work in the transmutation of

elements. He bemoaned the fact that his prize was awarded in chemistry, not in physics, as work with the elements was considered chemistry in those days. He was Thomson's successor as director of the Cavendish Laboratory.

5. Alpha particles, like all charged particles, lose energy by exciting and ionizing the molecules of the materials through which they are moving. The energy lost per unit path length ($-dE/dx$) is a function of the ionization potential of the molecules, the atomic number of the atoms, and the energy of the α particles. It can be computed (with some effort) and is relatively simple to measure experimentally.

6. Notice that $2\pi \sin \theta d\theta = d\Omega$, the differential solid angle subtended at the scattering nucleus by the surface in Figure 4-11. Since the cross section $\sigma = \pi b^2$, then $d\sigma = 2\pi b db$ and Equation 4-9 can be rewritten as

$$\frac{d\sigma}{d\Omega} = \left(\frac{kZe^2}{m_\alpha v^2} \right) \frac{1}{\sin^4(\theta/2)}$$

$d\sigma/d\Omega$ is called the *differential cross section*.

7. H. Geiger and E. Marsden, *Philosophical Magazine* (6), 25, 605 (1913).

8. The value of Z could not be measured directly in this experiment; however, relative values for different foil materials could be found and all materials heavier than aluminum had Z approximately equal to half the atomic weight.

9. This also introduces a deviation from the predicted ΔN associated with Rutherford's assumption that the nuclear mass was much larger than the α particle mass. For lighter-atomic-weight elements that assumption is not valid. Correction for the nuclear mass effect can be made, however, and the data in Figure 4-9b reflect the correction.

10. Niels H. D. Bohr (1885–1962), Danish physicist and first-rate soccer player. He went to the Cavendish Laboratory to work with J. J. Thomson after receiving his Ph.D.; however, Thomson is reported to have been impatient with Bohr's soft, accented English. Happily, the occasion of Thomson's annual birthday banquet brought Bohr in contact with Rutherford, whom he promptly followed to the latter's laboratory at Manchester, where he learned of the nuclear atom. A giant of twentieth-century physics, Bohr was awarded the Nobel Prize in 1922 for his explanation of the hydrogen spectrum. On a visit to the United States in 1939, he brought the news that the fission of uranium atoms had been observed. The story of his life makes absolutely fascinating reading.

11. N. Bohr, *Philosophical Magazine* (6), **26**, 1 (1913).

12. P. J. Mohr and B. N. Taylor, "The Fundamental Physical Constants," *Physics Today* (August 2004). Only 8 of the 14 current significant figures are given in Equation 4-27. The relative uncertainty in the value is about 1 part in 10^{12} !

13. Harold C. Urey (1893–1981), American chemist. His work opened the way for the use of isotopic tracers in biological systems. He was recognized with the Nobel Prize in 1934.

14. The basic reason that elliptical orbits solve this problem is that the frequency of the radiation emitted classically depends on the acceleration of the charge. The acceleration is constant for a circular orbit but varies for elliptical orbits, being dependent on the instantaneous distance from the focus. The energy of a particle in a circular orbit of radius r is the same as that of a particle in an elliptical orbit with a semimajor axis of r , so one would expect the only allowed elliptical orbits to be those whose semimajor axis was equal to an allowed Bohr circular orbit radius.

15. Viewed with spectrographs of high resolution, the spectral lines of hydrogen in Figure 4-2a—and, indeed, most spectral lines of all elements—are found to consist of very closely

spaced sets of lines, i.e., fine structure. We will discuss this topic in detail in Chapter 7.

16. Henry G.-J. Moseley (1887–1915), English physicist, considered by some the most brilliant of Rutherford's students. He would surely have been awarded the Nobel Prize had he not been killed in action in World War I. His father was a naturalist on the expedition of the HMS *Challenger*, the first vessel ever devoted to the exploration of the oceans.

17. The identifiers L and K were assigned by the English physicist C. G. Barkla, the discoverer of the characteristic x-ray lines, for which he received the Nobel Prize in 1917. He discovered two sets of x-ray lines for each of several elements, the longer wavelength of which he called the L series, the other the K series. The identifiers stuck and were subsequently used to label the atomic electron shells.

18. That the remaining K electron should result in $b = 1$, i.e., shielding of exactly $1e$, is perhaps a surprise. Actually it was a happy accident. It is the combined effect of the remaining K electron and the penetration of the electron waves of the outer L electrons that resulted in making $b = 1$, as we will see in Chapter 7.

19. Since in multielectron atoms the energies of the stationary states depend in part on the number of electrons in the atom (see Chapter 7), the energies E_n for a given atom change slightly when it is singly ionized, as in the production of characteristic x-ray lines, or doubly ionized, as in the Auger effect.

20. James Franck (1882–1964), German-American physicist; Gustav L. Hertz (1887–1975), German physicist. Franck won an Iron Cross as a soldier in World War I and later worked on the Manhattan Project. Hertz was a nephew of Heinrich Hertz, discoverer of the photoelectric effect. For their work on the inelastic scattering of electrons, Franck and Hertz shared the 1925 Nobel Prize in Physics.

21. We should note at this point that there is an energy state in the Hg atom at about 4.6 eV, slightly lower than the one found by Franck and Hertz. However, transitions from the ground state to the 4.6-eV level are not observed, and their absence is in accord with the prediction of more advanced quantum mechanics, as we will see in Chapter 7.

22. Since q/m for electrons is much larger than for ionized atoms, the radius for an electron magnetic spectrometer need not be as large as for a mass spectrometer, even for electron energies of several keV. (See Equation 3-2.)

Problems

Level I

Section 4-1 Atomic Spectra

4-1. Compute the wavelength and frequency of the series limit for the Lyman, Balmer, and Paschen spectral series of hydrogen.

4-2. The wavelength of a particular line in the Balmer series is measured to be 379.1 nm. What transition does it correspond to?

4-3. An astronomer finds a new absorption line with $\lambda = 164.1$ nm in the ultraviolet region of the Sun's continuous spectrum. He attributes the line to hydrogen's Lyman series. Is he right? Justify your answer.

4-4. The series of hydrogen spectral lines with $m = 4$ is called Brackett's series. Compute the wavelengths of the first four lines of Brackett's series.

4-5. In a sample that contains hydrogen, among other things, four spectral lines are found in the infrared with wavelengths 7460 nm, 4654 nm, 4103 nm, and 3741 nm. Which one does not belong to a hydrogen spectral series?

Section 4-2 Rutherford's Nuclear Model

4-6. A gold foil of thickness $2.0 \mu\text{m}$ is used in a Rutherford experiment to scatter α particles with energy 7.0 MeV. (a) What fraction of the particles will be scattered at angles greater than 90° ? (b) What fraction will be scattered at angles between 45° and 75° ? (c) Use N_A , ρ , and M for gold to compute the approximate radius of a gold atom. (For gold, $\rho = 19.3 \text{ g/cm}^3$ and $M = 197 \text{ g/mol}$.)

4-7. (a) What is the ratio of the number of particles per unit area on the screen scattered at 10° to those at 1° ? (b) What is the ratio of those scattered at 30° to those at 1° ?

4-8. For α particles of 7.7 MeV (those used by Geiger and Marsden), what impact parameter will result in a deflection of 2° for a thin gold foil?

4-9. What will be the distance of closest approach r_d to a gold nucleus for an α particle of 5.0 MeV? 7.7 MeV? 12 MeV?

4-10. What energy α particle would be needed to just reach the surface of an Al nucleus if its radius is 4 fm?

4-11. If a particle is deflected by 0.01° in each collision, about how many collisions would be necessary to produce an rms deflection of 10° ? (Use the result from the one-dimensional random walk problem in statistics stating that the rms deflection equals the magnitude of the individual deflections times the square root of the number of deflections.) Compare this result with the number of atomic layers in a gold foil of thickness 10^{-6} m , assuming that the thickness of each atom is $0.1 \text{ nm} = 10^{-10} \text{ m}$.

4-12. Consider the foil and α particle energy in Problem 4-6. Suppose that 1000 of those particles suffer a deflection of more than 25° . (a) How many of these are deflected by more than 45° ? (b) How many are deflected between 25° and 45° ? (c) How many are deflected between 75° and 90° ?

Section 4-3 The Bohr Model of the Hydrogen Atom

4-13. The radius of the $n = 1$ orbit in the hydrogen atom is $a_0 = 0.053 \text{ nm}$. (a) Compute the radius of the $n = 6$ orbit. (b) Compute the radius of the $n = 6$ orbit in singly ionized helium (He^+), which is hydrogen-like, i.e., it has only a single electron outside the nucleus.

4-14. Show that Equation 4-19 for the radius of the first Bohr orbit and Equation 4-20 for the magnitude of the lowest energy for the hydrogen atom can be written as

$$a_0 = \frac{hc}{\alpha mc^2} = \frac{\lambda_c}{2\pi\alpha} \quad E_1 = \frac{1}{2}\alpha^2 mc^2$$

where $\lambda_c = h/mc$ is the Compton wavelength of the electron and $\alpha = ke^2/hc$ is the fine-structure constant. Use these expressions to check the numerical values of the constants a_0 and E_1 .

4-15. Calculate the three longest wavelengths in the Lyman series ($n_f = 1$) in nm and indicate their position on a horizontal linear scale. Indicate the series limit (shortest wavelength) on this scale. Are any of these lines in the visible spectrum?

4-16. If the angular momentum of Earth in its motion around the Sun were quantized like a hydrogen electron according to Equation 4-17, what would Earth's quantum number be? How much energy would be released in a transition to the next lowest level? Would that energy release (presumably as a gravity wave) be detectable? What would be the radius of that orbit? (The radius of Earth's orbit is $1.50 \times 10^{11} \text{ m}$.)

4-17. On average, a hydrogen atom will exist in an excited state for about 10^{-8} sec before making a transition to a lower energy state. About how many revolutions does an electron in the $n = 2$ state make in 10^{-8} sec ?

4-18. An atom in an excited state will on average undergo a transition to a state of lower energy in about 10^{-8} seconds . If the electron in a doubly ionized lithium atom (Li^{+2} , which is hydrogenlike) is placed in the $n = 4$ state, about how many revolutions around the nucleus does it make before undergoing a transition to a lower energy state?

4-19. It is possible for a muon to be captured by a proton to form a muonic atom. A muon is identical to an electron except for its mass, which is $105.7 \text{ MeV}/c^2$. (a) Calculate the radius of the first Bohr orbit of a muonic atom. (b) Calculate the magnitude of the lowest energy state. (c) What is the shortest wavelength in the Lyman series for this atom?

4-20. In the lithium atom ($Z = 3$) two electrons are in the $n = 1$ orbit and the third is in the $n = 2$ orbit. (Only two are allowed in the $n = 1$ orbit because of the exclusion principle, which will be discussed in Chapter 7.) The interaction of the inner electrons with the outer one can be approximated by writing the energy of the outer electron as

$$E = -Z'^2(E_1/n^2)$$

where $E_1 = 13.6 \text{ eV}$, $n = 2$, and Z' is the effective nuclear charge, which is less than 3 because of the screening effect of the two inner electrons. Using the measured ionization energy of 5.39 eV , calculate Z' .

4-21. Draw to careful scale an energy-level diagram for hydrogen for levels with $n = 1, 2, 3, 4, \infty$. Show the following on the diagram: (a) the limit of the Lyman series, (b) the H_β line, (c) the transition between the state whose binding energy (= energy needed to remove the electron from the atom) is 1.51 eV and the state whose excitation energy is 10.2 eV , and (d) the longest wavelength line of the Paschen series.

4-22. A hydrogen atom at rest in the laboratory emits the Lyman α radiation. (a) Compute the recoil kinetic energy of the atom. (b) What fraction of the excitation energy of the $n = 2$ state is carried by the recoiling atom? (Hint: Use conservation of momentum.)

4-23. (a) Draw accurately to scale and label completely a partial energy-level diagram for C^{5+} , including at minimum the energy levels for $n = 1, 2, 3, 4, 5$, and ∞ . (b) Compute the wavelength of the spectral line resulting from the $n = 3$ to the $n = 2$ transition, the $C^{5+}H_\alpha$ line. (c) In what part of the EM spectrum does this line lie?

4-24. The electron-positron pair that was discussed in Chapter 2 can form a hydrogenlike system called *positronium*. Calculate (a) the energies of the three lowest states and (b) the wavelength of the Lyman α and β lines. (Detection of those lines is a “signature” of positronium formation.)

4-25. With the aid of tunable lasers, Rydberg atoms of sodium have been produced with $n \approx 100$. The resulting atomic diameter would correspond in hydrogen to $n \approx 600$. (a) What would be the diameter of a hydrogen atom whose electron is in the $n \approx 600$ orbit? (b) What would be the speed of the electron in that orbit? (c) How does the result in (b) compare with the speed in the $n \approx 1$ orbit?

Section 4-4 X-Ray Spectra

4-26. (a) Calculate the next two longest wavelengths in the K series (after the K_α line) of molybdenum. (b) What is the wavelength of the shortest wavelength in this series?

4-27. The wavelength of the K_α x-ray line for an element is measured to be 0.0794 nm . What is the element?

4-28. Moseley pointed out that elements with atomic numbers 43, 61, and 75 should exist and (at that time) had not been found. (a) Using Figure 4-19, what frequencies would Moseley's graphical data have predicted for the K_α x ray for each of these elements? (b) Compute the wavelengths for these lines predicted by Equation 4-37.

4-29. What is the approximate radius of the $n = 1$ orbit of gold ($Z = 79$)? Compare this with the radius of the gold nucleus, about 7.1 fm .

4-30. An electron in the K shell of Fe is ejected by a high-energy electron in the target of an x-ray tube. The resulting hole in the $n = 1$ shell could be filled by an electron from the $n = 2$ shell, the L shell; however, instead of emitting the characteristic $Fe\ K_\alpha$ x ray, the atom ejects an Auger electron from the $n = 2$ shell. Using Bohr theory, compute the energy of the Auger electron.

4-31. In a particular x-ray tube, an electron approaches the target moving at $2.25 \times 10^8 \text{ m/s}$. It slows down on being deflected by a nucleus of the target, emitting a photon of energy 32.5 keV . Ignoring the nuclear recoil, but not relativity, compute the final speed of the electron.

4-32. (a) Compute the energy of an electron in the $n = 1$ (K shell) of tungsten, using $Z - 1$ for the effective nuclear charge. (b) The experimental result for this energy is 69.5 keV . Assume that the effective nuclear charge is $Z - \sigma$, where σ is called the screening constant, and calculate σ from the experimental result.

4-33. Construct a Moseley plot similar to Figure 4-19 for the K_{β} x rays of the elements listed below (the x-ray energies are given in keV):

| | | | |
|----------|----------|----------|----------|
| Al 1.56 | Ar 3.19 | Sc 4.46 | Fe 7.06 |
| Ge 10.98 | Kr 14.10 | Zr 17.66 | Ba 36.35 |

Determine the slope of your plot, and compare it with the K_{β} line in Figure 4-19.

Section 4-5 The Franck-Hertz Experiment

4-34. Suppose that, in a Franck-Hertz experiment, electrons of energy up to 13.0 eV can be produced in the tube. If the tube contained atomic hydrogen, (a) what is the shortest-wavelength spectral line that could be emitted from the tube? (b) List all of the hydrogen lines that can be emitted by this tube.

4-35. Using the data in Figure 4-24b and a good ruler, draw a carefully scaled energy-level diagram covering the range from 0 eV to 60 eV for the vibrational states of this solid. What approximate energy is typical of the transitions between adjacent levels corresponding to the larger of each pair of peaks?

4-36. The transition from the first excited state to the ground state in potassium results in the emission of a photon with $\lambda = 770$ nm. If potassium vapor is used in a Franck-Hertz experiment, at what voltage would you expect to see the first decrease in current?

4-37. If we could somehow fill a Franck-Hertz tube with positronium, what cathode-grid voltage would be needed to reach the second current decrease in the positronium equivalent of Figure 4-23? (See Problem 4-24.)

4-38. Electrons in the Franck-Hertz tube can also have elastic collisions with the Hg atoms. If such a collision is a head-on, what fraction of its initial kinetic energy will an electron lose, assuming the Hg atom to be at rest? If the collision is not head-on, will the fractional loss be greater or less than this?

Level II

4-39. Derive Equation 4-8 along the lines indicated in the paragraph that immediately precedes it.

4-40. Geiger and Marsden used α particles with 7.7-MeV kinetic energy and found that when they were scattered from thin gold foil, the number observed to be scattered at all angles agreed with Rutherford's formula. Use this fact to compute an upper limit on the radius of the gold nucleus.

4-41. (a) The current i due to a charge q moving in a circle with frequency f_{rev} is $q f_{\text{rev}}$. Find the current due to the electron in the first Bohr orbit. (b) The magnetic moment of a current loop is iA , where A is the area of the loop. Find the magnetic moment of the electron in the first Bohr orbit in units $\text{A}\cdot\text{m}^2$. This magnetic moment is called a *Bohr magneton*.

4-42. Use a spreadsheet to calculate the wavelengths (in nm) of the first five spectral lines of the Lyman, Balmer, Paschen, and Brackett series of hydrogen. Show the positions of these lines on a linear scale and indicate which ones lie in the visible.

4-43. Show that a small change in the reduced mass of the electron produces a small change in a spectral line given by $\Delta\lambda/\lambda = \Delta\mu/\mu$. Use this to calculate the difference $\Delta\lambda$ in the Balmer red line $\lambda = 656.3$ nm between hydrogen and deuterium, which has a nucleus with twice the mass of hydrogen.

4-44. Consider the Franck-Hertz experiment with Hg vapor in the tube and the voltage between the cathode and the grid equal to 4.0 V, i.e., not enough for the electrons to excite the Hg atom's first excited state. Therefore, the electron-Hg atom collisions are elastic. (a) If the kinetic energy of the electrons is E_k , show that the maximum kinetic energy that a recoiling Hg atom can have is approximately $4mE_k/M$, where M is the Hg atom mass. (b) What is the approximate maximum kinetic energy that can be lost by an electron with $E_k = 2.5$ eV?

4-45. The Li^{2+} ion is essentially identical to the H atom in Bohr's theory, aside from the effect of the different nuclear charges and masses. (a) What transitions in Li^{2+} will yield emission lines whose wavelengths are very nearly equal to the first two lines of the Lyman series in hydrogen?

(b) Calculate the difference between the wavelength of the Lyman α line of hydrogen and the emission line from Li^{2+} that has very nearly the same wavelength.

4-46. In an α scattering experiment, the area of the α particle detector is 0.50 cm^2 . The detector is located 10 cm from a $1.0\text{-}\mu\text{m}$ -thick silver foil. The incident beam carries a current of 1.0 nA , and the energy of each α particle is 6.0 MeV . How many α particles will be counted per second by the detector at (a) $\theta = 60^\circ$? (b) $\theta = 120^\circ$?

4-47. The K_α , L_α , and M_α x rays are emitted in the $n = 2 \rightarrow n = 1$, $n = 3 \rightarrow n = 2$, and $n = 4 \rightarrow n = 3$ transitions, respectively. For calcium ($Z = 20$) the energies of these transitions are 3.69 keV , 0.341 keV , and 0.024 keV , respectively. Suppose that energetic photons impinging on a calcium surface cause ejection of an electron from the K shell of the surface atoms. Compute the energies of the Auger electrons that may be emitted from the L , M , and N shells ($n = 2, 3$, and 4) of the sample atoms, in addition to the characteristic x rays.

4-48. Figure 3-15b shows the K_α and K_β characteristic x rays emitted by a molybdenum (Mo) target in an x-ray tube whose accelerating potential is 35 kV . The wavelengths are $K_\alpha = 0.071 \text{ nm}$ and $K_\beta = 0.063 \text{ nm}$. (a) Compute the corresponding energies of these photons. (b) Suppose we wish to prepare a beam consisting primarily of K_α x rays by passing the molybdenum x rays through a material that absorbs K_β x rays more strongly than K_α x rays by photoelectric effect on K -shell electrons of the material. Which of the materials listed in the accompanying table with their K -shell binding energies would you choose? Explain your answer.

| Element | Zr | Nb | Mo | Tc | Ru |
|-------------|-------|-------|-------|-------|-------|
| Z | 40 | 41 | 42 | 43 | 44 |
| E_K (keV) | 18.00 | 18.99 | 20.00 | 21.04 | 22.12 |

Level III

4-49. A small shot of negligible radius hits a stationary smooth, hard sphere of radius R , making an angle β with the normal to the sphere, as shown in Figure 4-25. It is reflected at an equal angle to the normal. The scattering angle is $\theta = 180^\circ - 2\beta$, as shown. (a) Show by the geometry of the figure that the impact parameter b is related to θ by $b = R \cos \frac{1}{2}\theta$. (b) If the incoming intensity of the shot is I_0 particles/s \cdot area, how many are scattered through angles greater than θ ? (c) Show that the cross section for scattering through angles greater than 0° is πR^2 . (d) Discuss the implication of the fact that the Rutherford cross section for scattering through angles greater than 0° is infinite.

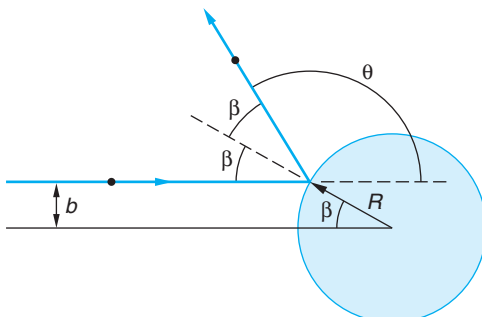


Figure 4-25 Small particle scattered by a hard sphere of radius R .

4-50. Singly ionized helium He^+ is hydrogenlike. (a) Construct a carefully scaled energy-level diagram for He^+ similar to that in Figure 4-16, showing the levels for $n = 1, 2, 3, 4, 5$, and ∞ . (b) What is the ionization energy of He^+ ? (c) Compute the difference in wavelength between each of the first two lines of the Lyman series of hydrogen and the first two lines of the He^+ Balmer series. Be sure to include the reduced mass correction for both atoms. (d) Show that for every spectral line of hydrogen, He^+ has a spectral line of very nearly the same wavelength. (Mass of $\text{He}^+ = 6.65 \times 10^{-27} \text{ kg}$.)

4-51. Listed in the table are the L_{α} x-ray wavelengths for several elements. Construct a Moseley plot from these data. Compare the slope with the appropriate one in Figure 4-19. Determine and interpret the intercept on your graph, using a suitably modified version of Equation 4-35.

| Element | P | Ca | Co | Kr | Mo | I |
|-----------------|-------|------|------|------|------|------|
| Z | 15 | 20 | 27 | 36 | 42 | 53 |
| Wavelength (nm) | 10.41 | 4.05 | 1.79 | 0.73 | 0.51 | 0.33 |

4-52. In this problem you are to obtain the Bohr results for the energy levels in hydrogen without using the quantization condition of Equation 4-17. In order to relate Equation 4-14 to the Balmer-Ritz formula, assume that the radii of allowed orbits are given by $r_n = n^2 r_0$, where n is an integer and r_0 is a constant to be determined. (a) Show that the frequency of radiation for a transition to $n_f = n - 1$ is given by $f \approx kZe^2/hr_0 n^3$ for large n . (b) Show that the frequency of revolution is given by

$$f_{\text{rev}}^2 = \frac{kZe^2}{4\pi^2 mr_0^3 n^6}$$

(c) Use the correspondence principle to determine r_0 and compare with Equation 4-19.

4-53. Calculate the energies and speeds of electrons in circular Bohr orbits in a hydrogenlike atom using the relativistic expressions for kinetic energy and momentum.

4-54. (a) Write a computer program for your personal computer or programmable calculator that will provide you with the spectral series of H-like atoms. Inputs to be included are n_i , n_f , Z , and the nuclear mass M . Outputs are to be the wavelengths and frequencies of the first six lines and the series limit for the specified n_f , Z , and M . Include the reduced mass correction. (b) Use the program to compute the wavelengths and frequencies of the Balmer series. (c) Pick an $n_f > 100$, name the series the [your name] series, and use your program to compute the wavelengths and frequencies of the first three lines and the limit.

4-55. Figure 4-26 shows an energy loss spectrum for He measured in an apparatus such as that shown in Figure 4-24a. Use the spectrum to construct and draw carefully to scale an energy-level diagram for He.

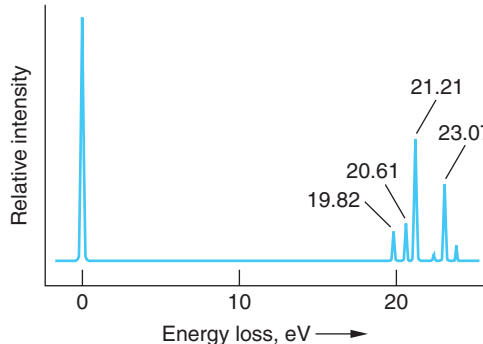
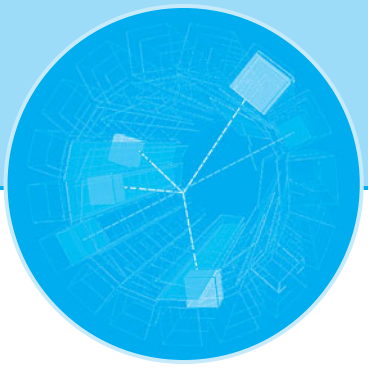


Figure 4-26 Energy-loss spectrum of helium. Incident electron energy was 34 eV. The elastically scattered electrons cause the peak at 0 eV.

4-56. If electric charge did not exist and electrons were bound to protons by the gravitational force to form hydrogen, derive the corresponding expressions for a_0 and E_n and compute the energy and frequency of the H_{α} line and the limit of the Balmer series. Compare these with the corresponding quantities for “real” hydrogen.

4-57. A sample of hydrogen atoms are all in the $n = 5$ state. If all the atoms return to the ground state, how many different photon energies will be emitted, assuming all possible transitions occur? If there are 500 atoms in the sample and assuming that from any state all possible downward transitions are equally probable, what is the total number of photons that will be emitted when all of the atoms have returned to the ground state?

4-58. Consider muonic atoms (see Problem 4-19). (a) Draw a correctly scaled and labeled partial energy level diagram including levels with $n = 1, 2, 3, 4, 5$, and ∞ for muonic hydrogen. (b) Compute the radius of the $n = 1$ muon orbit in muonic H, He^{1+} , Al^{12+} , and Au^{78+} . (c) Compare the results in (b) with the radii of these nuclei. (d) Compute the wavelength of the photon emitted in the $n = 2$ to $n = 1$ transition for each of these muonic atoms.



The Wavelike Properties of Particles

In 1924, a French graduate student, Louis de Broglie,¹ proposed in his doctoral dissertation that the dual—i.e., wave-particle—behavior that was by then known to exist for radiation was also a characteristic of matter, in particular, electrons. This suggestion was highly speculative, since there was yet no experimental evidence whatsoever for any wave aspects of electrons or any other particles. What had led him to this seemingly strange idea? It was a “bolt out of the blue,” like Einstein’s “happy thought” that led to the principle of equivalence (see Chapter 2). De Broglie described it with these words:

After the end of World War I, I gave a great deal of thought to the theory of quanta and to the wave-particle dualism. . . . It was then that I had a sudden inspiration. Einstein's wave-particle dualism was an absolutely general phenomenon extending to all physical nature.²

Since the visible universe consists entirely of matter and radiation, de Broglie's hypothesis is a fundamental statement about the grand symmetry of nature. (There is currently strong observational evidence that ordinary matter makes up only about 4 percent of the visible universe. About 22 percent is some unknown form of invisible “dark matter,” and approximately 74 percent consists of some sort of equally mysterious “dark energy.” See Chapter 13.)

5-1 The de Broglie Hypothesis

De Broglie stated his proposal mathematically with the following equations for the frequency and wavelength of the electron waves, which are referred to as the *de Broglie relations*:

$$f = \frac{E}{h} \quad 5-1$$

$$\lambda = \frac{h}{p} \quad 5-2$$

where E is the total energy, p is the momentum, and λ is called the *de Broglie wavelength* of the particle. For photons, these same equations result directly from

| | |
|--|------------|
| 5-1 The de Broglie Hypothesis | 185 |
| 5-2 Measurements of Particle Wavelengths | 187 |
| 5-3 Wave Packets | 196 |
| 5-4 The Probabilistic Interpretation of the Wave Function | 202 |
| 5-5 The Uncertainty Principle | 205 |
| 5-6 Some Consequences of the Uncertainty Principle | 208 |
| 5-7 Wave-Particle Duality | 212 |

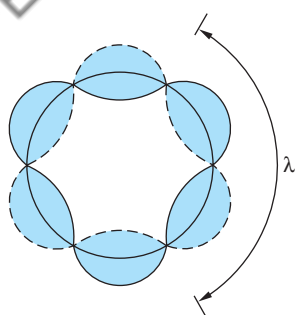


Figure 5-1 Standing waves around the circumference of a circle. In this case the circle is 3λ in circumference. If the vibrator were, for example, a steel ring that had been suitably tapped with a hammer, the shape of the ring would oscillate between the extreme positions represented by the solid and broken lines.

Einstein's quantization of radiation $E = hf$ and Equation 2-31 for a particle of zero rest energy $E = pc$ as follows:

$$E = pc = hf = \frac{hc}{\lambda}$$

By a more indirect approach using relativistic mechanics, de Broglie was able to demonstrate that Equations 5-1 and 5-2 also apply to particles with mass. He then pointed out that these equations lead to a physical interpretation of Bohr's quantization of the angular momentum of the electron in hydrogenlike atoms, namely, that the quantization is equivalent to a standing-wave condition. (See Figure 5-1.) We have

$$mv r = n\hbar = \frac{nh}{2\pi} \quad \text{for } n = \text{integer}$$

$$2\pi r = \frac{nh}{mv} = \frac{nh}{p} = n\lambda = \text{circumference of orbit} \quad 5-3$$

The idea of explaining discrete energy states in matter by standing waves thus seemed quite promising.

De Broglie's ideas were expanded and developed into a complete theory by Erwin Schrödinger late in 1925. In 1927, C. J. Davisson and L. H. Germer verified the de Broglie hypothesis directly by observing interference patterns, a characteristic of waves, with electron beams. We will discuss both Schrödinger's theory and the Davisson-Germer experiment in later sections, but first we have to ask ourselves why wavelike behavior of matter had not been observed before de Broglie's work. We can understand why if we first recall that the wave properties of light were not noticed either until apertures or slits with dimensions of the order of the wavelength of light could be obtained. This is because the wave nature of light is not evident in experiments where the primary dimensions of the apparatus are large compared with the wavelength of the light used. For example, if A represents the diameter of a lens or the width of a slit, then diffraction effects³ (a manifestation of wave properties) are limited to angles θ around the forward direction ($\theta = 0^\circ$) where $\sin \theta = \lambda/A$. In geometric (ray) optics $\lambda/A \rightarrow 0$, so $\theta \approx \sin \theta \rightarrow 0$, too. However, if a characteristic

Louis V. de Broglie,
who first suggested
that electrons might
have wave properties.
[Courtesy of
Culver Pictures.]



dimension of the apparatus becomes of the order of (or smaller than) λ , the wavelength of light passing through the system, then $\lambda/A \rightarrow 1$. In that event $\theta \approx \lambda/A$ is readily observable, and the wavelike properties of light become apparent. Because Planck's constant is so small, the wavelength given by Equation 5-2 is extremely small for any macroscopic object. This point is among those illustrated in the following section.

5-2 Measurements of Particle Wavelengths

Although we now have diffraction systems of nuclear dimensions, the smallest-scale systems to which de Broglie's contemporaries had access were the spacings between the planes of atoms in crystalline solids, about 0.1 nm. This means that even for an extremely small macroscopic particle, such as a grain of dust ($m \approx 0.1$ mg) moving through air with the average kinetic energy of the atmospheric gas molecules, the smallest diffraction systems available would have resulted in diffraction angles τ only of the order of 10^{-10} radian, far below the limit of experimental detectability. The small magnitude of Planck's constant ensures that λ will be smaller than any readily accessible aperture, placing diffraction beyond the limits of experimental observation. For objects whose momenta are larger than that of the dust particle, the possibility of observing *particle*, or *matter waves*, is even less, as the following example illustrates.

EXAMPLE 5-1 De Broglie Wavelength of a Ping-Pong Ball What is the de Broglie wavelength of a Ping-Pong ball of mass 2.0 g after it is slammed across the table with speed 5 m/s?

SOLUTION

$$\begin{aligned}\lambda &= \frac{h}{mv} = \frac{6.63 \times 10^{-34} \text{ J} \cdot \text{s}}{(2.0 \times 10^{-3} \text{ kg})(5 \text{ m/s})} \\ &= 6.6 \times 10^{-32} \text{ m} = 6.6 \times 10^{-23} \text{ nm}\end{aligned}$$

This is 17 orders of magnitude smaller than typical nuclear dimensions, far below the dimensions of any possible aperture.

The case is different for low-energy electrons, as de Broglie himself realized. At his *soutenance de thèse* (defense of the thesis), de Broglie was asked by Perrin⁴ how his hypothesis could be verified, to which he replied that perhaps passing particles, such as electrons, through very small slits would reveal the waves. Consider an electron that has been accelerated through V_0 volts. Its kinetic energy (nonrelativistic) is then

$$E = \frac{p^2}{2m} = eV_0$$

Solving for p and substituting into Equation 5-2,

$$\lambda = \frac{h}{p} = \frac{hc}{pc} = \frac{hc}{(2mc^2eV_0)^{1/2}}$$

Using $hc = 1.24 \times 10^3 \text{ eV} \cdot \text{nm}$ and $mc^2 = 0.511 \times 10^6 \text{ eV}$, we obtain

$$\lambda = \frac{1.226}{V_0^{1/2}} \text{ nm} \quad \text{for} \quad eV_0 \sim mc^2 \quad 5-4$$

The following example computes an electron de Broglie wavelength, giving a measure of just how small the slit must be.

EXAMPLE 5-2 De Broglie Wavelength of a Slow Electron Compute the de Broglie wavelength of an electron whose kinetic energy is 10 eV.

SOLUTION

1. The de Broglie wavelength is given by Equation 5-2:

$$\lambda = \frac{h}{p}$$

2. *Method 1:* Since a 10-eV electron is nonrelativistic, we can use the classical relation connecting the momentum and the kinetic energy:

$$E_k = \frac{p^2}{2m}$$

or

$$\begin{aligned} p &= \sqrt{2mE_k} \\ &= \sqrt{(2)(9.11 \times 10^{-31} \text{ kg})(10 \text{ eV})(1.60 \times 10^{-19} \text{ J/eV})} \\ &= 1.71 \times 10^{-24} \text{ kg} \cdot \text{m/s} \end{aligned}$$

3. Substituting this result into Equation 5-2:

$$\begin{aligned} \lambda &= \frac{6.63 \times 10^{-34} \text{ J} \cdot \text{s}}{1.71 \times 10^{-24} \text{ kg} \cdot \text{m/s}} \\ &= 3.88 \times 10^{-10} \text{ m} = 0.39 \text{ nm} \end{aligned}$$

4. *Method 2:* The electron's wavelength can also be computed from Equation 5-4 with $V_0 = 10 \text{ V}$:

$$\begin{aligned} \lambda &= \frac{1.226}{V^{1/2}} = \frac{1.226}{\sqrt{10}} \\ &= 0.39 \text{ nm} \end{aligned}$$

Remarks: Though this wavelength is small, it is just the order of magnitude of the size of an atom and of the spacing of atoms in a crystal.

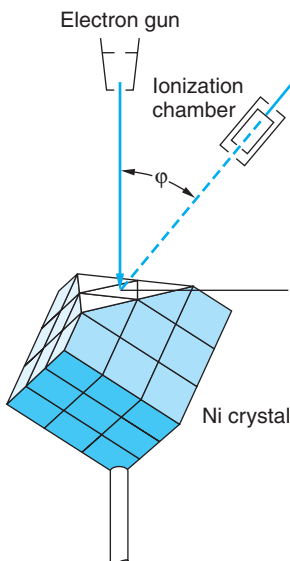


Figure 5-2 The Davisson-Germer experiment. Low-energy electrons scattered at angle ϕ from a nickel crystal are detected in an ionization chamber. The kinetic energy of the electrons could be varied by changing the accelerating voltage on the electron gun.

The Davisson-Germer Experiment

In a brief note in the August 14, 1925, issue of the journal *Naturwissenschaften*, Walter Elsasser, at the time a student of J. Franck's (of the Franck-Hertz experiment), proposed that the wave effects of low-velocity electrons might be detected by scattering them from single crystals. The first such measurements of the wavelengths of electrons were made in 1927 by C. J. Davisson⁵ and L. H. Germer, who were studying electron reflection from a nickel target at Bell Telephone Laboratories, unaware of either Elsasser's suggestion or de Broglie's work. After heating their target to remove an oxide coating that had accumulated during an accidental break in their vacuum system, they found that the scattered electron intensity as a function of the scattering angle showed maxima and minima. The surface atoms of their nickel target had, in the process of cooling, formed relatively large single crystals, and they were observing electron diffraction. Recognizing the importance of their accidental discovery, they then prepared a target consisting of a single crystal of nickel and extensively investigated the scattering of electrons from it. Figure 5-2 illustrates their experimental arrangement. Their data for 54-eV electrons, shown in Figure 5-3, indicate a strong maximum of scattering at $\phi = 50^\circ$. Consider the scattering from a set of Bragg

FÉUE WH

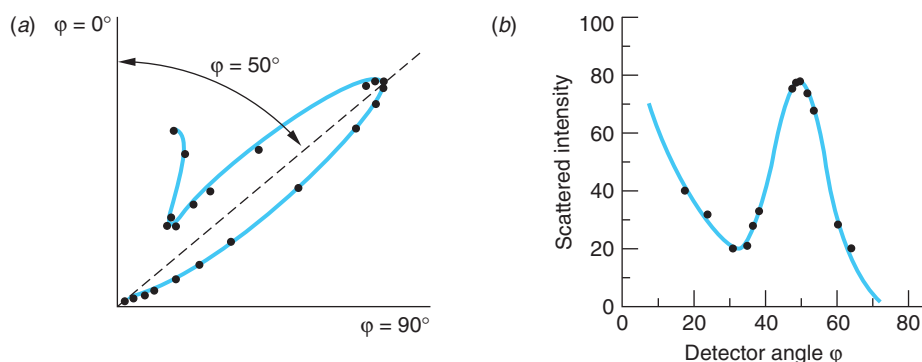


Figure 5-3 Scattered intensity vs. detector angle for 54-eV electrons. (a) Polar plot of the data. The intensity at each angle is indicated by the distance of the point from the origin. Scattering angle ϕ is plotted clockwise starting at the vertical axes. (b) The same data plotted on a Cartesian graph. The intensity scales are arbitrary but the same on both graphs. In each plot there is maximum intensity at $\phi = 50^\circ$, as predicted for Bragg scattering of waves having wavelength $\lambda = h/p$. [From Nobel Prize Lectures: Physics (Amsterdam and New York: Elsevier, © Nobel Foundation, 1964).]

planes, as shown in Figure 5-4. The Bragg condition for constructive interference is $n\lambda = 2d \sin \theta = 2d \cos \alpha$. The spacing of the Bragg planes d is related to the spacing of the atoms D by $d = D \sin \alpha$; thus

$$n\lambda = 2D \sin \alpha \cos \alpha = D \sin 2\alpha$$

or

$$n\lambda = D \sin \varphi \quad 5-5$$

where $\varphi = 2\alpha$ is the scattering angle.

The spacing D for Ni is known from x-ray diffraction to be 0.215 nm. The wavelength calculated from Equation 5-5 for the peak observed at $\varphi = 50^\circ$ by Davisson and Germer is, for $n = 1$,

$$\lambda = 0.215 \sin 50^\circ = 0.165 \text{ nm}$$

The value calculated from the de Broglie relation for 54-eV electrons is

$$\lambda = \frac{1.226}{(54)^{1/2}} = 0.167 \text{ nm}$$

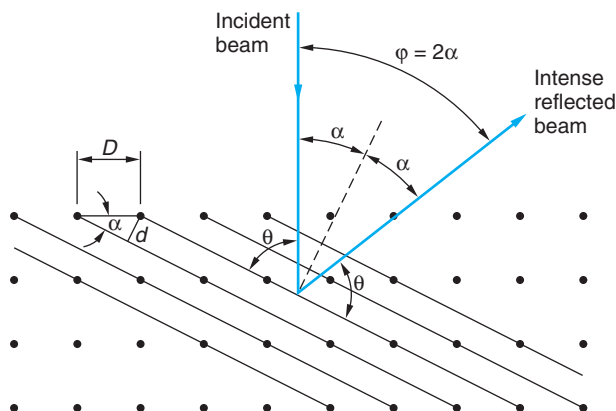


Figure 5-4 Scattering of electrons by a crystal. Electron waves are strongly scattered if the Bragg condition $n\lambda = 2d \sin \theta$ is met. This is equivalent to the condition $n\lambda = D \sin \varphi$.

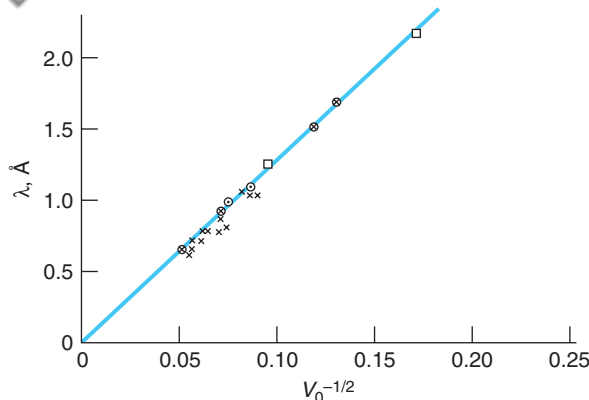


Figure 5-5 Test of the de Broglie formula $\lambda = h/p$. The wavelength is computed from a plot of the diffraction data plotted against $V_0^{-1/2}$, where V_0 is the accelerating voltage. The straight line is $1.226V_0^{-1/2}$ nm as predicted from $\lambda = h(2mE)^{-1/2}$. These are the data referred to in the quotation from Davisson's Nobel lecture. (× From observations with diffraction apparatus; ⊗ same, particularly reliable; □ same, grazing beams. ○ From observations with reflection apparatus.) [From Nobel Prize Lectures: Physics (Amsterdam and New York: Elsevier, © Nobel Foundation, 1964).]

The agreement with the experimental observation is excellent! With this spectacular result Davisson and Germer then conducted a systematic study to test the de Broglie relation using electrons up to about 400 eV and various experimental arrangements. Figure 5-5 shows a plot of measured wavelengths versus $V_0^{-1/2}$. The wavelengths measured by diffraction are slightly lower than the theoretical predictions because the refraction of the electron waves at the crystal surface has been neglected. We have seen from the photoelectric effect that it takes work of the order of several eV to remove an electron from a metal. Electrons entering a metal thus gain kinetic energy; therefore, their de Broglie wavelength is slightly less inside the crystal.⁶

A subtle point must be made here. Notice that the wavelength in Equation 5-5 depends only on D , the interatomic spacing of the crystal, whereas our derivation of that equation included the interplane spacing as well. The fact that the structure of the crystal really is essential shows up when the energy is varied, as was done in collecting the data for Figure 5-5. Equation 5-5 suggests that a change in λ , resulting from a change in the energy, would mean only that the diffraction maximum would occur at some other value of φ such that the equation remains satisfied. However, as can be seen from examination of

Figure 5-4, the value of φ is determined by α , the angle

of the planes determined by the crystal structure. Thus, if there are no crystal planes making an angle $\alpha = \varphi/2$ with the surface, then setting the detector at $\varphi = \sin^{-1}(\lambda/D)$ will not result in constructive interference and strong reflection for that value of λ , even though Equation 5-5 is satisfied. This is neatly illustrated by Figure 5-6, which shows a series of polar graphs (like Figure 5-3a) for electrons of energies from 36 eV through 68 eV. The building to a strong reflection at $\varphi = 50^\circ$ is evident for $V_0 = 54$ V, as we have already seen. But Equation 5-5 by itself would also lead us to expect, for example, a strong reflection at $\varphi = 64^\circ$ when $V_0 = 40$ V, which obviously does not occur.

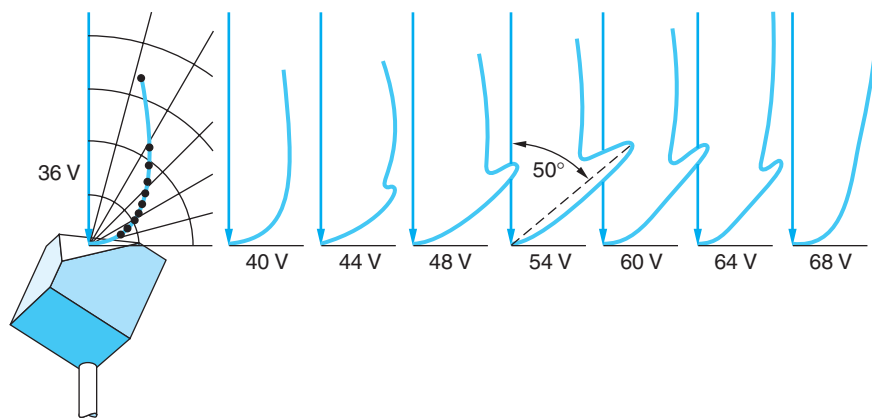


Figure 5-6 A series of polar graphs of Davisson and Germer's data at electron accelerating potentials from 36 V to 68 V. Note the development of the peak at $\varphi = 50^\circ$ to a maximum when $V_0 = 54$ V.



Clinton J. Davisson (left) and Lester H. Germer at Bell Laboratories, where electron diffraction was first observed. [Bell Telephone Laboratories, Inc.]

In order to show the dependence of the diffraction on the inner atomic layers, Davisson and Germer kept the detector angle φ fixed and varied the accelerating voltage rather than search for the correct angle for a given λ . Writing Equation 5-5 as

$$\lambda = \frac{D \sin \varphi}{n} = \frac{D \sin(2\alpha)}{n} \quad 5-6$$

and noting that $\lambda \propto V_0^{-1/2}$, a graph of intensity versus $V_0^{1/2} (\propto 1/\lambda)$ for a given angle φ should yield (1) a series of equally spaced peaks corresponding to successive values of the integer n , if $\alpha = \varphi/2$ is an existing angle for atomic planes, or (2) no diffraction peaks if $\varphi/2$ is not such an angle. Their measurements verified the dependence upon the interplane spacing, the agreement with the prediction being about ± 1 percent. Figure 5-7 illustrates the results for $\varphi = 50^\circ$. Thus, Davisson and Germer showed conclusively that particles with mass moving at speeds $v \ll c$ do indeed have wavelike properties, as de Broglie had proposed.

The diffraction pattern formed by high-energy electron waves scattered from nuclei provides a means by which nuclear radii and the internal distribution of the nuclear charge (the protons) are measured. See Chapter 11.

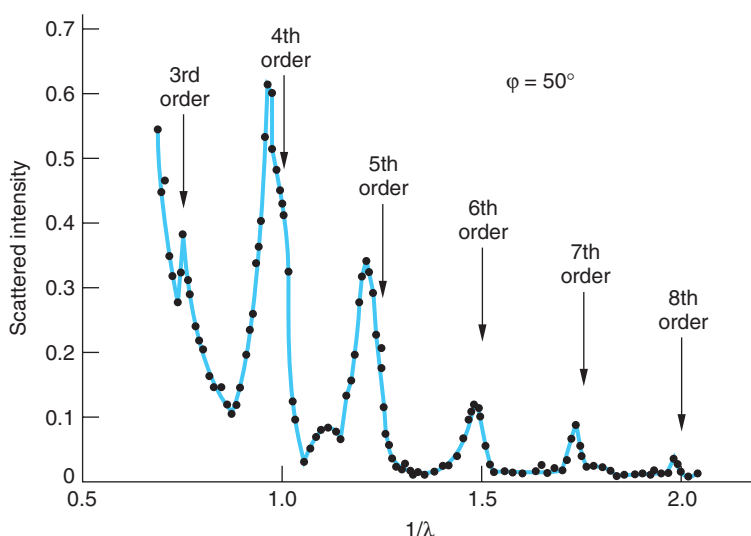


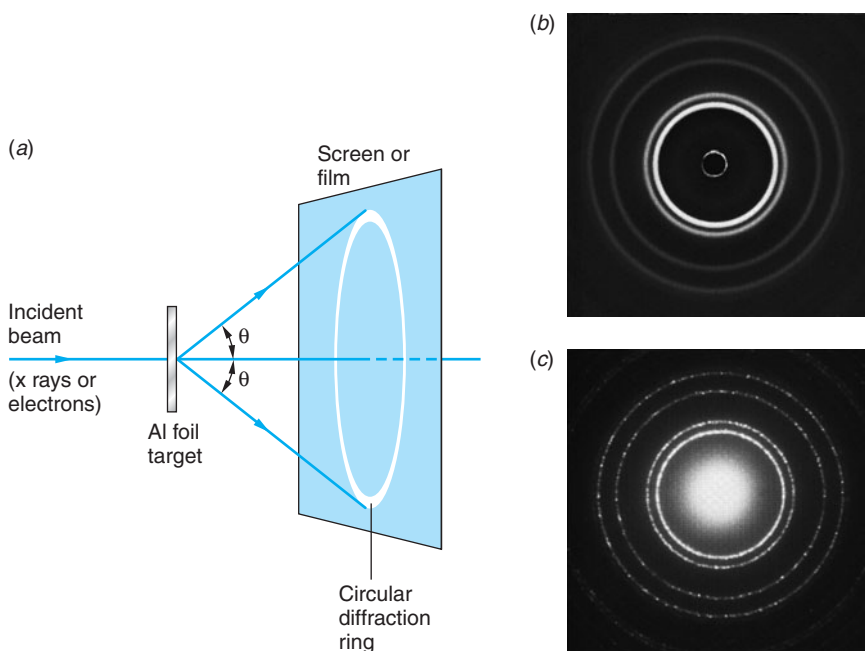
Figure 5-7 Variation of the scattered electron intensity with wavelength for constant φ . The incident beam in this case was 10° from the normal, the resulting refraction causing the measured peaks to be slightly shifted from the positions computed from Equation 5-5, as explained in note 6. [After C. J. Davisson and L. H. Germer, *Proceedings of the National Academy of Sciences*, **14**, 619 (1928).]

Here is Davisson's account of the connection between de Broglie's predictions and their experimental verification:

Perhaps no idea in physics has received so rapid or so intensive development as this one. De Broglie himself was in the van of this development, but the chief contributions were made by the older and more experienced Schrödinger. It would be pleasant to tell you that no sooner had Elsasser's suggestion appeared than the experiments were begun in New York which resulted in a demonstration of electron diffraction—pleasanter still to say that the work was begun the day after copies of de Broglie's thesis reached America. The true story contains less of perspicacity and more of chance... It was discovered, purely by accident, that the intensity of elastic scattering [of electrons] varies with the orientations of the scattering crystals. Out of this grew, quite naturally, an investigation of elastic scattering by a single crystal of predetermined orientation... Thus the New York experiment was not, at its inception, a test of wave theory. Only in the summer of 1926, after I had discussed the investigation in England with Richardson, Born, Franck and others, did it take on this character.⁷

A demonstration of the wave nature of relativistic electrons was provided in the same year by G. P. Thomson, who observed the transmission of electrons with energies in the range of 10 to 40 keV through thin metallic foils (G. P. Thomson, the son of J. J. Thomson, shared the Nobel Prize in 1937 with Davisson). The experimental arrangement (Figure 5-8a) was similar to that used to obtain Laue patterns with x rays (see Figure 3-11). Because the metal foil consists of many tiny crystals randomly oriented, the diffraction pattern consists of concentric rings. If a crystal is oriented at an angle θ with the incident beam, where θ satisfies the Bragg condition, this crystal will strongly scatter at an equal angle θ ; thus there will be a scattered beam making an angle 2θ with the incident beam. Figure 5-8b and c show the similarities in patterns produced by x rays and electron waves.

Figure 5-8 (a) Schematic arrangement used for producing a diffraction pattern from a polycrystalline aluminum target. (b) Diffraction pattern produced by x rays of wavelength 0.071 nm and an aluminum foil target. (c) Diffraction pattern produced by 600-eV electrons (de Broglie wavelength of about 0.05 nm) and an aluminum foil target. The pattern has been enlarged by 1.6 times to facilitate comparison with (b). [Courtesy of Film Studio, Education Development Center.]



Diffraction of Other Particles

The wave properties of neutral atoms and molecules were first demonstrated by O. Stern and I. Estermann in 1930 with beams of helium atoms and hydrogen molecules diffracted from a lithium fluoride crystal. Since the particles are neutral, there is no possibility of accelerating them with electrostatic potentials. The energy of the molecules was that of their average thermal motion, about 0.03 eV, which implies a de Broglie wavelength of about 0.10 nm for these molecules, according to Equation 5-2. Because of their low energy, the scattering occurs just from the array of atoms on the surface of the crystal, in contrast to Davisson and Germer's experiment. Figure 5-9 illustrates the geometry of the surface scattering, the experimental arrangement, and the results. Figure 5-9c indicates clearly the diffraction of He atom waves.

Since then, diffraction of other atoms, of protons, and of neutrons has been observed (see Figures 5-10, 5-11, and 5-12 on page 194). In all cases the measured wavelengths agree with de Broglie's prediction. There is thus no doubt that all matter has wavelike, as well as particlelike, properties, in symmetry with electromagnetic radiation.

The diffraction patterns formed by helium atom waves are used to study impurities and defects on the surfaces of crystals. Being a noble gas, helium does not react chemically with molecules on the surface nor "stick" to the surface.

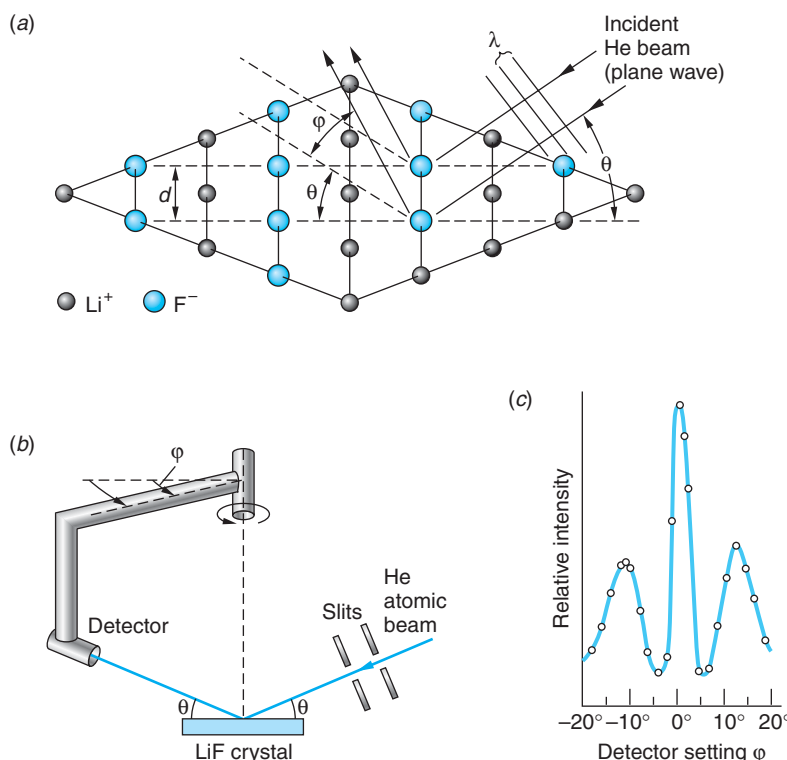


Figure 5-9 (a) He atoms impinge upon the surface of the LiF crystal at angle θ ($\theta = 18.5^\circ$ in Estermann and Stern's experiment). The reflected beam also makes the same angle θ with the surface but is also scattered at azimuthal angles φ relative to an axis perpendicular to the surface. (b) The detector views the surface at angle θ but can scan through the angle φ . (c) At angle φ where the path difference ($d \sin \varphi$) between adjacent "rays" is $n\lambda$, constructive interference, i.e., a diffraction peak, occurs. The $n = 1$ peaks occur on either side of the $n = 0$ maximum.

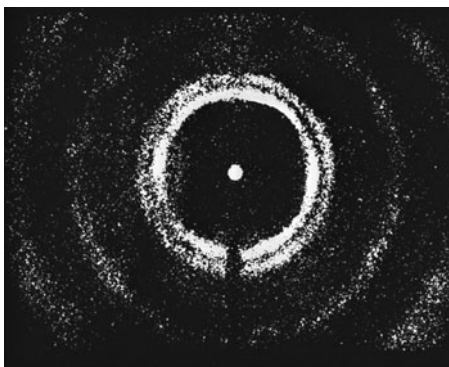


Figure 5-10 Diffraction pattern produced by 0.0568-eV neutrons (de Broglie wavelength of 0.120 nm) and a target of polycrystalline copper. Note the similarity in the patterns produced by x rays, electrons, and neutrons. [Courtesy of C. G. Shull.]

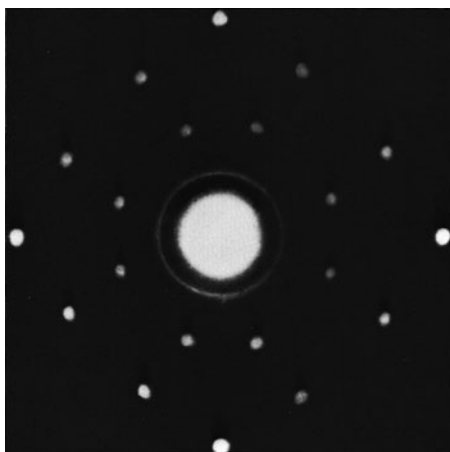


Figure 5-11 Neutron Laue pattern of NaCl. Compare this with the x-ray Laue pattern in Figure 3-14. [Courtesy of E. O. Wollan and C. G. Shull.]

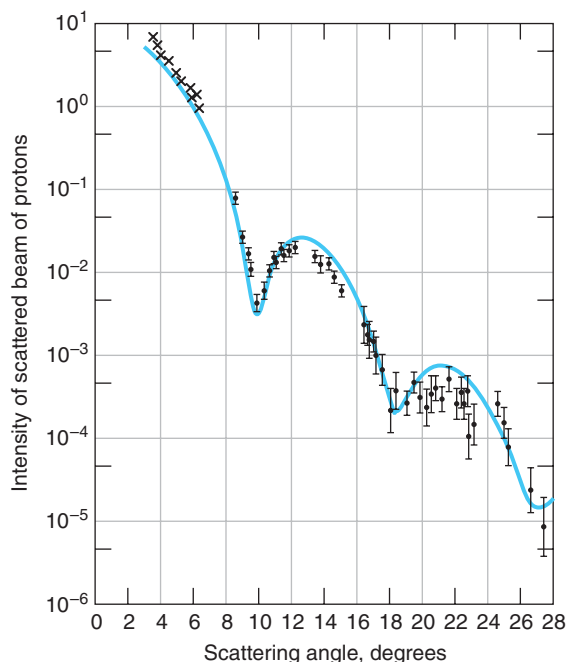


Figure 5-12 Nuclei provide scatterers whose dimensions are of the order of 10^{-15} m. Here the diffraction of 1-GeV protons from oxygen nuclei result in a pattern similar to that of a single slit.

An Easy Way to Determine de Broglie Wavelengths

It is frequently helpful to know the de Broglie wavelength for particles with a specific kinetic energy. For low energies where relativistic effects can be ignored, the equation leading to Equation 5-4 can be rewritten in terms of the kinetic energy as follows:

$$\lambda = \frac{h}{p} = \frac{h}{\sqrt{2mE_k}} \quad 5-7$$

To find the equivalent expression that covers both relativistic and nonrelativistic speeds, we begin with the relativistic equation relating the total energy to the momentum:

$$E^2 = (pc)^2 + (mc^2)^2 \quad 2-31$$

Writing E_0 for the rest energy mc^2 of the particle for convenience, this becomes

$$E^2 = (pc)^2 + E_0^2 \quad 5-8$$

Since the total energy $E = E_0 + E_k$, Equation 5-8 becomes

$$(E_0 + E_k)^2 = (pc)^2 + E_0^2$$

that, when solved for p , yields

$$p = \frac{(2E_0E_k + E_k^2)^{1/2}}{c}$$

from which Equation 5-2 gives

$$\lambda = \frac{hc}{(2E_0E_k + E_k^2)^{1/2}} \quad 5-9$$

This can be written in a particularly useful way applicable to any particle of any energy by dividing the numerator and denominator by the rest energy $E_0 = mc^2$ as follows:

$$\lambda = \frac{hc/mc^2}{(2E_0E_k + E_k^2)^{1/2}/E_0} = \frac{h/mc}{[2(E_k/E_0) + (E_k/E_0)^2]^{1/2}}$$

Recognizing h/mc as the Compton wavelength λ_c of the particle of mass m (see Section 3-4), we have that, for any particle,

$$\frac{\lambda}{\lambda_c} = \frac{1}{[2(E_k/E_0) + (E_k/E_0)^2]^{1/2}} \quad 5-10$$

A log-log graph of λ/λ_c versus E_k/E_0 is shown in Figure 5-13. It has two sections of nearly constant slope, one for $E_k \ll mc^2$ and the other for $E_k \gg mc^2$, connected by a curved portion lying roughly between $0.1 < E_k/E_0 < 10$. The following example illustrates the use of Figure 5-13.

EXAMPLE 5-3 The de Broglie Wavelength of a Cosmic Ray Proton Detectors on board a satellite measure the kinetic energy of a cosmic ray proton to be 150 GeV. What is the proton's de Broglie wavelength, as read from Figure 5-13?

SOLUTION

The rest energy of the proton is $mc^2 = 0.938$ GeV and the proton's mass is 1.67×10^{-27} kg. Thus, the ratio E_k/E_0 is

$$\frac{E_k}{E_0} = \frac{150 \text{ GeV}}{0.938 \text{ GeV}} = 160$$

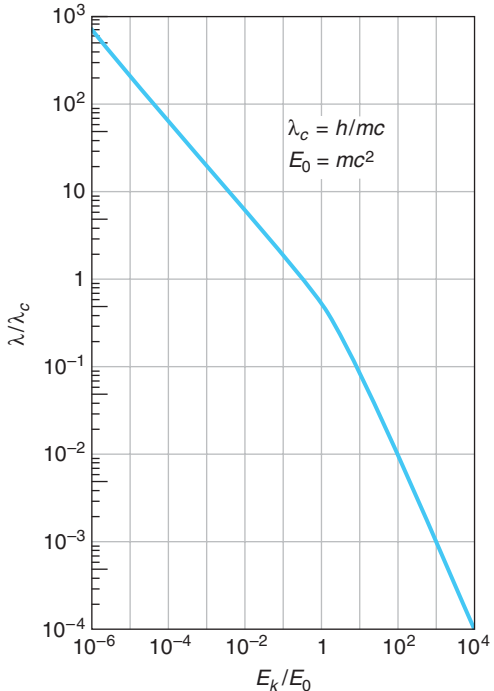


Figure 5-13 The de Broglie wavelength λ expressed in units of the Compton wavelength λ_c for a particle of mass m versus the kinetic energy of the particle E_k expressed in units of its rest energy $E_0 = mc^2$. For protons and neutrons $E_0 = 0.938$ GeV and $\lambda_c = 1.32$ fm. For electrons $E_0 = 0.511$ MeV and $\lambda_c = 0.00234$ nm.

This value on the curve corresponds to about 6×10^{-3} on the λ/λ_c axis. The Compton wavelength of the proton is

$$\lambda_c = \frac{h}{mc} = \frac{6.63 \times 10^{-34} \text{ J}\cdot\text{s}}{(1.67 \times 10^{-27} \text{ kg})(3 \times 10^8 \text{ m/s})} = 1.32 \times 10^{-15} \text{ m}$$

and we have then for the particle's de Broglie wavelength

$$\lambda = (6 \times 10^{-3})(1.32 \times 10^{-15} \text{ m}) = 7.9 \times 10^{-18} \text{ m} = 7.9 \times 10^{-3} \text{ fm}$$

Questions

1. Since the electrons used by Davisson and Germer were low energy, they penetrated only a few atomic layers into the crystal, so it is rather surprising that the effects of the inner layers shows so clearly. What feature of the diffraction is most affected by the relatively shallow penetration?
2. How might the frequency of de Broglie waves be measured?
3. Why is it not reasonable to do crystallographic studies with protons?

5-3 Wave Packets

In any discussion of waves the question arises, “What’s waving?” For some waves the answer is clear: for waves on the ocean, it is the water that “waves”; for sound waves in air, it is the molecules that make up the air; for light, it is the E and the B . So what is waving for matter waves? For matter waves as for light waves, there is no “ether.” As will be developed in this section and the next, for matter it is the *probability of finding the particle* that waves.

Classical waves are solutions of the classical *wave equation*

$$\frac{\partial^2 y}{\partial x^2} = \frac{1}{v^2} \frac{\partial^2 y}{\partial t^2} \quad 5-11$$

Important among classical waves is the *harmonic wave* of amplitude y_0 , frequency f , and period T , traveling in the $+x$ direction as written here:

$$y(x, t) = y_0 \cos(kx - \omega t) = y_0 \cos 2\pi \left(\frac{x}{\lambda} - \frac{t}{T} \right) = y_0 \cos \frac{2\pi}{\lambda} (x - vt) \quad 5-12$$

where the *angular frequency* ω and the *wave number*⁸ k are defined by

$$\omega = 2\pi f = \frac{2\pi}{T} \quad 5-13a$$

and

$$k = \frac{2\pi}{\lambda} \quad 5-13b$$

and the velocity v of the wave, the so-called *wave* or *phase velocity* v_p , is given by

$$v_p = f\lambda \quad 5-14$$

A familiar wave phenomenon that cannot be described by a single harmonic wave is a pulse, such as the flip of one end of a long string (Figure 5-14), a sudden noise, or the brief opening of a shutter in front of a light source. The main characteristic of a pulse is localization in time and space. A single harmonic wave is not localized in either time or space. The description of a pulse can be obtained by the superposition of a group of harmonic waves of different frequencies and wavelengths. Such a group is called a *wave packet*. The mathematics of representing arbitrarily shaped pulses by sums of sine or cosine functions involves Fourier series and Fourier integrals. We will illustrate the phenomenon of wave packets by considering some simple and somewhat artificial examples and discussing the general properties qualitatively. Wave groups are particularly important because a wave description of a particle must include the important property of localization.

Consider a simple group consisting of only two waves of equal amplitude and nearly equal frequencies and wavelengths. Such a group occurs in the phenomenon of beats and is described in most introductory textbooks. The quantities k , ω , and v are related to one another via Equations 5-13 and 5-14. Let the wave numbers be k_1 and k_2 , the angular frequencies ω_1 and ω_2 , and the speeds v_1 and v_2 . The sum of the two waves is

$$y(x, t) = y_0 \cos(k_1 x - \omega_1 t) + y_0 \cos(k_2 x - \omega_2 t)$$

which, with the use of a bit of trigonometry, becomes

$$y(x, t) = 2y_0 \cos\left(\frac{\Delta k}{2}x - \frac{\Delta \omega}{2}t\right) \cos\left(\frac{k_1 + k_2}{2}x - \frac{\omega_1 + \omega_2}{2}t\right)$$

where $\Delta k = k_2 - k_1$ and $\Delta \omega = \omega_2 - \omega_1$. Since the two waves have nearly equal values of k and ω , we will write $\bar{k} = (k_1 + k_2)/2$ and $\bar{\omega} = (\omega_1 + \omega_2)/2$ for the mean values. The sum is then

$$y(x, t) = 2y_0 \cos\left(\frac{1}{2}\Delta k x - \frac{1}{2}\Delta \omega t\right) \cos(\bar{k}x - \bar{\omega}t) \quad 5-15$$

Figure 5-15 shows a sketch of $y(x, t_0)$ versus x at some time t_0 . The dashed curve is the envelope of the group of two waves, given by the first cosine term in Equation 5-15. The wave within the envelope moves with the speed $\bar{\omega}/\bar{k}$, the phase velocity v_p due to the second cosine term. If we write the first (amplitude-modulating) term as $\cos[\frac{1}{2}\Delta k[x - (\Delta \omega/\Delta k)t]]$, we see that the envelope moves with speed $\Delta \omega/\Delta k$. The speed of the envelope is called the *group velocity* v_g .

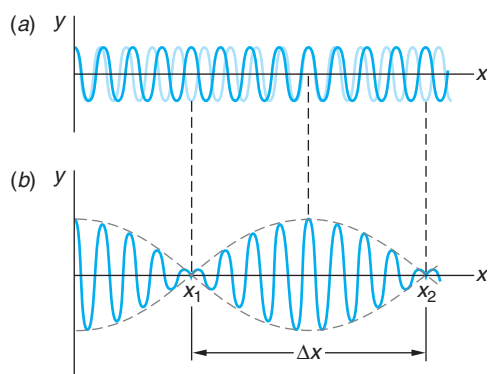


Figure 5-15 Two waves of slightly different wavelength and frequency produce beats. (a) Shows $y(x)$ at a given instant for each of the two waves. The waves are in phase at the origin, but because of the difference in wavelength, they become out of phase and then in phase again. (b) The sum of these waves. The spatial extent of the group Δx is inversely proportional to the difference in wave numbers Δk , where k is related to the wavelength by $k = 2\pi/\lambda$. Identical figures are obtained if y is plotted versus time t at a fixed point x . In that case the extent in time Δt is inversely proportional to the frequency difference $\Delta\omega$.

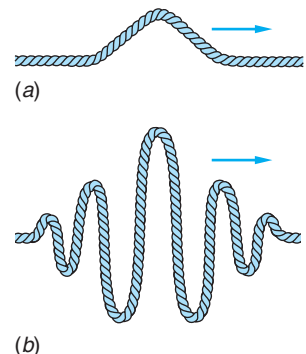


Figure 5-14 (a) Wave pulse moving along a string. A pulse has a beginning and an end; i.e., it is localized, unlike a pure harmonic wave, which goes on forever in space and time. (b) A wave packet formed by the superposition of harmonic waves.

A more general wave packet can be constructed if, instead of adding just two sinusoidal waves as in Figure 5-15, we superpose a larger, finite number with slightly different wavelengths and different amplitudes. For example, Figure 5-16a illustrates the superposing of seven cosines with wavelengths from $\lambda_9 = 1/9$ to $\lambda_{15} = 1/15$ (wave numbers from $k_9 = 18\pi$ to $k_{15} = 30\pi$) at time t_0 . The waves are all in phase at $x = 0$ and again at $x = \pm 12, x = \pm 24, \dots$. Their sum $y(x, t_0) = \sum_{i=9}^{15} y_i(x, t_0)$

oscillates with maxima at those values of x , decreasing and increasing at other values as a result of the changing phases of the waves (see Figure 5-16b). Now, if we superpose an infinite number of waves from the same range of wavelengths and wave numbers as in Figure 5-16 with infinitesimally different values of k , the central group around $x = 0$ will be essentially the same as in that figure. However, the additional groups will no longer be present since there is now no length along the x axis into which an exactly integral number of all of the infinite number of component waves can fit. Thus, we have formed a single wave packet throughout this (one-dimensional) space.

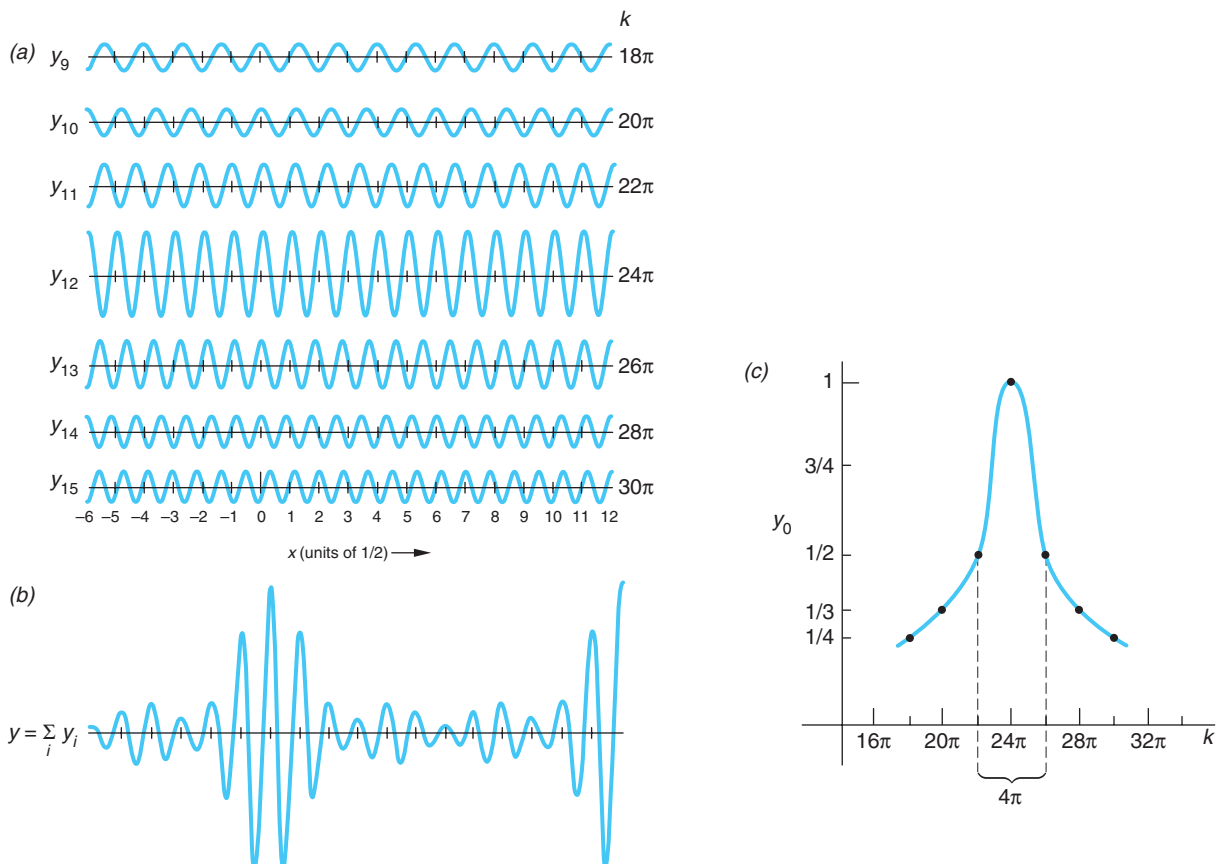


Figure 5-16 (a) Superposition of seven sinusoids $y_k(x, t) = y_{0k} \cos(kx - \omega t)$ with uniformly spaced wave numbers ranging from $k = (2\pi)9$ to $k = (2\pi)15$ with $t = 0$. The maximum amplitude is 1 at the center of the range ($k = (2\pi)12$), decreasing to $1/2, 1/3$, and $1/4$, respectively, for the waves on each side of the central wave. (b) The sum $y(x, 0) = \sum_{i=9}^{15} y_i(x, 0)$ is maximum at $x = 0$ with additional maxima equally spaced along the $\pm x$ axis. (c) Amplitudes of the sinusoids y_i versus wave number k .

This packet moves at the group velocity $v_g = d\omega/dk$. The mathematics needed to demonstrate the above involves use of the Fourier integral described in the Classical Concept Review.

The phase velocities of the individual harmonic waves are given by Equation 5-14:

$$v_p = f\lambda = \left(\frac{\omega}{2\pi}\right)\left(\frac{2\pi}{k}\right) = \frac{\omega}{k}$$



Writing this as $\omega = kv_p$, the relation between the group and phase velocities is given by Equation 5-16:

$$v_g = \frac{d\omega}{dk} = v_p + k \frac{dv_p}{dk} \quad 5-16$$

If the phase velocity is the same for all frequencies and wavelengths, then $dv_p/dk = 0$, and the group velocity is the same as the phase velocity. A medium for which the phase velocity is the same for all frequencies is said to be *nondispersive*. Examples are waves on a perfectly flexible string, sound waves in air, and electromagnetic waves in a vacuum. An important characteristic of a nondispersive medium is that, since all the harmonic waves making up a packet move with the same speed, the packet maintains its shape as it moves; thus, it does not change its shape in time. Conversely, if the phase velocity is different for different frequencies, the shape of the pulse will change as it travels. In that case the group velocity and phase velocity are not the same. Such a medium is called a *dispersive* medium; examples are water waves, waves on a wire that is not perfectly flexible, light waves in a medium such as glass or water in which the index of refraction has a slight dependence on frequency, and electron waves. It is the speed of the packet, the group velocity v_g , that is normally seen by an observer.

Classical Uncertainty Relations

Notice that the width of the group⁹ Δx of the superposition $y(x, t_0)$ in Figure 5-16b is just a bit larger than 1/12. Similarly, the graph of the amplitude of these waves versus k has width $\Delta k = 4\pi$, which is a bit more than 12 (Figure 5-16c), so we see that

$$\Delta k \Delta x \sim 1 \quad 5-17$$

By a similar analysis, we would also conclude that

$$\Delta\omega \Delta t \sim 1 \quad 5-18$$

The range of wavelengths or frequencies of the harmonic waves needed to form a wave packet depends on the extent in space and duration in time of the pulse. In general, if the extent in space Δx is to be small, the range Δk of wave numbers must be large. Similarly, if the duration in time Δt is small, the range of frequencies $\Delta\omega$ must be large. We have written these as order-of-magnitude equations because the exact value of the products $\Delta k \Delta x$ and $\Delta\omega \Delta t$ depends on how these ranges are defined, as well as on the particular shape of the packets. Equation 5-18 is sometimes known as the *response time-bandwidth* relation, expressing the result that a circuit component such as an amplifier must have a large bandwidth ($\Delta\omega$) if it is to be able to respond to signals of short duration.

The classical uncertainty relations define the range of signal frequencies to which all kinds of communications equipment and computer systems must respond, from cell phones to supercomputers.

There is a slight variation of Equation 5-17 that is also helpful in interpreting the relation between Δx and Δk . Differentiating the wave number in Equation 5-13b yields

$$dk = \frac{-2\pi d\lambda}{\lambda^2} \quad 5-19$$

Replacing the differentials by small intervals and concerning ourselves only with magnitudes, Equation 5-19 becomes

$$\Delta k = \frac{2\pi \Delta \lambda}{\lambda^2}$$

which when substituted into Equation 5-17 gives

$$\Delta x \Delta \lambda \approx \frac{\lambda^2}{2\pi} \quad 5-20$$

Equation 5-20 says that the product of the spatial extent of a classical wave Δx and the uncertainty (or “error”) in the determination of its wavelength $\Delta \lambda$ will always be of the order of $\lambda^2/2\pi$. The following brief examples will illustrate the meaning of Equations 5-17 and 5-18, often referred to as the *classical uncertainty relations*, and Equation 5-20.

EXAMPLE 5-4 $\Delta\lambda$ for Ocean Waves Standing in the middle of a 20-m-long pier, you notice that at any given instant there are 15 wave crests between the two ends of the pier. Estimate the minimum uncertainty in the wavelength that could be computed from this information.

SOLUTION

1. The minimum uncertainty $\Delta \lambda$ in the wavelength is given by Equation 5-20:

$$\Delta x \Delta \lambda = \frac{\lambda^2}{2\pi}$$

2. The wavelength λ of the waves is

$$\lambda = \frac{20 \text{ m}}{15 \text{ waves}} = 1.3 \text{ m}$$

3. The spatial extent of the waves used for this calculation is:

$$\Delta x = 20 \text{ m}$$

4. Solving Equation 5-20 for $\Delta \lambda$ and substituting these values gives

$$\begin{aligned} \Delta \lambda &= \frac{\lambda^2}{2\pi \Delta x} = \frac{(1.3)^2}{2\pi \times 20} \\ &= 0.013 \text{ m} \\ \Delta \lambda &\approx 0.01 \text{ m} = 1 \text{ cm} \end{aligned}$$

Remarks: This is the minimum uncertainty. Any error that may exist in the measurement of the number of wave crests and the length of the pier would add further uncertainty to the determination of λ .

EXAMPLE 5-5 Frequency Control The frequency of the alternating voltage produced at electric generating stations is carefully maintained at 60.00 Hz. The frequency is monitored on a digital frequency meter in the control room. For how long must the frequency be measured and how often can the display be updated if the reading is to be accurate to within 0.01 Hz?

SOLUTION

Since $\omega = 2\pi f$, then $\Delta\omega = 2\pi\Delta f = 2\pi(0.01)$ rad/s and

$$\Delta t \sim 1/\Delta\omega = 1/2\pi(0.01)$$

$$\Delta t \sim 16 \text{ s}$$

Thus, the frequency must be measured for about 16 s if the reading is to be accurate to 0.01 Hz and the display cannot be updated more often than once every 16 s.

Questions

4. Which is more important for communication, the group velocity or the phase velocity?
5. What are Δx and Δk for a purely harmonic wave of a single frequency and wavelength?

Particle Wave Packets

The quantity analogous to the displacement $y(x, t)$ for waves on a string, to the pressure $P(x, t)$ for a sound wave, or to the electric field $\mathcal{E}(x, t)$ for electromagnetic waves is called the *wave function for particles* and is usually designated $\Psi(x, t)$. It is $\Psi(x, t)$ that we will relate to the probability of finding the particle and, as we alerted you earlier, it is the probability that waves. Consider, for example, an electron wave consisting of a single frequency and wavelength; we could represent such a wave by any of the following, exactly as we did the classical wave: $\Psi(x, t) = A \cos(kx - \omega t)$, $\Psi(x, t) = A \sin(kx - \omega t)$, or $\Psi(x, t) = Ae^{i(kx - \omega t)}$.

The phase velocity for this wave is given by

$$v_p = f\lambda = (E/h)(h/p) = E/p$$

where we have used the de Broglie relations for the wavelength and frequency. Using the nonrelativistic expression for the energy of a particle moving in free space, i.e., no potential energy (with no forces acting upon it),

$$E = \frac{1}{2}mv^2 = \frac{p^2}{2m}$$

we see that the phase velocity is

$$v_p = E/p = (p^2/2m)/p = p/2m = v/2$$

i.e., the phase velocity of the wave is half the velocity of an electron with momentum p . The phase velocity does *not* equal the particle velocity. Moreover, a wave of a single frequency and wavelength is not localized but is spread throughout space, which makes it difficult to see how the particle and wave properties of the electron could be related.

An application of phase and particle speeds by nature:
produce a wave on a still pond (or in a bathtub) and watch the wavelets that make up the wave appear to "climb over" the wave crest at twice the speed of the wave.

Thus, for the electron to have the particle property of being localized, the matter waves of the electron must also be limited in spatial extent—i.e., realistically, $\Psi(x, t)$ must be a wave packet containing many more than one wave number k and frequency ω . It is the wave packet $\Psi(x, t)$ that we expect to move at a group velocity equal to the particle velocity, which we will show below is indeed the case. The particle, if observed, we will expect to find somewhere within the spatial extent of the wave packet $\Psi(x, t)$, precisely where within that space being the subject of the next section.

To illustrate the equality of the group velocity v_g and the particle velocity v , it is convenient to express de Broglie's relations in a slightly different form. Writing Equation 5-1 as follows,

$$E = hf = h\omega/2\pi \quad \text{or} \quad E = \hbar\omega \quad 5-21$$

and Equation 5-2 as

$$p = \frac{h}{\lambda} = \frac{h}{2\pi/k} = \frac{\hbar k}{2\pi} \quad \text{or} \quad p = \hbar k \quad 5-22$$

The group velocity is then given by

$$v_g = d\omega/dk = (dE/\hbar)/(dp/\hbar) = dE/dp$$

Again using the nonrelativistic expression $E = p^2/2m$, we have that

$$v_g = dE/dp = p/m = v$$

and *the wave packet $\Psi(x, t)$ moves with the velocity of the electron*. This was, in fact, one of de Broglie's reasons for choosing Equations 5-1 and 5-2. (De Broglie used the relativistic expression relating energy and momentum, which also leads to the equality of the group velocity and particle velocity.)

5-4 The Probabilistic Interpretation of the Wave Function

Let us consider in more detail the relation between the wave function $\Psi(x, t)$ and the location of the electron. We can get a hint about this relation from the case of light. The wave equation that governs light is Equation 5-11, with $y = \mathcal{E}$, the electric field, as the wave function. The energy per unit volume in a light wave is proportional to \mathcal{E}^2 , but the energy in a light wave is quantized in units of hf for each photon. We expect, therefore, that the number of photons in a unit volume is proportional to \mathcal{E}^2 , a connection first pointed out by Einstein.

Consider the famous double-slit interference experiment (Figure 5-17). The pattern observed on the screen is determined by the interference of the waves from the slits. At a point on the screen where the wave from one slit is 180° out of phase with that from the other, the resultant electric field is zero; there is no light energy at this point, and this point on the screen is dark. If we reduce the intensity to a very low value, we can still observe the interference pattern if we replace the ordinary screen by a scintillation screen or a two-dimensional array of tiny photon detectors (e.g., a CCD camera) and wait a sufficient length of time.

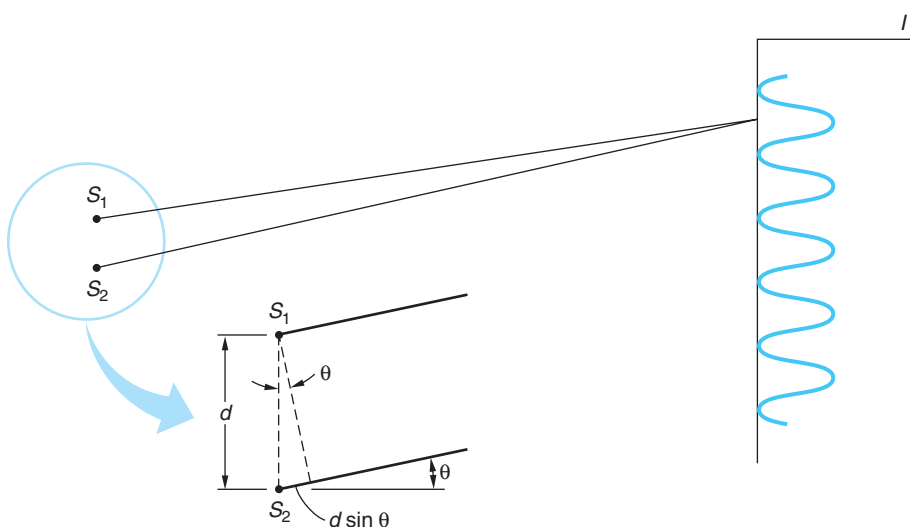


Figure 5-17 Two-source interference pattern. If the sources are coherent and in phase, the waves from the sources interfere constructively at points for which the path difference ($d \sin \theta$) is an integral number of wavelengths.

The interaction of light with the detector or scintillator is a quantum phenomenon. If we illuminate the scintillators or detectors for only a very short time with a low-intensity source, we do not see merely a weaker version of the high-intensity pattern; we see, instead, “dots” caused by the interactions of individual photons (Figure 5-18). At points where the waves from the slits interfere destructively, there are no dots, and at points where the waves interfere constructively, there are many dots. However,

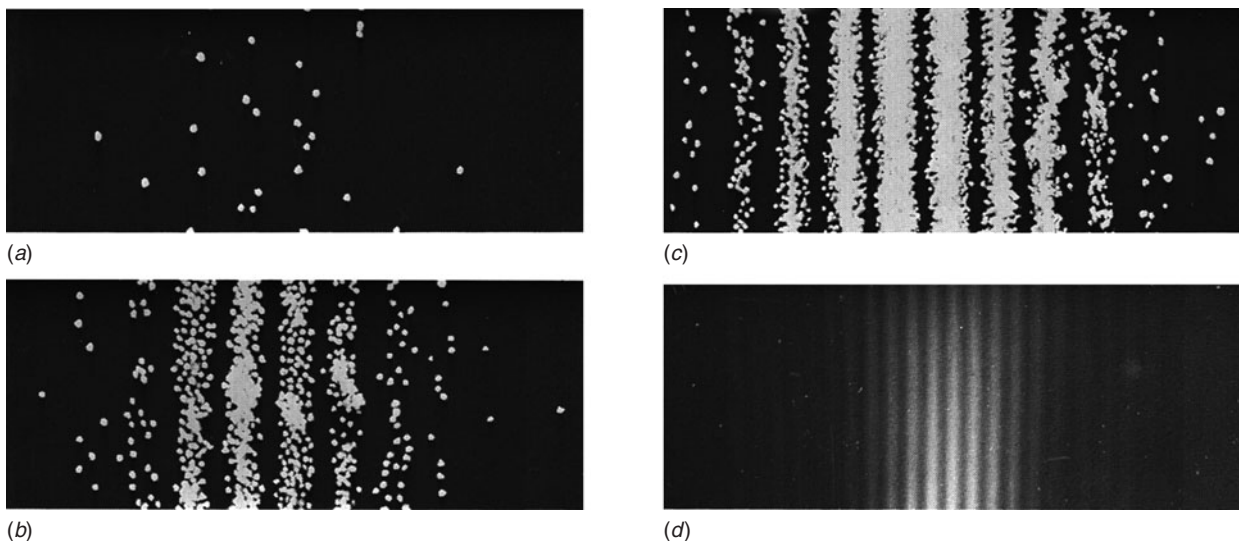


Figure 5-18 Growth of two-slit interference pattern. The photo (d) is an actual two-slit electron interference pattern in which the film was exposed to millions of electrons. The pattern is identical to that usually obtained with photons. If the film were to be observed at various stages, such as after being struck by 28 electrons, then after about 1000 electrons, and again after about 10,000 electrons, the patterns of individually exposed grains would be similar to those shown in (a), (b), and (c) except that the exposed dots would be smaller than the dots drawn here. Note that there are no dots in the region of the interference minima. The probability of any point of the film being exposed is determined by wave theory, whether the film is exposed by electrons or photons. [Parts (a), (b), and (c) from E. R. Huggins, *Physics 1*, © by W. A. Benjamin, Inc., Menlo Park, California. Photo (d) courtesy of C. Jonsson.]

when the exposure is short and the source weak, random fluctuations from the average predictions of the wave theory are clearly evident. If the exposure is long enough that many photons reach the detector, the fluctuations average out and the quantum nature of light is not noticed. The interference pattern depends only on the total number of photons interacting with the detector and not on the rate. *Even when the intensity is so low that only one photon at a time reaches the detector, the wave theory predicts the correct average pattern.* For low intensities, we therefore interpret \mathcal{E}^2 as proportional to the probability of detecting a photon in a unit volume of space. At points on the detector where \mathcal{E}^2 is zero, photons are never observed, whereas they are most likely to be observed at points where \mathcal{E}^2 is large.

It is not necessary to use light waves to produce an interference pattern. Such patterns can be produced with electrons and other particles as well. In the wave theory of electrons the de Broglie wave of a *single* electron is described by a wave function Ψ . The amplitude of Ψ at any point is related to the probability of finding the particle at that point. In analogy with the foregoing interpretation of \mathcal{E}^2 , the quantity $|\Psi|^2$ is proportional to the probability of detecting an electron in a unit volume, where $|\Psi|^2 \equiv \Psi^* \Psi$, the function Ψ^* being the complex conjugate of Ψ . In one dimension, $|\Psi|^2 dx$ is the probability of an electron being in the interval dx .¹⁰ (See Figure 5-19.) If we call this probability $P(x)dx$, where $P(x)$ is the probability distribution function, we have

$$P(x)dx = |\Psi|^2 dx \quad 5-23$$

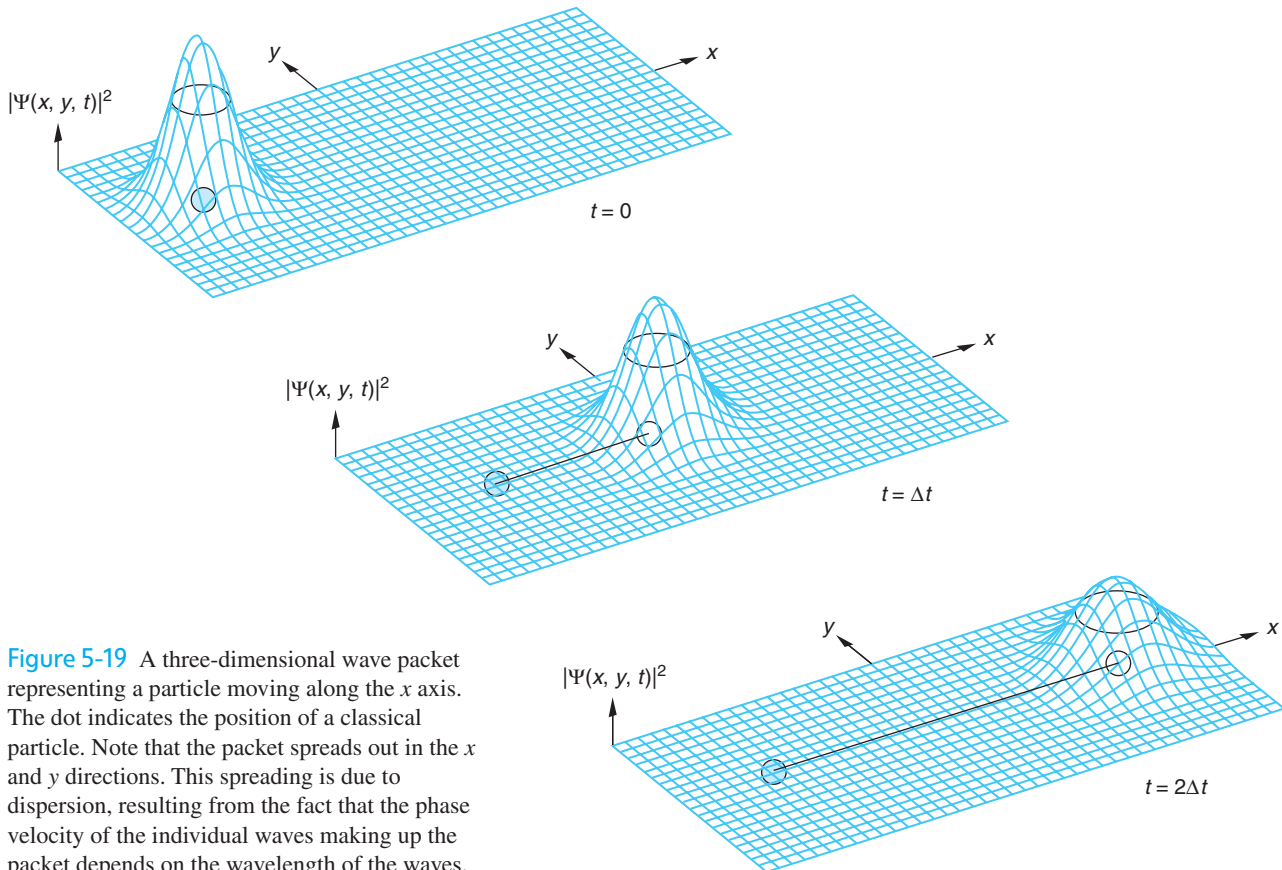


Figure 5-19 A three-dimensional wave packet representing a particle moving along the x axis. The dot indicates the position of a classical particle. Note that the packet spreads out in the x and y directions. This spreading is due to dispersion, resulting from the fact that the phase velocity of the individual waves making up the packet depends on the wavelength of the waves.

In the next chapter we will more thoroughly discuss the amplitudes of matter waves associated with particles, in particular developing the mathematical system for computing the amplitudes and probabilities in various situations. The uneasiness that you may feel at this point regarding the fact that we have not given a precise physical interpretation to the amplitude of the de Broglie matter wave can be attributed in part to the complex nature of the wave amplitude; i.e., it is in general a complex function with a real part and an imaginary part, the latter proportional to $i = (-1)^{1/2}$. We cannot directly measure or physically interpret complex numbers in our world of real numbers. However, as we will see, defining the probability in terms of $|\Psi|^2$, which is always real, presents no difficulty in its physical interpretation. Thus, even though the amplitudes of the wave functions Ψ have no simple meaning, the waves themselves behave just as classical waves do, exhibiting the wave characteristics of reflection, refraction, interference, and diffraction and obeying the principles of superposition.

5-5 The Uncertainty Principle

The uncertainty relations for classical wave packets (Equations 5-17 and 5-18) have very important matter wave analogs.

Consider a wave packet $\Psi(x, t)$ representing an electron. The most probable position of the electron is the value of x for which $|\Psi(x, t)|^2$ is a maximum. Since $|\Psi(x, t)|^2$ is proportional to the probability that the electron is located at x and $|\Psi(x, t)|^2$ is nonzero for a range of values of x , there is an *uncertainty* in the position of the electron (see Figure 5-19). This means that if we make a number of position measurements on identical electrons—electrons with the same wave function—we will not always obtain the same result. In fact, the distribution function for the results of such measurements will be given by $|\Psi(x, t)|^2$. If the wave packet is very narrow, the uncertainty in position will be small. However, a narrow wave packet must contain a wide range of wave numbers k . Since the momentum is related to the wave number by $p = \hbar k$, a wide range of k values means a wide range of momentum values. We have seen that for all wave packets the ranges Δx and Δk are related by

$$\Delta k \Delta x \sim 1 \quad 5-17$$

Similarly, a packet that is localized in time Δt must contain a range of frequencies $\Delta\omega$, where the ranges are related by

$$\Delta\omega \Delta t \sim 1 \quad 5-18$$

Equations 5-17 and 5-18 are inherent properties of waves. If we multiply these equations by \hbar and use $p = \hbar k$ and $E = \hbar\omega$, we obtain

$$\Delta x \Delta p \sim \hbar \quad 5-24$$

and

$$\Delta E \Delta t \sim \hbar \quad 5-25$$

Equations 5-24 and 5-25 provide a statement of the *uncertainty principle* first enunciated in 1927 by Werner K. Heisenberg.¹¹ Equation 5-24 expresses the fact that the distribution functions for position and momentum cannot both be made arbitrarily narrow simultaneously (see Figure 5-16); thus, measurements of position and momentum will have similar uncertainties, which are related by Equation 5-24. Of course, because of

Heisenberg's uncertainty principle is the key to the existence of virtual particles that hold the nuclei together (see Chapter 11) and is the root of quantum fluctuations that may have been the origin of the Big Bang (see Chapter 13).

inaccurate measurements, the product of Δx and Δp can be, and usually is, much larger than \hbar . The lower limit is not due to any technical problem in the design of measuring equipment that might be solved at some later time; it is instead due to the wave and particle nature of both matter and light.

If we define precisely what we mean by the uncertainty in the measurements of position and momentum, we can give a precise statement of the uncertainty principle. For example, if σ_x is the standard deviation for measurements of position and σ_k is the standard deviation for measurements of the wave number, the product $\sigma_x \sigma_k$ has its minimum value of $1/2$ when the distribution functions are Gaussian. If we define Δx and Δp to be the standard deviations, the minimum value of their product is $\hbar/2$. Thus,

$$\Delta x \Delta p \geq \frac{1}{2} \hbar \quad 5-26$$

Similarly,

$$\Delta E \Delta t \geq \frac{1}{2} \hbar \quad 5-27$$

Question

6. Does the uncertainty principle say that the momentum of a particle can never be precisely known?



EXPLORING The Gamma-Ray Microscope

Let us see how one might attempt to make a measurement so accurate as to violate the uncertainty principle. A common way to measure the position of an object such as an electron is to look at it with light, i.e., scatter light from it and observe the diffraction pattern. The momentum can be obtained by looking at it again a short time later and computing what velocity it must have had the instant before the light scattered from it. Because of diffraction effects, we cannot hope to make measurements of length (position) that are smaller than the wavelength of the light used, so we will use the shortest-wavelength light that can be obtained, gamma rays. (There is, in principle, no limit to how short the wavelength of electromagnetic radiation can be.) We also know that light carries momentum and energy, so that when it scatters off the electron, the motion of the electron will be disturbed, affecting the momentum. We must, therefore, use the minimum intensity possible so as to disturb the electron as little as possible. Reducing the intensity decreases the number of photons, but we must scatter at least one photon to observe the electron. The minimum possible intensity, then, is that corresponding to one photon. The scattering of a photon by a free electron is, of course, a Compton scattering, which was discussed in Section 3-4. The momentum of the photon is $hf/c = h/\lambda$. The smaller λ that is used to measure the position, the more the photon will disturb the electron, but we can correct for that with a Compton-effect analysis, provided only that we know the photon's momentum and the scattering angles of the event.

Figure 5-20 illustrates the problem. (This illustration was first given as a gedanken-experiment, or thought experiment, by Heisenberg. Since a single photon doesn't form a diffraction pattern, think of the diffraction pattern as being built up by photons from

many identical scattering experiments.) The position of the electron is to be determined by viewing it through a microscope. We will assume that only one photon is used. We can take for the uncertainty in position the minimum separation distance for which two objects can be resolved; this is¹²

$$\Delta x = \frac{\lambda}{2 \sin \theta}$$

where θ is the half angle subtended by the lens aperture, as shown in Figure 5-20a and b.

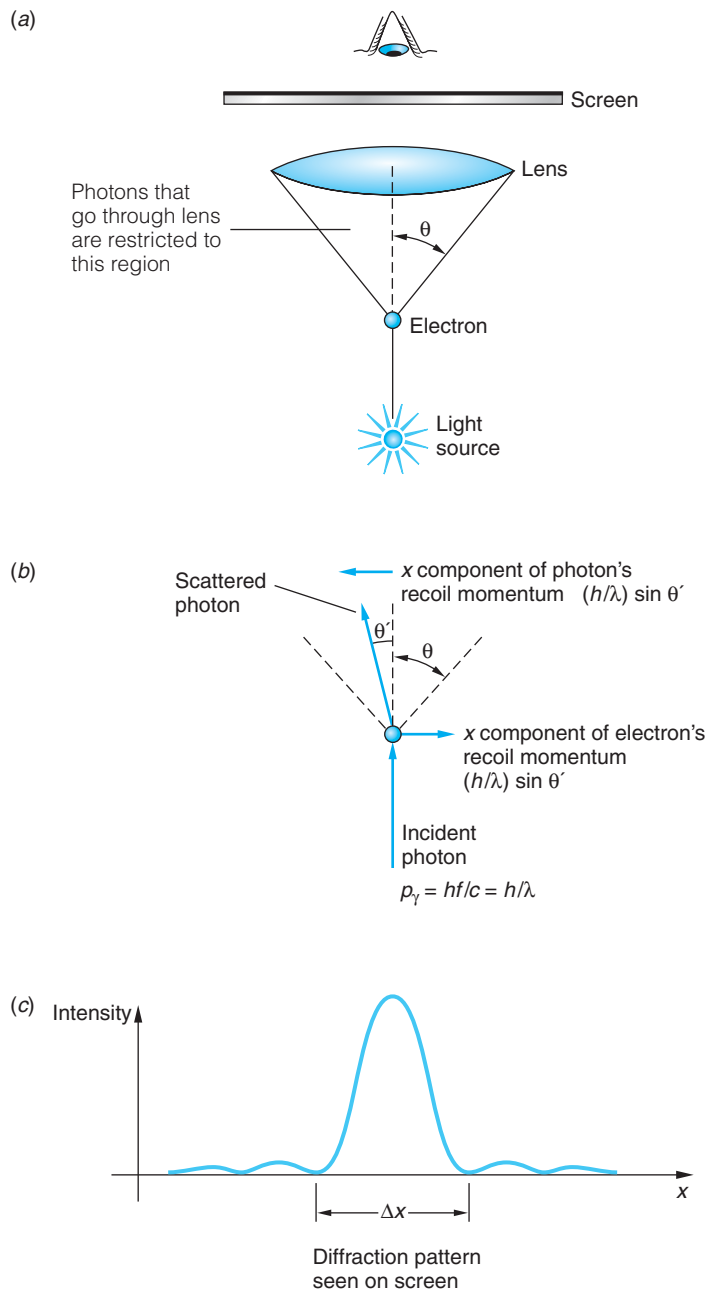


Figure 5-20 “Seeing an electron” with a gamma-ray microscope. (b) Because of the size of the lens, the momentum of the scattered photon is uncertain by $\Delta p_x \approx p \sin \theta = h \sin \theta / \lambda$. Thus the recoil momentum of the electron is also uncertain by at least this amount. (c) The position of the electron cannot be resolved better than the width of the central maximum of the diffraction pattern $\Delta x \approx \lambda / \sin \theta$. The product of the uncertainties $\Delta p_x \Delta x$ is therefore of the order of Planck’s constant h .

Let us assume that the x component of momentum of the incoming photon is known precisely from a previous measurement. To reach the screen and contribute to the diffraction pattern in Figure 5-20c, the scattered photon need only go through the lens aperture. Thus, the scattered photon can have any x component of momentum from 0 to $p_x = p \sin \theta$, where p is the total momentum of the scattered photon. By conservation of momentum, the uncertainty in the momentum of the electron after the scattering must be greater than or equal to that of the scattered photon (it would be equal, of course, if the electron's initial momentum were known precisely); therefore, we write

$$\Delta p_x \geq p \sin \theta = \frac{h}{\lambda} \sin \theta$$

and

$$\Delta x \Delta p_x \geq \frac{\lambda}{2 \sin \theta} \frac{h \sin \theta}{\lambda} = \frac{1}{2} h$$

Thus, even though the electron prior to our observation may have had a definite position and momentum, our observation has unavoidably introduced an uncertainty in the measured values of those quantities. This illustrates the essential point of the uncertainty principle—that this product of uncertainties cannot be less than about h *in principle*, that is, even in an ideal situation. If electrons rather than photons were used to locate the object, the analysis would not change since the relation $\lambda = h/p$ is the same for both.

5-6 Some Consequences of the Uncertainty Principle

In the next chapter we will see that the Schrödinger wave equation provides a straightforward method of solving problems in atomic physics. However, the solution of the Schrödinger equation is often laborious and difficult. Much semiquantitative information about the behavior of atomic systems can be obtained from the uncertainty principle alone without a detailed solution of the problem. The general approach used in applying the uncertainty principle to such systems will first be illustrated by considering a particle moving in a box with rigid walls. We then use that analysis in several numerical examples and as a basis for discussing some additional consequences.

Minimum Energy of a Particle in a Box

An important consequence of the uncertainty principle is that a particle confined to a finite space cannot have zero kinetic energy. Let us consider the case of a one-dimensional “box” of length L . If we know that the particle is in the box, Δx is not larger than L . This implies that Δp is at least \hbar/L . (Since we are interested in orders of magnitude, we will ignore the 1/2 in the minimum uncertainty product. In general, distributions are not Gaussian anyway, so $\Delta p \Delta x$ will be larger than $\hbar/2$.) Let us take the standard deviation as a measure of Δp ,

$$(\Delta p)^2 = (p - \bar{p})_{\text{av}}^2 = (p^2 - 2p\bar{p} + \bar{p}^2)_{\text{av}} = \bar{p}^2 - \bar{p}^2$$

If the box is symmetric, \bar{p} will be zero since the particle moves to the left as often as to the right. Then

$$(\Delta p)^2 = \bar{p}^2 \geq \left(\frac{\hbar}{L} \right)^2$$

and the average kinetic energy is

$$\bar{E} = \frac{\overline{p^2}}{2m} \geq \frac{\hbar^2}{2mL^2} \quad 5-28$$

Thus, we see that the uncertainty principle indicates that the minimum energy of a particle (*any* particle) in a “box” (*any* kind of “box”) cannot be zero. This minimum energy given by Equation 5-28 for a particle in a one-dimensional box is called the *zero point energy*.

EXAMPLE 5-6 A Macroscopic Particle in a Box Consider a small but macroscopic particle of mass $m = 10^{-6}$ g confined to a one-dimensional box with $L = 10^{-6}$ m, e.g., a tiny bead on a very short wire. Compute the bead’s minimum kinetic energy and the corresponding speed.

SOLUTION

1. The minimum kinetic energy is given by Equation 5-28:

$$\begin{aligned}\bar{E} &= \frac{\hbar^2}{2mL^2} = \frac{(1.055 \times 10^{-34} \text{ J} \cdot \text{s})^2}{(2)(10^{-9} \text{ kg})(10^{-6} \text{ m})^2} \\ &= 5.57 \times 10^{-48} \text{ J} \\ &= 3.47 \times 10^{-29} \text{ eV}\end{aligned}$$

2. The speed corresponding to this kinetic energy is:

$$\begin{aligned}v &= \sqrt{\frac{2\bar{E}}{m}} = \sqrt{\frac{2(5.57 \times 10^{-48} \text{ J})}{10^{-9} \text{ kg}}} \\ &= 1.06 \times 10^{-19} \text{ m/s}\end{aligned}$$

Remarks: We can see from this calculation that the minimum kinetic energy implied by the uncertainty principle is certainly not observable for macroscopic objects even as small as 10^{-6} g.

EXAMPLE 5-7 An Electron in an Atomic Box If the particle in a one-dimensional box of length $L = 0.1$ nm (about the diameter of an atom) is an electron, what will be its zero-point energy?

SOLUTION

Again using Equation 5-28, we find that

$$E = \frac{(\hbar c)^2}{2mc^2L^2} = \frac{(197.3 \text{ eV} \cdot \text{nm})^2}{2(0.511 \times 10^6 \text{ eV})(0.1 \text{ nm})^2} = 3.81 \text{ eV}$$

This is the correct order of magnitude for the kinetic energy of an electron in an atom.

Size of the Hydrogen Atom

The energy of an electron of momentum p a distance r from a proton is

$$E = \frac{p^2}{2m} - \frac{ke^2}{r}$$

If we take for the order of magnitude of the position uncertainty $\Delta x = r$, we have

$$(\Delta p)^2 = \overline{p^2} \geq \frac{\hbar^2}{r^2}$$

The energy is then

$$E = \frac{\hbar^2}{2mr^2} - \frac{ke^2}{r}$$

There is a radius r_m at which E is minimum. Setting $dE/dr = 0$ yields r_m and E_m :

$$r_m = \frac{\hbar^2}{ke^2 m} = a_0 = 0.0529 \text{ nm}$$

and

$$E_m = -\frac{k^2 e^4 m}{2\hbar^2} = -13.6 \text{ eV}$$

The fact that r_m came out to be exactly the radius of the first Bohr orbit is due to the judicious choice of $\Delta x = r$ rather than $2r$ or $r/2$, which are just as reasonable. It should be clear, however, that any reasonable choice for Δx gives the correct order of magnitude of the size of an atom.

Widths of Spectral Lines

Equation 5-27 implies that the energy of a system cannot be measured exactly unless an infinite amount of time is available for the measurement. If an atom is in an excited state, it does not remain in that state indefinitely but makes transitions to lower energy states until it reaches the ground state. The decay of an excited state is a statistical process.

We can take the mean time for decay τ , called the *lifetime*, to be a measure of the time available to determine the energy of the state. For atomic transitions, τ is of the order of 10^{-8} s. The uncertainty in the energy corresponding to this time is

$$\Delta E \geq \frac{\hbar}{\tau} = \frac{6.58 \times 10^{-16} \text{ eV} \cdot \text{s}}{10^{-8} \text{ s}} \approx 10^{-7} \text{ eV}$$

This uncertainty in energy causes a spread $\Delta\lambda$ in the wavelength of the light emitted. For transitions to the ground state, which has a perfectly certain energy E_0 because of its infinite lifetime, the percentage spread in wavelength can be calculated from

$$E - E_0 = \frac{hc}{\lambda}$$

$$dE = -hc \frac{d\lambda}{\lambda^2}$$

$$|\Delta E| \approx hc \frac{|\Delta\lambda|}{\lambda^2}$$

thus,

$$\frac{\Delta\lambda}{\lambda} \approx \frac{\Delta E}{E - E_0}$$

The energy width $\Delta E = \hbar/\tau$ is called the *natural line width* and is represented by Γ_0 . Other effects that cause broadening of spectral lines are the Doppler effect, the recoil of the emitting atom, and atomic collisions. For optical spectra in the eV energy range, the Doppler width D is about 10^{-6} eV at room temperature, i.e., roughly 10 times the natural width Γ_0 , and the recoil width is negligible. For nuclear transitions in the MeV range, both the Doppler width and the recoil width are of the order of eV, much larger than the natural line width. We will see in Chapter 11 that in some special cases of atoms in solids at low temperatures, the Doppler and recoil widths are essentially zero and the width of the spectral line is just the natural width. This effect, called the *Mössbauer effect* after its discoverer, is extremely important since it provides photons of well-defined energy that are useful in experiments demanding extreme precision. For example, the 14.4-keV photon from ^{57}Fe has a natural width of the order of 10^{-11} of its energy.

Questions

7. What happens to the zero-point energy of a particle in a one-dimensional box as the length of the box $L \rightarrow \infty$?
8. Why is the uncertainty principle not apparent for macroscopic objects?

EXAMPLE 5-8 Emission of a Photon Most excited atomic states decay, i.e., emit a photon, within about $\tau = 10^{-8}$ s following excitation. What is the minimum uncertainty in the (1) energy and (2) frequency of the emitted photon?

SOLUTION

1. The minimum energy uncertainty is the natural line width $\Gamma_0 = \hbar/\tau$; therefore,

$$\Gamma_0 = \frac{6.63 \times 10^{-34} \text{ J} \cdot \text{s}}{2\pi \times 10^{-8} \text{ s}} = \frac{4.14 \times 10^{-15} \text{ eV} \cdot \text{s}}{2\pi \times 10^{-8} \text{ s}} = 6.6 \times 10^{-8} \text{ eV}$$

2. From de Broglie's relation $E = \hbar\omega$ we have

$$\Delta E = \hbar\Delta\omega = \hbar(2\pi\Delta f) = h\Delta f$$

so that Equation 5-27 can be written as

$$\Delta E \Delta t = h\Delta f \Delta t \geq \hbar$$

and the minimum uncertainty in the frequency becomes

$$\begin{aligned}\Delta f &\geq \frac{1}{2\pi\Delta t} = \frac{1}{2\pi \times 10^{-8}} \\ \Delta f &\geq 1.6 \times 10^7 \text{ Hz}\end{aligned}$$

Remarks: The frequency of photons in the visible region of the spectrum is of the order of 10^{14} Hz.

5-7 Wave-Particle Duality

We have seen that electrons, which were once thought of as simply particles, exhibit the wave properties of diffraction and interference. In earlier chapters we saw that light, which we previously had thought of as a wave, also has particle properties in its interaction with matter, as in the photoelectric effect or the Compton effect. All phenomena—electrons, atoms, light, sound—have both particle and wave characteristics. It is sometimes said that an electron, for example, behaves both as a wave and a particle. This may seem confusing since, in classical physics, the concepts of waves and particles are mutually exclusive. A *classical particle* behaves like a pellet or BB shot from an air-powered rifle. It can be localized and scattered, it exchanges energy suddenly in a lump, and it obeys the laws of conservation of energy and momentum in collisions, but it does *not* exhibit interference and diffraction. A *classical wave* behaves like a water wave. It exhibits diffraction and interference patterns and has its energy spread out continuously in space and time, not quantized in lumps. Nothing, it was thought, could be both a classical particle and a classical wave.

We now see that the classical concepts do not adequately describe either waves or particles. Both matter and radiation have both particle and wave aspects. When emission and absorption are being studied, it is the particle aspects that are dominant. When matter and radiation propagate through space, wave aspects dominate. Notice that emission and absorption are events characterized by exchange of energy and discrete locations. For example, light strikes the retina of your eye and a photon is absorbed, transferring its energy to a particular rod or cone: an observation has occurred. This illustrates the point that *observations* of matter and radiation are described in terms of the particle aspects. On the other hand, predicting the intensity distribution of the light on your retina involves consideration of the amplitudes of waves that have propagated through space and been diffracted at the pupil. Thus, *predictions*, i.e., a priori statements about what may be observed, are described in terms of the wave aspects. Let's elaborate on this just a bit.

Every phenomenon is describable by a wave function that is the solution of a wave equation. The wave function for light is the electric field $\mathcal{E}(x, t)$ (in one space dimension), which is the solution of a wave equation like Equation 5-11. We have called the wave function for an electron $\Psi(x, t)$. We will study the wave equation of which Ψ is the solution, called the *Schrödinger equation*, in the next chapter. The magnitude squared of the wave function gives the probability per unit volume that the electron, if looked for, will be found in a given volume or region. The wave function exhibits the classical wave properties of interference and diffraction. In order to predict where an electron, or other particle, is likely to be, we must find the wave function by methods similar to those of classical wave theory. When the electron (or light) interacts and exchanges energy and momentum, the wave function is changed by the interaction. The interaction can be described by classical particle theory, as is done in the Compton effect. There are times when classical particle theory and classical wave theory give the same results. *If the wavelength is much smaller than any object or aperture, particle theory can be used as well as wave theory to describe wave propagation because diffraction and interference effects are too small to be observed.* Common examples are geometrical optics, which is really a particle theory, and the motion of baseballs and jet aircraft. If one is interested only in time averages of energy and momentum exchange, the wave theory works as well as the particle theory. For example, the wave theory of light correctly predicts that the total electron current in the photoelectric effect is proportional to the intensity of the light.



More

That matter can exhibit wavelike characteristics as well as particlelike behavior can be a difficult concept to understand. A wonderfully clear discussion of wave-particle duality was given by R. P. Feynman, and we have used it as the basis of our explanation on the home page of the *Two-Slit Interference Pattern* for electrons: whfreeman.com/tiplermodernphysics5e/. See also Figures 5-21 and 5-22 and Equation 5-29 here.

Summary

| TOPIC | RELEVANT EQUATIONS AND REMARKS | | |
|-------------------------------------|---|--|------|
| 1. De Broglie relations | $f = E/h$ $\lambda = h/p$ | 5-1 5-2 | |
| | Electrons and all other particles exhibit the wave properties of interference and diffraction | | |
| 2. Detecting electron waves | Davisson and Germer | Showed that electron waves diffracted from a single Ni crystal according to Bragg's equation | |
| | | $n\lambda = D \sin \varphi$ | 5-5 |
| 3. Wave packets | Wave equation | $\frac{d^2y}{dx^2} = \frac{1}{v^2} \frac{d^2y}{dt^2}$ | 5-11 |
| | Uncertainty relations | $\Delta k \Delta x \sim 1$ | 5-17 |
| | | $\Delta \omega \Delta t \sim 1$ | 5-18 |
| | Wave speed | $v_p = f\lambda = \omega/k$ | |
| | Group (packet) speed | $v_g = \frac{d\omega}{dk} = v_p + k \frac{dv_p}{dk}$ | 5-16 |
| | Matter waves | The wave packet moves with the particle speed; i.e., the particle speed is the group speed v_g . | |
| 4. Probabilistic interpretation | | The magnitude square of the wave function is proportional to the probability of observing a particle in the region dx at x and t . | |
| | | $P(x)dx = \Psi ^2 dx$ | 5-23 |
| 5. Heisenberg uncertainty principle | | $\Delta x \Delta p \geq \frac{1}{2} \hbar$ | 5-26 |
| | | $\Delta E \Delta t \geq \frac{1}{2} \hbar$ | 5-27 |
| | | where each of the uncertainties is defined to be the standard deviation. | |

| TOPIC | RELEVANT EQUATIONS AND REMARKS | |
|-------------------|--|------|
| Particle in a box | $\bar{E} \geq \frac{\hbar^2}{2mL^2}$ | 5-28 |
| Energy of H atom | The minimum energy of any particle in any “box” cannot be zero. The Heisenberg principle predicts $E_{\min} = -13.6$ eV in agreement with the Bohr model. | |

General References

The following general references are written at a level appropriate for the readers of this book.

- De Broglie, L., *Matter and Light: The New Physics*, Dover, New York, 1939. In this collection of studies is de Broglie’s lecture on the occasion of receiving the Nobel Prize, in which he describes his reasoning that led to the prediction of the wave nature of matter.
- Feynman, R., “Probability and Uncertainty—The Quantum-Mechanical View of Nature,” filmed lecture, available from Educational Services, Inc., Film Library, Newton, MA.
- Feynman, R. P., R. B. Leighton, and M. Sands, *Lectures on Physics*, Addison-Wesley, Reading, MA, 1965.

- Fowles, G. R., *Introduction to Modern Optics*, Holt, Rinehart & Winston, New York, 1968.
- Hecht, E., *Optics*, 2d ed., Addison-Wesley, Reading, MA, 1987.
- Jenkins, F. A., and H. E. White, *Fundamentals of Optics*, 4th ed., McGraw-Hill, New York, 1976.
- Mehra, J., and H. Rechenberg, *The Historical Development of Quantum Theory*, Vol. 1, Springer-Verlag, New York, 1982.
- Resnick, R., and D. Halliday, *Basic Concepts in Relativity and Early Quantum Theory*, 2d ed., Wiley, New York, 1992.
- Tipler, P. A., and G. Mosca, *Physics for Scientists and Engineers*, 6th ed., W. H. Freeman and Co., New York, 2008. Chapters 15 and 16 include a complete discussion of classical waves.

Notes

1. Louis V. P. R. de Broglie (1892–1987), French physicist. Originally trained in history, he became interested in science after serving as a radio engineer in the French army (assigned to the Eiffel Tower) and through the work of his physicist brother Maurice. The subject of his doctoral dissertation received unusual attention because his professor, Paul Langevin (who discovered the principle on which sonar is based), brought it to the attention of Einstein, who described de Broglie’s hypothesis to Lorentz as “the first feeble ray of light to illuminate . . . the worst of our physical riddles.” He received the Nobel Prize in Physics in 1929, the first person so honored for work done for a doctoral thesis.

2. L. de Broglie, *New Perspectives in Physics*, Basic Books, New York, 1962.

3. See, e.g., Tipler, *Physics for Scientists and Engineers*, 5th ed. (New York: W. H. Freeman and Co., 2008), Section 35-5.

4. Jean-Baptiste Perrin (1870–1942), French physicist. He was the first to show that cathode rays are actually charged particles, setting the stage for J. J. Thomson’s measurement of their q/m ratio. He was also the first to measure the approximate size of atoms and molecules and determined Avogadro’s number. He received the Nobel Prize in Physics for that work in 1926.

5. Clinton J. Davisson (1881–1958), American physicist. He shared the 1937 Nobel Prize in Physics with G. P. Thomson for demonstrating the diffraction of particles. Davisson’s Nobel Prize was the first ever awarded for work done somewhere other than at an academic institution. Germer was one of Davisson’s assistants at Bell Telephone Laboratory.

6. Matter (electron) waves, like other waves, change their direction in passing from one medium (e.g., Ni crystal) into another (e.g., vacuum) in the manner described by Snell’s law and the indices of refraction of the two media. For normal incidence Equation 5-5 is not affected, but for other incident angles it is altered a bit, and that change has not been taken into account in either Figure 5-6 or 5-7.

7. *Nobel Prize Lectures: Physics* (Amsterdam and New York: Elsevier, 1964).

8. In spectroscopy, the quantity $k = \lambda^{-1}$ is called the *wave number*. In the theory of waves, the term *wave number* is used for $k = 2\pi/\lambda$.

9. Following convention, the “width” is defined as the full width of the pulse or envelope measured at half the maximum amplitude.

10. This interpretation of $|\Psi|^2$ was first developed by German physicist Max Born (1882–1970). One of his positions early in his career was at the University of Berlin, where he was to relieve Planck of his teaching duties. Born received the Nobel Prize in Physics in 1954, in part for his interpretation of $|\Psi|^2$.

11. Werner K. Heisenberg (1901–1976), German physicist. After obtaining his Ph.D. under Sommerfeld, he served as an assistant to Born and to Bohr. He was the director of research for Germany's atomic bomb project during World War II. His work on quantum theory earned him the Nobel Prize in Physics in 1932.

12. The resolving power of a microscope is discussed in some detail in Jenkins and White, *Fundamentals of Optics*,

4th ed. (New York: McGraw-Hill, 1976), pp. 332–334. The expression for Δx used here is determined by Rayleigh's criterion, which states that two points are just resolved if the central maximum of the diffraction pattern from one falls at the first minimum of the diffraction pattern of the other.

13. Richard P. Feynman (1918–1988), American physicist. This discussion is based upon one in his classic text *Lectures on Physics* (Reading, MA: Addison-Wesley, 1965). He shared the 1965 Nobel Prize in Physics for his development of quantum electrodynamics (QED). It was Feynman who, while a member of the commission on the *Challenger* disaster, pointed out that the booster stage O-rings were at fault. A genuine legend in American physics, he was also an accomplished bongo drummer and safecracker.

Problems

Level I

Section 5-1 The de Broglie Hypothesis

5-1. (a) What is the de Broglie wavelength of a 1-g mass moving at a speed of 1 m per year?
(b) What should be the speed of such a mass if its de Broglie wavelength is to be 1 cm?

5-2. If the kinetic energy of a particle is much greater than its rest energy, the relativistic approximation $E \approx pc$ holds. Use this approximation to find the de Broglie wavelength of an electron of energy 100 MeV.

5-3. Electrons in an electron microscope are accelerated from rest through a potential difference V_0 so that their de Broglie wavelength is 0.04 nm. What is V_0 ?

5-4. Compute the de Broglie wavelengths of (a) an electron, (b) a proton, and (c) an alpha particle of 4.5-keV kinetic energy.

5-5. According to statistical mechanics, the average kinetic energy of a particle at temperature T is $3kT/2$, where k is the Boltzmann constant. What is the average de Broglie wavelength of nitrogen molecules at room temperature?

5-6. Find the de Broglie wavelength of a neutron of kinetic energy 0.02 eV (this is of the order of magnitude of kT at room temperature).

5-7. A free proton moves back and forth between rigid walls separated by a distance $L = 0.01$ nm.
(a) If the proton is represented by a one-dimensional standing de Broglie wave with a node at each wall, show that the allowed values of the de Broglie wavelength are given by $\lambda = 2L/n$ where n is a positive integer.
(b) Derive a general expression for the allowed kinetic energy of the proton and compute the values for $n = 1$ and 2.

5-8. What must be the kinetic energy of an electron if the ratio of its de Broglie wavelength to its Compton wavelength is (a) 10^2 , (b) 0.2, and (c) 10^{-3} ?

5-9. Compute the wavelength of a cosmic-ray proton whose kinetic energy is (a) 2 GeV and (b) 200 GeV.

Section 5-2 Measurements of Particle Wavelengths

5-10. What is the Bragg scattering angle φ for electrons scattered from a nickel crystal if their energy is (a) 75 eV, (b) 100 eV?

5-11. Compute the kinetic energy of a proton whose de Broglie wavelength is 0.25 nm. If a beam of such protons is reflected from a calcite crystal with crystal plane spacing of 0.304 nm, at what angle will the first-order Bragg maximum occur?

5-12. (a) The scattering angle for 50-eV electrons from MgO is 55.6° . What is the crystal spacing D ? (b) What would be the scattering angle for 100-eV electrons?

5-13. A certain crystal has a set of planes spaced 0.30 nm apart. A beam of neutrons strikes the crystal at normal incidence and the first maximum of the diffraction pattern occurs at $\varphi = 42^\circ$. What are the de Broglie wavelength and kinetic energy of the neutrons?

5-14. Show that in Davisson and Germer's experiment with 54-eV electrons using the $D = 0.215$ nm planes, diffraction peaks with $n = 2$ and higher are not possible.

5-15. A beam of electrons with kinetic energy 350 eV is incident normal to the surface of a KCl crystal that has been cut so that the spacing D between adjacent atoms in the planes parallel to the surface is 0.315 nm. Calculate the angle φ at which diffraction peaks will occur for all orders possible.

Section 5-3 Wave Packets

5-16. Information is transmitted along a cable in the form of short electric pulses at 100,000 pulses/s. (a) What is the longest duration of the pulses such that they do not overlap? (b) What is the range of frequencies to which the receiving equipment must respond for this duration?

5-17. Two harmonic waves travel simultaneously along a long wire. Their wave functions are $y_1 = 0.002 \cos(8.0x - 400t)$ and $y_2 = 0.002 \cos(7.6x - 380t)$, where y and x are in meters and t in seconds. (a) Write the wave function for the resultant wave in the form of Equation 5-15. (b) What is the phase velocity of the resultant wave? (c) What is the group velocity? (d) Calculate the range Δx between successive zeros of the group and relate it to Δk .

5-18. (a) Starting from Equation 5-16, show that the group velocity can also be expressed as

$$v_g = v_p - \lambda(dv_p/d\lambda)$$

(b) The phase velocity of each wavelength of white light moving through ordinary glass is a function of the wavelength; i.e., glass is a dispersive medium. What is the general dependence of v_p on λ in glass? Is $dv_p/d\lambda$ positive or negative?

5-19. A radar transmitter used to measure the speed of pitched baseballs emits pulses of 2.0-cm wavelength that are 0.25 μs in duration. (a) What is the length of the wave packet produced? (b) To what frequency should the receiver be tuned? (c) What must be the minimum bandwidth of the receiver?

5-20. A certain standard tuning fork vibrates at 880 Hz. If the tuning fork is tapped, causing it to vibrate, then stopped a quarter of a second later, what is the approximate range of frequencies contained in the sound pulse that reached your ear?

5-21. If a phone line is capable of transmitting a range of frequencies $\Delta f = 5000$ Hz, what is the approximate duration of the shortest pulse that can be transmitted over the line?

5-22. (a) You are given the task of constructing a double slit experiment for 5-eV electrons. If you wish the first minimum of the diffraction pattern to occur at 5° , what must be the separation of the slits? (b) How far from the slits must the detector plane be located if the first minima on each side of the central maximum are to be separated by 1 cm?

Section 5-4 The Probabilistic Interpretation of the Wave Function

5-23. A 100-g rigid sphere of radius 1 cm has a kinetic energy of 2 J and is confined to move in a force-free region between two rigid walls separated by 50 cm. (a) What is the probability of finding the center of the sphere exactly midway between the two walls? (b) What is the probability of finding the center of the sphere between the 24.9- and 25.1-cm marks?

5-24. A particle moving in one dimension between rigid walls separated by a distance L has the wave function $\Psi(x) = A \sin(\pi x/L)$. Since the particle must remain between the walls, what must be the value of A ?

- 5-25.** The wave function describing a state of an electron confined to move along the x axis is given at time zero by

$$\Psi(x, 0) = Ae^{-x^2/4\sigma^2}$$

Find the probability of finding the electron in a region dx centered at (a) $x = 0$, (b) $x = \sigma$, and (c) $x = 2\sigma$. (d) Where is the electron most likely to be found?

Section 5-5 The Uncertainty Principle

- 5-26.** A tuning fork of frequency f_0 vibrates for a time Δt and sends out a waveform that looks like that in Figure 5-23. This wave function is similar to a harmonic wave except that it is confined to a time Δt and space $\Delta x = v\Delta t$, where v is the phase velocity. Let N be the approximate number of cycles of vibration. We can measure the frequency by counting the cycles and dividing by Δt . (a) The number of cycles is uncertain by approximately ± 1 cycle. Explain why (see the figure). What uncertainty does this introduce in the determination of the frequency f ? (b) Write an expression for the wave number k in terms of Δx and N . Show that the uncertainty in N of ± 1 leads to an uncertainty in k of $\Delta k = 2\pi/\Delta x$.

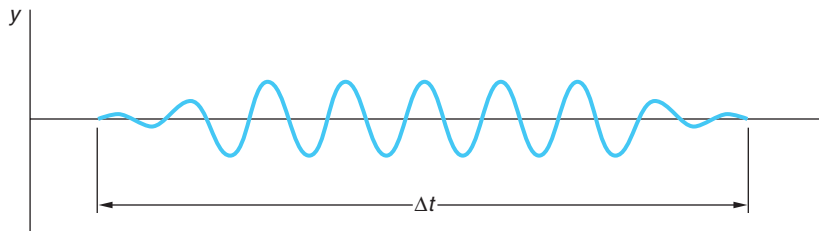


Figure 5-23

- 5-27.** If an excited state of an atom is known to have a lifetime of 10^{-7} s, what is the uncertainty in the energy of photons emitted by such atoms in the spontaneous decay to the ground state?

- 5-28.** A ladybug 5 mm in diameter with a mass of 1.0 mg being viewed through a low-power magnifier with a calibrated reticule is observed to be stationary with an uncertainty of 10^{-2} mm. How fast might the ladybug actually be walking?

- 5-29.** ^{222}Rn decays by the emission of an α particle with a lifetime of 3.823 days. The kinetic energy of the α particle is measured to be 5.490 MeV. What is the uncertainty in this energy? Describe in one sentence how the finite lifetime of the excited state of the radon nucleus translates into an energy uncertainty for the emitted α particle.

- 5-30.** If the uncertainty in the position of a wave packet representing the state of a quantum-system particle is equal to its de Broglie wavelength, how does the uncertainty in momentum compare with the value of the momentum of the particle?

- 5-31.** In one of G. Gamow's Mr. Tompkins tales, the hero visits a "quantum jungle" where \hbar is very large. Suppose that you are in such a place where $\hbar = 50 \text{ J} \cdot \text{s}$. A cheetah runs past you a few meters away. The cheetah is 2 m long from nose to tail tip and its mass is 30 kg. It is moving at 40 m/s. What is the uncertainty in the location of the "midpoint" of the cheetah? Describe in one sentence how the cheetah would look different to you than when \hbar has its actual value.

- 5-32.** In order to locate a particle, e.g., an electron, to within 5×10^{-12} m using electromagnetic waves ("light"), the wavelength must be at least this small. Calculate the momentum and energy of a photon with $\lambda = 5 \times 10^{-12}$ m. If the particle is an electron with $\Delta x = 5 \times 10^{-12}$ m, what is the corresponding uncertainty in its momentum?

- 5-33.** The decay of excited states in atoms and nuclei often leave the system in another, albeit lower-energy, excited state. (a) One example is the decay between two excited states of the nucleus of ^{48}Ti . The upper state has a lifetime of 1.4 ps, the lower state 3.0 ps. What is the fractional uncertainty $\Delta E/E$ in the energy of 1.3117-MeV gamma rays connecting the two states?

(a) Another example is the H_{α} line of the hydrogen Balmer series. In this case the lifetime of both states is about the same, 10^{-8} s. What is the uncertainty in the energy of the H_{α} photon?

5-34. Laser pulses of femtosecond duration can be produced but for such brief pulses it makes no sense to speak of the pulse's color. To see this, compute the time duration of a laser pulse whose range of frequencies covers the entire visible spectrum (4.0×10^{14} Hz to 7.5×10^{14} Hz).

Section 5-6 Some Consequences of the Uncertainty Principle

5-35. A neutron has a kinetic energy of 10 MeV. What size object is necessary to observe neutron diffraction effects? Is there anything in nature of this size that could serve as a target to demonstrate the wave nature of 10-MeV neutrons?

5-36. Protons and neutrons in nuclei are bound to the nucleus by exchanging pions (π mesons) with each other (see Chapter 11). This is possible to do without violating energy conservation provided the pion is reabsorbed within a time consistent with the Heisenberg uncertainty relations. Consider the emission reaction $p \rightarrow p + \pi$ where $m_{\pi} = 135 \text{ MeV}/c^2$. (a) Ignoring kinetic energy, by how much is energy conservation violated in this reaction? (b) Within what time interval must the pion be reabsorbed in order to avoid violation of energy conservation?

5-37. Show that the relation $\Delta p_s \Delta s > \hbar$ can be written $\Delta L \Delta \phi > \hbar$ for a particle moving in a circle about the z axis, where p_s is the linear momentum tangential to the circle, s is the arc length, and L is the angular momentum. How well can the angular position of the electron be specified in the Bohr atom?

5-38. An excited state of a certain nucleus has a half-life of 0.85 ns. Taking this to be the uncertainty Δt for emission of a photon, calculate the uncertainty in the frequency Δf , using Equation 5-25. If $\lambda = 0.01 \text{ nm}$, find $\Delta f/f$.

5-39. The lifetimes of so-called resonance particles cannot be measured directly but is computed from the energy width (or uncertainty) of the scattering cross section versus energy graph (see Chapter 12). For example, the scattering of a pion (π meson) and a proton can produce a short-lived Δ resonance particle with a mass of $1685 \text{ MeV}/c^2$ and an energy width of 250 MeV as shown in Figure 5-24: $\pi + p \rightarrow \Delta$. Compute the lifetime of the Δ .

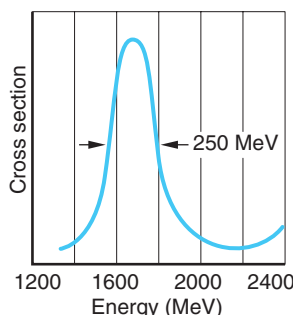


Figure 5-24

Section 5-7 Wave-Particle Duality

There are no problems for this section.

Level II

5-40. Neutrons and protons in atomic nuclei are confined within a region whose diameter is about 10^{-15} m . (a) At any given instant, how fast might an individual proton or neutron be moving? (b) What is the approximate kinetic energy of a neutron that is localized to within such a region? (c) What would be the corresponding energy of an electron localized to within such a region?

5-41. Using the relativistic expression $E^2 = p^2 c^2 + m^2 c^4$, (a) show that the phase velocity of an electron wave is greater than c . (b) Show that the group velocity of an electron wave equals the particle velocity of the electron.

5-42. Show that if y_1 and y_2 are solutions of Equation 5-11, the function $y_3 = C_1 y_1 + C_2 y_2$ is also a solution for any values of the constants C_1 and C_2 .

5-43. The London "Bobby" whistle has a frequency of 2500 Hz. If such a whistle is given a 3.0-s blast, (a) what is the uncertainty in the frequency? (b) How long is the wave train of this blast? (c) What would be the uncertainty in measuring the wavelength of this blast? (d) What is the wavelength of this blast?

5-44. A particle of mass m moves in a one-dimensional box of length L . (Take the potential energy of the particle in the box to be zero so that its total energy is its kinetic energy

$p^2/2m$.) Its energy is quantized by the standing-wave condition $n(\lambda/2) = L$, where λ is the de Broglie wavelength of the particle and n is an integer. (a) Show that the allowed energies are given by $E_n = n^2 E_1$ where $E_1 = h^2/8mL^2$. (b) Evaluate E_n for an electron in a box of size $L = 0.1$ nm and make an energy-level diagram for the state from $n = 1$ to $n = 5$. Use Bohr's second postulate $f = \Delta E/h$ to calculate the wavelength of electromagnetic radiation emitted when the electron makes a transition from (c) $n = 2$ to $n = 1$, (d) $n = 3$ to $n = 2$, and (e) $n = 5$ to $n = 1$.

5-45. (a) Use the results of Problem 5-44 to find the energy of the ground state ($n = 1$) and the first two excited states of a proton in a one-dimensional box of length $L = 10^{-15}$ m = 1 fm. (These are of the order of magnitude of nuclear energies.) Calculate the wavelength of electromagnetic radiation emitted when the proton makes a transition from (b) $n = 2$ to $n = 1$, (c) $n = 3$ to $n = 2$, and (d) $n = 3$ to $n = 1$.

5-46. (a) Suppose that a particle of mass m is constrained to move in a one-dimensional space between two infinitely high barriers located A apart. Using the uncertainty principle, find an expression for the zero-point (minimum) energy of the particle. (b) Using your result from (a), compute the minimum energy of an electron in such a space if $A = 10^{-10}$ m and $A = 1$ cm. (c) Calculate the minimum energy for a 100-mg bead moving on a thin wire between two stops located 2 cm apart.

5-47. A proton and a 10-g bullet each move with a speed of 500 m/s, measured with an uncertainty of 0.01 percent. If measurements of their respective positions are made simultaneous with the speed measurements, what is the minimum uncertainty possible in the position measurements?

Level III

5-48. Show that Equation 5-11 is satisfied by $y = f(\varphi)$, where $\varphi = x - vt$ for any function f .

5-49. An electron and a positron are moving toward each other with equal speeds of 3×10^6 m/s. The two particles annihilate each other and produce two photons of equal energy. (a) What were the de Broglie wavelengths of the electron and positron? Find the (b) energy, (c) momentum, and (d) wavelength of each photon.

5-50. It is possible for some fundamental particles to “violate” conservation of energy by creating and quickly reabsorbing another particle. For example, a proton can emit a π^+ according to $p = n + \pi^+$ where the n represents a neutron. The π^+ has a mass of 140 MeV/ c^2 . The reabsorption must occur within a time Δt consistent with the uncertainty principle. (a) Considering the example shown, by how much ΔE is energy conservation violated? (Ignore kinetic energy.) (b) For how long Δt can the π^+ exist? (c) Assuming that the π^+ is moving at nearly the speed of light, how far from the nucleus could it get in the time Δt ? (As we will discuss in Chapter 11, this is the approximate range of the strong nuclear force.) (d) Assuming that as soon as one pion is reabsorbed another is emitted, how many pions would be recorded by a “nucleon camera” with a shutter speed of 1 μ s?

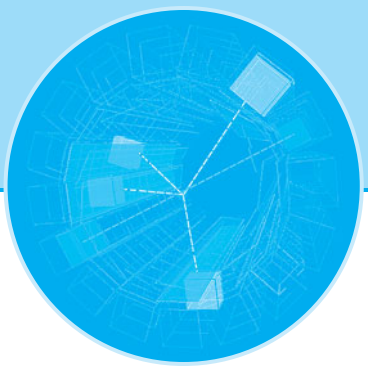
5-51. De Broglie developed Equation 5-2 initially for photons, assuming that they had a small but finite mass. His assumptions was that RF waves with $\lambda = 30$ m traveled at a speed of at least 99 percent of that of visible light with $\lambda = 500$ nm. Beginning with the relativistic expression $hf = \gamma mc^2$, verify de Broglie’s calculation that the upper limit of the rest mass of a photon is 10^{-44} g. (Hint: Find an expression for v/c in terms of hf and mc^2 , and then let $mc^2 \ll hf$) ($\gamma = 1/\sqrt{1 - v^2/c^2}$).

5-52. Suppose that you drop BBs onto a bull’s-eye marked on the floor. According to the uncertainty principle, the BBs do not necessarily fall straight down from the release point to the center of the bull’s-eye but are affected by the initial conditions. (a) If the location of the release point is uncertain by an amount Δx perpendicular to the vertical direction and the horizontal component of the speed is uncertain by Δv_x , derive an expression for the minimum spread ΔX

of impacts at the bull's-eye if it is located a distance y_0 below the release point. (b) Modify your result in (a) to include the effect on ΔX of uncertainties Δy and Δv_y at the release point.

5-53. Using the first-order Doppler-shift formula $f' = f_0(1 + v/c)$, calculate the energy shift of a 1-eV photon emitted from an iron atom moving toward you with energy $(3/2)kT$ at $T = 300$ K. Compare this Doppler line broadening with the natural line width calculated in Example 5-8. Repeat the calculation for a 1-MeV photon from a nuclear transition.

5-54. Calculate the order of magnitude of the shift in energy of a (a) 1-eV photon and (b) 1-MeV photon resulting from the recoil of an iron nucleus. Do this by first calculating the momentum of the photon and then by calculating $p^2/2m$ for the nucleus using that value of momentum. Compare with the natural line width calculated in Example 5-8.



The Schrödinger Equation

The success of the de Broglie relations in predicting the diffraction of electrons and other particles, and the realization that classical standing waves lead to a discrete set of frequencies, prompted a search for a wave theory of electrons analogous to the wave theory of light. In this electron wave theory, classical mechanics should appear as the short-wavelength limit, just as geometric optics is the short-wavelength limit of the wave theory of light. The genesis of the correct theory went something like this, according to Felix Bloch,¹ who was present at the time:

... in one of the next colloquia, Schrödinger gave a beautifully clear account of how de Broglie associated a wave with a particle and how he [i.e., de Broglie] could obtain the quantization rules ... by demanding that an integer number of waves should be fitted along a stationary orbit. When he had finished Debye² casually remarked that he thought this way of talking was rather childish ... [that to] deal properly with waves, one had to have a wave equation.

In 1926, Erwin Schrödinger³ published his now-famous wave equation, which governs the propagation of matter waves, including those of electrons. A few months earlier, Werner Heisenberg had published a seemingly different theory to explain atomic phenomena. In the Heisenberg theory, only measurable quantities appear. Dynamical quantities such as energy, position, and momentum are represented by matrices, the diagonal elements of which are the possible results of measurement. Though the Schrödinger and Heisenberg theories appear to be different, it was eventually shown by Schrödinger himself that they were equivalent, in that each could be derived from the other. The resulting theory, now called *wave mechanics* or *quantum mechanics*, has been amazingly successful. Though its principles may seem strange to us, whose experiences are limited to the macroscopic world, and though the mathematics required to solve even the simplest problem is quite involved, there seems to be no alternative to describe correctly the experimental results in atomic and nuclear physics. In this book we will confine our study to the Schrödinger theory because it is easier to learn and is a little less abstract than the Heisenberg theory. We will begin by restricting our discussion to problems in one space dimension.

| | | |
|------------|--|------------|
| 6-1 | The Schrödinger Equation in One Dimension | 222 |
| 6-2 | The Infinite Square Well | 229 |
| 6-3 | The Finite Square Well | 238 |
| 6-4 | Expectation Values and Operators | 242 |
| 6-5 | The Simple Harmonic Oscillator | 246 |
| 6-6 | Reflection and Transmission of Waves | 250 |

6-1 The Schrödinger Equation in One Dimension

The wave equation governing the motion of electrons and other particles with mass, which is analogous to the classical wave equation (Equation 5-11), was found by Schrödinger late in 1925 and is now known as the Schrödinger equation. Like the classical wave equation, the Schrödinger equation relates the time and space derivatives of the wave function. The reasoning followed by Schrödinger is somewhat difficult and not important for our purposes. In any case, it must be emphasized that we can't derive the Schrödinger equation just as we can't derive Newton's laws of motion. *Its validity, like that of any fundamental equation, lies in its agreement with experiment.* Just as Newton's second law is not relativistically correct, neither is Schrödinger's equation, which must ultimately yield to a relativistic wave equation. But, as you know, Newton's laws of motion are perfectly satisfactory for solving a vast array of nonrelativistic problems. So, too, will be Schrödinger's equation when applied to the equally extensive range of nonrelativistic problems in atomic, molecular, and solid-state physics. Schrödinger tried without success to develop a relativistic wave equation, a task accomplished in 1928 by Dirac.

Although it would be logical merely to postulate the Schrödinger equation, we can get some idea of what to expect by first considering the wave equation for photons, which is Equation 5-11 with speed $v = c$ and with $y(x, t)$ replaced by the electric field $\mathcal{E}(x, t)$.

$$\frac{\partial^2 \mathcal{E}}{\partial x^2} = \frac{1}{c^2} \frac{\partial^2 \mathcal{E}}{\partial t^2} \quad 6-1$$

As discussed in Chapter 5, a particularly important solution of this equation is the harmonic wave function $\mathcal{E}(x, t) = \mathcal{E}_0 \cos(kx - \omega t)$. Differentiating this function twice, we obtain

$$\frac{\partial^2 \mathcal{E}}{\partial t^2} = -\omega^2 \mathcal{E}_0 \cos(kx - \omega t) = -\omega^2 \mathcal{E}(x, t)$$

and

$$\frac{\partial^2 \mathcal{E}}{\partial x^2} = -k^2 \mathcal{E}(x, t)$$

Substitution into Equation 6-1 then gives

$$-k^2 = -\frac{\omega^2}{c^2}$$

or

$$\omega = kc \quad 6-2$$

Using $\omega = E/\hbar$ and $p = \hbar k$ for electromagnetic radiation, we have

$$E = pc \quad 6-3$$

which, as we saw earlier, is the relation between the energy and momentum of a photon.



Erwin Schrödinger. [Courtesy of the Niels Bohr Library, American Institute of Physics.]

Now let us use the de Broglie relations for a particle such as an electron to find the relation between ω and k that is analogous to Equation 6-2 for photons. We can then use this relation to work backward and see how the wave equation for electrons must differ from Equation 6-1. The total energy (nonrelativistic) of a particle of mass m is

$$E = \frac{p^2}{2m} + V \quad \text{6-4}$$

where V is the potential energy. Substituting the de Broglie relations (Equations 5-21 and 5-22) in Equation 6-4, we obtain

$$\hbar\omega = \frac{\hbar^2 k^2}{2m} + V \quad \text{6-5}$$

This differs from Equation 6-2 for a photon because it contains the potential energy V and because the angular frequency ω does not vary linearly with k . Note that we get a factor of ω when we differentiate a harmonic wave function with respect to time and a factor of k when we differentiate with respect to position. We expect, therefore, that the wave equation that applies to electrons will relate the *first* time derivative to the *second* space derivative and will also involve the potential energy of the electron.

Finally, we require that the wave equation for electrons will be a differential equation that is linear in the wave function $\Psi(x, t)$. This ensures that, if $\Psi_1(x, t)$ and $\Psi_2(x, t)$ are both solutions of the wave equation for the same potential energy, then any arbitrary linear combination of these solutions is also a solution—i.e., $\Psi(x, t) = a_1\Psi_1(x, t) + a_2\Psi_2(x, t)$ is a solution, with a_1 and a_2 being arbitrary constants. Such a combination is called *linear* because both $\Psi_1(x, t)$ and $\Psi_2(x, t)$ appear only to the first power. Linearity guarantees that the wave functions will add together to produce constructive and destructive interference, which we have seen to be a characteristic of matter waves, as well as all other wave phenomena. Note, in particular, that (1) the linearity requirement means that *every* term in the wave equation must be linear in $\Psi(x, t)$ and (2) that *any* derivative of $\Psi(x, t)$ is linear in $\Psi(x, t)$.⁴

The Schrödinger Equation

We are now ready to postulate the Schrödinger equation for a particle of mass m . In one dimension, it has the form

$$-\frac{\hbar^2}{2m} \frac{\partial^2 \Psi(x, t)}{\partial x^2} + V(x, t)\Psi(x, t) = i\hbar \frac{\partial \Psi(x, t)}{\partial t} \quad \text{6-6}$$

We will now show that this equation is satisfied by a harmonic wave function in the special case of a free particle, one on which no net force acts, so that the potential energy is constant, $V(x, t) = V_0$. First note that a function of the form $\cos(kx - \omega t)$ does not satisfy this equation because differentiation with respect to time changes the cosine to a sine, but the second derivative with respect to x gives back a cosine. Similar reasoning rules out the form $\sin(kx - \omega t)$. However, the exponential form of the harmonic wave function does satisfy the equation. Let

$$\begin{aligned} \Psi(x, t) &= A e^{i(kx - \omega t)} \\ &= A[\cos(kx - \omega t) + i \sin(kx - \omega t)] \end{aligned} \quad \text{6-7}$$

where A is a constant. Then

$$\frac{\partial \Psi}{\partial t} = -i\omega A e^{i(kx - \omega t)} = -i\omega \Psi$$

and

$$\frac{\partial^2 \Psi}{\partial x^2} = (ik)^2 A e^{i(kx - \omega t)} = -k^2 \Psi$$

Substituting these derivatives into the Schrödinger equation with $V(x, t) = V_0$ gives

$$\frac{-\hbar^2}{2m}(-k^2\Psi) + V_0\Psi = i\hbar(-i\omega)\Psi$$

or

$$\frac{\hbar^2 k^2}{2m} + V_0 = \hbar\omega$$

which is Equation 6-5.

An important difference between the Schrödinger equation and the classical wave equation is the explicit appearance⁵ of the imaginary number $i = (-1)^{1/2}$. The wave functions that satisfy the Schrödinger equation are not necessarily real, as we see from the case of the free-particle wave function of Equation 6-7. Evidently the wave function $\Psi(x, t)$ which solves the Schrödinger equation is not a directly measurable function as the classical wave function $y(x, t)$ is since measurements always yield real numbers. However, as we discussed in Section 5-4, the probability of

finding the electron in dx is certainly measurable, just as is the probability that a flipped coin will turn up heads. The probability $P(x)dx$ that the electron will be found in the volume dx was defined by Equation 5-23 to be equal to $|\Psi|^2 dx$. This probabilistic interpretation of Ψ was developed by Max Born and was recognized, over the early and formidable objections of both Schrödinger and Einstein, as the appropriate way of relating solutions of the Schrödinger equation to the results of physical measurements. The probability that an electron is in the region dx , a real number, can be measured by counting the fraction of time it is found there in a very large number of identical trials. In recognition of the complex nature of $\Psi(x, t)$, we must modify slightly the interpretation of the wave function discussed in Chapter 5 to accommodate Born's interpretation so that the probability of finding the electron in dx is real. We take for the probability

$$P(x, t) dx = \Psi^*(x, t)\Psi(x, t) dx = |\Psi(x, t)|^2 dx \quad 6-8$$

where Ψ^* , the complex conjugate of Ψ , is obtained from Ψ by replacing i with $-i$ wherever it appears.⁶ The complex nature of Ψ serves to emphasize the fact that, in reality, we should not ask or try to answer the question, "What is waving in a matter wave?" or inquire as to what medium supports the motion of a matter wave. The wave function is a computational device with utility in Schrödinger's theory of wave mechanics. Physical significance is associated not with Ψ itself, but with the product $\Psi^*\Psi = |\Psi|^2$, which is the probability distribution $P(x, t)$ or, as it is often called, the *probability density*. In keeping with the analogy with classical waves and wave functions, $\Psi(x, t)$ is also sometimes referred to as the *probability density amplitude*, or just the *probability amplitude*.

The probability of finding the electron in dx at x_1 or in dx at x_2 is the sum of separate probabilities, $P(x_1) dx + P(x_2) dx$. Since the electron must certainly be somewhere in space, the sum of the probabilities over all possible values of x must equal 1. That is⁷

$$\int_{-\infty}^{+\infty} \Psi^*\Psi dx = 1 \quad 6-9$$

Equation 6-9 is called the *normalization condition*. This condition plays an important role in quantum mechanics, for it places a restriction on the possible solutions of the Schrödinger equation. In particular, the wave function $\Psi(x, t)$ must approach zero sufficiently fast as $x \rightarrow \pm\infty$ so that the integral in Equation 6-9 remains finite. If it does not, then the probability becomes unbounded. As we will see in Section 6-3, it is this restriction together with boundary conditions imposed at finite values of x that leads to energy quantization for bound particles.

In the chapters that follow, we are going to be concerned with solutions to the Schrödinger equation for a wide range of real physical systems, but in what follows in this chapter, our intent is to illustrate a few of the techniques of solving the equation and to discover the various, often surprising properties of the solutions. To this end we will focus our attention on one-dimensional problems, as noted earlier, and use some potential energy functions with unrealistic physical characteristics, e.g., infinitely rigid walls, which will enable us to illustrate various properties of the solutions without obscuring the discussion with overly complex mathematics.

Separation of the Time and Space Dependencies of $\Psi(x, t)$

Schrödinger's first application of his wave equation was to problems such as the hydrogen atom (Bohr's work) and the simple harmonic oscillator (Planck's work), in which he showed that the energy quantization in those systems can be explained naturally in terms of standing waves. We referred to these in Chapter 4 as stationary states, meaning they did not change with time. Such states are also called *eigenstates*. For such problems that also have potential energy functions that are independent of time, the space and time dependence of the wave function can be separated, leading to a greatly simplified form of the Schrödinger equation.⁸ The separation is accomplished by first assuming that $\Psi(x, t)$ can be written as a product of two functions, one of x and one of t , as

$$\Psi(x, t) = \psi(x)\phi(t) \quad \text{6-10}$$

If Equation 6-10 turns out to be incorrect, we will find that out soon enough, but it turns out that *if* the potential function is *not* an explicit function of time, i.e., if the potential is given by $V(x)$, our assumption turns out to be valid. That this is true can be seen as follows:

Substituting $\Psi(x, t)$ from Equation 6-10 into the general, time-dependent Schrödinger equation (Equation 6-6) yields

$$\frac{-\hbar^2}{2m} \frac{\partial^2 \psi(x)\phi(t)}{\partial x^2} + V(x)\psi(x)\phi(t) = i\hbar \frac{\partial \psi(x)\phi(t)}{\partial t} \quad \text{6-11}$$

which is

$$\frac{-\hbar^2}{2m} \phi(t) \frac{d^2 \psi(x)}{dx^2} + V(x)\psi(x)\phi(t) = i\hbar \psi(x) \frac{d\phi(t)}{dt} \quad \text{6-12}$$

where the derivatives are now ordinary rather than partial ones. Dividing Equation 6-12 by Ψ in the assumed product form $\psi\phi$ gives

$$\frac{-\hbar^2}{2m} \frac{1}{\psi(x)} \frac{d^2 \psi(x)}{dx^2} + V(x) = i\hbar \frac{1}{\phi(t)} \frac{d\phi(t)}{dt} \quad \text{6-13}$$

Notice that each side of Equation 6-13 is a function of only one of the independent variables x and t . This means that, for example, changes in t cannot affect the value of the left side of Equation 6-13, and changes in x cannot affect the right side. Thus, both sides of the equation must be equal to the same constant C , called the *separation constant*, and we see that the assumption of Equation 6-10 is valid—the variables have been separated. We have thus replaced a partial differential equation containing two independent variables, Equation 6-6, with two ordinary differential equations each a function of only one of the independent variables:

$$\frac{-\hbar^2}{2m} \frac{1}{\psi(x)} \frac{d^2 \psi(x)}{dx^2} + V(x) = C \quad \text{6-14}$$

$$i\hbar \frac{1}{\phi(t)} \frac{d\phi(t)}{dt} = C \quad \text{6-15}$$

Let us solve Equation 6-15 first. The reason for doing so is twofold: (1) Equation 6-15 does not contain the potential $V(x)$; consequently, the time-dependent part $\phi(t)$ of all solutions $\Psi(x, t)$ to the Schrödinger equation will have the same form when the potential is not an explicit function of time, so we only have to do this once. (2) The separation constant C has particular significance that we want to discover before we tackle Equation 6-14. Writing Equation 6-15 as

$$\frac{d\phi(t)}{\phi(t)} = \frac{C}{i\hbar} dt = -\frac{iC}{\hbar} dt \quad 6-16$$

The general solution of Equation 6-16 is

$$\phi(t) = e^{-iCt/\hbar} \quad 6-17a$$

which can also be written as

$$\phi(t) = e^{-iCt/\hbar} = \cos\left(\frac{Ct}{\hbar}\right) - i \sin\left(\frac{Ct}{\hbar}\right) = \cos\left(2\pi\frac{Ct}{\hbar}\right) - i \sin\left(2\pi\frac{Ct}{\hbar}\right) \quad 6-17b$$

Thus, we see that $\phi(t)$, which describes the time variation of $\Psi(x, t)$, is an oscillatory function with frequency $f = C/\hbar$. However, according to the de Broglie relation (Equation 5-1), the frequency of the wave represented by $\Psi(x, t)$ is $f = E/\hbar$; therefore, we conclude that the separation constant $C = E$, the total energy of the particle, and we have

$$\phi(t) = e^{-iEt/\hbar} \quad 6-17c$$

for all solutions to Equation 6-6 involving time-independent potentials. Equation 6-14 then becomes, on multiplication by $\psi(x)$,

$$\frac{-\hbar^2}{2m} \frac{d^2\psi(x)}{dx^2} + V(x)\psi(x) = E\psi(x) \quad 6-18$$

Equation 6-18 is referred to as the *time-independent Schrödinger equation*.

The time-independent Schrödinger equation in one dimension is an ordinary differential equation in one variable x and is therefore much easier to handle than the general form of Equation 6-6. The normalization condition of Equation 6-9 can be expressed in terms of $\psi(x)$, since the time dependence of the absolute square of the wave function cancels. We have

$$\Psi^*(x, t)\Psi(x, t) = \psi^*(x)e^{+iEt/\hbar}\psi(x)e^{-iEt/\hbar} = \psi^*(x)\psi(x) \quad 6-19$$

and Equation 6-9 then becomes

$$\int_{-\infty}^{+\infty} \psi^*(x)\psi(x)dx = 1 \quad 6-20$$

Conditions for Acceptable Wave Functions

The form of the wave function $\psi(x)$ that satisfies Equation 6-18 depends on the form of the potential energy function $V(x)$. In the next few sections we will study some simple but important problems in which $V(x)$ is specified. Our example potentials will be approximations to real physical potentials, simplified to make calculations easier.

In some cases, the slope of the potential energy may be discontinuous, e.g., $V(x)$ may have one form in one region of space and another form in an adjacent region. (This is a useful mathematical approximation to real situations in which $V(x)$ varies rapidly over a small region of space, such as at the surface boundary of a metal.) The procedure in such cases is to solve the Schrödinger equation separately in each region of space and then require that the solutions join smoothly at the point of discontinuity.

Since the probability of finding a particle cannot vary discontinuously from point to point, the wave function $\psi(x)$ must be continuous.⁹ Since the Schrödinger equation involves the second derivative $d^2\psi/dx^2 = \psi''$, the first derivative ψ' (which is the slope) must also be continuous. That is, the graph of $\psi(x)$ versus x must be smooth. (In a special case in which the potential energy becomes infinite, this restriction is relaxed. Since no particle can have infinite potential energy, $\psi(x)$ must be zero in regions where $V(x)$ is infinite. Then, at the boundary of such a region, ψ' may be discontinuous.)

If either $\psi(x)$ or $d\psi/dx$ were not finite or not single valued, the same would be true of $\Psi(x, t)$ and $d\Psi/dx$. As we will shortly see, the predictions of wave mechanics regarding the results of measurements involve both of those quantities and would thus not necessarily predict finite or definite values for real physical quantities. Such results would not be acceptable since measurable quantities, such as angular momentum and position, are never infinite or multiple valued. A final restriction on the form of the wave function $\psi(x)$ is that in order to obey the normalization condition, $\psi(x)$ must approach zero sufficiently fast as $x \rightarrow \pm \infty$ so that normalization is preserved. For future reference, we may summarize the conditions that the wave function $\psi(x)$ must meet in order to be acceptable as follows:

1. $\psi(x)$ must exist and satisfy the Schrödinger equation.
2. $\psi(x)$ and $d\psi/dx$ must be continuous.
3. $\psi(x)$ and $d\psi/dx$ must be finite.
4. $\psi(x)$ and $d\psi/dx$ must be single valued.
5. $\psi(x) \rightarrow 0$ fast enough as $x \rightarrow \pm \infty$ so that the normalization integral, Equation 6-20, remains bounded.

Note that, given Equation 6-10, the acceptability conditions above ultimately apply to $\Psi(x, t)$.

Questions

1. Like the classical wave equation, the Schrödinger equation is linear. Why is this important?
2. There is no factor $i = (-1)^{1/2}$ in Equation 6-18. Does this mean that $\psi(x)$ must be real?
3. Why must the electric field $\mathcal{E}(x, t)$ be real? Is it possible to find a nonreal wave function that satisfies the classical wave equation?
4. Describe how the de Broglie hypothesis enters into the Schrödinger wave equation.
5. What would be the effect on the Schrödinger equation of adding a constant rest energy for a particle with mass to the total energy E in the de Broglie relation $f = E/h$?
6. Describe in words what is meant by normalization of the wave function.

EXAMPLE 6-1 A Solution to the Schrödinger Equation Show that for a free particle of mass m moving in one dimension, the function $\psi(x) = A \sin kx + B \cos kx$ is a solution to the time-independent Schrödinger equation for any values of the constants A and B .

SOLUTION

A free particle has no net force acting upon it, e.g., $V(x) = 0$, in which case the kinetic energy equals the total energy. Thus, $p = \hbar k = (2mE)^{1/2}$. Differentiating $\psi(x)$ gives

$$\frac{d\psi}{dx} = kA \cos kx - kB \sin kx$$

and differentiating again,

$$\begin{aligned}\frac{d^2\psi}{dx^2} &= -k^2A \sin kx - k^2B \cos kx \\ &= -k^2(A \sin kx + B \cos kx) = -k^2\psi(x)\end{aligned}$$

Substituting into Equation 6-18,

$$\begin{aligned}\frac{-\hbar^2}{2m}[(-k^2)(A \sin kx + B \cos kx)] &= E(A \sin kx + B \cos kx) \\ \frac{\hbar^2 k^2}{2m}\psi(x) &= E\psi(x)\end{aligned}$$

and, since $\hbar^2 k^2 = 2mE$, we have

$$E\psi(x) = E\psi(x)$$

and the given $\psi(x)$ is a solution of Equation 6-18.

6-2 The Infinite Square Well

A problem that provides several illustrations of the properties of wave functions and is also one of the easiest problems to solve using the time-independent, one-dimensional Schrödinger equation is that of the infinite square well, sometimes called the particle in a box. A macroscopic example is a bead moving on a frictionless wire between two massive stops clamped to the wire. We could also build such a “box” for an electron using electrodes and grids in an evacuated tube, as illustrated in Figure 6-1a. The walls of the box are provided by the increasing potential between the grids G and the electrode C as shown in Figures 6-1b and c. The walls can be made arbitrarily high and steep by increasing the potential V and reducing the separation between each grid-electrode pair. In the limit such a potential energy function looks like that in Figure 6-2, which is a graph of the potential energy of an infinite square well. For this problem the potential energy is of the form

$$\begin{aligned}V(x) &= 0 & 0 < x < L \\ V(x) &= \infty & x < 0 \quad \text{and} \quad x > L\end{aligned} \tag{6-21}$$

Although such a potential is clearly artificial, the problem is worth careful study for several reasons: (1) exact solutions to the Schrödinger equation can be obtained

Figure 6-1 (a) The electron placed between the two sets of electrodes C and grids G experiences no force in the region between the grids, which are at ground potential. However, in the regions between each C and G is a repelling electric field whose strength depends upon the magnitude of V . (b) If V is small, then the electron's potential energy versus x has low, sloping "walls." (c) If V is large, the "walls" become very high and steep, becoming infinitely high for $V \rightarrow \infty$.

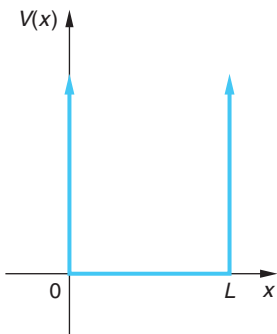
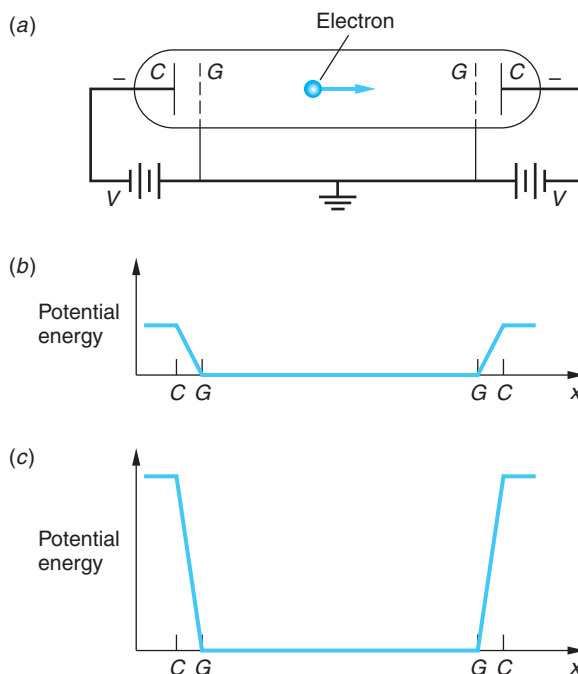


Figure 6-2 Infinite square well potential energy. For $0 < x < L$, the potential energy $V(x)$ is zero. Outside this region, $V(x)$ is infinite. The particle is confined to the region in the well $0 < x < L$.

without the difficult mathematics that usually accompanies its solution for more realistic potential functions, (2) the problem is closely related to the vibrating-string problem familiar in classical physics, (3) it illustrates many of the important features of all quantum-mechanical problems, and finally, (4) this potential is a relatively good approximation to some real situations; e.g., the motion of a free electron inside a metal.

Since the potential energy is infinite outside the well, the wave function is required to be zero there; that is, the particle must be inside the well. (As we proceed through this and other problems, keep in mind Born's interpretation: the probability density of the particle's position is proportional to $|\psi|^2$.) We then need only to solve Equation 6-18 for the region inside the well $0 < x < L$, subject to the condition that since the wave function must be continuous, $\psi(x)$ must be zero at $x = 0$ and $x = L$. Such a condition on the wave function at a boundary (here, the discontinuity of the potential energy function) is called a *boundary condition*. We will see that, mathematically, it is the boundary conditions together with the requirement that $\psi(x) \rightarrow 0$ as $x \rightarrow \pm\infty$ that lead to the quantization of energy. A classic example is the case of a vibrating string fixed at both ends. In that case the wave function $y(x, t)$ is the displacement of the string. If the string is fixed at $x = 0$ and $x = L$, we have the same boundary condition on the vibrating-string wave function: namely, that $y(x, t)$ be zero at $x = 0$ and $x = L$. These boundary conditions lead to discrete allowed frequencies of vibration of the string. It was this quantization of frequencies (which always occurs for standing waves in classical physics), along with de Broglie's hypothesis, that motivated Schrödinger to look for a wave equation for electrons.

The standing-wave condition for waves on a string of length L fixed at both ends is that *an integral number of half wavelengths fit into the length L* .

$$n \frac{\lambda}{2} = L \quad n = 1, 2, 3, \dots \quad 6-22$$

We will show below that the same condition follows from the solution of the Schrödinger equation for a particle in an infinite square well. Since the wavelength is related to the momentum of the particle by the de Broglie relation $p = h/\lambda$ and the total energy of the particle in the well is just the kinetic energy $p^2/2m$ (see Figure 6-2), this quantum condition on the wavelength implies that the energy is quantized and the allowed values are given by

$$E = \frac{p^2}{2m} = \frac{h^2}{2m\lambda^2} = \frac{h^2}{2m(2L/n)^2} = n^2 \frac{h^2}{8mL^2} \quad \text{6-23}$$

Since the energy depends on the integer n , it is customary to label it E_n . In terms of $\hbar = h/2\pi$ the energy is given by

$$E_n = n^2 \frac{\pi^2 \hbar^2}{2mL^2} = n^2 E_1 \quad n = 1, 2, 3, \dots \quad \text{6-24}$$

where E_1 is the lowest allowed energy¹⁰ and is given by

$$E_1 = \frac{\pi^2 \hbar^2}{2mL^2} \quad \text{6-25}$$

We now derive this result from the time-independent Schrödinger equation (Equation 6-18), which for $V(x) = 0$ is

$$-\frac{\hbar^2}{2m} \frac{d^2\psi(x)}{dx^2} = E\psi(x)$$

or

$$\psi''(x) = -\frac{2mE}{\hbar^2} \psi(x) = -k^2 \psi(x) \quad \text{6-26}$$

where we have substituted the square of the wave number k since

$$k^2 = \left(\frac{p}{\hbar}\right)^2 = \frac{2mE}{\hbar^2} \quad \text{6-27}$$

and we have written $\psi''(x)$ for the second derivative $d^2\psi(x)/dx^2$. Equation 6-26 has solutions of the form

$$\psi(x) = A \sin kx \quad \text{6-28a}$$

and

$$\psi(x) = B \cos kx \quad \text{6-28b}$$

where A and B are constants. The boundary condition $\psi(x) = 0$ at $x = 0$ rules out the cosine solution (Equation 6-28b) because $\cos 0 = 1$, so B must equal zero. The boundary condition $\psi(x) = 0$ at $x = L$ gives

$$\psi(L) = A \sin kL = 0 \quad \text{6-29}$$

This condition is satisfied if kL is any integer times π , i.e., if k is restricted to the values k_n given by

$$k_n = n \frac{\pi}{L} \quad n = 1, 2, 3, \dots \quad 6-30$$

If we write the wave number k in terms of the wavelength $\lambda = 2\pi/k$, we see that Equation 6-30 is the same as Equation 6-22 for standing waves on a string. The quantized energy values, or *energy eigenvalues*, are found from Equation 6-27, replacing k by k_n as given by Equation 6-30. We thus have

$$E_n = \frac{\hbar^2 k_n^2}{2m} = n^2 \frac{\hbar^2 \pi^2}{2m L^2} = n^2 E_1$$

which is the same as Equation 6-24. Figure 6-3 shows the energy level diagram and the potential energy function for the infinite square well potential.

The constant A in the wave function of Equation 6-28a is determined by the normalization condition:

$$\int_{-\infty}^{+\infty} \psi_n^* \psi_n dx = \int_0^L A_n^2 \sin^2\left(\frac{n\pi x}{L}\right) dx = 1 \quad 6-31$$

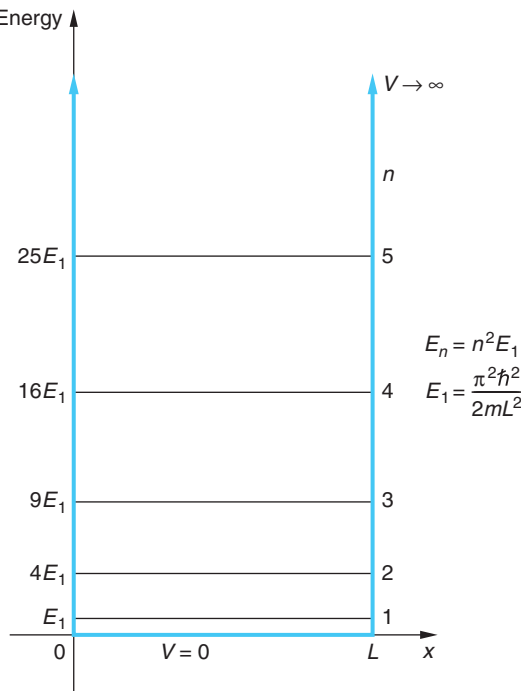


Figure 6-3 Graph of energy vs. x for a particle in an infinitely deep well. The potential energy $V(x)$ is shown with the colored lines. The set of allowed values for the particle's total energy E_n as given by Equation 6-24 form the energy-level diagram for the infinite square well potential. Classically, a particle can have any value of energy. Quantum mechanically, only the values given by $E_n = n^2(\hbar^2\pi^2/2mL^2)$ yield well-behaved solutions of the Schrödinger equation. As we become more familiar with energy-level diagrams, the x axis will be omitted.

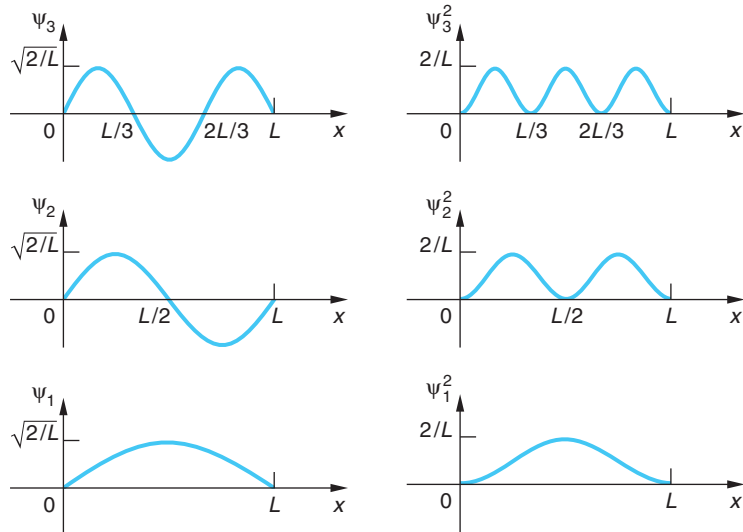


Figure 6-4 Wave functions $\psi_n(x)$ and probability densities $P_n(x) = \psi_n^2(x)$ for $n = 1, 2$, and 3 for the infinite square well potential. Though not shown, $\psi_n(x) = 0$ for $x < 0$ and $x > L$.

Since the wave function is zero in regions of space where the potential energy is infinite, the contributions to the integral from $-\infty$ to 0 and from L to $+\infty$ will both be zero. Thus, only the integral from 0 to L needs to be evaluated. Integrating, we obtain $A_n = (2/L)^{1/2}$ independent of n . The normalized wave function solutions for this problem, also called *eigenfunctions*, are then

$$\psi_n(x) = \sqrt{\frac{2}{L}} \sin \frac{n\pi x}{L} \quad n = 1, 2, 3, \dots \quad 6-32$$

These wave functions are exactly the same as the standing-wave functions $y_n(x)$ for the vibrating-string problem. The wave functions and the probability distribution functions $P_n(x)$ are sketched in Figure 6-4 for the lowest energy state $n = 1$, called the *ground state*, and for the first two *excited states*, $n = 2$ and $n = 3$. (Since these wave functions are real, $P_n(x) = \psi_n^* \psi_n = \psi_n^2$.) Notice in Figure 6-4 that the maximum amplitudes of each of the $\psi_n(x)$ are the same, $(2/L)^{1/2}$, as are those of $P_n(x)$, $2/L$. Note, too, that both $\psi_n(x)$ and $P_n(x)$ extend to $\pm \infty$. They just happen to be zero for $x < 0$ and $x > L$ in this case.

The number n in the equations above is called a *quantum number*. It specifies both the energy and the wave function. Given any value of n , we can immediately write down the wave function and the energy of the system. The quantum number n occurs because of the boundary conditions $\psi(x) = 0$ at $x = 0$ and $x = L$. We will see in Section 7-1 that for problems in three dimensions, three quantum numbers arise, one associated with boundary conditions on each coordinate.

Comparison with Classical Results

Let us compare our quantum-mechanical solution of this problem with the classical solution. In classical mechanics, if we know the potential energy function $V(x)$, we can find the force from $F_x = -dV/dx$ and thereby obtain the acceleration $a_x = d^2x/dt^2$ from Newton's second law. We can then find the position x as a function of time t if we know the initial position and velocity. In this problem there is no force when the

particle is between the walls of the well because $V = 0$ there. The particle therefore moves with constant speed in the well. Near the edge of the well the potential energy rises discontinuously to infinity—we may describe this as a very large force that acts over a very short distance and turns the particle around at the wall so that it moves away with its initial speed. Any speed, and therefore any energy, is permitted classically. The classical description breaks down because, according to the uncertainty principle, we can never precisely specify both the position and momentum (and therefore velocity) at the same time. We can therefore never specify the initial conditions precisely and cannot assign a definite position and momentum to the particle. Of course, for a macroscopic particle moving in a macroscopic box, the energy is much larger than E_1 of Equation 6-25, and the minimum uncertainty of momentum, which is of the order of \hbar/L , is much less than the momentum and less than experimental uncertainties. Then the difference in energy between adjacent states will be a small fraction of the total energy, quantization will be unnoticed, and the classical description will be adequate.¹¹

Let us also compare the classical prediction for the distribution of measurements of position with those from our quantum-mechanical solution. Classically, the probability of finding the particle in some region dx is proportional to the time spent in dx , which is dx/v , where v is the speed. Since the speed is constant, the classical distribution function is just a constant inside the well. The normalized classical distribution function is

$$P_c(x) = \frac{1}{L}$$

In Figure 6-4 we see that for the lowest energy states, the quantum distribution function is very different from this. According to Bohr's correspondence principle, the quantum distributions should approach the classical distribution when n is large, that is, at large energies. For any state n , the quantum distribution has n peaks. The distribution for $n = 10$ is shown in Figure 6-5. For very large n , the peaks are close together, and if there are many peaks in a small distance Δx , only the average value will be observed. But the average value of $\sin^2 k_n x$ over one or more cycles is $1/2$. Thus

$$\left[\Psi_n^2(x) \right]_{\text{av}} = \left[\frac{2}{L} \sin^2 k_n x \right]_{\text{av}} = \frac{2}{L} \frac{1}{2} = \frac{1}{L}$$

which is the same as the classical distribution.

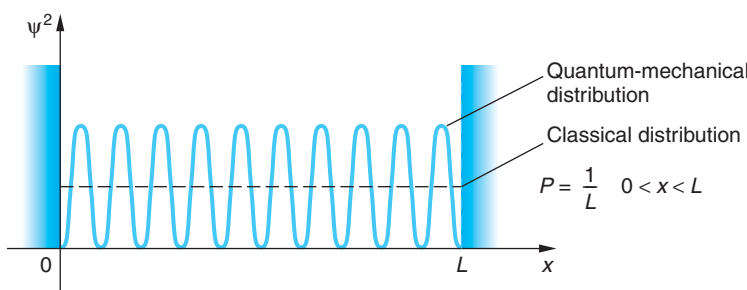


Figure 6-5 Probability distribution for $n = 10$ for the infinite square well potential. The dashed line is the classical probability density $P = 1/L$, which is equal to the quantum-mechanical distribution averaged over a region Δx containing several oscillations. A physical measurement with resolution Δx will yield the classical result if n is so large that $\psi^2(x)$ has many oscillations in Δx .

The Complete Wave Function

The complete wave function, including its time dependence, is found by multiplying the space part by

$$e^{-i\omega t} = e^{-i(E_n/\hbar)t}$$

according to Equation 6-17c. As mentioned previously, a wave function corresponding to a single energy oscillates with angular frequency $\omega_n = E_n/\hbar$, but the probability distribution $|\Psi_n(x, t)|^2$ is independent of time. This is the wave-mechanical justification for calling such a state a stationary state or eigenstate, as we have done earlier. It is instructive to look at the complete wave function for a particular state n .

$$\Psi_n(x, t) = \sqrt{\frac{2}{L}} \sin k_n x e^{-i\omega_n t}$$

If we use the identity

$$\sin k_n x = \frac{(e^{ik_n x} - e^{-ik_n x})}{2i}$$

we can write this wave function as

$$\Psi_n(x, t) = \frac{1}{2i} \sqrt{\frac{2}{L}} [e^{i(k_n x - \omega_n t)} - e^{-i(k_n x + \omega_n t)}]$$

Just as in the case of the standing-wave function for the vibrating string, we can consider this stationary-state wave function to be the superposition of a wave traveling to the right and a wave of the same frequency and amplitude traveling to the left. Since measurable quantities are related to $P \propto |\Psi|^2$, the fact that Ψ is complex is not a problem.

EXAMPLE 6-2 An Electron in a Wire An electron moving in a thin metal wire is a reasonable approximation of a particle in a one-dimensional infinite well. The potential inside the wire is constant on average but rises sharply at each end. Suppose the electron is in a wire 1.0 cm long. (a) Compute the ground-state energy for the electron. (b) If the electron's energy is equal to the average kinetic energy of the molecules in a gas at $T = 300$ K, about 0.03 eV, what is the electron's quantum number n ?

SOLUTION

- For question (a), the ground-state energy is given by Equation 6-25:

$$\begin{aligned} E_1 &= \frac{\pi^2 \hbar^2}{2mL^2} \\ &= \frac{\pi^2 (1.055 \times 10^{-34} \text{ J} \cdot \text{s})^2}{(2)(9.11 \times 10^{-31} \text{ kg})(10^{-2} \text{ m})^2} \\ &= 6.03 \times 10^{-34} \text{ J} = 3.80 \times 10^{-15} \text{ eV} \end{aligned}$$

- For question (b), the electron's quantum number is given by Equation 6-24:

$$E_n = n^2 E_1$$

3. Solving Equation 6-24 for n and substituting $E_n = 0.03$ eV and E_1 from above yields

$$n^2 = \frac{E_n}{E_1}$$

or

$$\begin{aligned} n &= \sqrt{\frac{E_n}{E_1}} = \sqrt{\frac{0.03 \text{ eV}}{3.80 \times 10^{-15} \text{ eV}}} \\ &= 2.81 \times 10^6 \end{aligned}$$

Remarks: The value of E_1 computed above is not only far below the limit of measurability, but also smaller than the uncertainty in the energy of an electron confined into 1 cm. For a value of n this large, the correspondence principle applies.

EXAMPLE 6-3 Calculating Probabilities Suppose that the electron in Example 6-2 could be measured while in its ground state. (a) What would be the probability of finding it somewhere in the region $0 < x < L/4$? (b) What would be the probability of finding it in a very narrow region $\Delta x = 0.01L$ wide centered at $x = 5L/8$?

SOLUTION

(a) The wave function for the $n = 1$ level, the ground state, is given by Equation 6-32 as

$$\psi_1(x) = \sqrt{\frac{2}{L}} \sin \frac{\pi x}{L}$$

The probability that the electron would be found in the region specified is

$$\int_0^{L/4} P_1(x) dx = \int_0^{L/4} \frac{2}{L} \sin^2 \left(\frac{\pi x}{L} \right) dx$$

Letting $u = \pi x/L$, hence $dx = L du/\pi$, and noting the appropriate change in the limits on the integral, we have that

$$\int_0^{\pi/4} \frac{2}{\pi} \sin^2 u du = \frac{2}{\pi} \left(\frac{u}{2} - \frac{\sin 2u}{4} \right) \Big|_0^{\pi/4} = \frac{2}{\pi} \left(\frac{\pi}{8} - \frac{1}{4} \right) = 0.091$$

Thus, if one looked for the particle in a large number of identical searches, the electron would be found in the region $0 < x < 0.25$ cm about 9 percent of the time. This probability is illustrated by the shaded area on the left side in Figure 6-6.

(b) Since the region $\Delta x = 0.01L$ is very small compared with L , we do not need to integrate but can calculate the approximate probability as follows:

$$P = P(x) \Delta x = \frac{2}{L} \sin^2 \frac{\pi x}{L} \Delta x$$

Substituting $\Delta x = 0.01L$ and $x = 5L/8$, we obtain

$$\begin{aligned} P &= \frac{2}{L} \sin^2 \frac{\pi(5L/8)}{L} (0.01L) \\ &= \frac{2}{L} (0.854)(0.01L) = 0.017 \end{aligned}$$

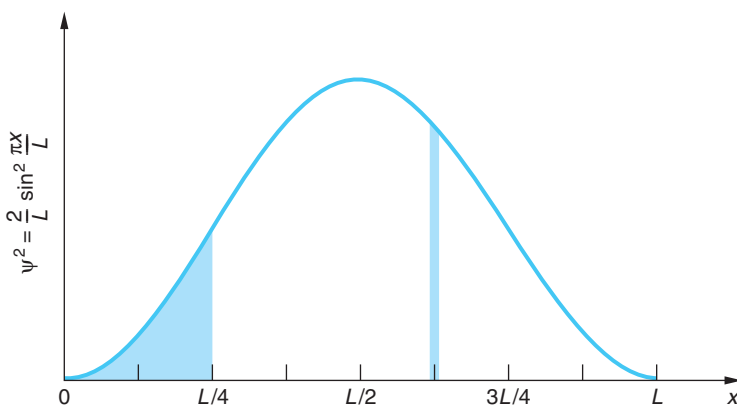


Figure 6-6 The probability density $\psi^2(x)$ versus x for a particle in the ground state of an infinite square well potential. The probability of finding the particle in the region $0 < x < L/4$ is represented by the larger shaded area. The narrow shaded band illustrates the probability of finding the particle within $\Delta x = 0.01L$ around the point where $x = 5L/8$.

This means that the probability of finding the electron within $0.01L$ around $x = 5L/8$ is about 1.7 percent. This is illustrated in Figure 6-6, where the area of the shaded narrow band at $x = 5L/8$ is 1.7 percent of the total area under the curve.

EXAMPLE 6-4 An Electron in an Atomic-Size Box (a) Find the energy in the ground state of an electron confined to a one-dimensional box of length $L = 0.1$ nm. (This box is roughly the size of an atom.) (b) Make an energy-level diagram and find the wavelengths of the photons emitted for all transitions beginning at state $n = 3$ or less and ending at a lower energy state.

SOLUTION

(a) The energy in the ground state is given by Equation 6-25. Multiplying the numerator and denominator by $c^2/4\pi^2$, we obtain an expression in terms of hc and mc^2 , the energy equivalent of the electron mass (see Chapter 2):

$$E_1 = \frac{(hc)^2}{8mc^2L^2}$$

Substituting $hc = 1240 \text{ eV} \cdot \text{nm}$ and $mc^2 = 0.511 \text{ MeV}$, we obtain

$$E_1 = \frac{(1240 \text{ eV} \cdot \text{nm})^2}{8(5.11 \times 10^5 \text{ eV})(0.1 \text{ nm})^2} = 37.6 \text{ eV}$$

This is of the same order of magnitude as the kinetic energy of the electron in the ground state of the hydrogen atom, which is 13.6 eV. In that case, the wavelength of the electron equals the circumference of a circle of radius 0.0529 nm, or about 0.33 nm, whereas for the electron in a one-dimensional box of length 0.1 nm, the wavelength in the ground state is $2L = 0.2$ nm.

(b) The energies of this system are given by

$$E_n = n^2 E_1 = n^2(37.6 \text{ eV})$$

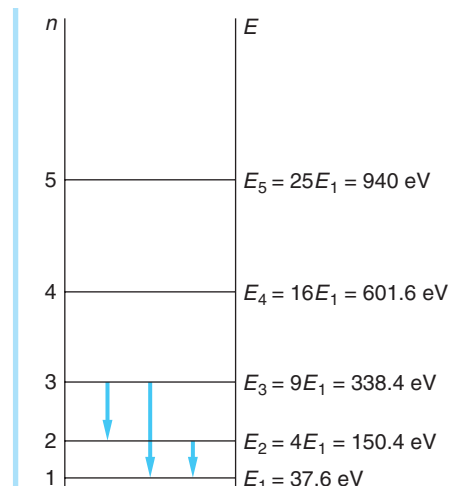


Figure 6-7 Energy-level diagram for Example 6-4. Transitions from the state $n = 3$ to the states $n = 2$ and $n = 1$, and from the state $n = 2$ to $n = 1$, are indicated by the vertical arrows.

Figure 6-7 shows these energies in an energy-level diagram. The energy of the first excited state is $E_2 = 4 \cdot (37.6 \text{ eV}) = 150.4 \text{ eV}$, and that of the second excited state is $E_3 = 9 \cdot (37.6 \text{ eV}) = 338.4 \text{ eV}$. The possible transitions from level 3 to level 2, from level 3 to level 1, and from level 2 to level 1 are indicated by the vertical arrows on the diagram. The energies of these transitions are

$$\begin{aligned}\Delta E_{3 \rightarrow 2} &= 338.4 \text{ eV} - 150.4 \text{ eV} = 188.0 \text{ eV} \\ \Delta E_{3 \rightarrow 1} &= 338.4 \text{ eV} - 37.6 \text{ eV} = 300.8 \text{ eV} \\ \Delta E_{2 \rightarrow 1} &= 150.4 \text{ eV} - 37.6 \text{ eV} = 112.8 \text{ eV}\end{aligned}$$

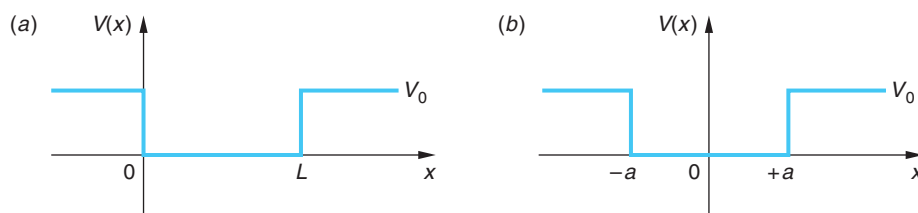
The photon wavelengths for these transitions are

$$\begin{aligned}\lambda_{3 \rightarrow 2} &= \frac{hc}{\Delta E_{3 \rightarrow 2}} = \frac{1240 \text{ eV} \cdot \text{nm}}{188.0 \text{ eV}} = 6.60 \text{ nm} \\ \lambda_{3 \rightarrow 1} &= \frac{hc}{\Delta E_{3 \rightarrow 1}} = \frac{1240 \text{ eV} \cdot \text{nm}}{300.8 \text{ eV}} = 4.12 \text{ nm} \\ \lambda_{2 \rightarrow 1} &= \frac{hc}{\Delta E_{2 \rightarrow 1}} = \frac{1240 \text{ eV} \cdot \text{nm}}{112.8 \text{ eV}} = 11.0 \text{ nm}\end{aligned}$$

6-3 The Finite Square Well

The quantization of energy that we found for a particle in an infinite square well is a general result that follows from the solution of the Schrödinger equation for any particle confined in some region of space. We will illustrate this by considering the qualitative behavior of the wave function for a slightly more general potential energy function, the finite square well shown in Figure 6-8. The solutions of the Schrödinger equation for this type of potential energy are quite different, depending on whether the total energy E is greater or less than V_0 . We will defer discussion of the case $E > V_0$ to Section 6-5 except to remark that in that case, the particle is not confined and any value of the energy is allowed; i.e., there is no energy quantization. Here we will assume that $E < V_0$.

FÉUE WHI



Inside the well, $V(x) = 0$ and the time-independent Schrödinger equation (Equation 6-18) becomes Equation 6-26, the same as for the infinite well:

$$\psi''(x) = -k^2\psi(x) \quad k^2 = \frac{2mE}{\hbar^2}$$

The solutions are sines and cosines (Equation 6-28) except that now we do not require $\psi(x)$ to be zero at the well boundaries, but rather we require that $\psi(x)$ and $\psi'(x)$ be continuous at these points. Outside the well, i.e., for $0 > x > L$, Equation 6-18 becomes

$$\psi''(x) = \frac{2m}{\hbar^2}(V_0 - E)\psi(x) = \alpha^2\psi(x) \quad 6-33$$

where

$$\alpha^2 = \frac{2m}{\hbar^2}(V_0 - E) > 0 \quad 6-34$$

The straightforward method of finding the wave functions and allowed energies for this problem is to solve Equation 6-33 for $\psi(x)$ outside the well and then require that $\psi(x)$ and $\psi'(x)$ be continuous at the boundaries. The solution of Equation 6-33 is not difficult [it is of the form $\psi(x) = Ce^{-\alpha x}$ for positive x], but applying the boundary conditions involves a method that may be new to you; we describe it in the More section on the Graphical Solution of the Finite Square Well.

First, we will explain in words unencumbered by the mathematics how the conditions of continuity of ψ and ψ' at the boundaries and the need for $\psi \rightarrow 0$ as $x \rightarrow \pm\infty$ leads to the selection of only certain wave functions and quantized energies for values of E within the well; i.e., $0 < E < V_0$. The important feature of Equation 6-33 is that the second derivative ψ'' , which is the curvature of the wave function, has the same sign as the wave function ψ . If ψ is positive, ψ'' is also positive and the wave function curves away from the axis, as shown in Figure 6-9a. Similarly, if ψ is negative, ψ'' is negative and, again, ψ curves away from the axis. This behavior is different from that inside the well, where $0 < x < L$. There, ψ and ψ'' have opposite signs so that ψ always curves toward the axis like a sine or cosine function. Because of this behavior outside the well,

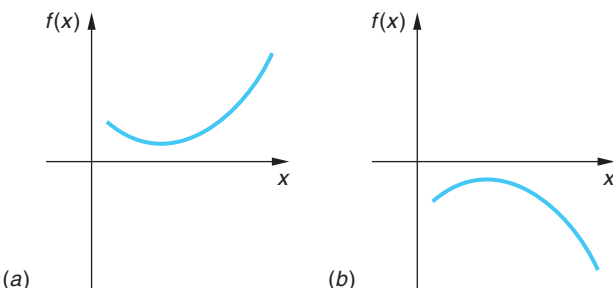


Figure 6-8 (a) The finite square well potential. (b) Region I is that with $x < -a$, II with $-a < x < +a$, and III with $x > +a$.

Figure 6-9 (a) Positive function with positive curvature; (b) negative function with negative curvature.

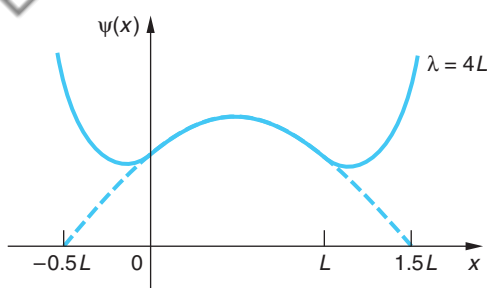


Figure 6-10 The function that satisfies the Schrödinger equation with $\lambda = 4L$ inside the well is not an acceptable wave function because it becomes infinite at large x . Although at $x = L$, the function is heading toward zero (slope is negative), the rate of increase of the slope ψ'' is so great that the slope becomes positive before the function becomes zero, and the function then increases. Since ψ'' has the same sign as ψ , the slope always increases and the function increases without bound. [This computer-generated plot courtesy of Paul Doherty, The Exploratorium.]

for most values of the energy the wave function becomes infinite as $x \rightarrow \pm\infty$; i.e., $\psi(x)$ is not well behaved. Such functions, though satisfying the Schrödinger equation, are not proper wave functions because they cannot be normalized.

Figure 6-10 shows the wave function for the energy $E = p^2/2m = h^2/2m\lambda^2$ for $\lambda = 4L$. Figure 6-11 shows a well-behaved wave function corresponding to wavelength $\lambda = \lambda_1$, which is the ground state wave function for the finite well, and the behavior of the wave functions for two nearby energies and wavelengths. The exact determination of the allowed energy levels in a finite square well can be obtained from a detailed solution of the problem. Figure 6-12 shows the wave functions and the probability distributions for the ground state and for the first two excited states. From this figure we see that the wavelengths inside the well are slightly longer than the corresponding wavelengths for the infinite well of the same width, so the corresponding energies are slightly less than those of the infinite well. Another feature of the finite well problem is that there are only a finite number of allowed energies, depending on the size of V_0 . For very small V_0 there is only one allowed energy level; i.e., only one bound state can exist. This will be quite apparent in the detailed solution in the More section.

Note that, in contrast to the classical case, there is some probability of finding the particle outside the well, in the regions $x > L$ or $x < 0$. In these regions, the total energy is less than the potential energy, so it would seem that the kinetic energy must be negative. Since negative kinetic energy has no meaning in classical physics, it is interesting to speculate about the meaning of this penetration of wave function beyond the well boundary. Does quantum mechanics predict that we could measure a negative kinetic energy? If so, this would be a serious defect in the theory. Fortunately, we are saved by the uncertainty principle. We can understand

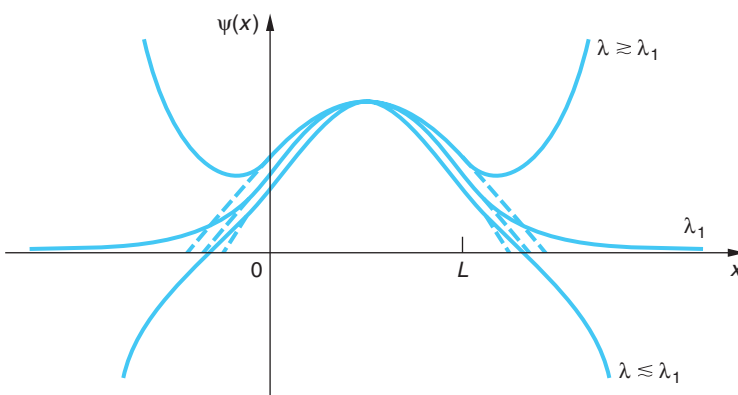


Figure 6-11 Functions satisfying the Schrödinger equation with wavelengths near the critical wavelength λ_1 . If λ is slightly greater than λ_1 , the function approaches infinity like that in Figure 6-10. At the wavelength λ_1 , the function and its slope approach zero together. This is an acceptable wave function corresponding to the energy $E_1 = h^2/2m\lambda_1^2$. If λ is slightly less than λ_1 , the function crosses the x axis while the slope is still negative. The slope becomes more negative because its rate of change ψ'' is now negative. This function approaches negative infinity at large x . [This computer-generated plot courtesy of Paul Doherty, The Exploratorium.]

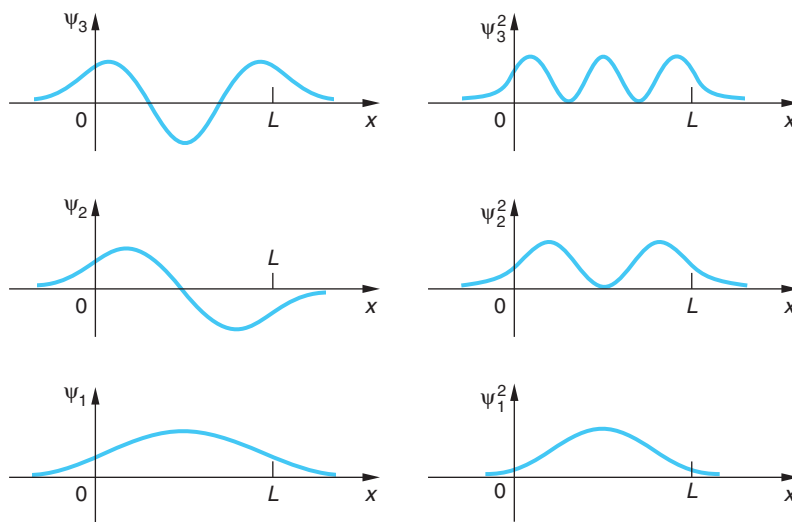


Figure 6-12 Wave functions $\psi_n(x)$ and probability distributions $\psi_n^2(x)$ for $n = 1, 2$, and 3 for the finite square well. Compare these with Figure 6-4 for the infinite square well, where the wave functions are zero at $x = 0$ and $x = L$. The wavelengths are slightly longer than the corresponding ones for the infinite well, so the allowed energies are somewhat smaller.

this qualitatively as follows (we will consider the region $x > L$ only). Since the wave function decreases as $e^{-\alpha x}$, with α given by Equation 6-34, the probability density $\psi^2 = e^{-2\alpha x}$ becomes very small in a distance of the order of $\Delta x \approx \alpha^{-1}$. If we consider $\psi(x)$ to be negligible beyond $x = L + \alpha^{-1}$, we can say that finding the particle in the region $x > L$ is roughly equivalent to localizing it in a region $\Delta x \approx \alpha^{-1}$. Such a measurement introduces an uncertainty in momentum of the order of $\Delta p \approx \hbar/\Delta x = \hbar\alpha$ and a minimum kinetic energy of the order of $(\Delta p)^2/2m = \hbar^2\alpha^2/2m = V_0 - E$. This kinetic energy is just enough to prevent us from measuring a negative kinetic energy! The penetration of the wave function into a classically forbidden region does have important consequences in tunneling or barrier penetration, which we will discuss in Section 6-6.

Much of our discussion of the finite well problem applies to any problem in which $E > V(x)$ in some region and $E < V(x)$ outside that region. Consider, for example, the potential energy $V(x)$ shown in Figure 6-13. Inside the well, the Schrödinger equation is of the form

$$\psi''(x) = -k^2\psi(x) \quad 6-35$$

where $k^2 = 2m[E - V(x)]/\hbar^2$ now depends on x . The solutions of this equation are no longer simple sine or cosine functions because the wave number $k = 2\pi/\lambda$ varies with x , but since ψ'' and ψ have opposite signs, ψ will always curve toward the axis and the solutions will oscillate. Outside the well, ψ will curve away from the axis so there will be only certain values of E for which solutions exist that approach zero as x approaches infinity.

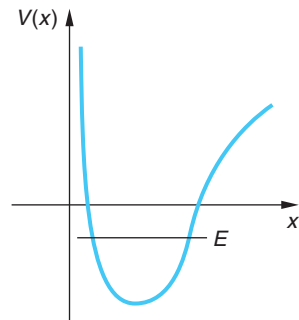


Figure 6-13 Arbitrary well-type potential with possible energy E . Inside the well [$E > V(x)$], $\psi(x)$ and $\psi'(x)$ have opposite signs, and the wave function will oscillate. Outside the well, $\psi(x)$ and $\psi'(x)$ have the same sign and, except for certain values of E , the wave function will not be well behaved.



More

In most cases the solution of finite well problems involves transcendental equations and is very difficult. For some finite potentials, however, graphical solutions are relatively simple and provide both insights and numerical results. As an example, we have included the *Graphical Solution of the Finite Square Well* on the home page: www.whfreeman.com/tiplermodernphysics5e. See also Equations 6-36 through 6-43 and Figure 6-14 here.

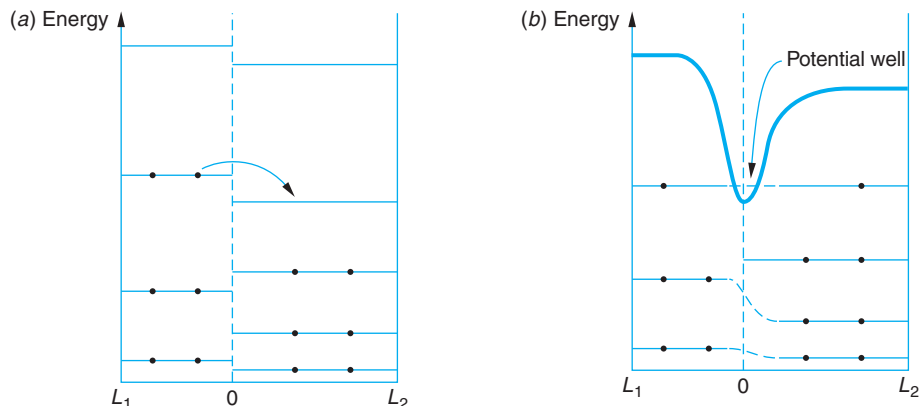


Figure 6-15 (a) Two infinite square wells of different widths L_1 and L_2 , each containing the same number of electrons, are put together. An electron from well 1 moves to the lowest empty level of well 2. (b) The energies of the two highest electrons are equalized, but the unequal charge in the two wells distorts the energy-level structure. The distortion of the lowest empty levels in each well results in a potential well at the junction between the wells. The orientation of the newly formed well is perpendicular to the plane of the figure.

Quantum Wells

Development of techniques for fabricating devices whose dimensions are of the order of nanometers, called *nanostructures*, has made possible the construction of *quantum wells*. These are finite potential wells of one, two, and three dimensions that can channel electron movement in selected directions. A one-dimensional quantum well is a thin layer of material that confines particles to within the dimension perpendicular to the layer's surface but does not restrict motion in the other two dimensions. In the case of three-dimensional wells, called *quantum dots*, electrons are restricted entirely to quantized energy states within the well. A ubiquitous current application of quantum wells is the diode lasers that read CDs, DVDs, and bar codes. Quantum dots have potential applications in data storage and *quantum computers*, devices that may greatly enhance computing power and speed.

One-dimensional quantum wells, called *quantum wires*, offer the possibility of dramatically increasing the speed that electrons move through a device in selected directions. This in turn would increase the speed with which signals move between circuit elements in computer systems. Figure 6-15 is an outline of how such a well might be formed.

6-4 Expectation Values and Operators

Expectation Values

The objective of theory is to explain experimental observations. In classical mechanics the solution of a problem is typically specified by giving the position of a particle or particles as a function of time. As we have discussed, the wave nature of matter prevents us from doing this for microscopic systems. Instead, we find the wave function

$\Psi(x, t)$ and the probability distribution function $|\Psi(x, t)|^2$. The most that we can know about a particle's position is the probability that a measurement will yield various values of x . The *expectation value* of x is defined as

$$\langle x \rangle = \int_{-\infty}^{+\infty} \Psi^*(x, t)x\Psi(x, t) dx \quad \text{6-44}$$

The expectation value of x is the average value of x that we would expect to obtain from a measurement of the positions of a large number of particles with the same wave function $\Psi(x, t)$. As we have seen, for a particle in a state of definite energy, the probability distribution is independent of time. The expectation value of x is then given by

$$\langle x \rangle = \int_{-\infty}^{+\infty} \Psi^*(x)x\Psi(x) dx \quad \text{6-45}$$

For example, for the infinite square well, we can see by symmetry (or by direct calculation) that $\langle x \rangle$ is $L/2$, the midpoint of the well.

In general, the expectation value of any function $f(x)$ is given by

$$\langle f(x) \rangle = \int_{-\infty}^{+\infty} \Psi^*f(x)\Psi dx \quad \text{6-46}$$

For example, $\langle x^2 \rangle$ can be calculated as above, for the infinite square well of width L . It is left as an exercise (see Problem 6-56) to show that

$$\langle x^2 \rangle = \frac{L^2}{3} - \frac{L^2}{2n^2\pi^2} \quad \text{6-47}$$

You may recognize the expectation values defined by Equations 6-45 and 6-46 as being weighted average calculations, borrowed by physics from probability and statistics. We should note that we don't necessarily expect to make a measurement whose result equals the expectation value. For example, for even n , the probability of measuring $x = L/2$ in some range dx around the midpoint of the well is zero because the wave function $\sin(n\pi x/L)$ is zero there. We get $\langle x \rangle = L/2$ because the probability density function $\Psi^*\Psi$ is symmetrical about that point. Remember that the expectation value is the average value that would result from many measurements.

Operators

If we knew the momentum p of a particle as a function of x , we could calculate the expectation value $\langle p \rangle$ from Equation 6-46. However, it is impossible in principle to find p as a function of x since, according to the uncertainty principle, both p and x cannot be determined at the same time. To find $\langle p \rangle$ we need to know the distribution function for momentum. If we know $\Psi(x)$, it can be found by Fourier analysis. The $\langle p \rangle$ also can be found from Equation 6-48, where $\left(\frac{\hbar}{i}\frac{\partial}{\partial x}\right)$ is the mathematical operator acting on Ψ that produces the x component of the momentum (see also Equation 6-6).

$$\langle p \rangle = \int_{-\infty}^{+\infty} \Psi^*\left(\frac{\hbar}{i}\frac{\partial}{\partial x}\right)\Psi dx \quad \text{6-48}$$

Similarly, $\langle p^2 \rangle$ can be found from

$$\langle p^2 \rangle = \int_{-\infty}^{+\infty} \Psi^* \left(\frac{\hbar}{i} \frac{\partial}{\partial x} \right) \left(\frac{\hbar}{i} \frac{\partial}{\partial x} \right) \Psi dx$$

Notice that in computing the expectation value the operator representing the physical quantity operates on $\Psi(x, t)$, not on $\Psi^*(x, t)$; i.e., its correct position is between Ψ^* and Ψ . This is not important to the outcome when the operator is simply some $f(x)$, but it is critical when the operator includes a differentiation, as in the case of the momentum operator. Note that $\langle p^2 \rangle$ is simply $2mE$ since, for the infinite square well, $E = p^2/2m$. The quantity $\left(\frac{\hbar}{i} \frac{\partial}{\partial x} \right)$, which operates on the wave function in Equation 6-48, is called the *momentum operator* p_{op} :

$$p_{\text{op}} = \frac{\hbar}{i} \frac{\partial}{\partial x} \quad \text{6-49}$$

EXAMPLE 6-5 Expectation Values for p and p^2 Find $\langle p \rangle$ and $\langle p^2 \rangle$ for the ground-state wave function of the infinite square well. (Before we calculate them, what do you think the results will be?)

SOLUTION

We can ignore the time dependence of Ψ , in which case we have

$$\begin{aligned} \langle p \rangle &= \int_0^L \left(\sqrt{\frac{2}{L}} \sin \frac{nx}{L} \right) \left(\frac{\hbar}{i} \frac{\partial}{\partial x} \right) \left(\sqrt{\frac{2}{L}} \sin \frac{nx}{L} \right) dx \\ &= \frac{\hbar}{i} \frac{2}{L} \frac{\pi}{L} \int_0^L \sin \frac{\pi x}{L} \cos \frac{\pi x}{L} dx = 0 \end{aligned}$$

The particle is equally as likely to be moving in the $-x$ as in the $+x$ direction, so its *average* momentum is zero.

Similarly, since

$$\begin{aligned} \frac{\hbar}{i} \frac{\partial}{\partial x} \left(\frac{\hbar}{i} \frac{\partial}{\partial x} \right) \Psi &= -\hbar^2 \frac{\partial^2 \Psi}{\partial x^2} = -\hbar^2 \left(-\frac{\pi^2}{L^2} \sqrt{\frac{2}{L}} \sin \frac{\pi x}{L} \right) \\ &= +\frac{\hbar^2 \pi^2}{L^2} \Psi \end{aligned}$$

we have

$$\langle p^2 \rangle = \frac{\hbar^2 \pi^2}{L^2} \int_0^L \Psi^* \Psi dx = \frac{\hbar^2 \pi^2}{L^2}$$

The time-independent Schrödinger equation (Equation 6-18) can now be written conveniently in terms of p_{op} :

$$\left(\frac{1}{2m} \right) p_{\text{op}}^2 \Psi(x) + V(x) \Psi(x) = E \Psi(x) \quad \text{6-50}$$

where

$$p_{\text{op}}^2 \Psi(x) = \frac{\hbar}{i} \frac{\partial}{\partial x} \left[\frac{\hbar}{i} \frac{\partial}{\partial x} \Psi(x) \right] = -\hbar^2 \frac{\partial^2 \Psi}{\partial x^2}$$

In classical mechanics, the total energy written in terms of the position and momentum variables is called the Hamiltonian function $H = p^2/2m + V$. If we replace the momentum by the momentum operator p_{op} and note that $V = V(x)$, we obtain the Hamiltonian operator H_{op} :

$$H_{\text{op}} = \frac{p_{\text{op}}^2}{2m} + V(x) \quad 6-51$$

The time-independent Schrödinger equation can then be written

$$H_{\text{op}}\psi = E\psi \quad 6-52$$

The advantage of writing the Schrödinger equation in this formal way is that it allows for easy generalization to more-complicated problems such as those with several particles moving in three dimensions. We simply write the total energy of the system in terms of position and momentum and replace the momentum variables by the appropriate operators to obtain the Hamiltonian operator for the system.

Table 6-1 summarizes the several operators representing physical quantities that we have discussed thus far and includes a few more that we will encounter later on.

Table 6-1 Some quantum-mechanical operators

| Symbol | Physical quantity | Operator |
|--------|--|---|
| $f(x)$ | Any function of x —e.g., the position x , the potential energy $V(x)$, etc. | $f(x)$ |
| p_x | x component of momentum | $\frac{\hbar}{i} \frac{\partial}{\partial x}$ |
| p_y | y component of momentum | $\frac{\hbar}{i} \frac{\partial}{\partial y}$ |
| p_z | z component of momentum | $\frac{\hbar}{i} \frac{\partial}{\partial z}$ |
| E | Hamiltonian (time independent) | $\frac{p_{\text{op}}^2}{2m} + V(x)$ |
| E | Hamiltonian (time dependent) | $i \hbar \frac{\partial}{\partial t}$ |
| E_k | kinetic energy | $-\frac{\hbar^2}{2m} \frac{\partial^2}{\partial x^2}$ |
| L_z | z component of angular momentum | $-i\hbar \frac{\partial}{\partial \phi}$ |

Questions

7. Explain (in words) why $\langle p \rangle$ and $\langle p^2 \rangle$ in Example 6-5 are not both zero.
8. Can $\langle x \rangle$ ever have a value that has zero probability of being measured?



More

In order for interesting things to happen in systems with quantized energies, the probability density must change in time. Only in this way can energy be emitted or absorbed by the system. *Transitions Between Energy States* on the home page (www.whfreeman.com/tiplermodernphysics5e) describes the process and applies it to the emission of light from an atom. See also Equations 6-52a–e and Figure 6-16 here.

6-5 The Simple Harmonic Oscillator

One of the problems solved by Schrödinger in the second of his six famous papers was that of the simple harmonic oscillator potential, given by

$$V(x) = \frac{1}{2}Kx^2 = \frac{1}{2}m\omega^2x^2$$

where K is the force constant and ω the angular frequency of vibration defined by $\omega = (K/m)^{1/2} = 2\pi f$. The solution of the Schrödinger equation for this potential is particularly important, as it can be applied to such problems as the vibration of molecules in gases and solids. This potential energy function is shown in Figure 6-17, with a possible total energy E indicated.

In classical mechanics, a particle in such a potential is in equilibrium at the origin $x = 0$, where $V(x)$ is minimum and the force $F_x = -dV/dx$ is zero. If disturbed, the particle will oscillate back and forth between $x = -A$ and $x = +A$, the points at which the kinetic energy is zero and the total energy is just equal to the potential energy. These points are called the classical turning points. The distance A is related to the total energy E by

$$E = \frac{1}{2}m\omega^2A^2 \quad 6-53$$

Classically, the probability of finding the particle in dx is proportional to the time spent in dx , which is dx/v . The speed of the particle can be obtained from the conservation of energy:

$$\frac{1}{2}mv^2 + \frac{1}{2}m\omega^2x^2 = E$$

The classical probability is thus

$$P_c(x) dx \propto \frac{dx}{v} = \frac{dx}{\sqrt{(2/m)(E - \frac{1}{2}m\omega^2x^2)}} \quad 6-54$$

Any value of the energy E is possible. The lowest energy is $E = 0$, in which case the particle is at rest at the origin.

The Schrödinger equation for this problem is

$$-\frac{\hbar^2}{2m} \frac{\partial^2\psi(x)}{\partial x^2} + \frac{1}{2}m\omega^2x^2\psi(x) = E\psi(x) \quad 6-55$$

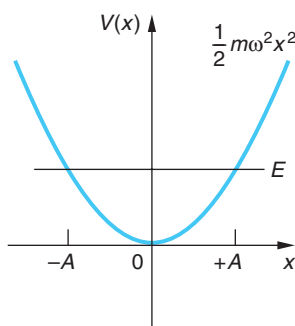


Figure 6-17 Potential energy function for a simple harmonic oscillator.

Classically, the particle is confined between the “turning points” $-A$ and $+A$.

The mathematical techniques involved in solving this type of differential equation are standard in mathematical physics but unfamiliar to most students at this level. We will, therefore, discuss the problem qualitatively. We first note that since the potential is symmetric about the origin $x = 0$, we expect the probability distribution function $|\psi(x)|^2$ also to be symmetric about the origin, i.e., to have the same value at $-x$ as at $+x$.

$$|\psi(-x)|^2 = |\psi(x)|^2$$

The wave function $\psi(x)$ must then be either symmetric $\psi(-x) = +\psi(x)$ or anti-symmetric $\psi(-x) = -\psi(x)$. We can therefore simplify our discussion by considering positive x only and find the solutions for negative x by symmetry. (The symmetry of Ψ is discussed further in the Exploring section, Parity; see page 250.)

Consider some value of total energy E . For x less than the classical turning point A defined by Equation 6-53, the potential energy $V(x)$ is less than the total energy E , whereas for $x > A$, $V(x)$ is greater than E . Our discussion in Section 6-3 applies directly to this problem. For $x < A$, the Schrödinger equation can be written

$$\psi''(x) = -k^2\psi(x)$$

where

$$k^2 = \frac{2m}{\hbar^2}[E - V(x)]$$

and $\psi(x)$ curves toward the axis and oscillates. For $x > A$, the Schrödinger equation becomes

$$\psi''(x) = +\alpha^2\psi(x)$$

with

$$\alpha^2 = \frac{2m}{\hbar^2}[V(x) - E]$$

and $\psi(x)$ curves away from the axis. Only certain values of E will lead to solutions that are well behaved, i.e., that approach zero as x approaches infinity. The allowed values of E for the simple harmonic oscillator must be determined by solving the Schrödinger equation; in this case they are given by

$$E_n = \left(n + \frac{1}{2}\right)\hbar\omega \quad n = 0, 1, 2, \dots \quad \text{6-56}$$

Thus, the ground-state energy is $\frac{1}{2}\hbar\omega$ and the energy levels are equally spaced, each excited state being separated from the levels immediately adjacent by $\hbar\omega$.

The wave functions of the simple harmonic oscillator in the ground state and in the first two excited states ($n = 0$, $n = 1$, and $n = 2$) are sketched in Figure 6-18. The ground-state wave function has the shape of a Gaussian curve, and the lowest energy $E = \frac{1}{2}\hbar\omega$ is the minimum energy consistent with the uncertainty principle.

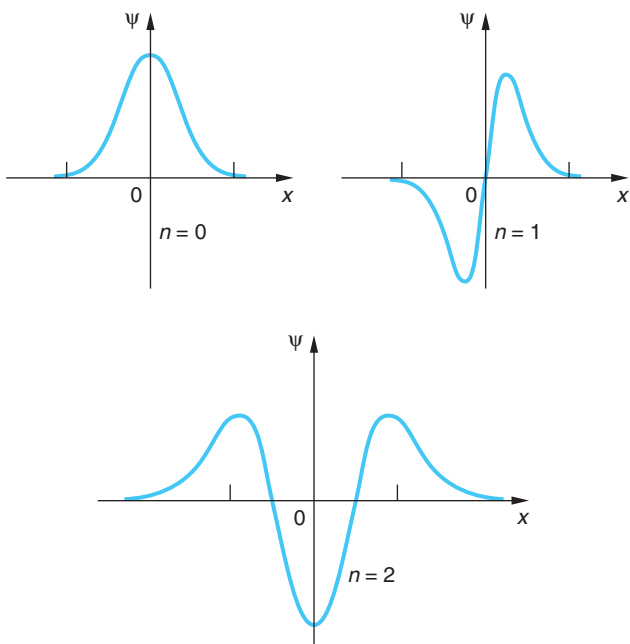


Figure 6-18 Wave functions for the ground state and the first two excited states of the simple harmonic oscillator potential, the states with $n = 0, 1$, and 2 .

The allowed solutions to the Schrödinger equation, the wave functions for the simple harmonic oscillator, can be written

$$\psi_n(x) = C_n e^{-m\omega x^2/2\hbar} H_n(x) \quad 6-57$$

where the constants C_n are determined by normalization and the functions $H_n(x)$ are polynomials of order n called the Hermite polynomials.¹³ The solutions for $n = 0, 1$, and 2 (see Figure 6-18) are

$$\begin{aligned}\psi_0(x) &= A_0 e^{-m\omega x^2/2\hbar} \\ \psi_1(x) &= A_1 \sqrt{\frac{m\omega}{\hbar}} x e^{-m\omega x^2/2\hbar} \\ \psi_2(x) &= A_2 \left(1 - \frac{2m\omega x^2}{\hbar}\right) e^{-m\omega x^2/2\hbar}\end{aligned} \quad 6-58$$

Molecules vibrate as harmonic oscillators.
Measuring vibration frequencies (see Chapter 9) enables determination of force constants, bond strengths, and properties of solids.

Notice that for even values of n , the wave functions are symmetric about the origin; for odd values of n , they are antisymmetric. In Figure 6-19 the probability distributions $\psi_n^2(x)$ are sketched for $n = 0, 1, 2, 3$, and 10 for comparison with the classical distribution.

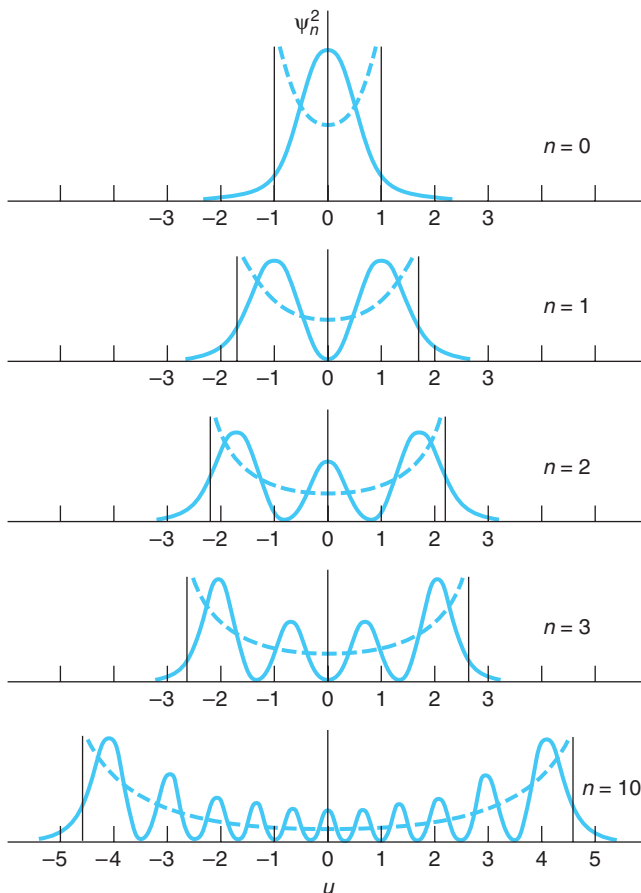


Figure 6-19 Probability density ψ_n^2 for the simple harmonic oscillator plotted against the dimensionless variable $u = (m\omega/\hbar)^{1/2}x$, for $n = 0, 1, 2, 3$, and 10 . The dashed curves are the classical probability densities for the same energy, and the vertical lines indicate the classical turning points $x = \pm A$.

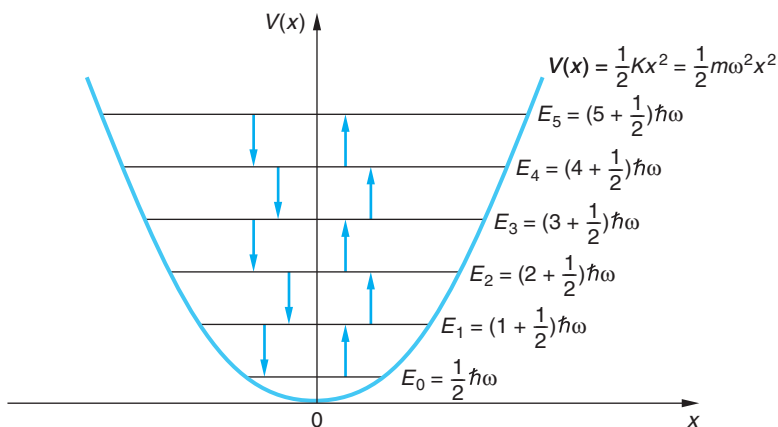


Figure 6-20 Energy levels in the simple harmonic oscillator potential. Transitions obeying the selection rule $\Delta n = \pm 1$ are indicated by the arrows (those pointing up indicate absorption). Since the levels have equal spacing, the same energy $\hbar\omega$ is emitted or absorbed in all allowed transitions. For this special potential, the frequency of the emitted or absorbed photon equals the frequency of oscillation, as predicted by classical theory.

A property of these wave functions that we will state without proof is that

$$\int_{-\infty}^{+\infty} \psi_n^* x \psi_m dx = 0 \quad \text{unless} \quad n = m \pm 1 \quad 6-59$$

This property places a condition on transitions that may occur between allowed states. This condition, called a *selection rule*, limits the amount by which n can change for (electric dipole) radiation emitted or absorbed by a simple harmonic oscillator:



The quantum number of the final state must be 1 less than or 1 greater than that of the initial state.

This selection rule is usually written

$$\Delta n = \pm 1 \quad 6-60$$

Since the difference in energy between two successive states is $\hbar\omega$, this is the energy of the photon emitted or absorbed in an electric dipole transition. The frequency of the photon is therefore equal to the classical frequency of the oscillator, as was assumed by Planck in his derivation of the blackbody radiation formula. Figure 6-20 shows an energy level diagram for the simple harmonic oscillator, with the allowed energy transitions indicated by vertical arrows.



More

Solution of the Schrödinger equation for the simple harmonic oscillator (Equation 6-55) involves some rather advanced differential equation techniques. However, a simpler exact solution is also possible using an approach invented by Schrödinger himself that we will call *Schrödinger's Trick*. With the authors' thanks to Wolfgang Lorenzon for bringing it to our attention, we include it on the home page www.whfreeman.com/tiplermodernphysics5e so that you, too, will know the trick.



EXPLORING Parity

We made a special point of arranging the simple harmonic oscillator potential symmetrically about $x = 0$ (see Figure 6-17), just as we had done with the finite square well in Figure 6-8b and will do with various other potentials in later discussions. The usual purpose in each case is to emphasize the symmetry of the physical situation and to simplify the mathematics. Notice that arranging the potential $V(x)$ symmetrically about the origin means that $V(x) = V(-x)$. This means that the Hamiltonian operator H_{op} , defined in Equation 6-51, is unchanged by a transformation that changes $x \rightarrow -x$. Such a transformation is called a *parity operation* and is usually denoted by the operator P . Thus, if $\psi(x)$ is a solution of the Schrödinger equation

$$H_{\text{op}}\psi(x) = E\psi(x) \quad \text{6-52}$$

then a parity operation P leads to

$$H_{\text{op}}\psi(-x) = E\psi(-x)$$

and $\psi(-x)$ is also a solution to the Schrödinger equation and corresponds to the same energy. When two (or more) wave functions are solutions corresponding to the same value of the energy E , that level is referred to as *degenerate*. In this case, where two wave functions, $\psi(x)$ and $\psi(-x)$, are both solutions with energy E , we call the energy level doubly degenerate.

It should be apparent from examining the two equations above that $\psi(x)$ and $\psi(-x)$ can differ at most by a multiplicative constant C ; i.e.,

$$\psi(x) = C\psi(-x) \quad \psi(-x) = C\psi(x)$$

or

$$\psi(x) = C\psi(-x) = C^2\psi(x)$$

from which it follows that $C = \pm 1$. If $C = 1$, $\psi(x)$ is an even function, i.e., $\psi(-x) = \psi(x)$. If $C = -1$, then $\psi(x)$ is an odd function, i.e., $\psi(-x) = -\psi(x)$. Parity is used in quantum mechanics to describe the symmetry properties of wave functions under a reflection of the *space* coordinates in the origin, i.e., under a parity operation. The terms even and odd parity describe the symmetry of the wave functions, not whether the quantum numbers are even or odd. We will have more on parity in Chapter 12.

6-6 Reflection and Transmission of Waves

Up to this point, we have been concerned with bound-state problems in which the potential energy is larger than the total energy for large values of x . In this section, we will consider some simple examples of unbound states for which E is greater than $V(x)$ as x gets larger in one or both directions. For these problems $d^2\psi(x)/dx^2$ and $\psi(x)$ have opposite signs for those regions of x where $E > V(x)$, so $\psi(x)$ in those regions curves toward the axis and does not become infinite at large values of $|x|$. Any value of E is allowed. Such wave functions are not normalizable since $\psi(x)$ does not approach zero as x goes to infinity in at least one direction and, as a consequence,

$$\int_{-\infty}^{+\infty} |\psi(x)|^2 dx \longrightarrow \infty$$

A complete solution involves combining infinite plane waves into a wave packet of finite width. The resulting finite packet is normalizable. However, for our purposes it is sufficient to note that the integral above is bounded between the limits a and b , provided only that $|b - a| < \infty$. Such wave functions are most frequently encountered, as we are about to do, in the scattering of beams of particles from potentials, so it is usual to normalize such wave functions in terms of the density of particles ρ in the beam. Thus,

$$\int_a^b |\psi(x)|^2 dx = \int_a^b \rho dx = \int_a^b dN = N$$

where dN is the number of particles in the interval dx and N is the number of particles in the interval $(b - a)$.¹⁴ The wave nature of the Schrödinger equation leads, even so, to some very interesting consequences.

Step Potential

Consider a region in which the potential energy is the step function

$$V(x) = 0 \quad \text{for } x < 0$$

$$V(x) = V_0 \quad \text{for } x > 0$$

as shown in Figure 6-21. We are interested in what happens when a beam of particles, each with the same total energy E , moving from left to right encounters the step.

The classical answer is simple. For $x < 0$, each particle moves with speed $v = (2E/m)^{1/2}$. At $x = 0$, an impulsive force acts on it. If the total energy E is less than V_0 , the particle will be turned around and will move to the left at its original speed; that is, it will be reflected by the step. If E is greater than V_0 , the particle will continue moving to the right but with reduced speed, given by $v = [2(E - V_0)/m]^{1/2}$. We might picture this classical problem as a ball rolling along a level surface and coming to a steep hill of height y_0 , given by $mgy_0 = V_0$. If its original kinetic energy is less than V_0 , the ball will roll partway up the hill and then back down and to the left along the level surface at its original speed. If E is greater than V_0 , the ball will roll up the hill and proceed to the right at a smaller speed.

The quantum-mechanical result is similar to the classical one for $E < V_0$ but quite different when $E > V_0$, as in Figure 6-22a. The Schrödinger equation in each of the two space regions shown in the diagram is given by

Region I

$$(x < 0) \quad \frac{d^2\psi(x)}{dx^2} = -k_1^2\psi(x) \quad \text{6-61}$$

Region II

$$(x > 0) \quad \frac{d^2\psi(x)}{dx^2} = -k_2^2\psi(x) \quad \text{6-62}$$

$$k_1 = \frac{\sqrt{2mE}}{\hbar} \quad \text{and} \quad k_2 = \frac{\sqrt{2m(E - V_0)}}{\hbar}$$

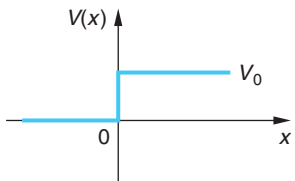


Figure 6-21 Step potential. A classical particle incident from the left, with total energy E greater than V_0 , is always transmitted. The potential change at $x = 0$ merely provides an impulsive force that reduces the speed of the particle. However, a wave incident from the left is partially transmitted and partially reflected because the wavelength changes abruptly at $x = 0$.

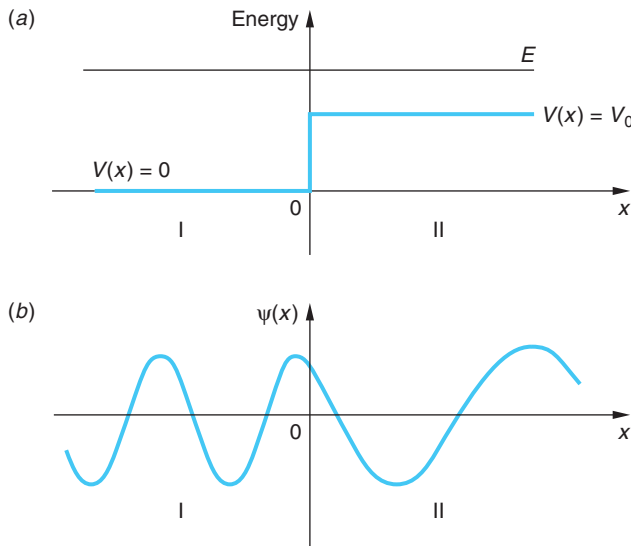


Figure 6-22 (a) A potential step. Particles are incident on the step from the left toward the right, each with total energy $E > V_0$. (b) The wavelength of the incident wave (Region I) is shorter than that of the transmitted wave (Region II). Since $k_2 < k_1$, $|C|^2 > |A|^2$; however, the transmission coefficient $T < 1$.

The general solutions are

Region I

$$(x < 0) \quad \psi_I(x) = Ae^{ik_1 x} + Be^{-ik_1 x} \quad 6-63$$

Region II

$$(x > 0) \quad \psi_{II}(x) = Ce^{ik_2 x} + De^{-ik_2 x} \quad 6-64$$

Specializing these solutions to our situation where we are assuming the incident beam of particles to be moving from left to right, we see that the first term in Equation 6-63 represents that beam since multiplying $Ae^{ik_1 x}$ by the time part of $\Psi(x, t)$, $e^{i\omega t}$, yields a plane wave (i.e., a beam of free particles) moving to the right. The second term, $Be^{-ik_1 x}$, represents particles moving to the left in Region I. In Equation 6-64, $D = 0$ since that term represents particles incident on the potential step from the right and there are none. Thus, we have that the constant A is known or at least obtainable (determined by normalization of $Ae^{ik_1 x}$ in terms of the density of particles in the beam as explained above) and the constants B and C are yet to be found. We find them by applying the continuity condition on $\psi(x)$ and $d\psi(x)/dx$ at $x = 0$, i.e., by requiring that $\psi_I(0) = \psi_{II}(0)$ and $d\psi_I(0)/dx = d\psi_{II}(0)/dx$. Continuity of ψ at $x = 0$ yields

$$\psi_I(0) = A + B = \psi_{II}(0) = C$$

or

$$A + B = C \quad 6-65a$$

Continuity of $d\psi/dx$ at $x = 0$ gives

$$k_1 A - k_1 B = k_2 C \quad 6-65b$$

Solving Equations 6-65a and b for B and C in terms of A (see Problem 6-47), we have

$$B = \frac{k_1 - k_2}{k_1 + k_2} A = \frac{E^{1/2} - (E - V_0)^{1/2}}{E^{1/2} + (E - V_0)^{1/2}} A \quad 6-66$$

$$C = \frac{2k_1}{k_1 + k_2} A = \frac{2E^{1/2}}{E^{1/2} + (E - V_0)^{1/2}} A \quad 6-67$$

where Equations 6-66 and 6-67 give the relative amplitude of the reflected and transmitted waves, respectively. It is usual to define the coefficients of reflection R and transmission T , the relative *rates* at which particles are reflected and transmitted, in terms of the squares of the amplitudes A , B , and C as¹⁵

$$R = \frac{|B|^2}{|A|^2} = \left(\frac{k_1 - k_2}{k_1 + k_2} \right)^2 \quad 6-68$$

$$T = \frac{k_2}{k_1} \frac{|C|^2}{|A|^2} = \frac{4k_1 k_2}{(k_1 + k_2)^2} \quad 6-69$$

from which it can be readily verified that

$$T + R = 1 \quad 6-70$$

Among the interesting consequences of the wave nature of the solutions to Schrödinger's equation, notice the following:

1. Even though $E > V_0$, R is *not* 0; i.e., in contrast to classical expectations, some of the particles are reflected from the step. (This is analogous to the internal reflection of electromagnetic waves at the interface of two media.)
2. The value of R depends on the difference between k_1 and k_2 but *not* on which is larger; i.e., a step down in the potential produces the same reflection as a step up of the same size.

Since $k = p/\hbar = 2\pi/\lambda$, the wavelength changes as the beam passes the step. We might also expect that the amplitude of ψ_{II} will be less than that of the incident wave; however, recall that the $|\psi|^2$ is proportional to the particle density. Since particles move more slowly in Region II ($k_2 < k_1$), $|\psi_{II}|^2$ may be larger than $|\psi_I|^2$. Figure 6-22b illustrates these points. Figure 6-23 shows the time development of a wave packet incident on a potential step for $E > V_0$.

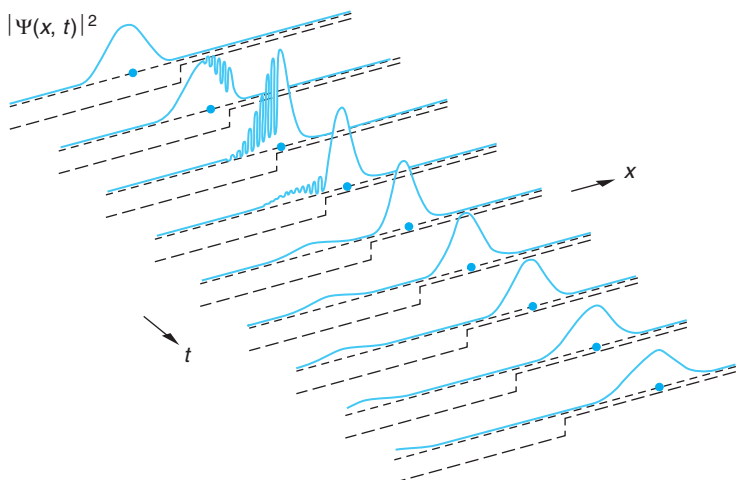
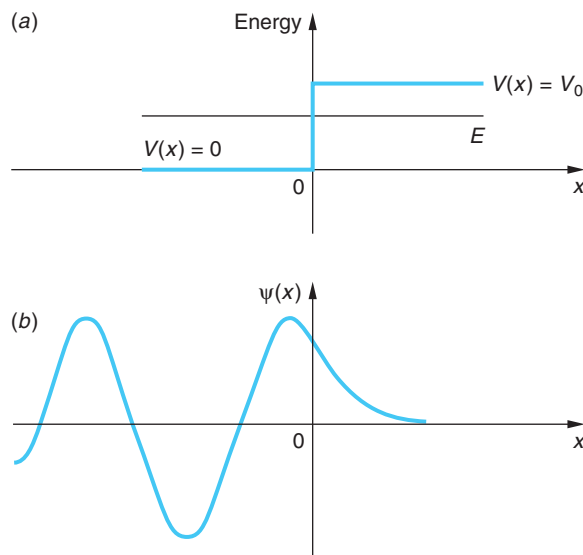


Figure 6-23 Time development of a one-dimensional wave packet representing a particle incident on a step potential for $E > V_0$. The position of a classical particle is indicated by the dot. Note that part of the packet is transmitted and part is reflected. The sharp spikes that appear are artifacts of the discontinuity in the slope of $V(x)$ at $x = 0$.

Figure 6-24 (a) A potential step. Particles are incident on the step from the left moving toward the right, each with total energy $E < V_0$. (b) The wave transmitted into region II is a decreasing exponential. However, the value of R in this case is 1 and no net energy is transmitted.



Now let us consider the case shown in Figure 6-24a, where $E < V_0$. Classically, we expect all particles to be reflected at $x = 0$; however, we note that k_2 in Equation 6-64 is now an imaginary number since $E < V_0$. Thus,

$$\psi_{II}(x) = Ce^{ik_2 x} = Ce^{-\alpha x} \quad 6-71$$

is a *real* exponential function where $\alpha = \sqrt{2m(V_0 - E)/\hbar}$. (We choose the positive root so that $\psi_{II} \rightarrow 0$ as $x \rightarrow \infty$.) This means that the numerator and denominator of the right side of Equation 6-66 are complex conjugates of each other; hence $|B|^2 = |A|^2$ and $R = 1$ and $T = 0$. Figure 6-25 is a graph of both R and T versus energy for a potential step. In agreement with the classical prediction, all of the particles (waves) are reflected back into Region I. However, another interesting result of our solution of Schrödinger's equation is that the particle waves do not all reflect at $x = 0$.

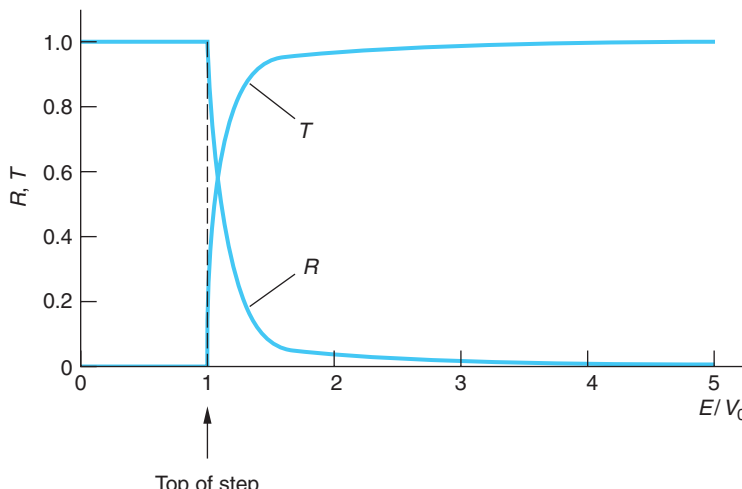


Figure 6-25 Reflection coefficient R and transmission coefficient T for a potential step V_0 high versus energy E (in units of V_0).

Since ψ_{II} is an exponential decreasing toward the right, the particle density in Region II is proportional to

$$|\psi_{II}|^2 = |C|^2 e^{-2\alpha x} \quad 6-72$$

Figure 6-24b shows the wave function for the case $E < V_0$. The wave function does not go to zero at $x = 0$ but decays exponentially, as does the wave function for the bound state in a finite square well problem. The wave penetrates slightly into the classically forbidden region $x > 0$ but eventually is completely reflected. (As discussed in Section 6-3, there is no prediction that a negative kinetic energy will be *measured* in such a region because to locate the particle in such a region introduces an uncertainty in the momentum corresponding to a minimum kinetic energy greater than $V_0 - E$.) This situation is similar to that of total internal reflection in optics.

EXAMPLE 6-6 **Reflection from a Step with $E < V_0$** A beam of electrons, each with energy $E = 0.1 V_0$, is incident on a potential step with $V_0 = 2$ eV. This is of the order of magnitude of the work function for electrons at the surface of metals. Graph the relative probability $|\psi|^2$ of particles penetrating the step up to a distance $x = 10^{-9}$ m, or roughly five atomic diameters.

SOLUTION

For $x > 0$, the wave function is given by Equation 6-71. The value of $|C|^2$ is, from Equation 6-67,

$$|C|^2 = \left| \frac{2(0.1 V_0)^{1/2}}{(0.1 V_0)^{1/2} + (-0.9 V_0)^{1/2}} \right|^2 = 0.4$$

where we have taken $|A|^2 = 1$. Computing $e^{-2\alpha x}$ for several values of x from 0 to 10^{-9} m gives, with $2\alpha = 2[2m(0.9 V_0)]^{1/2}/\hbar$, the first two columns of the Table 6-2. Taking $e^{-2\alpha x}$ and then multiplying by $|C|^2 = 0.4$ yields $|\psi|^2$, which is graphed in Figure 6-26.

Table 6-2 $|\psi|^2$

| x (m) | $2\alpha x$ | $ \psi ^2$ |
|------------------------|-------------|-------------|
| 0 | 0 | 0.40 |
| 0.1×10^{-10} | 0.137 | 0.349 |
| 1.0×10^{-10} | 1.374 | 0.101 |
| 2.0×10^{-10} | 2.748 | 0.026 |
| 5.0×10^{-10} | 6.869 | 0.001 |
| 10.0×10^{-10} | 13.74 | ≈ 0 |

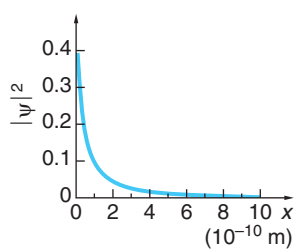


Figure 6-26

Barrier Potential

Now let us consider one of the more interesting quantum-mechanical potentials, the barrier, illustrated by the example in Figure 6-27. The potential is

$$V(x) = \begin{cases} V_0 & \text{for } 0 < x < a \\ 0 & \text{for } 0 > x \text{ and } x > a \end{cases} \quad 6-73$$

Classical particles incident on the barrier from the left in Region I with $E > V_0$ will all be transmitted, slowing down while passing through Region II but moving at their original speed again in Region III. For classical particles with $E < V_0$ incident from the left, all are reflected back into Region I. The quantum-mechanical behavior of particles incident on the barrier in both energy ranges is *much* different!

First, let us see what happens when a beam of particles, all with the same energy $E < V_0$, as illustrated in Figure 6-27a, are incident from the left. The general solutions to the wave equation are, following the example of the potential step,

$$\begin{aligned} \psi_I(x) &= Ae^{ik_1x} + Be^{-ik_1x} & x < 0 \\ \psi_{II}(x) &= Ce^{-\alpha x} + De^{\alpha x} & 0 < x < a \\ \psi_{III}(x) &= Fe^{ik_1x} + Ge^{-ik_1x} & x > a \end{aligned} \quad 6-74$$

where, as before, $k_1 = \sqrt{2mE/\hbar}$ and $\alpha = \sqrt{2m(V_0 - E)/\hbar}$. Note that ψ_{II} involves real exponentials, whereas ψ_I and ψ_{III} contain complex exponentials. Since the particle beam is incident on the barrier from the left, we can set $G = 0$. Once again, the value of A is determined by the particle density in the beam and the four constants B , C , D , and F are found in terms of A by applying the continuity condition on ψ and $d\psi/dx$ at $x = 0$ and at $x = a$. The details of the calculation are not of concern to us here, but several of the more interesting results are.

As we discovered for the potential step with $E < V_0$, the wave function incident from the left does not decrease immediately to zero at the barrier but instead will decay exponentially in the region of the barrier. Upon reaching the far wall of the barrier, the wave function must join smoothly to a sinusoidal wave function to the right of the barrier, as shown in Figure 6-27b. This implies that there will be some probability of the particles represented by the wave function being found on the far right side of the

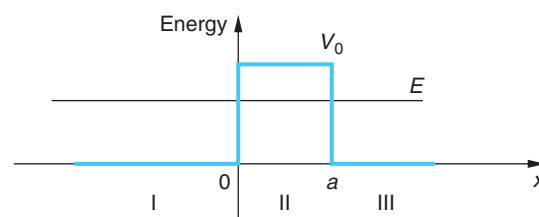
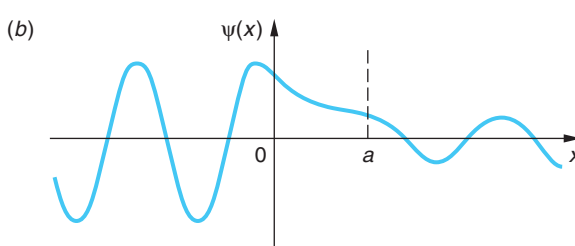


Figure 6-27 (a) Square barrier potential.

(b) Penetration of the barrier by a wave with energy less than the barrier energy. Part of the wave is transmitted by the barrier even though, classically, the particle cannot enter the region $0 < x < a$ in which the potential energy is greater than the total energy.



barrier, although classically they should never be able to get through; i.e., there is a probability that the particles approaching the barrier can penetrate it. This phenomenon is called *barrier penetration* or *tunneling* (see Figure 6-28). The relative probability of its occurrence in any given situation is given by the transmission coefficient.

The coefficient of transmission T from Region I into Region III is found to be (see Problem 6-64)

$$T = \frac{|F|^2}{|A|^2} = \left[1 + \frac{\sinh^2 \alpha a}{4 \frac{E}{V_0} \left(1 - \frac{E}{V_0} \right)} \right]^{-1} \quad 6-75$$

If $\alpha a \gg 1$, Equation 6-75 takes on the somewhat simpler form to evaluate

$$T \approx 16 \frac{E}{V_0} \left(1 - \frac{E}{V_0} \right) e^{-2\alpha a} \quad 6-76$$

Scanning Tunneling Microscope In the *scanning tunneling microscope* (STM), developed in the 1980s by G. Binnig and H. Rohrer, a narrow gap between a conducting specimen and the tip of a tiny probe acts as a potential barrier to electrons bound in the specimen, as illustrated in Figure 6-29. A small bias voltage applied between the probe and the specimen causes the electrons to tunnel through the barrier separating the two surfaces if the surfaces are close enough together. The tunneling current is extremely sensitive to the size of the gap, i.e., the width of the barrier, between the probe and specimen. A change of only 0.5 nm (about the diameter of one atom) in the width of the barrier can cause the tunneling current to change by as much as a factor of 10^4 . As the probe scans the specimen, a constant tunneling current is maintained by a piezoelectric feedback system that keeps the gap constant. Thus, the surface of the specimen can be mapped out by the vertical motions of the probe. In this way, the surface features of a specimen can be measured by STMs with a resolution of the order of the size of a single atom (see Figure 6-29).

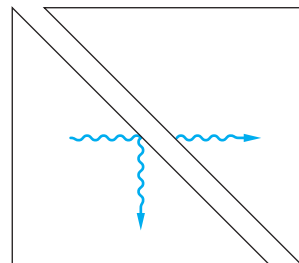


Figure 6-28 Optical barrier penetration, sometimes called frustrated total internal reflection. Because of the presence of the second prism, part of the wave penetrates the air barrier even though the angle of incidence in the first prism is greater than the critical angle. This effect can be demonstrated with two 45° prisms and a laser or a microwave beam and 45° prisms made of paraffin.

An important application of tunneling is the tunnel diode, a common component of electronic circuits. Another is *field emission*, tunneling of electrons facilitated by an electric field, now being used in wide-angle, flat-screen displays on some laptop computers.

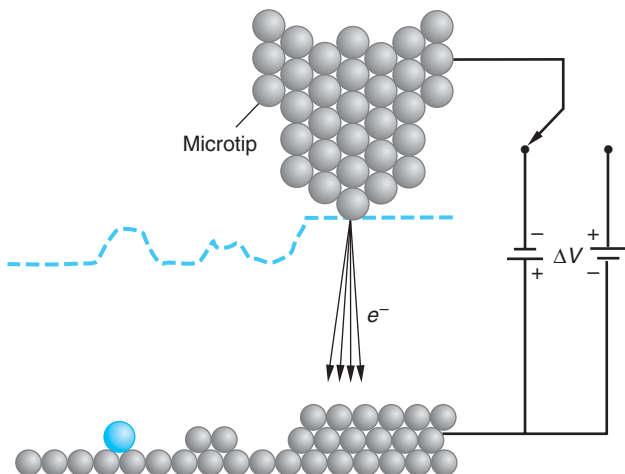
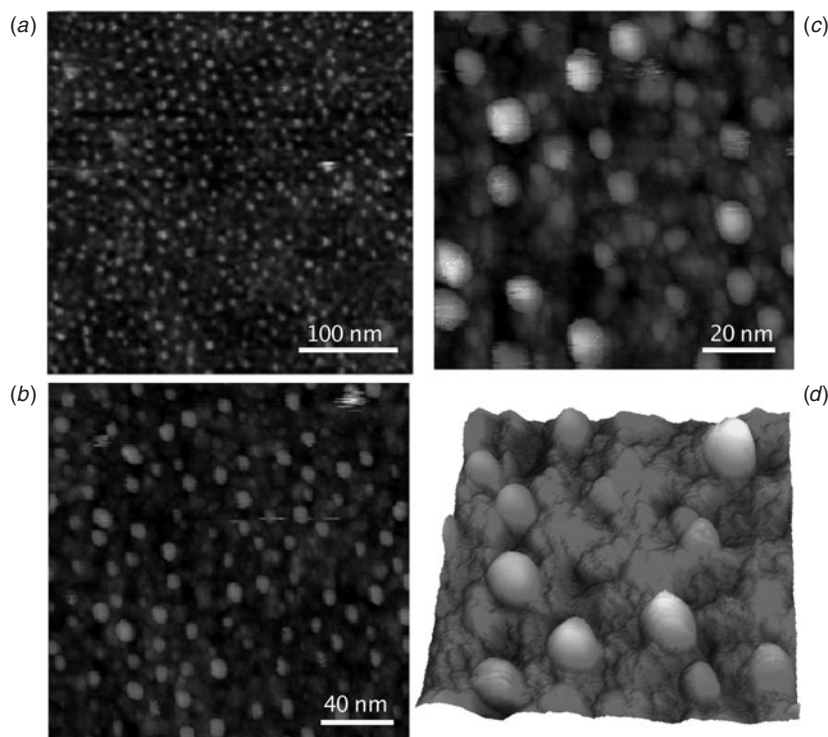


Figure 6-29 Schematic illustration of the path of the probe of an STM (dashed line) scanned across the surface of a sample while maintaining constant tunneling current. The probe has an extremely sharp microtip of atomic dimensions. Tunneling occurs over a small area across the narrow gap, allowing very small features (even individual atoms) to be imaged, as indicated by the dashed line.

Room temperature UHV-STM images of gold (Au) nanoparticles supported on TiC after annealing at 500°C. Images are
 (a) 375 nm × 375 nm,
 (b) 200 × 200 nm, and
 (c) 100 × 100 nm.
 (d) A 3-D image of a 70 nm × 70 nm section of (c). [The authors thank Beatriz Roldán Cuenya for permission to use these STM images.]



EXPLORING Alpha Decay

Barrier penetration was used by G. Gamow, E. U. Condon, and R. W. Gurney in 1928 to explain the enormous variation in the mean life for α decay of radioactive nuclei and the seemingly paradoxical very existence of α decay.¹⁶ While radioactive α decay will be discussed more thoroughly in Chapter 11, in general, the smaller the energy of the emitted α particle, the larger the mean life. The energies of α particles from natural radioactive sources range from about 4 to 7 MeV, whereas the mean lifetimes range from about 10^{10} years to 10^{-6} s. Gamow represented the radioactive nucleus by a potential well containing an α particle, as shown in Figure 6-30a. For r less than the nuclear radius R , the α particle is attracted by the nuclear force. Without knowing much about this force, Gamow and his co-workers represented it by a square well. Outside the nucleus, the α particle is repelled by the Coulomb force. This is represented by the Coulomb potential energy $+kZze^2/r$, where $z = 2$ for the α particle and Ze is the remaining nuclear charge. The energy E is the measured kinetic energy of the emitted α particle, since when it is far from the nucleus its potential energy is zero. We see from the figure that a small increase in E reduces the relative height of the barrier $V - E$ and also reduces the thickness. Because the probability of transmission varies exponentially with the relative height and barrier thickness, as indicated by Equation 6-76, a small increase in E leads to a large increase in the probability of transmission and in turn to a shorter lifetime. Gamow and his co-workers were able to derive an expression for the α decay rate and the mean lifetime as a function of energy E that was in good agreement with experimental results as follows:

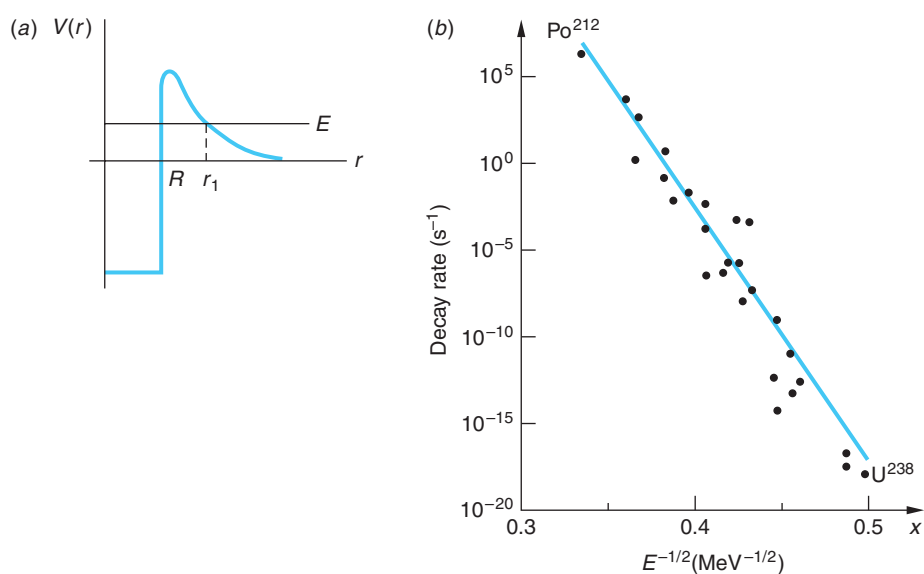


Figure 6-30 (a) Model of potential-energy function for an α particle and a nucleus. The strong attractive nuclear force for r less than the nuclear radius R can be approximately described by the potential well shown. Outside the nucleus the nuclear force is negligible, and the potential is given by Coulomb's law, $V(r) = +kZze^2/r$, where Ze is the nuclear charge and ze is the charge of the α particle. An α particle inside the nucleus oscillates back and forth, being reflected at the barrier at R . Because of its wave properties, when the α particle hits the barrier, there is a small chance that it will penetrate and appear outside the well at $r = r_1$. The wave function is similar to that shown in Figure 6-27b. (b) The decay rate for the emission of α particles from radioactive nuclei. The solid curve is the prediction of Equation 6-79; the points are experimental results.

The probability that an α particle will tunnel through the barrier in any one approach is given by T from Equation 6-76. In fact, in this case αa is so large that the exponential dominates the expression and

$$T \approx e^{-2\sqrt{2m(V_0 - E)a}/\hbar} \quad 6-77$$

which is a very small number; i.e., the α particle is usually reflected. The number of times per second N that the α particle approaches the barrier is given roughly by

$$N \approx \frac{v}{2R} \quad 6-78$$

where v equals the particle's speed inside the nucleus. Thus, the decay rate, or the probability per second that the nucleus will emit an α particle, which is also the reciprocal of the mean life τ , is given by

$$\text{decay rate} = \frac{1}{\tau} = \frac{v}{2R} e^{-2\sqrt{2m(V_0 - E)a}/\hbar} \quad 6-79$$

Figure 6-30b illustrates the good agreement between the barrier penetration calculation and experimental measurements.

In the event that $E/V_0 > 1$, there is no reflected wave for $\alpha a = \pi, 2\pi, \dots$ as a result of destructive interference. For electrons incident on noble gas atoms the resulting 100 percent transmission is called Ramsauer-Townsend effect and is a way of measuring atomic diameters for those elements.



EXPLORING NH_3 Atomic Clock

Barrier penetration also takes place in the case of the periodic *inversion* of the ammonia molecule. The NH_3 molecule has two equilibrium configurations, as illustrated in Figure 6-31a. The three hydrogen atoms are arranged in a plane. The nitrogen atom oscillates between two equilibrium positions equidistant from each of the H atoms above and below the plane. The potential energy function $V(x)$ acting on the N atom has two minima located symmetrically about the center of the plane, as shown in Figure 6-31b. The N atom is bound to the molecule, so the energy is quantized and the lower states lie well below the central maximum of the potential. The central maximum presents a barrier to the N atoms in the lower states through which they slowly tunnel back and forth.¹⁷ The oscillation frequency $f = 2.3786 \times 10^{10}$ Hz when the atom is in the state characterized by the energy E_1 in Figure 6-31b. This frequency is quite low compared with the frequencies of most molecular vibrations, a fact that allowed the N atom tunneling frequency in NH_3 to be used as the standard in the first *atomic clocks*, devices that now provide the world's standard for precision timekeeping.

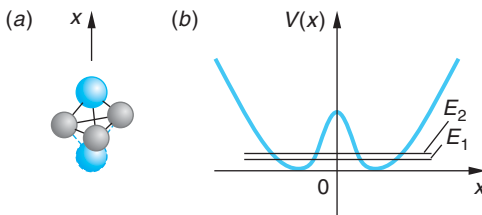


Figure 6-31 (a) The NH_3 molecule oscillates between the two equilibrium positions shown. The H atoms form a plane; the N atom is colored. (b) The potential energy of the N atom, where x is the distance above and below the plane of the H atoms. Several of the allowed energies, including the two lowest shown, lie below the top of the central barrier through which the N atom tunnels.



More

Quantum-mechanical tunneling involving two barriers is the basis for a number of devices such as the tunnel diode and the Josephson junction, both of which have a wide variety of useful applications. As an example of such systems, the *Tunnel Diode* is described on the home page: www.whfreeman.com/tiplermodernphysics5e. See also Equation 6-80 and Figure 6-32 here.

Summary

TOPIC

RELEVANT EQUATIONS AND REMARKS

1. Schrödinger equation

Time dependent, one space dimension

$$-\frac{\hbar^2}{2m} \frac{\partial^2 \psi(x, t)}{\partial x^2} + V(x, t)\psi(x, t) = i\hbar \frac{\partial \psi(x, t)}{\partial t} \quad \text{6-6}$$

TOPIC

RELEVANT EQUATIONS AND REMARKS

Time independent, one space dimension

$$\frac{-\hbar^2}{2m} \frac{d^2\psi(x)}{dx^2} + V(x)\psi(x) = E\psi(x) \quad \text{6-18}$$

Normalization condition

$$\int_{-\infty}^{+\infty} \Psi^*(x, t)\Psi(x, t) dx = 1 \quad \text{6-9}$$

and

$$\int_{-\infty}^{+\infty} \psi^*(x)\psi(x) dx = 1 \quad \text{6-20}$$

Acceptability conditions

1. $\psi(x)$ must exist and satisfy the Schrödinger equation.
2. $\psi(x)$ and $d\psi/dx$ must be continuous.
3. $\psi(x)$ and $d\psi/dx$ must be finite.
4. $\psi(x)$ and $d\psi/dx$ must be single valued.
5. $\psi(x) \rightarrow 0$ fast enough as $x \rightarrow \pm\infty$ so that the normalization integral, Equation 6-20, remains bounded.

2. Infinite square well

Allowed energies

$$E_n = n^2 \frac{\pi^2 \hbar^2}{2mL^2} = n^2 E_1 \quad n = 1, 2, 3, \dots \quad \text{6-24}$$

Wave functions

$$\psi_n(x) = \sqrt{\frac{2}{L}} \sin \frac{n\pi x}{L} \quad n = 1, 2, 3, \dots \quad \text{6-32}$$

3. Finite square well

For a finite well of width L the allowed energies E_n in the well are lower than the corresponding levels for an infinite well. There is always at least one allowed energy (bound state) in a finite well.

4. Expectation values and operators

The expectation or average value of a physical quantity represented by an operator, such as the momentum operator p_{op} , is given by

$$\langle p \rangle = \int_{-\infty}^{+\infty} \psi^* p_{\text{op}} \psi dx = \int_{-\infty}^{+\infty} \psi^* \left(\frac{\hbar}{i} \frac{\partial}{\partial x} \right) \psi dx \quad \text{6-48}$$

5. Simple harmonic oscillator

Allowed energies

$$E_n = \left(n + \frac{1}{2} \right) \hbar\omega \quad n = 0, 1, 2, \dots \quad \text{6-56}$$

6. Reflection and transmission

When the potential changes abruptly in a distance small compared to the de Broglie wavelength, a particle may be reflected even though $E > V(x)$. A particle may also penetrate into a region where $E < V(x)$.

General References

The following general references are written at a level appropriate for the readers of this book.

- Brandt, S., and H. D. Dahmen, *The Picture Book of Quantum Mechanics*, Wiley, New York, 1985.
 Eisberg, R., and R. Resnick, *Quantum Physics*, 2d ed., Wiley, New York, 1985.
 Feynman, R. P., R. B. Leighton, and M. Sands, *Lectures on Physics*, Addison-Wesley, Reading, MA, 1965.
 Ford, K. W., *The Quantum World*, Harvard University Press, Cambridge, MA, 2004.

French, A. P., and E. F. Taylor, *An Introduction to Quantum Physics*, Norton, New York, 1978.

Mehra, J., and H. Rechenberg, *The Historical Development of Quantum Theory*, Vol. 1, Springer-Verlag, New York, 1982.

Park, D., *Introduction to the Quantum Theory*, 3d ed., McGraw-Hill, New York, 1992.

Visual Quantum Mechanics, Kansas State University, Manhattan, 1996. Computer simulation software allows the user to analyze a variety of one-dimensional potentials, including the square wells and harmonic oscillator discussed in this chapter.

Notes

1. Felix Bloch (1905–1983), Swiss American physicist. He was a student at the University of Zurich and attended the colloquium referred to. The quote is from an address before the American Physical Society in 1976. Bloch shared the 1952 Nobel Prize in Physics for measuring the magnetic moment of the neutron, using a method that he invented that led to the development of the analytical technique of nuclear magnetic resonance (NMR) spectroscopy.

2. Peter J. W. Debye (1884–1966), Dutch American physical chemist. He succeeded Einstein in the chair of theoretical physics at the University of Zurich and received the Nobel Prize in Chemistry in 1936.

3. Erwin R. J. A. Schrödinger (1887–1961), Austrian physicist. He succeeded Planck in the chair of theoretical physics at the University of Berlin in 1928 following Planck's retirement and two years after publishing in rapid succession six papers that set forth the theory of wave mechanics. For that work he shared the Nobel Prize in Physics with P. A. M. Dirac in 1933. He left Nazi-controlled Europe in 1940, moving his household to Ireland.

4. To see that this is indeed the case, consider the effect on $\partial^2\Psi(x, t)/\partial x^2$ of multiplying $\Psi(x, t)$ by a factor C . Then $\partial^2C\Psi(x, t)/\partial x^2 = C\partial^2\Psi(x, t)/\partial x^2$, and the derivative is increased by the same factor. Thus, the derivative is proportional to the first power of the function; i.e., it is linear in $\Psi(x, t)$.

5. The imaginary i appears because the Schrödinger equation relates a *first* time derivative to a *second* space derivative as a consequence of the fact that the total energy is related to the *square* of the momentum. This is unlike the classical wave equation (Equation 5-11), which relates two second derivatives. The implication of this is that, in general, the $\Psi(x, t)$ will be complex functions, whereas the $y(x, t)$ are real.

6. The fact that Ψ is in general complex does not mean that its imaginary part doesn't contribute to the values of measurements, which are real. Every complex number can be

written in the form $z = a + bi$, where a and b are real numbers and $i = (-1)^{1/2}$. The magnitude or absolute value of z is defined as $(a^2 + b^2)^{1/2}$. The complex conjugate of z is $z^* = a - bi$, so $z^*z = (a - bi)(a + bi) = a^2 + b^2 = |z|^2$; thus, the value of $|\Psi|^2$ will contain a contribution from its imaginary part.

7. Here we are using the convention of probability and statistics that certainty is represented by a probability of 1.

8. This method for solving partial differential equations is called *separation of variables*, for obvious reasons. Since most potentials in quantum mechanics, as in classical mechanics, are time independent, the method may be applied to the Schrödinger equation in numerous situations.

9. We should note that there is an exception to this in the quantum theory of measurement.

10. $E = 0$ corresponding to $n=0$ is not a possible energy for a particle in a box. As discussed in Section 5-6, the uncertainty principle limits the minimum energy for such a particle to values $> \hbar^2/2mL^2$.

11. Recalling that linear combinations of solutions to Schrödinger's equation will also be solutions, we should note here that simulation of the classical behavior of a macroscopic particle in a macroscopic box requires wave functions that are the superpositions of many stationary states. Thus, the classical particle never has definite energy in the quantum mechanical sense.

12. To simplify the notation in this section, we will sometimes omit the functional dependence and merely write ψ_n for $\psi_n(x)$ and Ψ_n for $\Psi_n(x, t)$.

13. The Hermite polynomials are known functions that are tabulated in most books on quantum mechanics.

14. It is straightforward to show that the only difference between a $\psi(x)$ normalized in terms of the particle density and one for which $|\psi(x)|^2$ is the probability density is a multiplicative constant.

15. T and R are derived in terms of the particle currents, i.e., particles/unit time, in most introductory quantum mechanics books.

16. Rutherford had shown that the scattering of 8.8-MeV α particles from the decay of ^{212}Po obeyed the Coulomb force law down to distances of the order of 3×10^{-14} m, i.e., down to about nuclear dimensions. Thus, the Coulomb barrier at that distance was at least 8.8 MeV high; however, the energy of α particles emitted by ^{238}U is only 4.2 MeV, less than half the barrier height. How that could be possible presented classical physics with a paradox.

17. Since the molecule's center of mass is fixed in an inertial reference frame, the plane of H atoms also oscillates back and forth in the opposite direction to the N atom; however, their mass being smaller than that of the N atom, the amplitude of the plane's motion is actually larger than that of the N atom. It is the relative motion that is important.

18. See, for example, F. Capasso and S. Datta, "Quantum Electron Devices," *Physics Today*, **43**, 74 (1990). Leo Esaki was awarded the Nobel Prize in Physics in 1973 for inventing the resonant tunnel diode.

Problems

Level I

Section 6-1 The Schrödinger Equation in One Dimension

6-1. Show that the wave function $\Psi(x, t) = Ae^{kx - \omega t}$ does not satisfy the time-dependent Schrödinger equation.

6-2. Show that $\Psi(x, t) = Ae^{i(kx - \omega t)}$ satisfies both the time-dependent Schrödinger equation and the classical wave equation (Equation 6-1).

6-3. In a region of space, a particle has a wave function given by $\psi(x) = Ae^{-x^2/2L^2}$ and energy $\hbar^2/2mL^2$, where L is some length. (a) Find the potential energy as a function of x , and sketch V versus x . (b) What is the classical potential that has this dependence?

6-4. (a) For Problem 6-3, find the kinetic energy as a function of x . (b) Show that $x = L$ is the classical turning point. (c) The potential energy of a simple harmonic oscillator in terms of its angular frequency ω is given by $V(x) = \frac{1}{2}m\omega^2x^2$. Compare this with your answer to part (a) of Problem 6-3, and show that the total energy for this wave function can be written $E = \frac{1}{2}\hbar\omega$.

6-5. (a) Show that the wave function $\Psi(x, t) = A \sin(kx - \omega t)$ does *not* satisfy the time-dependent Schrödinger equation. (b) Show that $\Psi(x, t) = A \cos(kx - \omega t) + iA \sin(kx - \omega t)$ does satisfy this equation.

6-6. The wave function for a free electron, i.e., one on which no net force acts, is given by $\psi(x) = A \sin(2.5 \times 10^{10}x)$, where x is in meters. Compute the electron's (a) momentum, (b) total energy, and (c) de Broglie wavelength.

6-7. A particle with mass m and total energy zero is in a particular region of space where its wave function is $\psi(x) = Ce^{-x^2/L^2}$. (a) Find the potential energy $V(x)$ versus x and (b) make a sketch of $V(x)$ versus x .

6-8. Normalize the wave function in Problem 6-2 between $-a$ and $+a$. Why can't that wave function be normalized between $-\infty$ and $+\infty$?

Section 6-2 The Infinite Square Well

6-9. A particle is in an infinite square well of width L . Calculate the ground-state energy if (a) the particle is a proton and $L = 0.1$ nm, a typical size for a molecule; (b) the particle is a proton and $L = 1$ fm, a typical size for a nucleus.

6-10. A particle is in the ground state of an infinite square well potential given by Equation 6-21. Find the probability of finding the particle in the interval $\Delta x = 0.002 L$ at (a) $x = L/2$, (b) $x = 2L/3$, and (c) $x = L$. (Since Δx is very small, you need not do any integration.)

6-11. Do Problem 6-10 for a particle in the second excited state ($n = 3$) of an infinite square well potential.

6-12. A mass of 10^{-6} g is moving with a speed of about 10^{-1} cm/s in a box of length 1 cm. Treating this as a one-dimensional infinite square well, calculate the approximate value of the quantum number n .

6-13. (a) For the classical particle of Problem 6-12, find Δx and Δp , assuming that $\Delta x/L = 0.01$ percent and $\Delta p/p = 0.01$ percent. (b) What is $(\Delta x \Delta p)/\hbar$?

6-14. A particle of mass m is confined to a tube of length L . (a) Use the uncertainty relationship to estimate the smallest possible energy. (b) Assume that the inside of the tube is a force-free region and that the particle makes elastic reflections at the tube ends. Use Schrödinger's equation to find the ground-state energy for the particle in the tube. Compare the answer to that of part (a).

6-15. (a) What is the wavelength associated with the particle of Problem 6-14 if the particle is in its ground state? (b) What is the wavelength if the particle is in its second excited state (quantum number $n = 3$)? (c) Use de Broglie's relationship to find the magnitude for the momentum of the particle in its ground state. (d) Show that $p^2/2m$ gives the correct energy for the ground state of this particle in the box.

6-16. The wavelength of light emitted by a ruby laser is 694.3 nm. Assuming that the emission of a photon of this wavelength accompanies the transition of an electron from the $n = 2$ level to the $n = 1$ level of an infinite square well, compute L for the well.

6-17. The allowed energies for a particle of mass m in a one-dimensional infinite square well are given by Equation 6-24. Show that a level with $n = 0$ violates the Heisenberg uncertainty principle.

6-18. Suppose a macroscopic bead with a mass of 2.0 g is constrained to move on a straight frictionless wire between two heavy stops clamped firmly to the wire 10 cm apart. If the bead is moving at a speed of 20 nm/y (i.e., to all appearances it is at rest), what is the value of its quantum number n ?

6-19. An electron moving in a one-dimensional infinite square well is trapped in the $n = 5$ state. (a) Show that the probability of finding the electron between $x = 0.2 L$ and $x = 0.4 L$ is $1/5$. (b) Compute the probability of finding the electron within the “volume” $\Delta x = 0.01 L$ at $x = L/2$.

6-20. In the early days of nuclear physics before the neutron was discovered, it was thought that the nucleus contained only electrons and protons. If we consider the nucleus to be a one-dimensional infinite well with $L = 10$ fm and ignore relativity, compute the ground-state energy for (a) an electron and (b) a proton in the nucleus. (c) Compute the energy difference between the ground state and the first excited state for each particle. (Differences between energy levels in nuclei are found to be typically of the order of 1 MeV.)

6-21. An electron is in the ground state with energy E_n of a one-dimensional infinite well with $L = 10^{-10}$ m. Compute the force that the electron exerts on the wall during an impact on either wall. (*Hint:* $F = -dE_n/dL$. Why?) How does this result compare with the weight of an electron at the surface of Earth?

6-22. The wave functions of a particle in a one-dimensional infinite square well are given by Equation 6-32. Show that for these functions $\int \psi_n(x)\psi_m(x) dx = 0$, i.e., that $\psi_n(x)$ and $\psi_m(x)$ are orthogonal.

Section 6-3 The Finite Square Well

6-23. Sketch (a) the wave function and (b) the probability distribution for the $n = 4$ state for the finite square well potential.

6-24. A finite square well 1.0 fm wide contains one neutron. How deep must the well be if there are only two allowed energy levels for the neutron?

6-25. An electron is confined to a finite square well whose “walls” are 8.0 eV high. If the ground-state energy is 0.5 eV, estimate the width of the well.

6-26. Using arguments concerning curvature, wavelength, and amplitude, sketch very carefully the wave function corresponding to a particle with energy E in the finite potential well shown in Figure 6-33.

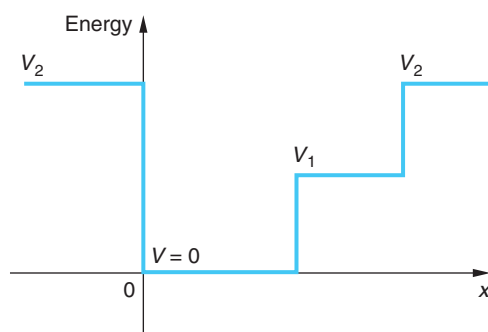


Figure 6-33 Problem 6-26.

- 6-27.** For a finite square well potential that has six quantized levels, if $a = 10 \text{ nm}$ (a) sketch the finite well, (b) sketch the wave function from $x = -2a$ to $x = +2a$ for $n = 3$, and (c) sketch the probability density for the same range of x .

Section 6-4 Expectation Values and Operators

- 6-28.** Compute the expectation value of the x component of the momentum of a particle of mass m in the $n = 3$ level of a one-dimensional infinite square well of width L . Reconcile your answer with the fact that the kinetic energy of the particle in this level is $9\pi^2\hbar^2/2mL^2$.

- 6-29.** Find (a) $\langle x \rangle$ and (b) $\langle x^2 \rangle$ for the second excited state ($n = 3$) in an infinite square well potential.

- 6-30.** (a) Show that the classical probability distribution function for a particle in a one-dimensional infinite square well potential of length L is given by $P(x) = 1/L$. (b) Use your result in (a) to find $\langle x \rangle$ and $\langle x^2 \rangle$ for a classical particle in such a well.

- 6-31.** Show directly from the time-independent Schrödinger equation that $\langle p^2 \rangle = \langle 2m[E - V(x)] \rangle$ in general and that $\langle p^2 \rangle = \langle 2mE \rangle$ for the infinite square well. Use this result to compute $\langle p^2 \rangle$ for the ground state of the infinite square well.

- 6-32.** Find $\sigma_x = \sqrt{\langle x^2 \rangle - \langle x \rangle^2}$, $\sigma_p = \sqrt{\langle p^2 \rangle - \langle p \rangle^2}$, and $\sigma_x \sigma_p$ for the ground-state wave function of an infinite square well. (Use the fact that $\langle p \rangle = 0$ by symmetry and $\langle p^2 \rangle = \langle 2mE \rangle$ from Problem 6-31.)

- 6-33.** Compute $\langle x \rangle$ and $\langle x^2 \rangle$ for the ground state of a harmonic oscillator (Equation 6-58). Use $A_0 = (m\omega/\hbar\pi)^{1/4}$.

- 6-34.** Use conservation of energy to obtain an expression connecting x^2 and p^2 for a harmonic oscillator, then use it along with the result from Problem 6-33 to compute $\langle p^2 \rangle$ for the harmonic oscillator ground state.

- 6-35.** (a) Using A_0 from Problem 6-33, write down the total wave function $\Psi_0(x, t)$ for the ground state of a harmonic oscillator. (b) Use the operator for p_x from Table 6-1 to compute $\langle p^2 \rangle$.

Section 6-5 The Simple Harmonic Oscillator

- 6-36.** For the harmonic oscillator ground state $n = 0$ the Hermite polynomial $H_n(x)$ in Equation 6-57 is given by $H_0 = 1$. Find (a) the normalization constant C_0 , (b) $\langle x^2 \rangle$, and (c) $\langle V(x) \rangle$ for this state. (Hint: Use the Probability Integral in Appendix B1 to compute the needed integrals.)

- 6-37.** For the first excited state, $H_1(x) = x$. Find (a) the normalization constant C_1 , (b) $\langle x \rangle$, (c) $\langle x^2 \rangle$, (d) $\langle V(x) \rangle$ for this state (see Problem 6-36).

- 6-38.** A quantum harmonic oscillator of mass m is in the ground state with classical turning points at $\pm A$. (a) With the mass confined to the region $\Delta x \approx 2A$, compute Δp for this state. (b) Compare the kinetic energy implied by Δp with (1) the ground-state total energy and (2) the expectation value of the kinetic energy.

6-39. Compute the spacing between adjacent energy levels per unit energy, i.e., $\Delta E_n/E_n$, for the quantum harmonic oscillator and show that the result agrees with Bohr's correspondence principle (see Section 4-3) by letting $n \rightarrow \infty$.

6-40. Compute $\langle x \rangle$ and $\langle x^2 \rangle$ for (a) the ground state and (b) the first excited state of the harmonic oscillator.

6-41. The period of a macroscopic pendulum made with a mass of 10 g suspended from a massless cord 50 cm long is 1.42 s. (a) Compute the ground-state (zero-point) energy. (b) If the pendulum is set into motion so that the mass raises 0.1 mm above its equilibrium position, what will be the quantum number of the state? (c) What is the frequency of the motion in (b)?

6-42. Show that the wave functions for the ground state and the first excited state of the simple harmonic oscillator, given in Equation 6-58, are orthogonal; that is, show that $\int \psi_0(x)\psi_1(x) dx = 0$.

Section 6-6 Reflection and Transmission of Waves

6-43. A free particle of mass m with wave number k_1 is traveling to the right. At $x = 0$, the potential jumps from zero to V_0 and remains at this value for positive x . (a) If the total energy is $E = \hbar^2 k_1^2/2m = 2V_0$, what is the wave number k_2 in the region $x > 0$? Express your answer in terms of k_1 and V_0 . (b) Calculate the reflection coefficient R at the potential step. (c) What is the transmission coefficient T ? (d) If one million particles with wave number k_1 are incident upon the potential step, how many particles are expected to continue along in the positive x direction? How does this compare with the classical prediction?

6-44. In Problem 6-43, suppose that the potential jumps from zero to $-V_0$ at $x = 0$ so that the free particle speeds up instead of slowing down. The wave number for the incident particle is again k_1 , and the total energy is $2V_0$. (a) What is the wave number for the particle in the region of positive x ? (b) Calculate the reflection coefficient R at the potential step. (c) What is the transmission coefficient T ? (d) If one million particles with wave number k_1 are incident upon the potential step, how many particles are expected to continue along in the positive x direction? How does this compare with the classical prediction?

6-45. In a particular semiconductor device an oxide layer forms a barrier 0.6 nm wide and 9 V high between two conducting wires. Electrons accelerated through 4 V approach the barrier. (a) What fraction of the incident electrons will tunnel through the barrier? (b) Through what potential difference should the electrons be accelerated in order to increase the tunneling fraction by a factor of 2?

6-46. For particles incident on a step potential with $E < V_0$, show that $T = 0$ using Equation 6-70.

6-47. Derive Equations 6-66 and 6-67 from those that immediately precede them.

6-48. A beam of electrons, each with kinetic energy $E = 2.0$ eV, is incident on a potential barrier with $V_0 = 6.5$ eV and width 5.0×10^{-10} m. (See Figure 6-26.) What fraction of the electrons in the beam will be transmitted through the barrier?

6-49. A beam of protons, each with kinetic energy 40 MeV, approaches a step potential of 30 MeV. (a) What fraction of the beam is reflected and transmitted? (b) Does your answer change if the particles are electrons?

Level II

6-50. A proton is in an infinite square well potential given by Equation 6-21 with $L = 1$ fm. (a) Find the ground-state energy in MeV. (b) Make an energy-level diagram for this system. Calculate the wavelength of the photon emitted for the transitions (c) $n = 2$ to $n = 1$, (d) $n = 3$ to $n = 2$, and (e) $n = 3$ to $n = 1$.

6-51. A particle is in the ground state of an infinite square well potential given by Equation 6-21. Calculate the probability that the particle will be found in the region (a) $0 < x < \frac{1}{2}L$, (b) $0 < x < \frac{1}{3}L$, and (c) $0 < x < \frac{3}{4}L$.

6-52. (a) Show that for large n , the fractional difference in energy between state n and state $n + 1$ for a particle in an infinite square well is given approximately by

$$\frac{E_{n+1} - E_n}{E_n} \approx \frac{2}{n}$$

(b) What is the approximate percentage energy difference between the states $n_1 = 1000$ and $n_2 = 1001$? (c) Comment on how this result is related to Bohr's correspondence principle.

6-53. Compute the expectation value of the kinetic energy of a particle of mass m moving in the $n = 2$ level of a one-dimensional infinite square well of width L .

6-54. A particle of mass m is in an infinite square well potential given by

$$\begin{aligned} V &= \infty & x < -L/2 \\ V &= 0 & -L/2 < x < +L/2 \\ V &= \infty & +L/2 < x \end{aligned}$$

Since this potential is symmetric about the origin, the probability density $|\psi(x)|^2$ must also be symmetric. (a) Show that this implies that either $\psi(-x) = \psi(x)$ or $\psi(-x) = -\psi(x)$. (b) Show that the proper solutions of the time-independent Schrödinger equation can be written

$$\psi(x) = \sqrt{\frac{2}{L}} \cos \frac{n\pi x}{L} \quad n = 1, 3, 5, 7, \dots$$

and

$$\psi(x) = \sqrt{\frac{2}{L}} \sin \frac{n\pi x}{L} \quad n = 2, 4, 6, 8, \dots$$

(c) Show that the allowed energies are the same as those for the infinite square well given by Equation 6-24.

6-55. The wave function $\psi_0(x) = Ae^{-x^2/2L^2}$ represents the ground-state energy of a harmonic oscillator. (a) Show that $\psi_1(x) = L d\psi_0(x)/dx$ is also a solution of Schrödinger's equation. (b) What is the energy of this new state? (c) From a look at the nodes of this wave function, how would you classify this excited state?

6-56. For the wave functions

$$\psi(x) = \sqrt{\frac{2}{L}} \sin \frac{n\pi x}{L} \quad n = 1, 2, 3, \dots$$

corresponding to an infinite square well of width L , show that

$$\langle x^2 \rangle = \frac{L^2}{3} - \frac{L^2}{2n^2\pi^2}$$

6-57. A 10-eV electron is incident on a potential barrier of height 25 eV and width 1 nm. (a) Use Equation 6-76 to calculate the order of magnitude of the probability that the electron will tunnel through the barrier. (b) Repeat your calculation for a width of 0.1 nm.

6-58. A particle of mass m moves in a region in which the potential energy is constant $V = V_0$. (a) Show that neither $\Psi(x, t) = A \sin(kx - \omega t)$ nor $\Psi(x, t) = A \cos(kx - \omega t)$ satisfies the time-dependent Schrödinger equation. (Hint: If $C_1 \sin \phi + C_2 \cos \phi = 0$ for all values of ϕ , then C_1 and C_2 must be zero.) (b) Show that $\Psi(x, t) = A[\cos(kx - \omega t) + i \sin(kx - \omega t)] = Ae^{i(kx - \omega t)}$ does satisfy the time-independent Schrödinger equation providing that k , V_0 , and ω are related by Equation 6-5.

Level III

6-59. A particle of mass m on a table at $z = 0$ can be described by the potential energy

$$\begin{aligned} V &= mgz & \text{for } z > 0 \\ V &= \infty & \text{for } z < 0 \end{aligned}$$

For some positive value of total energy E , indicate the classically allowed region on a sketch of $V(z)$ versus z . Sketch also the kinetic energy versus z . The Schrödinger equation for this problem is quite difficult to solve. Using arguments similar to those in Section 6-3 about the curvature of a wave function as given by the Schrödinger equation, sketch your "educated guesses" for the shape of the wave function for the ground state and the first two excited states.

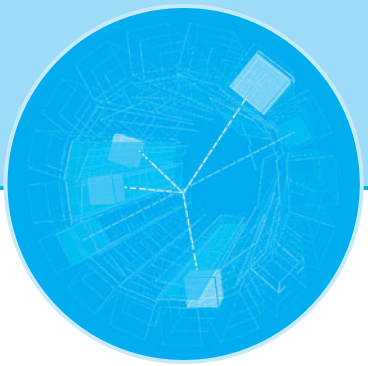
6-60. Use the Schrödinger equation to show that the expectation value of the kinetic energy of a particle is given by

$$\langle E_k \rangle = \int_{-\infty}^{+\infty} \psi(x) \left(-\frac{\hbar^2}{2m} \frac{d^2\psi(x)}{dx^2} \right) dx$$

6-61. An electron in an infinite square well with $L = 10^{-12}$ m is moving at relativistic speed; hence, the momentum is *not* given by $p = (2mE)^{1/2}$. (a) Use the uncertainty principle to verify that the speed is relativistic. (b) Derive an expression for the electron's allowed energy levels and (c) compute E_1 . (d) By what fraction does E_1 computed in (c) differ from the nonrelativistic E_1 ?

6-62. (a) Derive Equation 6-75. (b) Show that, if $\alpha x \gg 1$, Equation 6-76 follows from Equation 6-75 as an approximation.

6-63. A beam of protons, each with energy $E = 20$ MeV, is incident on a potential step 40 MeV high. Graph the relative probability of finding protons at values of $x > 0$ from $x = 0$ to $x = 5$ fm. (*Hint:* Take $|A|^2 = 1$ and refer to Example 6-6.)



Atomic Physics

In this chapter we will apply quantum theory to atomic systems. For all neutral atoms except hydrogen, the Schrödinger equation cannot be solved exactly. Despite this, it is in the realm of atomic physics that the Schrödinger equation has had its greatest success because the electromagnetic interaction of the electrons with one another and with the atomic nucleus is well understood. With powerful approximation methods and high-speed computers, many features of complex atoms, such as their energy levels and the wavelengths and intensities of their spectra, can be calculated, often to whatever accuracy is desired. The Schrödinger equation for the hydrogen atom was first solved in Schrödinger's first paper on quantum mechanics, published in 1926. This problem is of considerable importance not only because the Schrödinger equation can be solved exactly in this case, but also because the solutions obtained form the basis for the approximate solutions for other atoms. We will therefore discuss this problem in some detail. Although the mathematics that arises in solving the Schrödinger equation is a bit difficult in a few places, we will be as quantitative as possible, presenting results without proof and discussing important features of these results qualitatively only when necessary. Whenever possible, we will give simple physical arguments to make important results plausible.

7-1 The Schrödinger Equation in Three Dimensions

In Chapter 6 we considered motion in just one dimension, but of course the real world is three-dimensional. Although in many cases the one-dimensional form brings out the essential physical features, there are some considerations introduced in three-dimensional problems that we want to examine. In rectangular coordinates, the time-independent Schrödinger equation is

$$-\frac{\hbar^2}{2m} \left(\frac{\partial^2 \psi}{\partial x^2} + \frac{\partial^2 \psi}{\partial y^2} + \frac{\partial^2 \psi}{\partial z^2} \right) + V\psi = E\psi \quad 7-1$$

The wave function and the potential energy are generally functions of all three coordinates x , y , and z .

| | |
|---|------------|
| 7-1 The Schrödinger Equation in Three Dimensions | 269 |
| 7-2 Quantization of Angular Momentum and Energy in the Hydrogen Atom | 272 |
| 7-3 The Hydrogen Atom Wave Functions | 281 |
| 7-4 Electron Spin | 285 |
| 7-5 Total Angular Momentum and the Spin-Orbit Effect | 291 |
| 7-6 The Schrödinger Equation for Two (or More) Particles | 295 |
| 7-7 Ground States of Atoms: The Periodic Table | 297 |
| 7-8 Excited States and Spectra of Atoms | 301 |

Infinite Square Well in Three Dimensions

Let us consider the three-dimensional version of a particle in a cubical box. The potential energy function $V(x, y, z) = 0$ for $0 < x < L$, $0 < y < L$, and $0 < z < L$. V is infinite outside this region. For this problem, the wave function must be zero at the walls of the box and will be a sine function inside the box. In fact, if we consider just one coordinate such as x , the solution will be the same as in the one-dimensional box discussed in Section 6-2. That is, the x dependence of the wave function will be of the form $\sin k_1 x$ with the restriction $k_1 L = n_1 \pi$, where n_1 is an integer. The complete wave function $\psi(x, y, z)$ can be written as a product of a function of x only, a function of y only, and a function of z only.

$$\psi(x, y, z) = \psi_1(x)\psi_2(y)\psi_3(z) \quad 7-2$$

where each of the functions ψ_n is a sine function as in the one-dimensional problem. For example, if we try the solution

$$\psi(x, y, z) = A \sin k_1 x \sin k_2 y \sin k_3 z \quad 7-3$$

we find by inserting this function into Equation 7-1 that the energy is given by

$$E = \frac{\hbar^2}{2m}(k_1^2 + k_2^2 + k_3^2)$$

which is equivalent to

$$E = \frac{(p_x^2 + p_y^2 + p_z^2)}{2m}$$

with $p_x = \hbar k_1$ and so forth. Using the restrictions on the wave numbers $k_i = n_i \pi / L$ from the boundary condition that the wave function be zero at the walls, we obtain for the total energy

$$E_{n_1 n_2 n_3} = \frac{\hbar^2 \pi^2}{2mL^2} (n_1^2 + n_2^2 + n_3^2) \quad 7-4$$

where n_1 , n_2 , and n_3 are integers greater than zero, as in Equation 6-24.

Notice that *the energy and wave function are characterized by three quantum numbers, each arising from a boundary condition on one of the coordinates*. In this case the quantum numbers are independent of one another, but in more-general problems the value of one quantum number may affect the possible values of the others. For example, as we will see in a moment, in problems such as the hydrogen atom that have a spherical symmetry, the Schrödinger equation is most readily solved in spherical coordinates r , θ , and φ . The quantum numbers associated with the boundary conditions on these coordinates are interdependent.

The lowest energy state, the ground state for the cubical box, is given by Equation 7-4 with $n_1 = n_2 = n_3 = 1$. The first excited energy level can be obtained in three different ways: either $n_1 = 2, n_2 = n_3 = 1$ or $n_2 = 2, n_1 = n_3 = 1$ or $n_3 = 2, n_1 = n_2 = 1$ since we see from Equation 7-4 that $E_{211} = E_{121} = E_{112}$. Each has a different wave function.

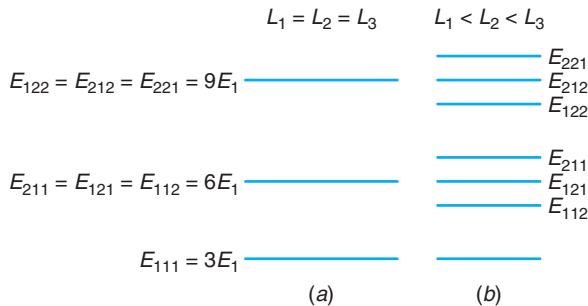


Figure 7-1 Energy-level diagram for (a) cubic infinite square well potential and (b) noncubic infinite square well. In the cubic well, the energy levels above the ground state are threefold degenerate; i.e., there are three wave functions having the same energy. The degeneracy is removed when the symmetry of the potential is removed, as in (b). The diagram is only schematic, and none of the levels in (b) necessarily has the same value of the energy as any level in (a).

For example, the wave function for $n_1 = 2$ and $n_2 = n_3 = 1$ is of the form

$$\psi_{211} = A \sin \frac{2\pi x}{L} \sin \frac{\pi y}{L} \sin \frac{\pi z}{L}$$

An energy level that has more than one wave function associated with it is said to be *degenerate*. In this case there is threefold degeneracy because there are three wave functions $\psi(x, y, z)$ corresponding to the same energy. The degeneracy is related to the symmetry of the problem, and anything that destroys or breaks the symmetry will also destroy or remove the degeneracy.¹ If, for example, we considered a noncubical box $V = 0$ for $0 < x < L_1$, $0 < y < L_2$, and $0 < z < L_3$, the boundary condition at the walls would lead to the quantum conditions $k_1 L_1 = n_1 \pi$, $k_2 L_2 = n_2 \pi$, and $k_3 L_3 = n_3 \pi$, and the total energy would be

7-5

Figure 7-1 shows the energy levels for the ground state and first two excited states when $L_1 = L_2 = L_3$, for which the excited states are degenerate, and when L_1 , L_2 , and L_3 are slightly different, in which case the excited levels are slightly split apart and the degeneracy is removed.

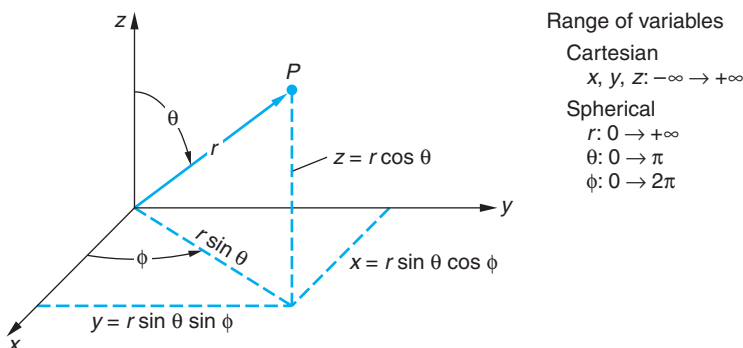
The Schrödinger Equation in Spherical Coordinates

In the next section we are going to consider another, different potential, that of a real atom. Assuming the proton to be at rest, we can treat the hydrogen atom as a single particle, an electron moving with kinetic energy $p^2/2m_e$ and a potential energy $V(r)$ due to the electrostatic attraction of the proton:

$$V(r) = -\frac{Zke^2}{r} \quad \text{7-6}$$

As in the Bohr theory, we include the atomic number Z , which is 1 for hydrogen, so we can apply our results to other similar systems, such as ionized helium He^+ , where $Z = 2$. We also note that we can account for the motion of the nucleus by replacing

Figure 7-2 Geometric relations between spherical (polar) and rectangular coordinates.



Hydrogenlike atoms, those with a single electron, have been produced from elements up to and including U⁹¹⁺. Highly ionized atomic beams are used to further our understanding of relativistic effects and atomic structure. Collision of two completely ionized Au atoms, each moving at nearly the speed of light, produced the “star” of thousands of particles reproduced on page 562 in Chapter 12.

the electron mass m_e by the reduced mass $\mu = m_e/(1 + m_e/M_N)$, where M_N is the mass of the nucleus. The time-independent Schrödinger equation for a particle of mass μ moving in three dimensions is Equation 7-1, with m replaced by μ :

$$-\frac{\hbar^2}{2\mu} \left(\frac{\partial^2 \psi}{\partial x^2} + \frac{\partial^2 \psi}{\partial y^2} + \frac{\partial^2 \psi}{\partial z^2} \right) + V\psi = E\psi \quad 7-7$$

Since the potential energy $V(r)$ depends only on the radial distance $r = (x^2 + y^2 + z^2)^{1/2}$, the problem is most conveniently treated in spherical coordinates r , θ , and ϕ . These are related to x , y , and z by

$$\begin{aligned} x &= r \sin \theta \cos \phi \\ y &= r \sin \theta \sin \phi \\ z &= r \cos \theta \end{aligned} \quad 7-8$$

These relations are shown in Figure 7-2. The transformation of the three-dimensional Schrödinger equation into spherical coordinates is straightforward but involves much tedious calculation, which we will omit. The result is

$$-\frac{\hbar^2}{2\mu} \frac{1}{r^2} \frac{\partial}{\partial r} \left(r^2 \frac{\partial \psi}{\partial r} \right) - \frac{\hbar^2}{2\mu r^2} \left[\frac{1}{\sin \theta} \frac{\partial}{\partial \theta} \left(\sin \theta \frac{\partial \psi}{\partial \theta} \right) + \frac{1}{\sin^2 \theta} \frac{\partial^2 \psi}{\partial \phi^2} \right] + V(r)\psi = E\psi \quad 7-9$$

Despite the formidable appearance of this equation, it was not difficult for Schrödinger to solve because it is similar to other partial differential equations that arise in classical physics, and such equations had been thoroughly studied. We will present the solution of this equation in detail, taking care to point out the origin of the quantum number associated with each dimension. As was the case with the three-dimensional square well, the new quantum numbers will arise as a result of boundary conditions on the solution of the wave equation, Equation 7-9 in this case.

7-2 Quantization of Angular Momentum and Energy in the Hydrogen Atom

In this section we will solve the time-independent Schrödinger equation for hydrogen and hydrogenlike atoms. We will see how the quantization of both the energy and the angular momentum arise as natural consequences of the acceptability conditions on the wave function (see Section 6-1) and discover the origin and physical meaning of the quantum numbers n , ℓ , and m .

The first step in the solution of a partial differential equation such as Equation 7-9 is to search for separable solutions by writing the wave function $\psi(r, \theta, \phi)$ as a product of functions of each single variable. We write

$$\psi(r, \theta, \phi) = R(r)f(\theta)g(\phi) \quad 7-10$$

where R depends only on the radial coordinate r , f depends only on θ , and g depends only on ϕ . When this form of $\psi(r, \theta, \phi)$ is substituted into Equation 7-9, the partial differential equation can be transformed into three ordinary differential equations, one for $R(r)$, one for $f(\theta)$, and one for $g(\phi)$. Most of the solutions of Equation 7-9 are, of course, not of this separable product form; however, if enough product solutions of the form of Equation 7-10 can be found,² all solutions can be expressed as superpositions of them. Even so, the separable solutions given by Equation 7-10 turn out to be the most important ones physically because they correspond to definite values (*eigenvalues*) of energy and angular momentum. When Equation 7-10 is substituted into Equation 7-9 and the indicated differentiations are performed, we obtain

$$\begin{aligned} -\frac{\hbar^2}{2\mu} fg \frac{1}{r^2} \frac{d}{dr} \left(r^2 \frac{dR}{dr} \right) - \frac{\hbar^2}{2\mu r^2} Rg \frac{1}{\sin \theta} \frac{d}{d\theta} \left(\sin \theta \frac{df}{d\theta} \right) \\ - \frac{\hbar^2}{2\mu r^2} \frac{Rf}{\sin^2 \theta} \frac{d^2 g}{d\phi^2} + VRfg = ERfg \end{aligned} \quad 7-11$$

since derivatives with respect to r do not affect $f(\theta)$ and $g(\phi)$, derivatives with respect to θ do not affect $R(r)$ and $g(\phi)$, and those with respect to ϕ do not affect $R(r)$ and $f(\theta)$. Separation of the r -dependent functions from the θ - and ϕ -dependent ones is accomplished by multiplying Equation 7-11 by $-2\mu r^2/(\hbar^2 R f g)$ and rearranging slightly to obtain

$$\begin{aligned} \frac{1}{R(r)} \frac{d}{dr} \left(r^2 \frac{dR(r)}{dr} \right) + \frac{2\mu r^2}{\hbar^2} \left[E - V(r) \right] = \\ - \left[\frac{1}{f(\theta) \sin \theta} \frac{d}{d\theta} \left(\sin \theta \frac{df(\theta)}{d\theta} \right) + \frac{1}{g(\phi) \sin^2 \theta} \frac{d^2 g(\phi)}{d\phi^2} \right] \end{aligned} \quad 7-12$$

Note two points about Equation 7-12: (1) The left side contains only terms that are functions of r , while the right side has only terms depending on θ and ϕ . Since the variables are independent, changes in r cannot change the value of the right side of the equation, nor can changes in θ and ϕ have any effect on the left side. Thus, the two sides of the equation must be equal to the same constant, which we will call, with foresight, $\ell(\ell + 1)$. (2) The potential is a function only of r so the solution of the right side, the angular part, of Equation 7-12 will be the same for all potentials that are only functions³ of r .

In view of the second point above, we will first solve the angular equation so that its results will be available to us as we consider solutions to the r -dependent equation, referred to usually as the *radial equation*, for various $V(r)$. Setting the right side of Equation 7-12 equal to $\ell(\ell + 1)$, multiplying by $\sin^2 \theta$, and rearranging slightly, we obtain

$$\frac{1}{g(\phi)} \frac{d^2 g(\phi)}{d\phi^2} = -\ell(\ell + 1) \sin^2 \theta - \frac{\sin \theta}{f(\theta)} \frac{d}{d\theta} \left[\sin \theta \frac{df(\theta)}{d\theta} \right] \quad 7-13$$

Once again we see that the two sides of the relation, Equation 7-13, are each a function of only one of the independent variables hence both sides must be equal to the same constant, which we will, again with foresight, call $-m^2$. Setting the left side of Equation 7-13 equal to $-m^2$ and solving for $g(\phi)$ yields

$$g_m(\phi) = e^{im\phi} \quad 7-14$$

The single valued condition on ψ (see Section 6-1) implies that $g(\phi + 2\pi) = g(\phi)$, which in turn requires that m be a positive or negative integer or zero.

Now letting the right side of Equation 7-13 equal $-m^2$ and solving for $f(\theta)$, we obtain (not intended to be obvious; for the detailed solution see Weber and Arfken, Chapter 11):

$$f_{\ell m}(\theta) = \frac{(\sin \theta)^{|m|}}{2^\ell \ell!} \left[\frac{d}{d(\cos \theta)} \right]^{\ell+|m|} (\cos^2 \theta - 1)^\ell \quad 7-15$$

The condition that ψ be finite requires that $f(\theta)$ be finite at $\theta = 0$ and $\theta = \pi$, which restricts the values of ℓ to zero and positive integers and limits $m \leq \ell$. The notation reflects the link between ℓ and m , namely, that each value of ℓ has associated values of m ranging from 0 up to $\pm\ell$. The functions $f_{\ell m}(\theta)$, given by Equation 7-15, are called the *associated Legendre functions*. The subset of those with $m = 0$ is referred to as the *Legendre polynomials*.

The product of $f_{\ell m}(\theta)$ and $g_m(\phi)$, which describes the angular dependence of $\psi(r, \theta, \phi)$ for all spherically symmetric potentials, forms an often-encountered family of functions $Y_{\ell m}(\theta, \phi)$,

$$Y_{\ell m}(\theta, \phi) = f_{\ell m}(\theta)g_m(\phi) \quad 7-16$$

called the *spherical harmonics*. The first few of these functions, which give the combined angular dependence of the motion of the electron in the hydrogen atom, are given in Table 7-1. The associated Legendre functions and the Legendre polynomials ($m = 0$) can, if needed, be easily taken from the same table. (Extended tables of both functions can be found in Weber and Arfken.) In the following section we will discover the physical significance of ℓ and m .

Table 7-1 Spherical harmonics

| | | |
|------------|----------|---|
| $\ell = 0$ | $m = 0$ | $Y_{00} = \sqrt{\frac{1}{4\pi}}$ |
| $\ell = 1$ | $m = 1$ | $Y_{11} = -\sqrt{\frac{3}{8\pi}} \sin \theta e^{i\phi}$ |
| | $m = 0$ | $Y_{10} = \sqrt{\frac{3}{4\pi}} \cos \theta$ |
| | $m = -1$ | $Y_{1-1} = \sqrt{\frac{3}{8\pi}} \sin \theta e^{-i\phi}$ |
| $\ell = 2$ | $m = 2$ | $Y_{22} = \sqrt{\frac{15}{32\pi}} \sin^2 \theta e^{2i\phi}$ |
| | $m = 1$ | $Y_{21} = -\sqrt{\frac{15}{8\pi}} \sin \theta \cos \theta e^{i\phi}$ |
| | $m = 0$ | $Y_{20} = \sqrt{\frac{5}{16\pi}} (3 \cos^2 \theta - 1)$ |
| $\ell = 3$ | $m = -1$ | $Y_{3-1} = \sqrt{\frac{15}{8\pi}} \sin \theta \cos \theta e^{-i\phi}$ |
| | $m = -2$ | $Y_{3-2} = \sqrt{\frac{15}{32\pi}} \sin^2 \theta e^{-2i\phi}$ |

Quantization of the Angular Momentum

The definition of the angular momentum \mathbf{L} of a mass m moving with velocity \mathbf{v} , hence momentum \mathbf{p} , at some location \mathbf{r} relative to the origin, given in most introductory physics textbooks, is

$$\mathbf{L} = \mathbf{r} \times \mathbf{p}$$

where the momentum $\mathbf{p} = m(d\mathbf{r}/dt)$. In cases where $V = V(r)$, such as the electron in the hydrogen atom, \mathbf{L} is conserved (see Problem 7-15) and the classical motion of the mass m lies in a fixed plane perpendicular to \mathbf{L} , which contains the coordinate origin. The momentum \mathbf{p} has components (in that plane) \mathbf{p}_r along \mathbf{r} and \mathbf{p}_t perpendicular to \mathbf{r} , as illustrated in Figure 7-3, whose magnitudes are given by

$$p_r = \mu \left(\frac{dr}{dt} \right) \quad \text{and} \quad p_t = \mu r \left(\frac{dA}{dt} \right)$$

and the magnitude of the conserved (i.e., constant) vector \mathbf{L} is

$$L = rp \sin A = rp_t$$

The kinetic energy can be written in terms of these components as

$$\frac{p^2}{2\mu} = \frac{p_r^2 + p_t^2}{2\mu} = \frac{p_r^2}{2\mu} + \frac{L^2}{2\mu r^2}$$

from which the classical total energy E is given by

$$\frac{p_r^2}{2\mu} + \frac{L^2}{2\mu r^2} + V(r) = E \quad 7-17$$

Rewriting Equation 7-17 in terms of the “effective” potential $V_{\text{eff}}(r) = L^2/2\mu r^2 + V(r)$, as is often done, we obtain

$$\frac{p_r^2}{2\mu} + V_{\text{eff}}(r) = E \quad 7-18$$

which is identical in form to Equation 6-4, which we used as a basis for our introduction to the Schrödinger equation.

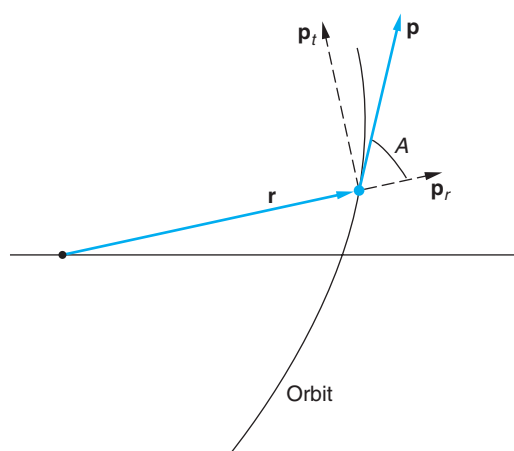


Figure 7-3 The orbit of a classical particle with $V = V(r)$ lies in a plane perpendicular to \mathbf{L} . The components of the momentum \mathbf{p} parallel and perpendicular to \mathbf{r} are \mathbf{p}_r and \mathbf{p}_t , respectively. The momentum \mathbf{p} makes an angle A with the displacement \mathbf{r} .

Equation 7-17 can be used to write the Schrödinger equation, just as we did in Chapter 6 by inserting de Broglie's relation and the appropriate differential operators in spherical coordinates for p_r^2 and L^2 . Doing so is a lengthy though not particularly difficult exercise whose details we will omit here. For p_r^2 the operator turns out to be

$$(p_r^2)_{\text{op}} = -\hbar^2 \frac{1}{r^2} \frac{\partial}{\partial r} \left(r^2 \frac{\partial}{\partial r} \right) \quad 7-19$$

which, divided by 2μ and operating on ψ , you recognize as the first term (kinetic energy) of the Schrödinger equation in spherical coordinates (Equation 7-9). Similarly, the operator for L^2 turns out to be

$$(L^2)_{\text{op}} = -\hbar^2 \left[\frac{1}{\sin \theta} \frac{\partial}{\partial \theta} \left(\sin \theta \frac{\partial}{\partial \theta} \right) + \frac{1}{\sin^2 \theta} \frac{\partial^2}{\partial \phi^2} \right] \quad 7-20$$

which, divided by $2\mu r^2$ and operating on ψ , is the second term of the Schrödinger equation in spherical coordinates (Equation 7-9). The right side of Equation 7-12, which equals $\ell(\ell + 1)$, can now be written as follows when multiplied by $\hbar^2 f(\theta)g(\phi)$, remembering that $f_{\ell m}(0)g_m(\phi) = Y_{\ell m}(\theta, \phi)$:

$$-\hbar^2 \left[\frac{1}{\sin \theta} \frac{\partial}{\partial \theta} \left(\sin \theta \frac{\partial}{\partial \theta} \right) + \frac{1}{\sin^2 \theta} \frac{\partial^2}{\partial \phi^2} \right] Y_{\ell m}(\theta, \phi) = \ell(\ell + 1) \hbar^2 Y_{\ell m}(\theta, \phi) \quad 7-21a$$

or

$$(L^2)_{\text{op}} Y_{\ell m}(\theta, \phi) = \ell(\ell + 1) \hbar^2 Y_{\ell m}(\theta, \phi) \quad 7-21b$$

or, since $\psi(r, \theta, \phi) = R(r)Y(\theta, \phi)$,

$$(L^2)_{\text{op}} \psi(r, \theta, \phi) = \ell(\ell + 1) \hbar^2 \psi(r, \theta, \phi) \quad 7-21c$$

Thus, we have the very important result that, for all potentials where $V = V(r)$, *the angular momentum is quantized* and its allowed magnitudes (eigenvalues) are given by

$$|\mathbf{L}| = L = \sqrt{\ell(\ell + 1)} \hbar \quad \text{for } \ell = 0, 1, 2, 3, \dots \quad 7-22$$

where ℓ is referred to as the *angular momentum quantum number* or the *orbital quantum number*.

In addition, if we use the same substitution method on L_z , the z component of \mathbf{L} , we find that *the z component of the angular momentum is also quantized* and its allowed values are given by

$$L_z = m\hbar \quad \text{for } m = 0, \pm 1, \pm 2, \dots, \pm \ell \quad 7-23$$

The physical significance of Equation 7-23 is that the angular momentum \mathbf{L} , whose magnitude is quantized with values $\sqrt{\ell(\ell + 1)} \hbar$, can only point in those directions *in space* such that the projection of \mathbf{L} on the z axis is one or another of the values given by $m\hbar$. Thus, \mathbf{L} is also *space quantized*. The quantum number m is referred to as the *magnetic quantum number*. (Why "magnetic"? See Section 7-4.)

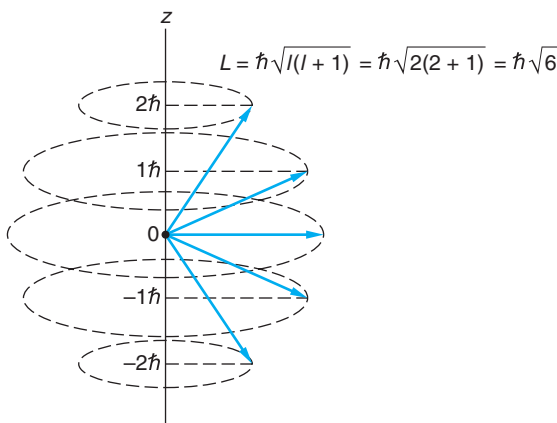


Figure 7-4 Vector model illustrating the possible orientations of \mathbf{L} in space and the possible values of L_z for the case where $\ell = 2$.

Figure 7-4 shows a diagram, called the *vector model* of the atom, illustrating the possible orientations of the angular momentum vector. Note the perhaps unexpected result that the angular momentum vector never points in the z direction, since the maximum z component $m\hbar$ is always less than the magnitude $\sqrt{\ell(\ell + 1)}\hbar$. This is a consequence of the uncertainty principle for angular momentum (which we will not derive) that implies that no two components of angular momentum can be precisely known simultaneously,⁴ except in the case of zero angular momentum. It is worth noting that *for a given value of ℓ there are $2\ell + 1$ possible values of m , ranging from $-\ell$ to $+\ell$ in integral steps.* Operators for L_x and L_y can also be obtained by the substitution method; however, operating with them on ψ does not produce eigenvalues. This is mainly because specifying rotation about the x and y axes requires measurement of both θ and ϕ .

EXAMPLE 7-1 Quantized Values of \mathbf{L} If a system has angular momentum characterized by the quantum number $\ell = 2$, what are the possible values of L_z , what is the magnitude L , and what is the smallest possible angle between \mathbf{L} and the z axis?

SOLUTION

1. The possible values of L_z are given by Equation 7-23: $L_z = m\hbar$
2. The values of m for $\ell = 2$ are $m = 0, \pm 1, \pm 2$
3. Thus, allowed values of L_z are $L_z = -2\hbar, -1\hbar, 0, \hbar, 2\hbar$
4. The magnitude of \mathbf{L} is given by Equation 7-22. For $\ell = 2$ $|\mathbf{L}| = \sqrt{\ell(\ell + 1)}\hbar = \sqrt{6}\hbar = 2.45\hbar$
5. From Figure 7-4 the angle θ between \mathbf{L} and the z axis is given by: $\cos \theta = \frac{L_z}{L} = \frac{m\hbar}{\sqrt{\ell(\ell + 1)}\hbar} = \frac{m}{\sqrt{\ell(\ell + 1)}}$
6. The smallest possible angle θ between \mathbf{L} and the z axis is that for $m = \pm \ell$, which for $\ell = 2$ gives $\cos \theta = \frac{2}{\sqrt{6}} = 0.816$ or $\theta = 35.5^\circ$

Quantization of the Energy

The results discussed so far apply to any system that is spherically symmetric, that is, one for which the potential energy depends on r only. The solution of the radial equation for $R(r)$, on the other hand, depends on the detailed form of $V(r)$. The new quantum number associated with the coordinate r is called the *principal quantum number* n . This quantum number, as we will see, is related to the energy in the hydrogen atom. Figure 7-5 shows a sketch of the potential energy function of Equation 7-6. If the total energy is positive, the electron is not bound to the atom. We are interested here only in bound-state solutions, for which the values of E are negative. For this case, the potential energy function becomes greater than E for large r , as shown in the figure. As we have discussed previously, for bound systems only certain values of the energy E lead to well-behaved solutions. These values are found by solving the radial equation, which is formed by equating the left side of Equation 7-12 to the constant $\ell(\ell + 1)$. For $V(r)$ of the hydrogen atom, given by Equation 7-6, the radial equation is

$$-\frac{\hbar^2}{2\mu r^2} \frac{\partial}{\partial r} \left(r^2 \frac{\partial R(r)}{\partial r} \right) + \left[-\frac{kZe^2}{r} + \frac{\hbar^2 \ell(\ell + 1)}{2\mu r^2} \right] R(r) = ER(r) \quad 7-24$$

The radial equation can be solved using standard methods of differential equations whose details we will omit here, except to note that (1) we expect a link to appear between the principal quantum number n and the angular momentum quantum number ℓ (since the latter already appears in Equation 7-24) and (2) in order that the solutions of Equation 7-24 be well behaved, only certain values of the energy are allowed, just as we discovered for the square well and the harmonic oscillator. The allowed values of E are given by

$$E_n = -\left(\frac{kZe^2}{\hbar}\right)^2 \frac{\mu}{2n^2} = -\frac{Z^2 E_1}{n^2} \quad 7-25$$

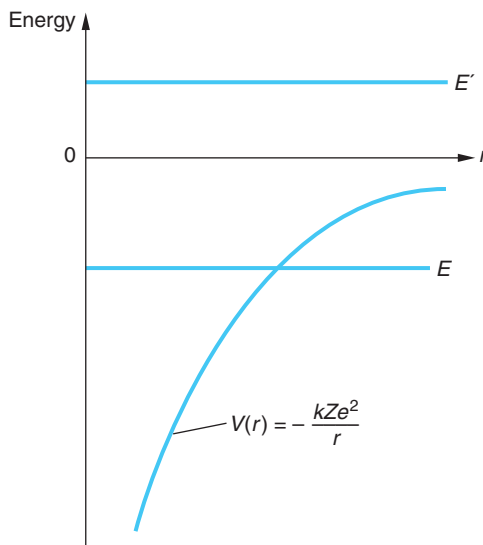


Figure 7-5 Potential energy of an electron in a hydrogen atom. If the total energy is greater than zero, as E' , the electron is not bound and the energy is not quantized. If the total energy is less than zero, as E , the electron is bound. Then, as in one-dimensional problems, only certain discrete values of the total energy lead to well-behaved wave functions.

Table 7-2 Radial functions for hydrogen

| | | |
|---------|------------|---|
| $n = 1$ | $\ell = 0$ | $R_{10} = \frac{2}{\sqrt{a_0^3}} e^{-r/a_0}$ |
| $n = 2$ | $\ell = 0$ | $R_{20} = \frac{1}{\sqrt{2a_0^3}} \left(1 - \frac{r}{2a_0}\right) e^{-r/2a_0}$ |
| | $\ell = 1$ | $R_{21} = \frac{1}{2\sqrt{6a_0^3}} \frac{r}{a_0} e^{-r/2a_0}$ |
| | $\ell = 0$ | $R_{30} = \frac{2}{3\sqrt{3a_0^3}} \left(1 - \frac{2r}{3a_0} + \frac{2r^2}{27a_0^2}\right) e^{-r/3a_0}$ |
| $n = 3$ | $\ell = 1$ | $R_{31} = \frac{8}{27\sqrt{6a_0^3}} \frac{r}{a_0} \left(1 - \frac{r}{6a_0}\right) e^{-r/3a_0}$ |
| | $\ell = 2$ | $R_{32} = \frac{4}{81\sqrt{30a_0^3}} \frac{r^2}{a_0^2} e^{-r/3a_0}$ |

where $E_1 = (1/2)(ke^2/\hbar)^2\mu \approx 13.6$ eV and the principal quantum number n can take on the values $n = 1, 2, 3, \dots$, with the further restriction that n must be greater than ℓ . These energy values are identical to those found from the Bohr model. The radial functions resulting from the solution of Equation 7-24 for hydrogen are given by Equation 7-26, where the $\mathcal{L}_{n\ell}(r/a_0)$ are standard functions called Laguerre polynomials.

$$R_{n\ell}(r) = A_{n\ell} e^{-r/a_0 n} r^\ell \mathcal{L}_{n\ell}(r/a_0) \quad 7-26$$

and the Bohr radius $a_0 = \hbar^2/(ke^2\mu)$. The radial functions $R_{n\ell}(r)$ for $n = 1, 2$, and 3 are given in Table 7-2. (For a detailed solution of Equation 7-24 and an extended table of Laguerre polynomials, see Weber and Arfken, Chapter 13.)

Summary of the Quantum Numbers

The allowed values of and restrictions on the quantum numbers n , ℓ , and m associated with the variables r , θ , and ϕ are summarized as follows:

$$\begin{aligned} n &= 1, 2, 3, \dots \\ \ell &= 0, 1, 2, \dots, (n-1) \\ m &= -\ell, (-\ell+1), \dots, 0, 1, 2, \dots, +\ell \end{aligned} \quad 7-27$$

The fact that the energy of the hydrogen atom depends only on the principal quantum number n and not on ℓ is a peculiarity of the inverse-square force. It is related to the result in classical mechanics that the energy of a mass moving in an elliptical orbit in an inverse-square force field depends only on the major axis of the orbit and not on the eccentricity. The largest value of angular momentum ($\ell = n-1$) corresponds most nearly to a circular orbit, whereas a small value of ℓ corresponds to a highly eccentric orbit. (Zero angular momentum corresponds to oscillation along a line through the force center, i.e., through the nucleus, in the case of the hydrogen atom.) For central forces that do not obey an inverse-square law, the energy does depend on the angular momentum (both classically and quantum mechanically) and thus depends on both n and ℓ .

The quantum number m is related to the z component of angular momentum. Since there is no preferred direction for the z axis for any central force, the energy cannot depend on m . We will see later that if we place an atom in an external magnetic field, there is a preferred direction in space (the direction of the field) and the energy then does depend on the value of m . (This effect, called the Zeeman effect, is discussed in a More section on the Web site. See page 303.)

Figure 7-6 shows an energy-level diagram for hydrogen. This diagram is similar to Figure 4-16a except that states with the same n but different ℓ are shown separately. These states are referred to by giving the value of n along with a code letter: S stands for $\ell = 0$, P for $\ell = 1$, D for $\ell = 2$, and F for $\ell = 3$. These code letters are remnants of the spectroscopist's descriptions of various series of spectral lines as *Sharp*, *Principal*, *Diffuse*, and *Fundamental*. (For values of ℓ greater than 3, the letters follow alphabetically; thus G for $\ell = 4$, etc.) The allowed electric dipole transitions between energy levels obey the *selection rules*

$$\Delta m = 0 \quad \text{or} \quad \pm 1$$

$$\Delta \ell = \pm 1$$

7-28

That the quantum number ℓ of the atom must change by ± 1 when the atom emits or absorbs a photon results from conservation of angular momentum and the fact that the photon itself has an intrinsic angular momentum of $1 \hbar$. For the principal quantum number, Δn is unrestricted.

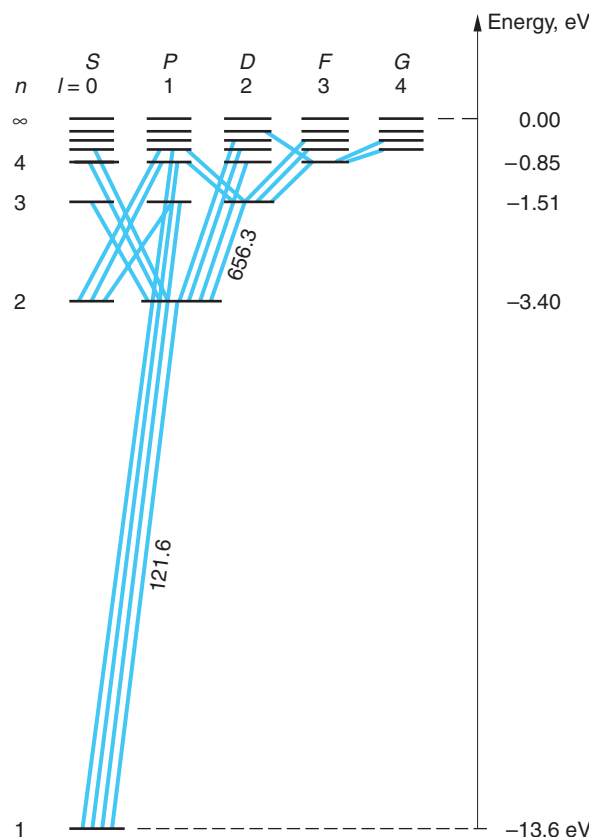


Figure 7-6 Energy-level diagram for the hydrogen atom, showing transitions obeying the selection rule $\Delta \ell = \pm 1$. States with the same n value but different ℓ value have the same energy, $-E_1/n^2$, where $E_1 = 13.6 \text{ eV}$, as in the Bohr theory. The wavelengths of the Lyman α ($n = 2 \rightarrow n = 1$) and Balmer α ($n = 3 \rightarrow n = 2$) lines are shown in nm. Note that the latter has two possible transitions due to the ℓ degeneracy.

Questions

1. Why wasn't quantization of angular momentum noticed in classical physics?
2. What are the similarities and differences between the quantization of angular momentum in the Schrödinger theory and in the Bohr model?
3. Why doesn't the energy of the hydrogen atom depend on ℓ ? Why doesn't it depend on m ?

7-3 The Hydrogen Atom Wave Functions

The wave functions $\psi_{n\ell m}(r, \theta, \phi)$ satisfying the Schrödinger equation for the hydrogen atom are rather complicated functions of r , θ , and ϕ . In this section we will write some of these functions and display some of their more important features graphically.

As we have seen, the ϕ dependence of the wave function, given by Equation 7-14, is simply $e^{im\phi}$. The θ dependence is described by the associated Legendre functions $f_{\ell m}(\theta)$ given by Equation 7-15. The complete angular dependence is then given by the spherical harmonic functions $Y_{\ell m}(\theta, \phi)$, the product of $g_m(\phi)$ and $f_{\ell m}(\theta)$ as indicated by Equation 7-16 and, for the first few, tabulated in Table 7-1. The solutions to the radial equation $R_{n\ell}(r)$ are of the form indicated by Equation 7-26 and are listed in Table 7-2 for the three lowest values of the principal quantum number n . Referring to Equation 7-10, our assumed product solutions of the time-independent Schrödinger equation, we have that the complete wave function of the hydrogen atom is

$$\psi_{n\ell m}(r, \theta, \phi) = C_{n\ell m} R_{n\ell}(r) f_{\ell m}(\theta) g_m(\phi) \quad 7-29$$

where $C_{n\ell m}$ is a constant determined by the normalization condition.

We see from the form of this expression that the complete wave function depends on the quantum numbers n , ℓ , and m that arose because of the boundary conditions on $R(r)$, $f(\theta)$, and $g(\phi)$. The energy, however, depends only on the value of n . From Equation 7-27 we see that for any value of n , there are n possible values of ℓ ($\ell = 0, 1, 2, \dots, n - 1$), and for each value of ℓ , there are $2\ell + 1$ possible values of m ($m = -\ell, -\ell + 1, \dots, +\ell$). Except for the lowest energy level (for which $n = 1$ and therefore ℓ and m can only be zero) there are generally many different wave functions corresponding to the same energy. As discussed in the previous section, the origins of this degeneracy are the $1/r$ dependence of the potential energy and the fact that there is no preferred direction in space.

The Ground State

Let us examine the wave functions for several particular states beginning with the lowest-energy level, the ground state, which has $n = 1$. Then ℓ and m must both be zero. The Laguerre polynomial L_{10} in Equation 7-26 is equal to 1, and the wave function is

$$\psi_{100} = C_{100} e^{-Zr/a_0} \quad 7-30$$

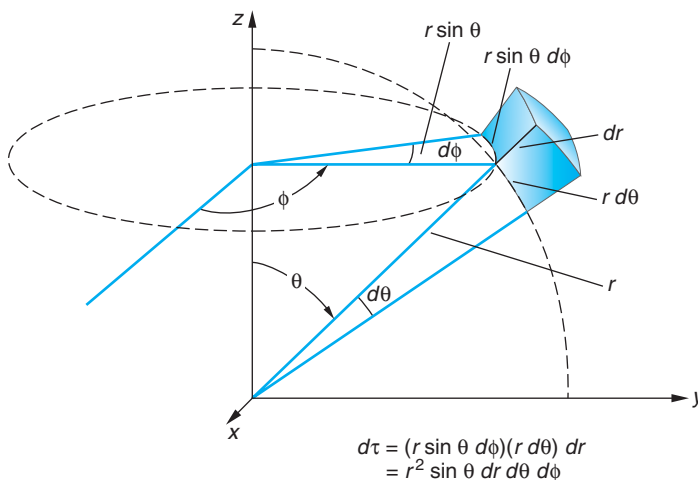


Figure 7-7 Volume element $d\tau$ in spherical coordinates.

The constant C_{100} is determined by normalization:

$$\int \psi^* \psi d\tau = \int_0^\infty \int_0^\pi \int_0^{2\pi} \psi^* \psi r^2 \sin \theta d\phi d\theta dr = 1$$

using for the volume element in spherical coordinates (see Figure 7-7)

$$d\tau = (r \sin \theta d\phi)(r d\theta)(dr)$$

Because $\psi^* \psi$ for this state is spherically symmetric, the integration over angles gives 4π . Carrying out the integration over r gives⁵

$$C_{100} = \frac{1}{\sqrt{\pi}} \left(\frac{Z}{a_0} \right)^{3/2} = \frac{1}{\sqrt{\pi}} \left(\frac{1}{a_0} \right)^{3/2} \quad \text{for } Z = 1 \quad 7-31$$

The probability of finding the electron in the volume $d\tau$ is $\psi^* \psi d\tau$.

The probability density $\psi^* \psi$ is illustrated in Figure 7-8. The probability density for the ground state is maximum at the origin. It is often of more interest to determine the probability of finding the electron in a spherical shell between r and $r + dr$. This probability, $P(r)dr$, is just the probability density $\psi^* \psi$ times the volume of the spherical shell of thickness dr :

$$P(r) dr = \psi^* \psi 4\pi r^2 dr = 4\pi r^2 C_{100}^2 e^{-2Zr/a_0} dr \quad 7-32$$

Figure 7-9 shows a sketch of $P(r)$ versus r/a_0 . It is left as a problem (see Problem 7-21) to show that $P(r)$ has its maximum value at $r = a_0/Z$. In contrast to the Bohr model for hydrogen, in which the electron stays in a well-defined orbit at $r = a_0$, we see that it is possible for the electron to be found at any distance from the nucleus.

The angular dependence of the electron probability distributions is critical to our understanding of the bonding of atoms into molecules and solids (see Chapters 9 and 10).

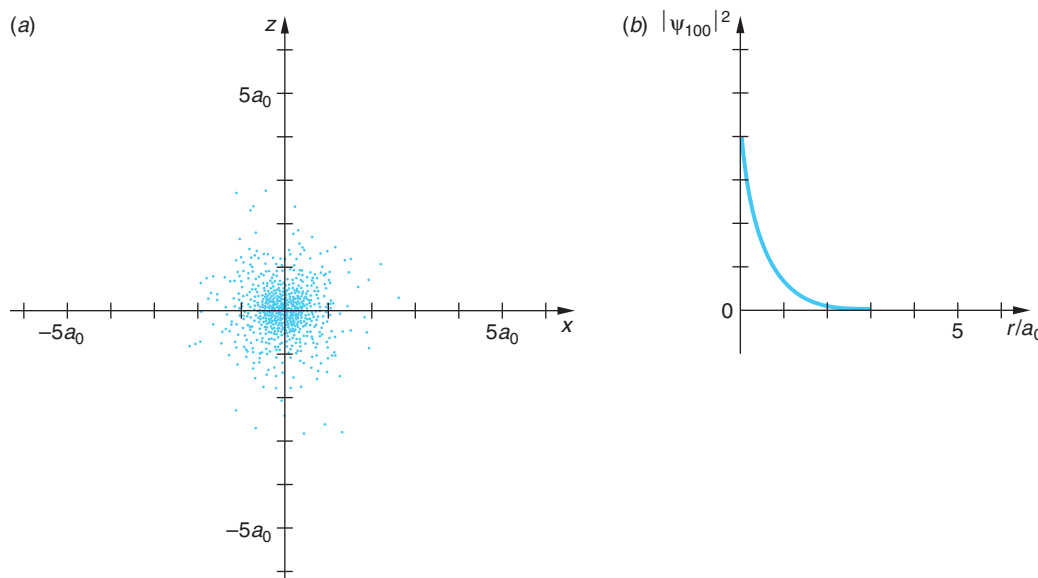


Figure 7-8 Probability density $\psi^*\psi$ for the ground state in hydrogen. The quantity $e\psi^*\psi$ can be thought of as the electron charge density in the atom. (a) The density is spherically symmetric, is greatest at the origin, and decreases exponentially with r . This computer-generated plot was made by making hundreds of “searches” for the hydrogen electron in the x - z plane (i.e., for $\phi = 0$), recording each finding with a dot. (b) The more conventional graph of the probability density $|\psi_{100}|^2$ vs. r/a_0 . Compare the two graphs carefully.

[This computer-generated plot courtesy of Paul Doherty, The Exploratorium.]

However, the most probable distance is a_0 , and the chance of finding the electron at a much different distance is small. It is useful to think of the electron as a charged cloud of charge density $\rho = e\psi^*\psi$. (We must remember, though, that the electron is always *observed* as one charge.) Note that the angular momentum in the ground state is zero, contrary to the Bohr model assumption of $1\ \hbar$.

The Excited States

In the first excited state, $n = 2$ and ℓ can be either 0 or 1. For $\ell = 0$, $m = 0$, and again we have a spherically symmetric wave function, given by

$$\psi_{200} = C_{200} \left(2 - \frac{Zr}{a_0} \right) e^{-Zr/2a_0} \quad 7-33$$

For $\ell = 1$, m can be +1, 0, or -1. The corresponding wave functions are (see Tables 7-1 and 7-2)

$$\psi_{210} = C_{210} \frac{Zr}{a_0} e^{-Zr/2a_0} \cos \theta \quad 7-34$$

$$\psi_{21\pm 1} = C_{21\pm 1} \frac{Zr}{a_0} e^{-Zr/2a_0} \sin \theta e^{\pm i\phi} \quad 7-35$$

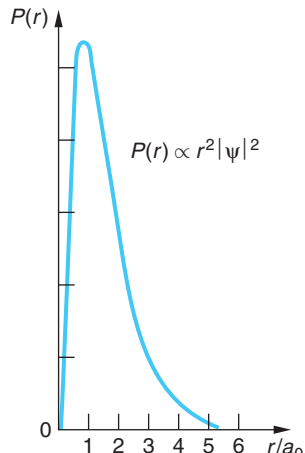


Figure 7-9 Radial probability density $P(r)$ versus r/a_0 for the ground state of the hydrogen atom. $P(r)$ is proportional to $r^2 |\psi_{100}|^2$. The most probable distance r is the Bohr radius a_0 .

Figure 7-10 (a) Radial probability density $P(r)$ vs. r/a_0 for the $n = 2$ states in hydrogen. $P(r)$ for $\ell = 1$ has a maximum at the Bohr value $2^2 a_0$. For $\ell = 0$, there is a maximum near this value and a smaller submaximum near the origin. The markers on the r/a_0 axis denote the values of $\langle r/a_0 \rangle$. (b) $P(r)$ vs. r/a_0 for the $n = 3$ states in hydrogen.

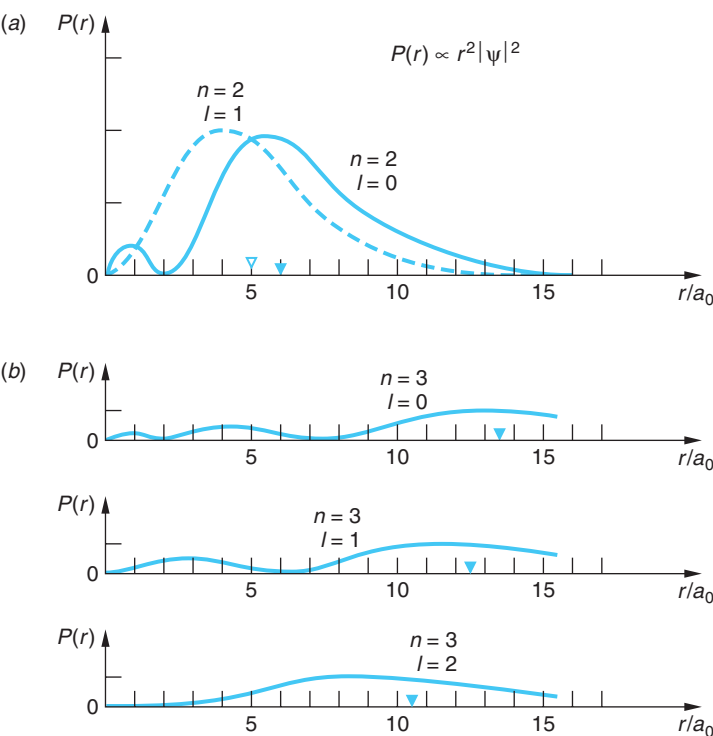


Figure 7-10a shows $P(r)$ for these wave functions. The distribution for $n = 2$, $\ell = 1$ is maximum at the radius of the second Bohr orbit,

$$r_{\max} = 2^2 a_0$$

while for $n = 2$ and $\ell = 0$, $P(r)$ has two maxima, the larger of which is near this radius.

Radial probability distributions can be obtained in the same way for the other excited states of hydrogen. For example, those for the second excited state $n = 3$ are shown in Figure 7-10b. The main radial dependence of $P(r)$ is contained in the factor e^{-Zr/na_0} , except near the origin. A detailed examination of the Laguerre polynomials shows that $\psi \rightarrow r^\ell$ as $r \rightarrow 0$. Thus, for a given n , $\psi_{n\ell m}$ is greatest near the origin when ℓ is small.

An important feature of these wave functions is that for $\ell = 0$, the probability densities are spherically symmetric, whereas for $\ell \neq 0$, they depend on the angle θ . The probability density plots of Figure 7-11 illustrate this result for the first excited state $n = 2$. These angular distributions of the electron charge density depend only on the value of ℓ and not on the radial part of the wave function. Similar charge distributions for the valence electrons in more complicated atoms play an important role in the chemistry of molecular bonding.

Question

4. At what value of r is $\psi^* \psi$ maximum for the ground state of hydrogen? Why is $P(r)$ maximum at a different value of r ?

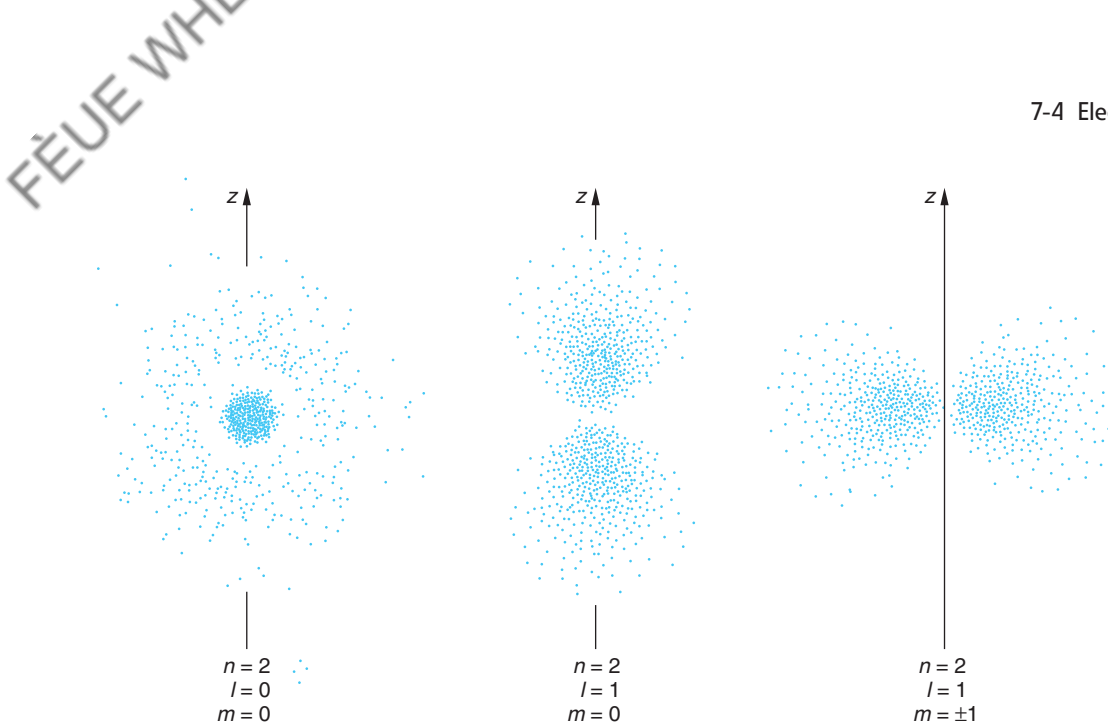


Figure 7-11 Probability densities $\psi^*\psi$ for the $n = 2$ states in hydrogen. The probability is spherically symmetric for $\ell = 0$. It is proportional to $\cos^2\theta$ for $\ell = 1, m = 0$, and to $\sin^2\theta$ for $\ell = 1, m = \pm 1$. The probability densities have rotational symmetry about the z axis. Thus, the three-dimensional charge density for the $\ell = 1, m = 0$ state is shaped roughly like a dumbbell, while that for the $\ell = 1, m = \pm 1$ states resembles a doughnut, or toroid. The shapes of these distributions are typical for all atoms in S states ($\ell = 0$) and P states ($\ell = 1$) and play an important role in molecular bonding. [This computer-generated plot courtesy of Paul Doherty, The Exploratorium.]

7-4 Electron Spin

As was mentioned in Chapter 4, when a spectral line of hydrogen or other atoms is viewed with high resolution, it shows a *fine structure*; that is, it is seen to consist of two or more closely spaced lines. As we noted then, Sommerfeld's relativistic calculation based on the Bohr model agrees with the experimental measurements of this fine structure for hydrogen, but the agreement turned out to be accidental since his calculation predicts fewer lines than are seen for other atoms. In order to explain fine structure and to clear up a major difficulty with the quantum-mechanical explanation of the periodic table (Section 7-6), W. Pauli⁶ in 1925 suggested that in addition to the quantum numbers n , ℓ , and m , the electron has a fourth quantum number, which could take on just two values.

As we have seen, quantum numbers arise from boundary conditions on some coordinate (see Equations 7-14 and 7-15). Pauli originally expected that the fourth quantum number would be associated with the time coordinate in a relativistic theory, but this idea was not pursued. In the same year, S. Goudsmit and G. Uhlenbeck,⁷ graduate students at Leiden, suggested that this fourth quantum number was the z component, m_s , of an intrinsic angular momentum of the electron, euphemistically called *spin*. They represented the spin vector \mathbf{S} with the same form that Schrödinger's wave mechanics gave for \mathbf{L} :

$$|\mathbf{S}| = S = \sqrt{s(s+1)}\hbar \quad 7-36$$

Since this intrinsic spin angular momentum \mathbf{S} is described by a quantum number s like the orbital angular momentum quantum number ℓ , we expect $2s + 1$ possible values of the z component just as there are $2\ell + 1$ possible z components of the orbital angular momentum \mathbf{L} . If m_s is to have only two values, as Pauli had suggested, then s could only be $\frac{1}{2}$ and m_s only $\pm \frac{1}{2}$. In addition to explaining fine structure and the periodic table, this proposal of electron spin explained the unexpected results of an interesting experiment that had been performed by O. Stern and W. Gerlach in 1922, which is described briefly in an Exploring section later on (see pages 288–289). To understand why the electron spin results in the splitting of the energy levels needed to account for the fine structure, we must consider the connection between the angular momentum and the magnetic moment of any charged particle system.

Magnetic Moment

If a system of charged particles is rotating, it has a *magnetic moment* proportional to its angular momentum. This result is sometimes known as the *Larmor theorem*. Consider a particle of mass M and charge q moving in a circle of radius r with speed v and frequency $f = v/2\pi r$; this constitutes a current loop. The angular momentum of the particle is $L = Mvr$. The magnetic moment of the current loop is the product of the current and the area of the loop. For a circulating charge, the current is the charge times the frequency,

$$i = qf = \frac{qv}{2\pi r} \quad 7-37$$

and the magnetic moment μ is⁸

$$\mu = iA = q\left(\frac{v}{2\pi r}\right)(\pi r^2) = \frac{1}{2}q\left(\frac{L}{M}\right) \quad 7-38$$

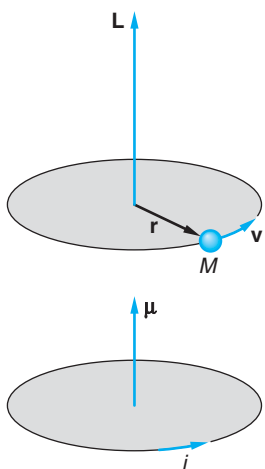


Figure 7-12 A particle moving in a circle has angular momentum \mathbf{L} . If the particle has a positive charge, the magnetic moment due to the current is parallel to \mathbf{L} .

From Figure 7-12 we see that, if q is positive, the magnetic moment is in the same direction as the angular momentum. If q is negative, μ and \mathbf{L} point in opposite directions; i.e., they are antiparallel. This enables us to write Equation 7-38 as a vector equation:

$$\mu = \frac{q}{2M}\mathbf{L} \quad 7-39$$

Equation 7-39, which we have derived for a single particle moving in a circle, also holds for a system of particles in any type of motion if the charge-to-mass ratio q/M is the same for each particle in the system.

Applying this result to the *orbital* motion of the electron in the hydrogen atom and substituting the magnitude of \mathbf{L} from Equation 7-22, we have for the magnitude of μ

$$\mu = \frac{e}{2m_e}L = \frac{e\hbar}{2m_e}\sqrt{\ell(\ell + 1)} = \sqrt{\ell(\ell + 1)}\mu_B \quad 7-40$$

and, from Equation 7-23, a z component of

$$\mu_z = -\frac{e\hbar}{2m_e}m = -m\mu_B \quad 7-41$$

where m_e is the mass of the electron, $m\hbar$ is the z component of the angular momentum, and μ_B is a natural unit of magnetic moment called the *Bohr magneton*, which has the value

$$\begin{aligned}\mu_B &= \frac{e\hbar}{2m_e} = 9.27 \times 10^{-24} \text{ joule/tesla} \\ &= 5.79 \times 10^{-9} \text{ eV/gauss} = 5.79 \times 10^{-5} \text{ eV/tesla}\end{aligned}\quad 7-42$$

The proportionality between μ and \mathbf{L} is a general property of rotating charge distributions; however, the particular relation expressed by Equation 7-39 is for a single charge q rotating in a circle. To allow the same mathematical form to be used for other, more complicated situations, it is customary to express the magnetic moment in terms of μ_B and a dimensionless quantity g called the *gyromagnetic ratio*, or simply the *g factor*, where the value of g is determined by the details of the charge distribution. In the case of the orbital angular momentum \mathbf{L} of the electron, $g_L = 1$ and Equation 7-39 would be written

$$\mu = \frac{-g_L \mu_B \mathbf{L}}{\hbar} \quad 7-43$$

and Equations 7-40 and 7-41 as

$$\mu = \sqrt{\ell(\ell + 1)} g_L \mu_B \quad 7-44$$

$$\mu_z = -mg_L \mu_B \quad 7-45$$

There are minus signs in Equations 7-43 and 7-45 because the electron has a negative charge. The magnetic moment and the angular momentum vectors associated with the orbital motion are therefore oppositely directed, and we see that *quantization of angular momentum implies quantization of magnetic moments*. Other magnetic moments and g factors that we will encounter will have the same form.

Finally, the behavior of a system with a magnetic moment in a magnetic field can be visualized by considering a small bar magnet (Figure 7-13). When placed in an external magnetic field \mathbf{B} there is a torque $\tau = \mu \times \mathbf{B}$ that tends to align the magnet with the field \mathbf{B} . If the magnet is spinning about its axis, the effect of the torque is to make the spin axis precess about the direction of the external field, just as a spinning top or gyroscope precesses about the direction of the gravitational field.

To change the orientation of the magnet relative to the applied field direction (whether or not it is spinning), work must be done on it. If it moves through angle $d\theta$, the work required is

$$dW = \tau d\theta = \mu B \sin \theta d\theta = d(-\mu B \cos \theta) = d(-\mu \cdot \mathbf{B})$$

The potential energy of the magnetic moment μ in the magnetic field \mathbf{B} can thus be written

$$U = -\mu \cdot \mathbf{B} \quad 7-46$$

If \mathbf{B} is in the z direction, the potential energy is

$$U = -\mu_z B \quad 7-47$$

The orbital motion and spin of the electrons are the origin of magnetism in metals, such as iron, cobalt, and nickel (see Chapter 10). Devices ranging from giant electricity transformers to decorative refrigerator magnets rely on these quantum properties of electrons.

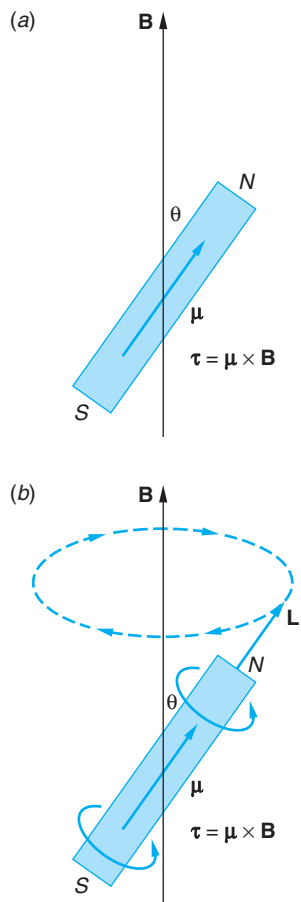


Figure 7-13 Bar-magnet model of magnetic moment. (a) In an external magnetic field, the moment experiences a torque that tends to align it with the field. If the magnet is spinning (b), the torque causes the system to precess around the external field.

Applying these arguments to the *intrinsic spin* of the electron results in the predictions (with $s = \frac{1}{2}$)

$$\mu = \sqrt{s(s+1)}\mu_B = \sqrt{\frac{3}{4}}\mu_B \quad \text{and} \quad \mu_z = m_s\mu_B = \pm\frac{1}{2}\mu_B \quad 7-48$$

Since the atomic electron is in a magnetic field arising from the apparent motion of the nuclear charge around the electron, the two values of m_s correspond to two different energies, according to Equation 7-47. *It is this splitting of the energy levels that results in the fine structure of the spectral lines.*

The restriction of the spin, and hence the intrinsic magnetic moment, to two orientations in space with $m_s = \pm\frac{1}{2}$ is another example of space quantization. The magnitude of the magnetic moment due to the spin angular momentum can be determined from quantitative measurement of the deflection of the beam in a Stern-Gerlach experiment. The result is *not* $\frac{1}{2}$ Bohr magneton, as predicted by Equation 7-41 with $m = m_s = \frac{1}{2}$, but twice this value. (This type of experiment is not an accurate way to measure magnetic moments, although the measurement of angular momentum this way is accurate because that involves simply counting the number of lines.) The g factor for the electron, g_s in Equation 7-49, has been precisely measured to be $g_s = 2.002319$.

$$\mu_z = -m_s g_s \mu_B \quad 7-49$$

This result, and the fact that s is a half integer rather than an integer like the orbital quantum number ℓ , makes it clear that the classical model of the electron as a spinning ball is not to be taken literally. Like the Bohr model of the atom, the classical picture is useful in describing results of quantum-mechanical calculations, and it often gives useful guidelines as to what to expect from an experiment. The phenomenon of spin, while not a part of Schrödinger's wave mechanics, is included in the relativistic wave mechanics formulated by Dirac. In its nonrelativistic limit, Dirac's wave equation predicts $g_s = 2$, which is approximately correct. The exact value of g_s is correctly predicted by *quantum electrodynamics* (QED), the relativistic quantum theory that describes the interaction of electrons with electromagnetic fields. Although beyond the scope of our discussions, QED is arguably the most precisely tested theory in physics.



EXPLORING

Stern-Gerlach Experiment

If a magnetic moment μ is placed in an *inhomogeneous* external magnetic field \mathbf{B} , the μ will feel an external force that depends on μ_z and the gradient of \mathbf{B} . This is because the force \mathbf{F} is the negative gradient of the potential, so

$$\mathbf{F} = -\nabla U = -\nabla(-\mu \cdot \mathbf{B}) \quad 7-50$$

from Equation 7-46. If we arrange the inhomogeneous \mathbf{B} field so that it is homogeneous in the x and y directions, then the gradient has only $\partial B / \partial z \neq 0$ and \mathbf{F} has only a z component, i.e.,

$$F_z = \mu_z (dB/dz) = -mg_L \mu_B (dB/dz) \quad 7-51$$

This effect was used by Stern and Gerlach⁹ in 1922 (before spin) to measure the possible orientations in space, i.e., the space quantization, of the magnetic moments of silver atoms. The experiment was repeated in 1927 (after spin) by Phipps and Taylor using hydrogen atoms.

The experimental setup is shown in Figure 7-14. Atoms from an oven are collimated and sent through a magnet whose poles are shaped so that the magnetic field B_z increases slightly with z , while B_x and B_y are constant in the x and y directions, respectively. The atoms then strike a collector plate. Figure 7-15 illustrates the effect of the dB/dz on several magnetic moments of different orientations. In addition to the torque, which merely causes the magnetic moment to precess about the field direction, there is the force F_z in the positive or negative z direction, depending on whether μ_z is positive or negative, since dB/dz is always positive. This force deflects the magnetic moment up or down by an amount that depends on the magnitudes of both dB/dz and the z component of the magnetic moment μ_z . Classically, one would expect a continuum of possible orientations of the magnetic moments. However, since the magnetic moment is proportional to \mathbf{L} , which is quantized, quantum mechanics predicts that μ_z also can have only the $2\ell + 1$ values corresponding to the $2\ell + 1$ possible values of m . We therefore expect $2\ell + 1$ deflections (counting 0 as a deflection). For example, for $\ell = 0$ there should be one line on the collector plate corresponding to no deflection, and for $\ell = 1$ there should be three lines corresponding to the three values $m = -1$, $m = 0$, and $m = +1$. The $\ell = 1$ case is illustrated in Figure 7-15.

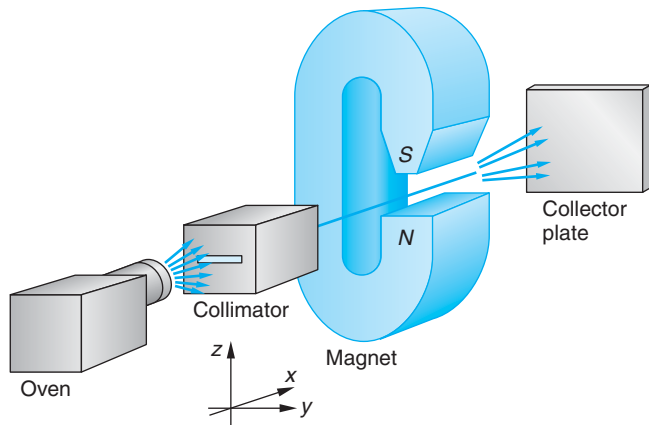


Figure 7-14 In the Stern-Gerlach experiment, atoms from an oven are collimated, passed through an inhomogeneous magnetic field, and detected on a collector plate.

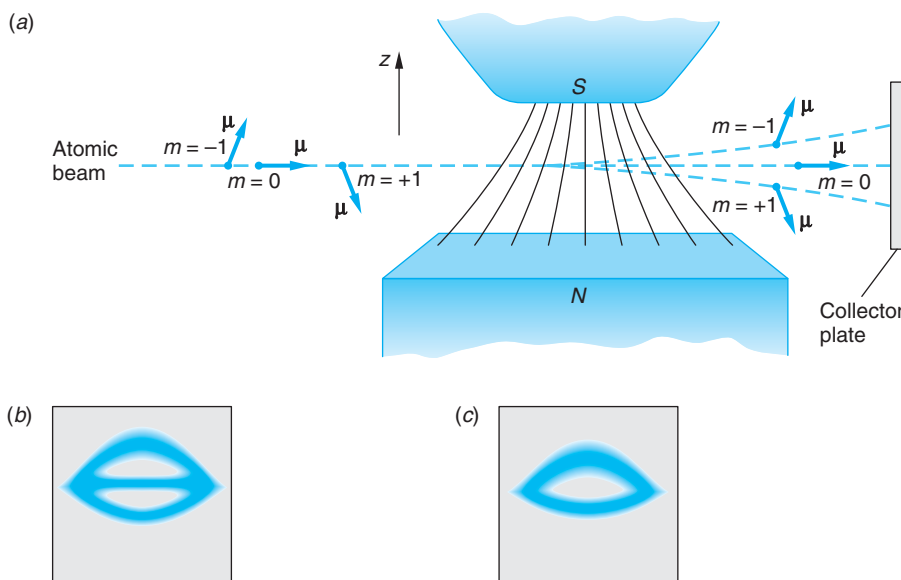


Figure 7-15 (a) In an inhomogeneous magnetic field the magnetic moment μ experiences a force F_z whose direction depends on the direction of the z component μ_z of μ and whose magnitude depends on those of μ_z and dB/dz . The beam from an oven (not shown) is collimated into a horizontal line. (b) The pattern for the $\ell = 1$ case illustrated in (a). The three images join at the edges and have different detailed shapes due to differences in the field inhomogeneity. (c) The pattern observed for silver and hydrogen.

Using neutral silver atoms, Stern and Gerlach expected to see only a single line, the middle line in Figure 7-15b, because the ground state of silver was known to be an $\ell = 0$ state; therefore, $m = 0$ and $\mu = 0$. The force F_z would then be zero, and no deflection of the atomic beam should occur. However, when the experiment was done with either silver or hydrogen atoms, there were *two* lines, as shown in Figure 7-15c. Since the ground state of hydrogen also has $\ell = 0$, we should again expect only one line, were it not for the electron spin. If the electron has spin angular momentum of magnitude $|S| = \sqrt{s(s+1)}\hbar$, where $s = \frac{1}{2}$, the z component can be either $+\hbar/2$ or $-\hbar/2$. Since the orbital angular momentum is zero, the total internal angular momentum of the atom is simply the spin¹⁰ and two lines would be expected. Stern and Gerlach had made the first direct observation of electron spin and space quantization.

The Complete Hydrogen Atom Wave Functions

Our description of the hydrogen atom wave functions in Section 7-3 is not complete because we did not include the spin of the electron. The hydrogen atom wave functions are also characterized by the spin quantum number m_s , which can be $+\frac{1}{2}$ or $-\frac{1}{2}$. (We need not include the quantum number s because it always has the value $s = \frac{1}{2}$.) A general wave function is then written $\psi_{n\ell m_\ell m_s}$, where we have included the subscript ℓ on m_ℓ to distinguish it from m_s . There are now two wave functions for the ground state of the hydrogen atom, $\psi_{100+1/2}$ and $\psi_{100-1/2}$, corresponding to an atom with its electron spin “parallel” or “antiparallel” to the z axis (as defined, for example, by a external magnetic field). In general, the ground state of a hydrogen atom is a linear combination of these wave functions:

$$\psi = C_1 \psi_{100+1/2} + C_2 \psi_{100-1/2}$$

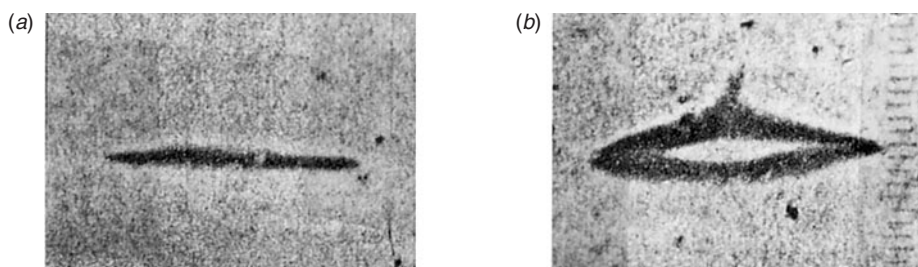
The probability of measuring $m_s = +\frac{1}{2}$ (for example, by observing to which spot the atom goes in the Stern-Gerlach experiment) is $|C_1|^2$. Unless atoms have been preselected in some way (such as by passing them through a previous inhomogeneous magnetic field or by their having recently emitted a photon), $|C_1|^2$ and $|C_2|^2$ will each be $\frac{1}{2}$, so that measuring the spin “up” ($m_s = +\frac{1}{2}$) and measuring the spin “down” ($m_s = -\frac{1}{2}$) are equally likely.

Questions

5. Does a system have to have a net charge to have a magnetic moment?
6. Consider the two beams of hydrogen atoms emerging from the magnetic field in the Stern-Gerlach experiment. How does the wave function for an atom in one beam differ from that of an atom in the other beam? How does it differ from the wave function for an atom in the incoming beam before passing through the magnetic field?

Photographs made by Stern and Gerlach with an atomic beam of silver atoms.

- (a) When the magnetic field is zero, all atoms strike in a single, undeviated line.
 (b) When the magnetic field is nonzero, the atoms strike in upper and lower lines, curved due to differing inhomogeneities. [From O. Stern and W. Gerlach, *Zeitschr. f. Physik* **9**, 349 (1922).]



7-5 Total Angular Momentum and the Spin-Orbit Effect

In general, an electron in an atom has both orbital angular momentum characterized by the quantum number ℓ and spin angular momentum characterized by the quantum number s . Analogous classical systems that have two kinds of angular momentum are Earth, which is spinning about its axis of rotation in addition to revolving about the Sun, or a precessing gyroscope, which has angular momentum of precession in addition to its spin. Classically the total angular momentum

$$\mathbf{J} = \mathbf{L} + \mathbf{S} \quad 7-52$$

is an important quantity because the resultant torque on a system equals the rate of change of the total angular momentum, and in the case of central forces, the total angular momentum is conserved. For a classical system, the magnitude of the total angular momentum J can have any value between $L + S$ and $|L - S|$. We have already seen that in quantum mechanics, angular momentum is more complicated: both \mathbf{L} and \mathbf{S} are quantized and their relative directions are restricted. The quantum-mechanical rules for combining orbital and spin angular momenta or any two angular momenta (such as for two particles) are somewhat difficult to derive, but they are not difficult to understand. For the case of orbital and spin angular momenta, the magnitude of the total angular momentum \mathbf{J} is given by

$$|\mathbf{J}| = \sqrt{j(j+1)}\hbar \quad 7-53$$

where the *total angular momentum quantum number* j can be either

$$j = \ell + s \quad \text{or} \quad j = |\ell - s| \quad 7-54$$

and the z component of \mathbf{J} is given by

$$J_z = m_j \hbar \quad \text{where} \quad m_j = -j, -j+1, \dots, j-1, j \quad 7-55$$

(If $\ell = 0$, the total angular momentum is simply the spin, and $j = s$.) Figure 7-16a is a simplified vector model illustrating the two possible combinations $j = 1 + \frac{1}{2} = \frac{3}{2}$ and $j = 1 - \frac{1}{2} = \frac{1}{2}$ for the case of an electron with $\ell = 1$. The lengths of the vectors are proportional to $[\ell(\ell+1)]^{1/2}$, $[s(s+1)]^{1/2}$, and $[j(j+1)]^{1/2}$. The spin and orbital angular momentum vectors are said to be “parallel” when $j = \ell + s$ and “antiparallel” when $j = |\ell - s|$. A quantum mechanically more accurate vector addition is shown in Figure 7-16b. The quantum number m_j can take on $2j + 1$ possible values in integer steps between $-j$ and $+j$, as indicated by Equation 7-55. Equation 7-55 also implies that $m_j = m_\ell + m_s$ since $J_z = L_z + S_z$.

Equation 7-54 is a special case of a more-general rule for combining two angular momenta that is useful when dealing with more than one particle. For example, there are two electrons in the helium atom, each with spin, orbital, and total angular momentum. The general rule is

If \mathbf{J}_1 is one angular momentum (orbital, spin, or a combination) and \mathbf{J}_2 is another, the resulting total angular momentum $\mathbf{J} = \mathbf{J}_1 + \mathbf{J}_2$ has the value $[j(j+1)]^{1/2}\hbar$ for its magnitude, where j can be any of the values

$$j_1 + j_2, j_1 + j_2 - 1, \dots, |j_1 - j_2|$$

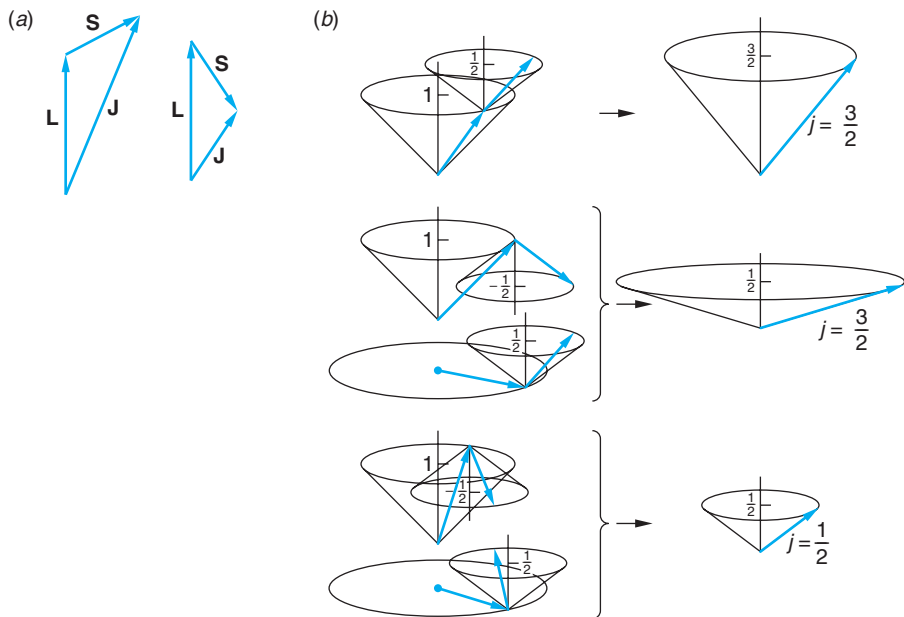


Figure 7-16 (a) Simplified vector model illustrating the addition of orbital and spin angular momenta. The case shown is for $\ell = 1$ and $s = \frac{1}{2}$. There are two possible values of the quantum number for the total angular momentum: $j = \ell + s = \frac{3}{2}$ and $j = \ell - s = \frac{1}{2}$. (b) Vector addition of the orbital and spin angular momenta, also for the case $\ell = 1$ and $s = \frac{1}{2}$. According to the uncertainty principle, the vectors can lie anywhere on the cones, corresponding to the definite values of their z components. Note in the middle sketch that there are two ways of forming the states with $j = \frac{3}{2}$, $m_j = \frac{1}{2}$ and $j = \frac{1}{2}$, $m_j = \frac{1}{2}$.

EXAMPLE 7-2 Addition of Angular Momenta I Two electrons each have zero orbital angular momentum. What are the possible quantum numbers for the total angular momentum of the two-electron system? (For example, these could be the He atom electrons in any of the S states.)

SOLUTION

In this case $j_1 = j_2 = \frac{1}{2}$. The general rule then gives two possible results, $j = 1$ and $j = 0$. These combinations are commonly called parallel and antiparallel, respectively.

EXAMPLE 7-3 Addition of Angular Momenta II An electron in an atom has orbital angular momentum \mathbf{L}_1 with quantum number $\ell_1 = 2$, and a second electron has orbital angular momentum \mathbf{L}_2 with quantum number $\ell_2 = 3$. What are the possible quantum numbers for the total orbital angular momentum $\mathbf{L} = \mathbf{L}_1 + \mathbf{L}_2$?

SOLUTION

Since $\ell_1 + \ell_2 = 5$ and $|\ell_1 - \ell_2| = 1$, the possible values of ℓ are 5, 4, 3, 2, and 1.

Spectroscopic Notation



Spectroscopic notation, a kind of shorthand developed in the early days of spectroscopy to condense information and simplify the description of transitions between states, has since been adopted for general use in atomic, molecular, nuclear, and

particle physics. The notation code appears to be arbitrary,¹¹ but it is easy to learn and, as you will discover, convenient to use. For single electrons we have:

1. For single-electron states the letter code $s\ p\ d\ f\ g\ h\dots$ is used in one-to-one correspondence with the values of the orbital angular momentum quantum number $\ell : 0\ 1\ 2\ 3\ 4\ 5\dots$. For example, an electron with $\ell = 2$ is said to be a d electron or in a d state.
2. The single-electron (Bohr) energy levels are called *shells*, labeled $K\ L\ M\ N\ O\dots$ in one-to-one correspondence with the values of the principal quantum number $n : 1\ 2\ 3\ 4\ 5\dots$. For example, an electron with $n = 3$ in an atom is said to be in the M shell. (This notation is less commonly used.)

For atomic states that may contain one or more electrons, the notation includes the principal quantum number and the angular momenta quantum numbers. The total orbital angular momentum quantum number is denoted by a capital letter in the same sequence as in rule 1 above, i.e., $S\ P\ D\ F\dots$ correspond to ℓ values $0\ 1\ 2\ 3\dots$. The value of n is written as a prefix and the value of the total angular momentum quantum number j by a subscript. The magnitude of the total spin quantum number s appears as a left superscript in the form $2s + 1$.¹² Thus, a state with $\ell = 1$, a P state, would be written as

$$n^{2s+1}P_j$$

For example, the ground state of the hydrogen atom ($n = 1$, $\ell = 0$, $s = 1/2$) is written $1^2S_{1/2}$, read “one doublet S one-half.” The $n = 2$ state can have $\ell = 0$ or $\ell = 1$, so the spectroscopic notation for these states is $2^2S_{1/2}$, $2^2P_{3/2}$, and $2^2P_{1/2}$. (The principal quantum number and spin superscript are sometimes not included if they are not needed in specific situations.)

Spin-Orbit Coupling

Atomic states with the same n and ℓ values but different j values have slightly different energies because of the interaction of the spin of the electron with its orbital motion. This is called the *spin-orbit effect*. The resulting splitting of the spectral lines such as the one that results from the splitting of the $2P$ level in the transition $2P \rightarrow 1S$ in hydrogen is called *fine-structure splitting*. We can understand the spin-orbit effect qualitatively from a simple Bohr model picture, as shown in Figure 7-17. In this picture, the electron moves in a circular orbit with speed v around a fixed proton. In the figure, the orbital angular momentum \mathbf{L} is up. In the frame of reference of the electron, the proton moves in a circle around it, thus constituting a circular loop current that produces a magnetic field \mathbf{B} at the position of the electron. The direction of \mathbf{B} is also up, parallel to \mathbf{L} . Recall that the potential energy of a magnetic moment in a magnetic field depends on its orientation relative to the field direction and is given by

$$U = -\boldsymbol{\mu} \cdot \mathbf{B} = -\mu_z B \quad 7-56$$

The potential energy is lowest when the magnetic moment is parallel to \mathbf{B} and highest when it is antiparallel. Since the intrinsic magnetic moment of the electron is directed opposite to its spin (because the electron has a negative charge), the spin-orbit energy is highest when the spin is parallel to \mathbf{B} and thus to \mathbf{L} . The energy of the $2P_{3/2}$ state in

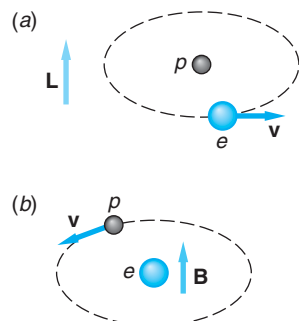
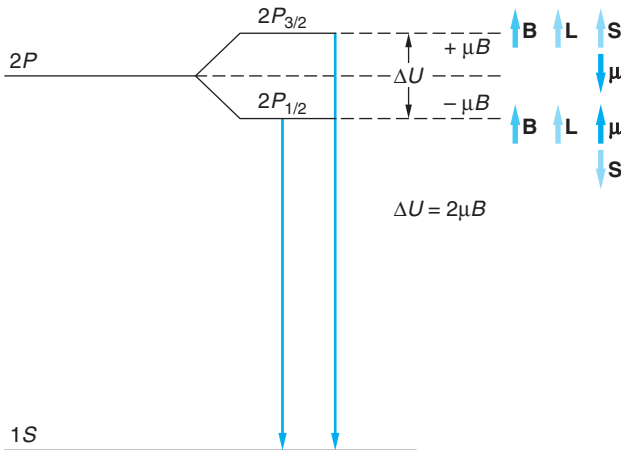


Figure 7-17 (a) An electron moving about a proton with angular momentum \mathbf{L} up. (b) The magnetic field \mathbf{B} seen by the electron due to the apparent (relative) motion of the proton is also up. When the electron spin is parallel to \mathbf{L} , the magnetic moment is antiparallel to \mathbf{L} and \mathbf{B} , so the spin-orbit energy has its largest value.

Figure 7-18 Fine-structure energy-level diagram.

On the left, the levels in the absence of a magnetic field are shown. The effect of the magnetic field due to the relative motion of the nucleus is shown on the right. Because of the spin-orbit interaction, the magnetic field splits the $2P$ level into two energy levels, with the $j = \frac{3}{2}$ level having slightly greater energy than the $j = \frac{1}{2}$ level. The spectral line due to the transition $2P \rightarrow 1S$ is therefore split into two lines of slightly different wavelengths. (Diagram is not to scale.)



hydrogen, in which \mathbf{L} and \mathbf{S} are parallel, is therefore slightly higher than the $2P_{1/2}$ state, in which \mathbf{L} and \mathbf{S} are antiparallel (Figure 7-18).¹³ The measured splitting is about 4.5×10^{-5} eV for the $2P_{1/2}$ and $2P_{3/2}$ levels in hydrogen. For other atoms, the fine-structure splitting is larger than this. For example, for sodium it is about 2×10^{-3} eV, as will be discussed in Section 7-7. Recalling that transitions resulting in spectral lines in the visible region are of the order of 1.5 to 3.0 eV, you can see that the fine-structure splitting is quite small.

EXAMPLE 7-4 **Fine-Structure Splitting** The fine-structure splitting of the $2P_{3/2}$ and $2P_{1/2}$ levels in hydrogen is 4.5×10^{-5} eV. From this, estimate the magnetic field that the $2p$ electron in hydrogen experiences. Assume \mathbf{B} is parallel to the z axis.

SOLUTION

- The energy of the $2p$ electrons is shifted in the presence of a magnetic field by an amount given by Equation 7-56:
$$U = -\boldsymbol{\mu} \cdot \mathbf{B} = -\mu_z B$$
- U is positive or negative depending on the relative orientation of $\boldsymbol{\mu}$ and \mathbf{B} , so the total energy difference ΔE between the two levels is:
$$\Delta E = 2U = 2\mu_z B$$
- Since the magnetic moment of the electron is μ_B , $\mu_z \approx \mu_B$ and
$$\Delta E \approx 2\mu_B B$$
- Solving this for B substituting for μ_B and the energy splitting ΔE gives
$$B \approx \frac{\Delta E}{2\mu_B}$$

$$\approx \frac{4.5 \times 10^{-5} \text{ eV}}{(2)(5.79 \times 10^{-5} \text{ eV/T})}$$

$$\approx 0.39 \text{ T}$$

Remarks: This is a substantial magnetic field, nearly 10,000 times Earth's average magnetic field.

When an atom is placed in an *external* magnetic field \mathbf{B} , the total angular momentum \mathbf{J} is quantized in space relative to the direction of \mathbf{B} and the energy of the atomic state characterized by the angular momentum quantum number j is split into $2j + 1$ energy levels corresponding to the $2j + 1$ possible values of the z component of \mathbf{J} and therefore to the $2j + 1$ possible values of the z component of the total magnetic moment. This splitting of the energy levels in the atom gives rise to a splitting of the spectral lines emitted by the atom. The splitting of the spectral lines of an atom placed in an external magnetic field was discovered by P. Zeeman and is known as the *Zeeman effect*. (See the second More section on page 303 and Section 3-1.) Zeeman and Lorentz shared the Nobel Prize in Physics for the discovery and explanation of the Zeeman effect.

7-6 The Schrödinger Equation for Two (or More) Particles

Our discussion of quantum mechanics so far has been limited to situations in which a single particle moves in some force field characterized by a potential energy function V . The most important physical problem of this type is the hydrogen atom, in which a single electron moves in the Coulomb potential of the proton nucleus. This problem is actually a two-body problem, as the proton also moves in the Coulomb potential of the electron. However, as in classical mechanics, we can treat this as a one-body problem by considering the proton to be at rest and replacing the electron mass with the reduced mass. When we consider more complicated atoms we must face the problem of applying quantum mechanics to two or more electrons moving in an external field. Such problems are complicated by the interaction of the electrons with each other and also by the fact that the electrons are identical.

The interaction of the electrons with each other is electromagnetic and essentially the same as that expected classically for two charged particles. The Schrödinger equation for an atom with two or more electrons cannot be solved exactly, and approximation methods must be used. This is not very different from the situation in classical problems with three or more particles. The complication arising from the identity of electrons is purely quantum mechanical and has no classical counterpart.

The indistinguishability of identical particles has important consequences related to the *Pauli exclusion principle*. We will illustrate the origin of this important principle in this section by considering the simple case of two noninteracting identical particles in a one-dimensional infinite square well.

The time-independent Schrödinger equation for two particles of mass m is

$$-\frac{\hbar^2}{2m} \frac{\partial^2 \psi(x_1, x_2)}{\partial x_1^2} - \frac{\hbar^2}{2m} \frac{\partial^2 \psi(x_1, x_2)}{\partial x_2^2} + V\psi(x_1, x_2) = E\psi(x_1, x_2) \quad 7-57$$

where x_1 and x_2 are the coordinates of the two particles. If the particles are interacting, the potential energy V contains terms with both x_1 and x_2 , which cannot usually be separated. For example, if the particles are charged, their mutual electrostatic potential energy (in one dimension) is $+ke^2/|x_2 - x_1|$. If they do not interact, however, we can write V as $V_1(x_1) + V_2(x_2)$. For the case of an infinite square well potential, we need solve the Schrödinger equation only inside the well where $V = 0$ and require the wave function to be zero at the walls of the well. Solutions of Equation 7-57 can be written as products of single-particle solutions and linear combinations of such solutions.

The single-particle product solutions are

$$\psi_{nm}(x_1, x_2) = \psi_n(x_1)\psi_m(x_2) \quad 7-58$$

where $\psi_n(x_1)$ and $\psi_m(x_2)$ are the single-particle wave functions for an infinite square well given by Equation 6-32. Thus, for $n = 1$ and $m = 2$,

$$\psi_{12} = C \sin \frac{\pi x_1}{L} \sin \frac{2\pi x_2}{L} \quad 7-59$$

The probability of finding particle 1 in dx_1 and particle 2 in dx_2 is $|\psi(x_1, x_2)|^2 dx_1 dx_2$, which is just the product of the separate probabilities $|\psi(x_1)|^2 dx_1$ and $|\psi(x_2)|^2 dx_2$. However, even though we have labeled the particles 1 and 2, if they are identical, we cannot distinguish which is in dx_1 and which is in dx_2 . For identical particles, therefore, we must construct the wave function so that the probability density is the same if we interchange the labels:

$$|\psi(x_1, x_2)|^2 = |\psi(x_2, x_1)|^2 \quad 7-60$$

Equation 7-60 holds if $\psi(x_1, x_2)$ is either symmetric or antisymmetric on exchange of particles—that is,

$$\psi(x_2, x_1) = +\psi(x_1, x_2) \quad \text{symmetric}$$

$$\psi(x_2, x_1) = -\psi(x_1, x_2) \quad \text{antisymmetric}$$

We note that the general wave function of the form of Equation 7-58 and the example (Equation 7-59) are neither symmetric nor antisymmetric. If we interchange x_1 and x_2 , we get a different wave function, implying that the particles can be distinguished. These forms are thus *not* consistent with the indistinguishability of identical particles. However, from among all of the possible linear combination solutions of the single product functions, we see that, if ψ_{nm} and ψ_{mn} are added or subtracted, we form symmetric or antisymmetric wave functions necessary to preserve the indistinguishability of the two particles:

$$\psi_S = C[\psi_n(x_1)\psi_m(x_2) + \psi_n(x_2)\psi_m(x_1)] \quad \text{symmetric}$$

$$\psi_A = C[\psi_n(x_1)\psi_m(x_2) - \psi_n(x_2)\psi_m(x_1)] \quad \text{antisymmetric}$$

Pauli Exclusion Principle

There is an important difference between the antisymmetric and symmetric combinations. If $n = m$, the antisymmetric wave function is identically zero for all x_1 and x_2 , whereas the symmetric function is not. More generally, it is found that electrons (and many other particles, including protons and neutrons) can only have antisymmetric *total* wave functions, that is

$$\Psi_{n\ell m_\ell m_s} = R_{n\ell} Y_{\ell m_\ell} X_{m_s} \quad 7-61$$

where $R_{n\ell}$ is the radial wave function, $Y_{\ell m_\ell}$ is the spherical harmonic, and X_{m_s} is the spin wave function. Thus, single-particle wave functions such as $\psi_n(x_1)$ and $\psi_m(x_1)$ for two such particles cannot have exactly the same set of values for the quantum numbers.

This is an example of the *Pauli exclusion principle*. For the case of electrons in atoms and molecules, four quantum numbers describe the state of each electron, one for each space coordinate and one associated with spin. The Pauli exclusion principle for electrons states that

No more than one electron may occupy a given quantum state specified by a particular set of single-particle quantum numbers n, ℓ, m_ℓ, m_s .

The effect of the exclusion principle is to exclude certain states in the many-electron system. It is an additional quantum condition imposed on solutions of the Schrödinger equation. It will be applied to the development of the periodic table in the following section. Particles such as α particles, deuterons, photons, and mesons have symmetric wave functions and do not obey the exclusion principle.

7-7 Ground States of Atoms: The Periodic Table

We now consider qualitatively the wave functions and energy levels for atoms more complicated than hydrogen. As we have mentioned, the Schrödinger equations for atoms other than hydrogen cannot be solved exactly because of the interaction of the electrons with one another, so approximate methods must be used. We will discuss the energies and wave functions for the ground states of atoms in this section and consider the excited states and spectra for some of the less complicated cases in the following section. We can describe the wave function for a complex atom in terms of single-particle wave functions. By neglecting the interaction energy of the electrons, that description can be simplified to products of the single-particle wave functions. These wave functions are similar to those of the hydrogen atom and are characterized by the quantum numbers n, ℓ, m_ℓ, m_s . The energy of an electron is determined mainly by the quantum numbers n (which is related to the radial part of the wave function) and ℓ (which characterizes the orbital angular momentum). Generally, the lower the value of n and ℓ , the lower the energy of the state. (See Figure 7-19.) The specification of n and ℓ for each electron in an atom is called the *electron configuration*. Customarily, the value of ℓ and the various electron shells are specified with the same code defined in the subsection “Spectroscopic Notation” (page 292) in Section 7-5. The electron configurations of the atomic ground states are given in Appendix C.

The Ground States of the Atoms

Helium ($Z = 2$) The energy of the two electrons in the helium atom consists of the kinetic energy of each electron, a potential energy of the form $-kZe^2/r_i$ for each electron corresponding to its attraction to the nucleus, and a potential energy of interaction V_{int} corresponding to the mutual repulsion of the two electrons. If \mathbf{r}_1 and \mathbf{r}_2 are the position vectors for the two electrons, V_{int} is given by

$$V_{\text{int}} = +\frac{ke^2}{|\mathbf{r}_2 - \mathbf{r}_1|} \quad 7-62$$

Because this interaction term contains the position variables of the two electrons, its presence in the Schrödinger equation prevents the separation of the equation into separate equations for each electron. If we neglect the interaction term, however, the

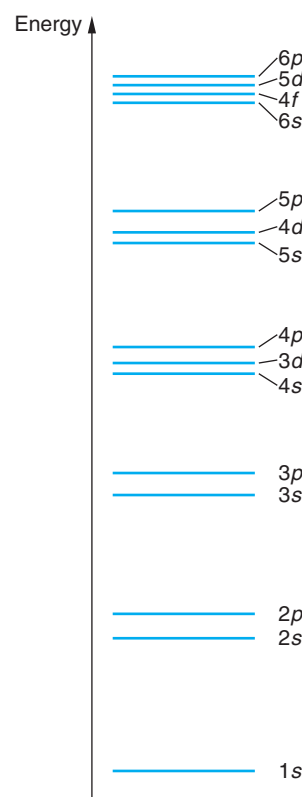


Figure 7-19 Relative energies of the atomic shells and subshells.

Schrödinger equation can be separated and solved exactly. We then obtain separate equations for each electron, with each equation identical to that for the hydrogen atom except that $Z = 2$. The allowed energies are then given by

$$E = -\frac{Z^2 E_0}{n_1^2} - \frac{Z^2 E_0}{n_2^2} \quad \text{where } E_0 = 13.6 \text{ eV} \quad 7-63$$

The lowest energy, $E_1 = -2(2)^2 E_0 \approx -108.8$ eV, occurs for $n_1 = n_2 = 1$. For this case, $\ell_1 = \ell_2 = 0$. The total wave function, neglecting the spin of the electrons, is of the form

$$\psi = \psi_{100}(r_1, \theta_1, \phi_1) \psi_{100}(r_2, \theta_2, \phi_2) \quad 7-64$$

The quantum numbers n , ℓ , and m_ℓ can be the same for the two electrons only if the fourth quantum number m_s is different, i.e., if one electron has $m_s = +\frac{1}{2}$ and the other has $m_s = -\frac{1}{2}$. The resulting total spin of the two electrons must therefore be zero.

We can obtain a first-order correction to the ground-state energy by using the approximate wave function of Equation 7-64 to calculate the average value of the interaction energy V_{int} , which is simply the expectation value $\langle V_{\text{int}} \rangle$. The result of this calculation is

$$\langle V_{\text{int}} \rangle = +34 \text{ eV} \quad 7-65$$

With this correction, the ground-state energy is

$$E \approx -108.8 + 34 = -74.8 \text{ eV} \quad 7-66$$

This approximation method, in which we neglect the interaction of the electrons to find an approximate wave function and then use this wave function to calculate the interaction energy, is called *first-order perturbation theory*. The approximation can be continued to higher orders: for example, the next step is to use the new ground-state energy to find a correction to the ground-state wave function. This approximation method is similar to that used in classical mechanics to calculate the orbits of the planets about the Sun. In the first approximation the interaction of the planets is neglected and the elliptical orbits are found for each planet. Then, using this result for the position of each planet, the perturbing effects of the nearby planets can be calculated.

The experimental value of the energy needed to remove both electrons from the helium atom is about 79 eV. The discrepancy between this result and the value 74.8 eV is due to the inaccuracy of the approximation used to calculate $\langle V_{\text{int}} \rangle$, as indicated by the rather large value of the correction (about 30 percent). (It should be pointed out that there are better methods of calculating the interaction energy for helium that give much closer agreement with experiment.) The helium *ion* He^+ , formed by removing one electron, is identical to the hydrogen atom except that $Z = 2$; so the ground-state energy is

$$-Z^2(13.6) = -54.4 \text{ eV}$$

The energy needed to remove the first electron from the helium atom is 24.6 eV. The corresponding potential, 24.6 V, is called the *first ionization potential* of the atom. The ionization energies are given in Appendix C.

The configuration of the ground state of the helium atom is written $1s^2$. The 1 signifies $n = 1$, the s signifies $\ell = 0$, and the 2 signifies that there are two electrons in this state. Since ℓ can only be zero for $n = 1$, the two electrons fill the K shell ($n = 1$).

Lithium ($Z = 3$) Lithium has three electrons. Two are in the K shell ($n = 1$), but the third cannot have $n = 1$ because of the exclusion principle. The next-lowest energy state for this electron has $n = 2$. The possible ℓ values are $\ell = 1$ or $\ell = 0$.

In the hydrogen atom, these ℓ values have the same energy because of the degeneracy associated with the inverse-square nature of the force. This is not true in lithium and other atoms because the charge “seen” by the outer electron is not a point charge.¹⁴ The positive charge of the nucleus $+Ze$ can be considered to be approximately a point charge, but the negative charge of the K shell electrons $-2e$ is spread out in space over a volume whose radius is of the order of a_0/Z . We can in fact take for the charge density of each inner electron $\rho = -e|\psi|^2$, where ψ is a hydrogenlike $1s$ wave function (neglecting the interaction of the two electrons in the K shell). The probability distribution for the outer electron in the $2s$ or $2p$ states is similar to that shown in Figure 7-10. We see that the probability distribution in both cases has a large maximum well outside the inner K -shell electrons but that the $2s$ distribution also has a small bump near the origin. We could describe this by saying that the electron in the $2p$ state is nearly always outside the shielding of the two $1s$ electrons in the K shell so that it sees an effective central charge of $Z_{\text{eff}} \approx 1$, whereas in the $2s$ state the electron penetrates this “shielding” more often and therefore sees a slightly larger effective positive central charge. The energy of the outer electron is therefore lower in the $2s$ state than in the $2p$ state, and the lowest energy configuration of the lithium atom is $1s^22s$.

The total angular momentum of the electrons in this atom is $\frac{1}{2}\hbar$ due to the spin of the outer electron since each of the electrons has zero orbital angular momentum and the inner K -shell electrons are paired to give zero spin. The first ionization potential for lithium is only 5.39 V. We can use this result to calculate the effective positive charge seen by the $2s$ electron. For $Z = Z_{\text{eff}}$ and $n = 2$, we have

$$E = \frac{Z^2 E_0}{n^2} = \frac{Z_{\text{eff}}^2 (13.6 \text{ eV})}{2^2} = 5.39 \text{ eV}$$

which gives $Z_{\text{eff}} \approx 1.3$. It is generally true that the smaller the value of ℓ , the greater the penetration of the wave function into the inner shielding cloud of electrons: The result is that in a multielectron atom, *for given n, the energy of the electron increases with increasing ℓ* . (See Figure 7-19.)

Beryllium ($Z = 4$) The fourth electron has the least energy in the $2s$ state. The exclusion principle requires that its spin be antiparallel to the other electron in this state so that the total angular momentum of the four electrons in this atom is zero. The electron configuration of beryllium is $1s^22s^2$. The first ionization potential is 9.32 V. This is greater than that for lithium because of the greater value of Z .

Boron to Neon ($Z = 5$ to $Z = 10$) Since the $2s$ subshell is filled, the fifth electron must go into the $2p$ subshell; that is, $n = 2$ and $\ell = 1$. Since there are three possible values of m_ℓ (+1, 0, and -1) and two values of m_s for each, there can be up to six electrons in this subshell. The electron configuration for boron is $1s^22s^22p$. Although it might be expected that boron would have a greater ionization potential than beryllium because of the greater Z , the $2p$ wave function penetrates the shielding of the core electrons to a lesser extent and the ionization potential of boron is actually about 8.3 V, slightly less than that of beryllium. The electron configuration of the elements carbon ($Z = 6$) to neon ($Z = 10$) differs from boron only by the number of electrons in the $2p$ subshell. The ionization potential increases slightly with Z for these elements, reaching the value of 21.6 V for the last element in the group, neon. Neon has the



George Gamow and Wolfgang Pauli in Switzerland in 1930.
[Courtesy of George Gamow.]

maximum number of electrons allowed in the $n = 2$ shell. The electron configuration of neon is $1s^22s^22p^6$. Because of its very high ionization potential, neon, like helium, is chemically inert. The element just before this, fluorine, has a “hole” in this shell; that is, it has room for one more electron. It readily combines with elements such as lithium, which has one outer electron that is donated to the fluorine atom to make an F^- ion and a Li^+ ion, which bond together. This is an example of ionic bonding, to be discussed in Chapter 9.

Sodium to Argon ($Z = 11$ to $Z = 18$) The eleventh electron must go into the $n = 3$ shell. Since this electron is weakly bound in the Na atom, Na combines readily with atoms such as F. The ionization potential for sodium is only 5.14 V. Because of the lowering of the energy due to penetration of the electronic shield formed by the other 10 electrons—similar to that discussed for Li—the $3s$ state is lower than the $3p$ or $3d$ states. (With $n = 3$, ℓ can have the values 0, 1, or 2.) This energy difference between subshells of the same n value becomes greater as the number of electrons increases. The configuration of Na is thus $1s^22s^22p^63s$. As we move to higher-Z elements, the $3s$ subshell and then the $3p$ subshell begin to fill up. These two subshells can accommodate $2 + 6 = 8$ electrons. The configuration of argon ($Z = 18$) is $1s^22s^22p^63s^23p^6$. There is another large energy difference between the eighteenth and nineteenth electrons, and argon, with its full $3p$ subshell, is stable and inert.

Atoms with $Z > 18$ One might expect that the nineteenth electron would go into the $3d$ subshell, but the shielding or penetration effect is now so strong that the energy is lower in the $4s$ shell than in the $3d$ shell. The nineteenth electron in potassium ($Z = 19$) and the twentieth electron in calcium ($Z = 20$) go into the $4s$ rather than the $3d$ subshell. The electron configurations of the next 10 elements, scandium ($Z = 21$) through zinc ($Z = 30$), differ only in the number of electrons in the $3d$ subshell except for chromium ($Z = 24$) and copper ($Z = 29$), each of which has only one $4s$ electron. These elements are called *transition elements*. Since their chemical properties are mainly due to their $4s$ electrons, they are quite similar chemically.

Figure 7-20 shows a plot of the first ionization potential of an atom versus Z up to $Z = 90$. The sudden decrease in ionization potential after the Z numbers 2, 10, 18, 36, 54, and 86 marks the closing of a shell or subshell. A corresponding sudden increase occurs in the atomic radii, as illustrated in Figure 7-21. The ground-state electron configurations of the elements are tabulated in Appendix C.

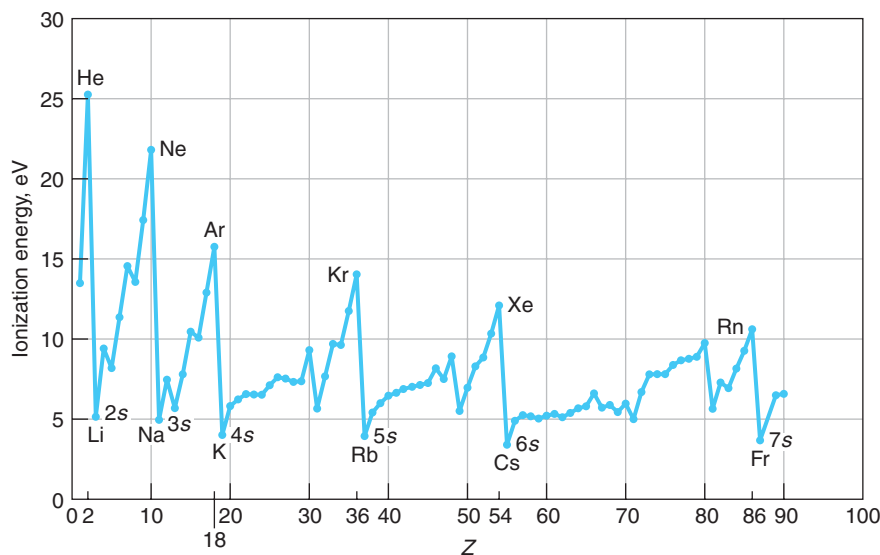


Figure 7-20 First ionization energy vs. Z up to $Z = 90$. The energy is the binding energy of the last electron in the atom. This energy increases with Z until a shell is closed at Z values of 2, 10, 18, 36, 54, and 86. The next electron must go into the next higher shell and hence is farther from the center of core charge and thus less tightly bound. The ionization potential (in volts) is numerically equal to the ionization energy (in eV).

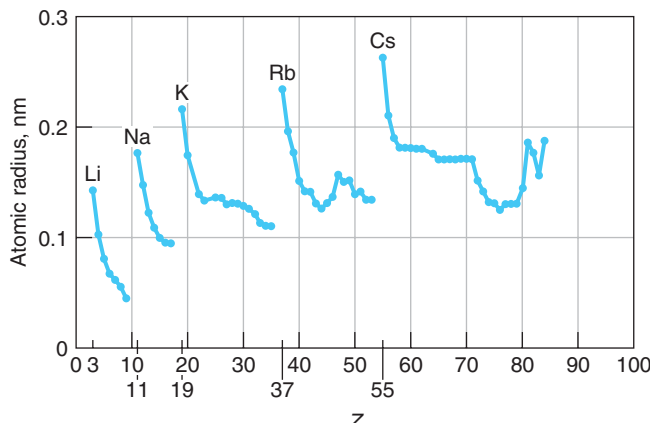


Figure 7-21 The atomic radii versus Z shows a sharp rise following the completion of a shell as the next electron must have the next larger n . The radii then decline with increasing Z , reflecting the penetration of wave functions of the electrons in the developing shell. The recurring patterns here and in Figure 7-20 are examples of the behavior of many atomic properties that give the periodic table its name.

Questions

- Why is the energy of the $3s$ state considerably lower than that of the $3p$ state for sodium, whereas in hydrogen these states have essentially the same energy?
- Discuss the evidence from the periodic table of the need for a fourth quantum number. How would the properties of He differ if there were only three quantum numbers, n , ℓ , and m ?

The concept of shell structure for the electrons in the atomic systems was a significant aid to the later understanding of molecular bonding (see Chapter 9) and the complex structure of the atomic nuclei (see Chapter 11).

7-8 Excited States and Spectra of Atoms

Alkali Atoms

In order to understand atomic spectra, we need to understand the excited states of atoms. The situation for an atom with many electrons is, in general, much more complicated than that of hydrogen. An excited state of the atom usually involves a change in the state of one of the electrons or more rarely two or even more electrons. Even in the case of the excitation of only one electron, the change in state of this electron changes the energies of the others. Fortunately, there are many cases in which this effect is negligible, and the energy levels can be calculated accurately from a relatively simple model of one electron plus a stable core. This model works particularly well for the alkali metals: Li, Na, K, Rb, and Cs. These elements are in the first column of the periodic table. The optical spectra of these elements are similar in many ways to the spectrum of hydrogen.

Another simplification is possible because of the wide difference between excitation energy of a core electron and the excitation energy of an outer electron. Consider the case of sodium, which has a neon core (except $Z = 11$ rather than $Z = 10$) and an outer $3s$ electron. If this electron did not penetrate the core, it would see an effective nuclear charge of $Z_{\text{eff}} = 1$ resulting from the $+11e$ nuclear charge and the $-10e$ of the completed electron shells. The ionization energy would be the same as the energy of the $n = 3$ electron in hydrogen, about 1.5 eV. Penetration into the core increases Z_{eff} and so lowers the energy of the outer electron, i.e., binds it more tightly, thereby increasing the ionization energy. The measured ionization energy of sodium is about 5 eV. The energy needed to remove one of the outermost core electrons, a $2p$ electron, is about 31 eV, whereas that needed to remove one of the $1s$ electrons is about 1041 eV.

Among the many applications of atomic spectra is their use in answering questions about the composition of stars and the evolution of the universe (see Chapter 13).

An electron in the inner core cannot be excited to any of the filled $n = 2$ states because of the exclusion principle. Thus, the minimum excitation of an $n = 1$ electron is to the $n = 3$ shell, which requires an energy only slightly less than that needed to remove this electron completely from the atom. Since the energies of photons in the visible range (about 400 to 800 nm) vary only from about 1.5 to 3 eV, the optical (*i.e.*, visible) spectrum of sodium must be due to transitions involving only the outer electron. Transitions involving the core electrons produce line spectra in the ultraviolet and x-ray regions of the electromagnetic spectrum.

Figure 7-22 shows an energy-level diagram for the optical transitions in sodium. Since the spin angular momentum of the neon core adds up to zero, the spin of each state in sodium is $\frac{1}{2}$. Because of the spin-orbit effect, the states with $j = \ell - \frac{1}{2}$ have a slightly lower energy than those with $j = \ell + \frac{1}{2}$. Each state is therefore a doublet (except for the S states). The doublet splitting is very small and is not evident on the energy scale of Figure 7-22 but is shown in Figure 7-18. The states are labeled by the usual spectroscopic notation, with the superscript 2 before the letter indicating that the state is a doublet. Thus, $^2P_{3/2}$, read as “doublet P three-halves,” denotes a state

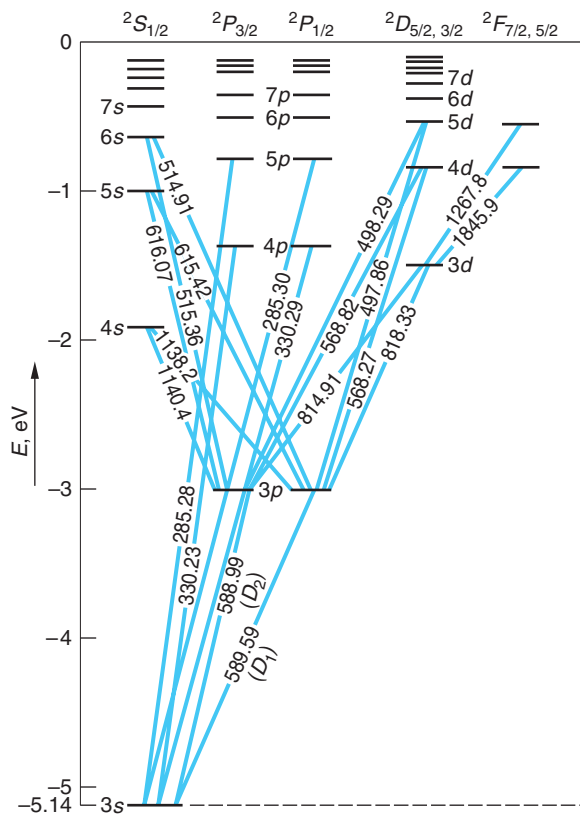


Figure 7-22 Energy-level diagram for sodium (Na) with some transitions indicated. Wavelengths shown are in nanometers. The spectral lines labeled D_1 and D_2 are very intense and are responsible for the yellow color of lamps containing sodium. The energy splittings of the D and F levels, also doublets, are not shown.

in which $\ell = 1$ and $j = \frac{3}{2}$. (The S states are customarily labeled as if they were doublets even though they are not. This is done because they belong to the set of levels with $S = \frac{1}{2}$ but, unlike the others, have $\ell = 0$ and are thus not split. The number indicating the n value of the electron is often omitted.) In the first excited state, the outer electron is excited from the $3s$ level to the $3p$ level, which is about 2.1 eV above the ground state. The spin-orbit energy difference between the $P_{3/2}$ and $P_{1/2}$ states due to the spin-orbit effect is about 0.002 eV. Transitions from these states to the ground state give the familiar sodium yellow doublet

$$\begin{aligned} 3p(^2P_{1/2}) &\rightarrow 3s(^2S_{1/2}) & \lambda &= 589.6 \text{ nm} \\ 3p(^2P_{3/2}) &\rightarrow 3s(^2S_{1/2}) & \lambda &= 589.0 \text{ nm} \end{aligned}$$

The energy levels and spectra of other alkali atoms are similar to those for sodium.

It is important to distinguish between doublet energy states and doublet spectral lines. All transitions beginning or ending on an S state give double lines because they involve one doublet state and one singlet state (the selection rule $\Delta\ell = \pm 1$ rules out transitions between two S states). There are four possible energy differences between two doublet states. One of these is ruled out by a selection rule on j , which is¹⁵

$$\Delta j = \pm 1 \text{ or } 0 \quad (\text{but no } j = 0 \rightarrow j = 0) \quad 7-67$$

Transitions between pairs of doublet energy states therefore result in three spectral lines, i.e., a triplet. Under relatively low resolution the three lines look like two, as illustrated in Figure 7-23, because two of them are very close together. For this reason, they are often referred to as a *compound doublet* to preserve the verbal hint that they involve doublet energy states.



More

Atoms with more than one electron in the outer shell have more complicated energy-level structures. Additional total spin possibilities exist for the atom, resulting in multiple sets of nearly independent energy states and multiple sets of spectral lines. *Multielectron Atoms* and their spectra are described on the home page: www.whfreeman.com/tiplermodernphysics5e. See also Equations 7-68 and 7-69 and Figures 7-24 through 7-27 here.



More

Tradition tells us that Mrs. Bohr encountered an obviously sad young Wolfgang Pauli sitting in the garden of Bohr's Institute for Theoretical Physics in Copenhagen and asked considerately if he was unhappy. His reply was, "Of course I'm unhappy! I don't understand the anomalous Zeeman effect!" On the home page we explain *The Zeeman Effect* so you, too, won't be unhappy: www.whfreeman.com/tiplermodernphysics5e. See also Equations 7-70 through 7-74 and Figures 7-28 through 7-31 here.

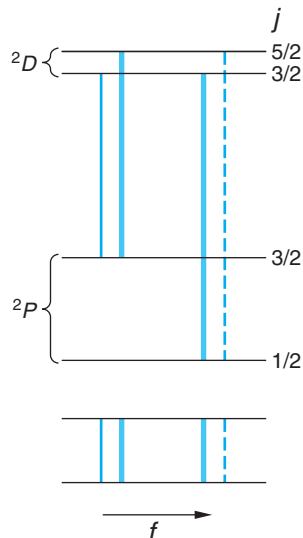


Figure 7-23 The transitions between a pair of doublet energy states in singly ionized calcium. The transition represented by the dotted line is forbidden by the $\Delta j = \pm 1, 0$ selection rule. The darkness of the lines indicates relative intensity. Under low resolution the faint line on the left of the spectrum at the bottom merges with its neighbor and the compound doublet (or triplet) looks like a doublet.



EXPLORING Frozen Light

Using the quantum properties of atomic energy states, tunable lasers, and a Bose-Einstein (BE) condensate of sodium atoms (see Chapter 8), physicists have been able to slow a light pulse to a dead stop, then regenerate it some time later and send it on its way. Here is how it's done.

Consider the $3s$ and $3p$ energy levels of sodium in Figure 7-22. L-S coupling does not cause splitting of the $3s$ state because the orbital angular momentum of that state is zero; however, we will discover in Chapter 11 (see also Problem 7-72) that protons and neutrons also have intrinsic spins and magnetic moments, resulting in a *nuclear* spin and magnetic moment. Although the latter is smaller than the electron's magnetic moment by a factor of about 1000, it causes a very small splitting of the $3s$ level exactly analogous to that due to L-S coupling in states with nonzero orbital angular momenta. Called *hyperfine structure* (because it's smaller than the fine-structure splitting discussed earlier), the $3s$ level is split into two levels spaced about 3.5×10^{-6} eV above and below the original $3s$ state.

Producing the BE condensate results in a cigar-shaped “cloud” about one centimeter long suspended by a magnetic field in a vacuum chamber. The cloud contains several million sodium atoms *all with their spins aligned and all in the lower of the two 3s hyperfine levels*, the new ground state. (See Figure 7-32a.) The light pulse that we wish to slow (the probe beam) is provided by a laser precisely tuned to the energy difference between the lower of the $3s$ hyperfine levels (the new ground state) and the $3p$ state. A second laser (the coupling beam) is precisely tuned to the energy difference between the higher of the $3s$ hyperfine levels and the $3p$ state and illuminates the BE condensate perpendicular to the probe beam.

If the probe beam alone were to enter the sample, all of the atoms would be excited to the $3p$ level, absorbing the beam completely. As the atoms relaxed back to the ground state, sodium yellow light would be emitted randomly in all directions. If the coupling beam alone entered the sample, no excitation of the $3p$ level would result because the coupling beam photons do not have enough energy to excite electrons from the ground state to the $3p$ state. However, if the coupling beam is illuminating the sample with all atoms in the ground state and the probe beam is turned on, as the leading edge of the probe pulse enters the sample (Figure 7-32b), the two beams together shift the sodium atoms into a quantum superposition of both states, meaning that in that region of the sample *each atom is in both* hyperfine states (Figure 7-32c). Instead of both beams now being able to excite those atoms to the $3p$ level, the two processes cancel, a phenomenon called *quantum interference*, and the BE condensate becomes transparent to the probe beam, as in Figure 7-32c. A similar cancellation causes the index of refraction of the sample to change very steeply over the narrow frequency range of the probe pulse, slowing the leading edge from 3×10^8 m/s to about 15 m/s. As the rest of the probe pulse (still moving at 3×10^8 m/s) enters the sample and slows, it piles up behind the leading edge, dramatically compressing the pulse to about 0.05 mm in length, which fits easily within the sample. Over the region occupied by the compressed pulse, the quantum superposition shifts the atomic spins in synchrony with the superposition, as illustrated in Figure 7-32d.

At this point the coupling beam is turned off. The BE condensate immediately becomes opaque to the probe beam; the pulse comes to a stop and turns off. The light has “frozen”! The information imprinted on the pulse is now imprinted like a hologram on the spins of the atoms in the superposition states. (See Figure 7-32e.) When the coupling pulse is again turned on, the sample again becomes transparent to the probe pulse.

The “frozen” probe pulse is regenerated carrying the original information, moves slowly to the edge of the sample, then zooms away at 3×10^8 m/s. (See Figure 7-32f.)

The ability to slow and stop light raises new opportunities in many areas. For example, it may make possible the development of quantum communications that cannot be eavesdropped upon. Building large-scale quantum computers may depend upon the ultra-high-speed switching potential of quantum superpositions in slow light systems. Astrophysicists may be able to use BE condensates in vortex states, already achieved experimentally, with slow light to simulate in the laboratory the dragging of light into black holes. Stay tuned!

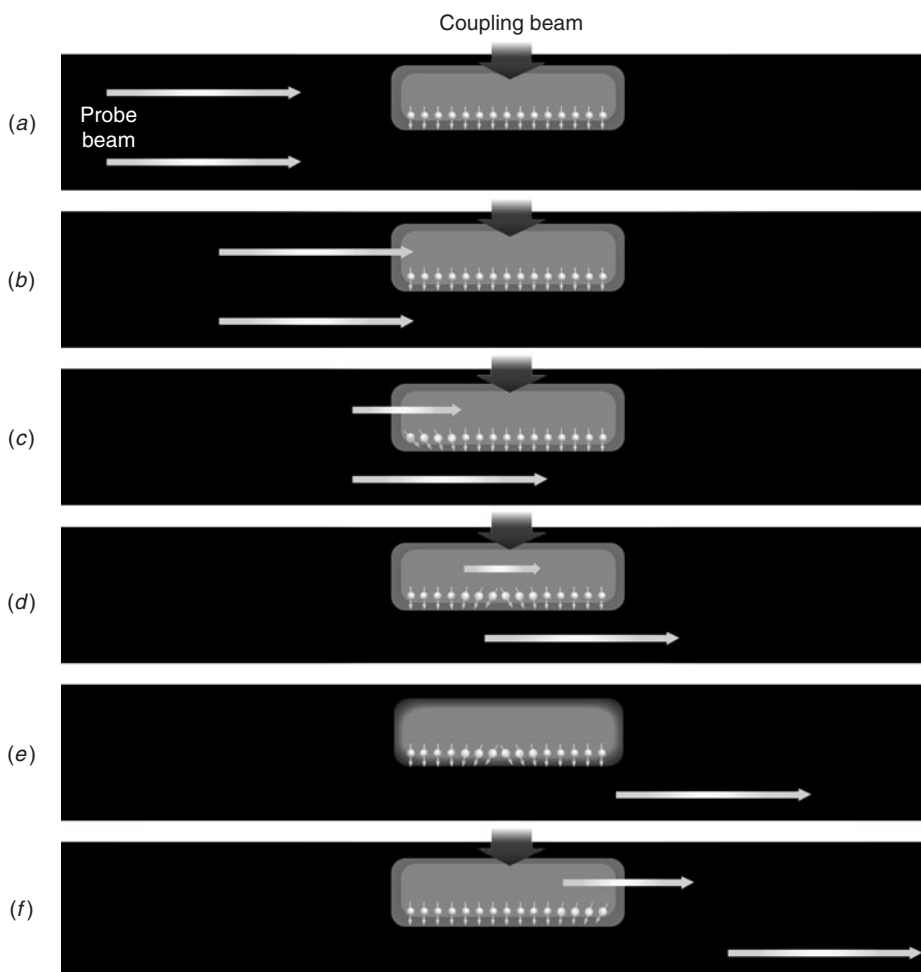


Figure 7-32 (a) The coupling beam illuminates the sodium Bose-Einstein condensate, whose atoms are in the ground state with spins aligned. (b) The leading edge of the probe beam pulse enters the sample. (c) Quantum superposition shifts the spins, and the rapidly changing refractive index dramatically slows and shortens the probe beam inside the condensate. (d) Now completely contained inside the sample, the speed of the probe pulse is about 15 m/s. (e) The coupling beam is turned off and the probe pulse stops, its information stored in the shifted spins of the atoms. (f) The coupling beam is turned back on and the probe pulse regenerates, moves slowly to the edge of the sample, then leaves at 3×10^8 m/s. [Courtesy of Samuel Velasco.]

Summary

| TOPIC | RELEVANT EQUATIONS AND REMARKS | |
|---|---|------|
| 1. Schrödinger equation in three dimensions | The equation is solved for the hydrogen atom by separating it into three ordinary differential equations, one for each coordinate r, θ, ϕ . The quantum numbers n, ℓ , and m arise from the boundary conditions to the solutions of these equations. | |
| 2. Quantization | | |
| Angular momentum | $ \mathbf{L} = \sqrt{\ell(\ell + 1)}\hbar \quad \text{for } \ell = 0, 1, 2, 3, \dots$ | 7-22 |
| z component of \mathbf{L} | $L_z = m\hbar \quad \text{for } m = 0, \pm 1, \pm 2, \dots, \pm \ell$ | 7-23 |
| Energy | $E_n = -\left(\frac{kZe^2}{\hbar}\right)^2 \frac{\mu}{2n^2} = -13.6 \frac{Z^2}{n^2} \text{ eV}$ | 7-24 |
| 3. Hydrogen wave functions | $\Psi_{n\ell m} = C_{n\ell m} R_{n\ell}(r) Y_{\ell m}(\theta, \phi)$ where $C_{n\ell m}$ are normalization constants, $R_{n\ell}$ are the radial functions, and $Y_{\ell m}$ are the spherical harmonics. | |
| 4. Electron spin | The electron spin is not included in Schrödinger's wave equation. | |
| Magnitude of \mathbf{S} | $ \mathbf{S} = \sqrt{s(s + 1)}\hbar \quad s = \frac{1}{2}$ | 7-36 |
| z component of \mathbf{S} | $S_z = m_s \hbar \quad m_s = \pm \frac{1}{2}$ | |
| Stern-Gerlach experiment | This was the first direct observation of the electron spin. | |
| 5. Spin-orbit coupling | \mathbf{L} and \mathbf{S} add to give the total angular momentum $\mathbf{J} = \mathbf{L} + \mathbf{S}$, whose magnitude is given by $ \mathbf{J} = \sqrt{j(j + 1)}\hbar$ | 7-53 |
| | where $j = \ell + s$ or $ \ell - s $. This interaction leads to the fine-structure splitting of the energy levels. | |
| 6. Exclusion principle | No more than one electron can occupy a given quantum state specified by a particular set of the single-particle quantum numbers n, ℓ, m_ℓ , and m_s . | |

General References

The following general references are written at a level appropriate for the readers of this book.

- Brehm, J. J., and W. J. Mullin, *Introduction to the Structure of Matter*, Wiley, New York, 1989.
 Eisberg, R., and R. Resnick, *Quantum Physics*, 2d ed., Wiley, New York, 1985.
 Herzberg, G., *Atomic Spectra and Atomic Structure*, Dover, New York, 1944.

- Kuhn, H. G., *Atomic Spectra*, Academic Press, New York, 1962.
 Mehra, J., and H. Rechenberg, *The Historical Development of Quantum Theory*, Vol. 1, Springer-Verlag, New York, 1982.
 Pauling, L., and S. Goudsmit, *The Structure of Line Spectra*, McGraw-Hill, New York, 1930.
 Weber, H. J., and G. B. Arfken, *Essential Mathematical Methods for Physicists*, Elsevier Academic Press, New York, 2004.

Notes

1. Degeneracy may arise because of a particular symmetry of the physical system, such as the symmetry of the potential energy described here. Degeneracy may also arise for completely different reasons and can certainly occur for nonproduct wave functions. The latter are sometimes called accidental degeneracies, and both types can exist in the same system.

2. “Enough” means a complete set in the mathematical sense.

3. Such potentials are called central field or, sometimes, conservative potentials. The Coulomb potential and the gravitational potential are the most frequently encountered examples.

4. $L_z = |\mathbf{L}|$ would mean that $L_x = L_y = 0$. All three components of \mathbf{L} would then be known exactly, a violation of the uncertainty principle.

5. The functions $Y_{\ell m}$ and R_{nl} listed in Tables 7-1 and 7-2 are normalized. The $C_{n\ell m}$ are simply the products of those corresponding normalization constants.

6. Wolfgang Pauli (1900–1958), Austrian physicist. A bona fide child prodigy, while a graduate student at Munich he wrote a paper on general relativity that earned Einstein’s interest and admiration. Pauli was 18 at the time. A brilliant theoretician, he became the conscience of the quantum physicists, assaulting “bad physics” with an often devastatingly sharp tongue, one of his oft-quoted dismissals of a certain poor paper being, “It isn’t even wrong.” He belatedly won the Nobel Prize in Physics in 1945 for his discovery of the exclusion principle.

7. Samuel A. Goudsmit (1902–78) and George E. Uhlenbeck (1900–88), Dutch-American physicists. While graduate students at Leiden, they proposed the idea of electron spin to their thesis adviser Paul Ehrenfest, who suggested that they ask H. A. Lorentz his opinion. After some delay, Lorentz pointed out that an electron spin of the magnitude necessary to explain the fine structure was inconsistent with special relativity. Returning to Ehrenfest with this disturbing news, they found that he had already sent their paper to a journal for publication.

8. Since the same symbol μ is used for both the reduced mass and the magnetic moment, some care is needed to keep these unrelated concepts clear. The symbol m is sometimes used to designate the magnetic moment, but there is confusion enough between the symbol m of the quantum number for the z component of angular momentum and m_e as the electron mass.

9. Otto Stern (1888–1969), German-American physicist, and Walther Gerlach (1899–1979), German physicist. After working as Einstein’s assistant for two years, Stern developed the atomic/molecular beam techniques that enabled him and Gerlach, an excellent experimentalist, to show the existence of space quantization in silver. Stern received the 1943 Nobel Prize in Physics for his pioneering molecular beam work.

10. The nucleus of an atom also has angular momentum and therefore a magnetic moment, but the mass of the nucleus is about 2000 times that of the electron for hydrogen and greater still for other atoms. From Equation 7-39 we expect the magnetic moment of the nucleus to be on the order of 1/2000 of a

Bohr magneton since M is now m_p rather than m_e . This small effect does not show up in the Stern-Gerlach experiment.

11. The letters first used, s , p , d , f , weren’t really arbitrary. They described the visual appearance of certain groups of spectral lines. After improved instrumentation vastly increased the number of measurable lines, the letters went on alphabetically. As we noted in Chapter 4, the K , L , etc., notation was assigned by Barkla.

12. This particular form for writing the total spin was chosen because it also corresponded to the number of lines in the fine structure of the spectrum; e.g., hydrogen lines were doublets and $s = \frac{1}{2}$, so $2s + 1 = 2$.

13. A more precise interpretation is that the electron, possessing an intrinsic magnetic moment due to its spin, carries with it a dipole magnetic field. This field varies in time due to the orbital motion of the electron, thus generating a time-varying electric field at the (stationary) proton, which produces the energy shift.

14. Actually, it’s not quite true for hydrogen either. W. Lamb showed that the $2S$ and $2P$ levels of hydrogen differ slightly in energy. That difference together with the spin-orbit splitting of the $2P$ state puts the $2^2P_{1/2}$ level 4.4×10^{-6} eV below the $2^2S_{1/2}$ level, an energy difference called the Lamb shift. It enables the $2^2S_{1/2}$ state, which would otherwise have been metastable due to the $\Delta\ell = \pm 1$ selection rule, to deactivate to the $1^2S_{1/2}$ ground state via a transition to the $2^2P_{1/2}$ level. The Lamb shift is accounted for by relativistic quantum theory.

15. We can think of this rule in terms of the conservation of angular momentum. The intrinsic spin angular momentum of a photon has the quantum number $s = 1$. For electric dipole radiation, the photon spin is its total angular momentum relative to the center of mass of the atom. If the initial angular momentum quantum number of the atom is j_1 and the final is j_2 , the rules for combining angular momenta imply that $j_2 = j_1 + 1, j_1$, or $j_1 - 1$, if $j_1 \neq 0$. If $j_1 = 0$, j_2 must be 1.

16. This is true for nearly all two-electron atoms, such as He, Be, Mg, and Ca, except for the triplet P states in the very heavy atom mercury, where fine-structure splitting is of about the same order of magnitude as the singlet-triplet splitting.

17. Pieter Zeeman (1865–1943), Dutch physicist. His discovery of the Zeeman effect, which so enlightened our understanding of atomic structure, was largely ignored until its importance was pointed out by Lord Kelvin. Zeeman shared the 1902 Nobel Prize in Physics with his professor H. A. Lorentz for its discovery.

18. The terminology is historical, arising from the fact that the effect in transitions between singlet states could be explained by Lorentz’s classical electron theory and hence was “normal,” while the effects in other transitions could not and were thus mysterious or “anomalous.”

19. This calculation can be found in Herzberg (1944).

20. After Alfred Landé (1888–1975), German physicist. His collaborations with Born and Heisenberg led to the correct interpretation of the anomalous Zeeman effect.

Problems

Level I

Section 7-1 The Schrödinger Equation in Three Dimensions

7-1. Find the energies E_{311} , E_{222} , and E_{321} and construct an energy-level diagram for the three-dimensional cubic well that includes the third, fourth, and fifth excited states. Which of the states on your diagram are degenerate?

7-2. A particle is confined to a three-dimensional box that has sides L_1 , $L_2 = 2L_1$, and $L_3 = 3L_1$. Give the sets of quantum numbers n_1 , n_2 , and n_3 that correspond to the lowest 10 energy levels of this box.

7-3. A particle moves in a potential well given by $V(x, y, z) = 0$ for $-L/2 < x < L/2$, $0 < y < L$, and $0 < z < L$ and $V = \infty$ outside these ranges. (a) Write an expression for the ground-state wave function for this particle. (b) How do the allowed energies compare with those for a box having $V = 0$ for $0 < x < L$ rather than for $-L/2 < x < L/2$?

7-4. Write down the wave functions for the 5 lowest energy levels of the particle in Problem 7-2.

7-5. (a) Repeat Problem 7-2 for the case $L_2 = 2L_1$ and $L_3 = 4L_1$. (b) What sets of quantum numbers correspond to degenerate energy levels?

7-6. Write down the wave functions for the lowest 10 quantized energy states for the particle in Problem 7-5.

7-7. Suppose the particle in Problem 7-1 is an electron and $L = 0.10$ nm. Compute the energy of the transitions from each of the third, fourth, and fifth excited states to the ground state.

7-8. Consider a particle moving in a two-dimensional space defined by $V = 0$ for $0 < x < L$ and $0 < y < L$ and $V = \infty$ elsewhere. (a) Write down the wave functions for the particle in this well. (b) Find the expression for the corresponding energies. (c) What are the sets of quantum numbers for the lowest-energy degenerate state?

Section 7-2 Quantization of Angular Momentum and Energy in the Hydrogen Atom

7-9. If $n = 3$, (a) what are the possible values of ℓ ? (b) For each value of ℓ in (a), list the possible values of m . (c) Using the fact that there are two quantum states for each combination of values of ℓ and m because of electron spin, find the total number of electron states with $n = 3$.

7-10. Determine the minimum angle that \mathbf{L} can make with the z axis when the angular momentum quantum number is (a) $\ell = 4$ and (b) $\ell = 2$.

7-11. The moment of inertia of a compact disc is about 10^{-5} kg \cdot m². (a) Find the angular momentum $L = I\omega$ when the disc rotates at $\omega/2\pi = 735$ rev/min and (b) find the approximate value of the quantum number ℓ .

7-12. Draw an accurately scaled vector model diagram illustrating the possible orientations of the angular momentum vector \mathbf{L} for (a) $\ell = 1$, (b) $\ell = 2$, (c) $\ell = 4$. (d) Compute the magnitude of \mathbf{L} in each case.

7-13. For $\ell = 2$, (a) what is the minimum value of $L_x^2 = L_y^2$? (b) What is the maximum value of $L_x^2 = L_y^2$? (c) What is $L_x^2 = L_y^2$ for $\ell = 2$ and $m = 1$? Can either L_x or L_y be determined from this? (d) What is the minimum value of n that this state can have?

7-14. For $\ell = 1$, find (a) the magnitude of the angular momentum L and (b) the possible values of m . (c) Draw to scale a vector diagram showing the possible orientations of \mathbf{L} with the z axis. (d) Repeat the above for $\ell = 3$.

7-15. Show that, if V is a function only of r , then $d\mathbf{L}/dt = 0$, i.e., that \mathbf{L} is conserved.

7-16. What are the possible values of n and m if (a) $\ell = 3$, and (b) $\ell = 4$, and (c) $\ell = 0$? (d) Compute the minimum possible energy for each case.

7-17. A hydrogen atom electron is in the $6f$ state. (a) What are the values of n and ℓ ? (b) Compute the energy of the electron. (c) Compute the magnitude of \mathbf{L} . (d) Compute the possible values of L_z in this situation.

7-18. At what values of r/a_0 is the radial function R_{30} equal to zero? (See Table 7-2.)

Section 7-3 The Hydrogen Atom Wave Functions

7-19. For the ground state of the hydrogen atom, find the values of (a) ψ , (b) ψ^2 , and (c) the radial probability density $P(r)$ at $r = a_0$. Give your answers in terms of a_0 .

7-20. For the ground state of the hydrogen atom, find the probability of finding the electron in the range $\Delta r = 0.03a_0$ at (a) $r = a_0$ and at (b) $r = 2a_0$.

7-21. The radial probability distribution function for the hydrogen's ground state can be written $P(r) = Cr^2e^{-2Zr/a_0}$, where C is a constant. Show that $P(r)$ has its maximum value at $r = a_0/Z$.

7-22. Compute the normalization constant C_{210} in Equation 7-34.

7-23. Find the probability of finding the electron in the range $\Delta r = 0.02a_0$ at (a) $r = a_0$ and (b) $r = 2a_0$ for the state $n = 2$, $\ell = 0$, $m = 0$ in hydrogen. (See Problem 7-25 for the value of C_{200} .)

7-24. Show that the radial probability density for the $n = 2$, $\ell = 1$, $m = 0$ state of a one-electron atom can be written as

$$P(r) = A \cos^2 \theta r^2 e^{-Zr/a_0}$$

where A is a constant.

7-25. The value of the constant C_{200} in Equation 7-33 is

$$C_{200} = \frac{1}{\sqrt{2\pi}} \left(\frac{Z}{a_0} \right)^{3/2}$$

Find the values of (a) ψ , (b) ψ^2 , and (c) the radial probability density $P(r)$ at $r = a_0$ for the state $n = 2$, $\ell = 0$, $m = 0$ in hydrogen. Give your answers in terms of a_0 .

7-26. Show that an electron in the $n = 2$, $\ell = 1$ state of hydrogen is most likely to be found at $r = 4a_0$.

7-27. Write down the wave function for the hydrogen atom when the electron's quantum numbers are $n = 3$, $\ell = 2$, and $m_\ell = -1$. Check to be sure that the wave function is normalized.

7-28. Verify that the wave function ψ_{100} is a solution of the time-independent Schrödinger equation, Equation 7-9.

Section 7-4 Electron Spin

7-29. If a classical system does not have a constant charge-to-mass ratio throughout the system, the magnetic moment can be written

$$\mu = g \frac{Q}{2M} L$$

where Q is the total charge, M is the total mass, and $g \neq 1$. (a) Show that $g = 2$ for a solid cylinder ($I = \frac{1}{2}MR^2$) that spins about its axis and has a uniform charge on its cylindrical surface. (b) Show that $g = 2.5$ for a solid sphere ($I = 2MR^2/5$) that has a ring of charge on the surface at the equator, as shown in Figure 7-33.

7-30. Assuming the electron to be a classical particle, a sphere of radius 10^{-15} m and a uniform mass density, use the magnitude of the spin angular momentum $|\mathbf{S}| = s(s + 1)^{1/2}\hbar = (3/4)^{1/2}\hbar$ to compute the speed of rotation at the electron's equator. How does your result compare with the speed of light?

7-31. How many lines would be expected on the detector plate of a Stern-Gerlach experiment (see Figure 7-15) if we use a beam of (a) potassium atoms, (b) calcium atoms, (c) oxygen atoms, and (d) tin atoms?

7-32. The force on a magnetic moment with z component μ_z moving in an inhomogeneous magnetic field is given by Equation 7-51. If the silver atoms in the Stern-Gerlach experiment traveled horizontally 1 m through the magnet and 1 m in a field-free region at a speed of 250 m/s, what must have been the gradient of B_z , dB_z/dz in order that the beams each be deflected a maximum of 0.5 mm from the central, or no-field, position?

7-33. (a) The angular momentum of the yttrium atom in the ground state is characterized by the quantum number $j = 3/2$. How many lines would you expect to see if you could do a Stern-Gerlach experiment with yttrium atoms? (b) How many lines would you expect to see if the beam consisted of atoms with zero spin but $\ell = 1$?

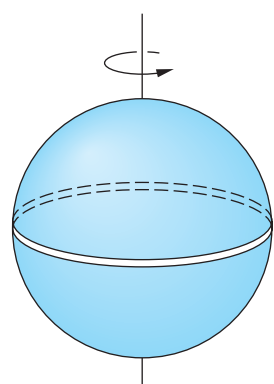


Figure 7-33 Solid sphere with charge Q uniformly distributed on ring.

Section 7-5 Total Angular Momentum and the Spin-Orbit Effect

7-34. The spin-orbit effect removes a symmetry in the hydrogen atom potential, splitting the energy levels. (a) Considering the state with $n = 4$, write down in spectroscopic notation the identification of each state and list them in order of increasing energy. (b) If a weak external magnetic field is applied to the atoms, into how many levels will each state in (a) be split?

7-35. Suppose the outer electron in a potassium atom is in a state with $\ell = 2$. Compute the magnitude of \mathbf{L} . What are the possible values of j and the possible magnitudes of \mathbf{J} ?

7-36. A hydrogen atom is in the $3D$ state ($n = 3, \ell = 2$). (a) What are the possible values of j ? (b) What are the possible values of the magnitude of the total angular momentum? (c) What are the possible z components of the total angular momentum?

7-37. Compute the angle between \mathbf{L} and \mathbf{S} in (a) the $d_{5/2}$ and (b) the $d_{3/2}$ states of atomic hydrogen.

7-38. Write down all possible sets of quantum numbers for an electron in a (a) $4f$, (b) $3d$, and (c) $2p$ subshell.

7-39. Consider a system of two electrons, each with $\ell = 1$ and $s = \frac{1}{2}$. (a) What are the possible values of the quantum number for the total orbital angular momentum $\mathbf{L} = \mathbf{L}_1 + \mathbf{L}_2$? (b) What are the possible values of the quantum number S for the total spin $\mathbf{S} = \mathbf{S}_1 + \mathbf{S}_2$? (c) Using the results of parts (a) and (b), find the possible quantum numbers j for the combination $\mathbf{J} = \mathbf{L} + \mathbf{S}$. (d) What are the possible quantum numbers j_1 and j_2 for the total angular momentum of each particle? (e) Use the results of part (d) to calculate the possible values of j from the combinations of j_1 and j_2 . Are these the same as in part (c)?

7-40. The prominent yellow doublet lines in the spectrum of sodium result from transitions from the $3P_{3/2}$ and $3P_{1/2}$ states to the ground state. The wavelengths of these two lines are 589.0 nm and 589.6 nm. (a) Calculate the energies in eV of the photons corresponding to these wavelengths. (b) The difference in energy of these photons equals the difference in energy ΔE of the $3P_{3/2}$ and $3P_{1/2}$ states. This energy difference is due to the spin-orbit effect. Calculate ΔE . (c) If the $3p$ electron in sodium sees an internal magnetic field B , the spin-orbit energy splitting will be of the order of $\Delta E = 2\mu_B B$, where μ_B is the Bohr magneton. Estimate B from the energy difference ΔE found in part (b).

Section 7-6 The Schrödinger Equation for Two (or More) Particles

7-41. Show that the wave function of Equation 7-59 satisfies the Schrödinger equation (Equation 7-57) with $V = 0$ and find the energy of this state.

7-42. Two neutrons are in an infinite square well with $L = 2.0$ fm. What is the minimum total energy that the system can have? (Neutrons, like electrons, have antisymmetric wave functions. Ignore spin.)

7-43. Five identical noninteracting particles are placed in an infinite square well with $L = 1.0$ nm. Compare the slowest total energy for the system if the particles are (a) electrons and (b) pions. Pions have symmetric wave functions and their mass is $264 m_e$.

Section 7-7 Ground States of Atoms: The Periodic Table

7-44. Write the electron configuration of (a) carbon, (b) oxygen, and (c) argon.

7-45. Using Figure 7-34, determine the ground-state electron configurations of tin (Sn, $Z = 50$), neodymium (Nd, $Z = 60$), and ytterbium (Yb, $Z = 70$). Check your answers with Appendix C. Are there any disagreements? If so, which one(s)?

7-46. In Figure 7-20 there are small dips in the ionization potential curve at $Z = 31$ (gallium), $Z = 49$ (indium), and $Z = 81$ (thallium) that are not labeled in the figure. Explain these dips, using the electron configuration of these atoms given in Appendix C.

7-47. Which of the following atoms would you expect to have its ground state split by the spin-orbit interaction: Li, B, Na, Al, K, Ag, Cu, Ga? (Hint: Use Appendix C to see which elements have $\ell = 0$ in their ground state and which do not.)

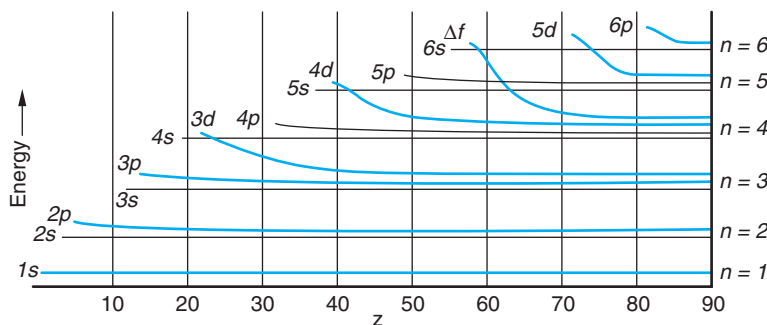


Figure 7-34 Energy of electron ground-state configurations versus Z .

7-48. If the $3s$ electron in sodium did not penetrate the inner core its energy would be $-13.6 \text{ eV}/3^2 = -1.51 \text{ eV}$. Because it does penetrate, it sees a higher effective Z and its energy is lower. Use the measured ionization potential of 5.14 V to calculate Z_{eff} for the $3s$ electron in sodium.

7-49. What elements have these ground-state electron configurations? (a) $1s^2 2s^2 2p^6 3s^2 3p^2$ and (b) $1s^2 2s^2 2p^6 3s^2 3p^6 4s^2$?

7-50. Give the possible values of the z component of the orbital angular momentum of (a) a d electron, (b) an f electron, and (c) an s electron.

Section 7-8 Excited States and Spectra of Atoms

7-51. Which of the following elements should have an energy-level diagram similar to that of sodium and which should be similar to mercury: Li, He, Ca, Ti, Rb, Ag, Cd, Mg, Cs, Ba, Fr, Ra?

7-52. The optical spectra of atoms with two electrons in the same outer shell are similar, but they are quite different from the spectra of atoms with just one outer electron because of the interaction of the two electrons. Separate the following elements into two groups such that those in each group have similar spectra: lithium, beryllium, sodium, magnesium, potassium, calcium, chromium, nickel, cesium, and barium.

7-53. Which of the following elements should have optical spectra similar to that of hydrogen and which should have optical spectra similar to that of helium: Li, Ca, Ti, Rb, Ag, Cd, Ba, Hg, Fr, Ra?

7-54. The quantum numbers n , ℓ , and j for the outer electron in potassium have the values 4, 0, and $\frac{1}{2}$, respectively, in the ground state; 4, 1, and $\frac{1}{2}$ in the first excited state; and 4, 1, and $\frac{3}{2}$ in the second excited state. Make a table giving the n , ℓ , and j values for the 12 lowest-energy states in potassium (see Figure 7-24).

7-55. Which of the following transitions in sodium do not occur as electric dipole transitions? (Give the selection rule that is violated.)



7-56. Transitions between the inner electron levels of heavier atoms result in the emission of characteristic x rays, as was discussed in Section 4-4. (a) Calculate the energy of the electron in the K shell for tungsten using $Z - 1$ for the effective nuclear charge. (b) The experimental result for this energy is 69.5 keV . Assume that the effective nuclear charge is $(Z - \sigma)$, where σ is called the screening constant, and calculate σ from the experimental result for the energy.

7-57. Since the P states and the D states of sodium are all doublets, there are four possible energies for transitions between these states. Indicate which three transitions are allowed and which one is not allowed by the selection rule of Equation 7-67.

7-58. The relative penetration of the inner-core electrons by the outer electron in sodium can be described by the calculation of Z_{eff} from $E = -[Z_{\text{eff}}^2(13.6 \text{ eV})]/n^2$ and comparing with $E = -13.6 \text{ eV}/n^2$ for no penetration (see Problem 7-45). (a) Find the energies of the outer electron in the $3s$, $3p$, and $3d$ states from Figure 7-22. (*Hint:* An accurate method is to use -5.14 eV for the ground state as given and find the energy of the $3p$ and $3d$ states from the photon energies of the indicated transitions.) (b) Find Z_{eff} for the $3p$ and $3d$ states. (c) Is the approximation $-13.6 \text{ eV}/n^2$ good for any of these states?

7-59. A hydrogen atom in the ground state is placed in a magnetic field of strength $B_z = 0.55 \text{ T}$. (a) Compute the energy splitting of the spin states. (b) Which state has the higher energy? (c) If you wish to excite the atom from the lower to the higher energy state with a photon, what frequency must the photon have? In what part of the electromagnetic spectrum does this lie?

7-60. Show that the change in wavelength $\Delta\lambda$ of a transition due to a small change in energy is

$$\Delta\lambda \approx -\frac{\lambda^2}{hc}\Delta E$$

(*Hint:* Differentiate $E = hc/\lambda$.)

7-61. (a) Find the normal Zeeman energy shift $\Delta E = e\hbar B/2m_e$ for a magnetic field of strength $B = 0.05 \text{ T}$. (b) Use the result of Problem 7-57 to calculate the wavelength changes for the singlet transition in mercury of wavelength $\lambda = 579.07 \text{ nm}$. (c) If the smallest wavelength change that can be measured in a spectrometer is 0.01 nm , what is the strength of the magnetic field needed to observe the Zeeman effect in this transition?

Level II

7-62. If the outer electron in lithium moves in the $n = 2$ Bohr orbit, the effective nuclear charge would be $Z_{\text{eff}}e = 1e$ and the energy of the electron would be $-13.6 \text{ eV}/2^2 = -3.4 \text{ eV}$. However, the ionization energy of lithium is 5.39 eV , not 3.4 eV . Use this fact to calculate the effective nuclear charge Z_{eff} seen by the outer electron in lithium. Assume that $r = 4a_0$ for the outer electron.

7-63. Show that the expectation value of r for the electron in the ground state of a one-electron atom is $\langle r \rangle = (3/2)a_0/Z$.

7-64. If a rigid body has moment of inertia I and angular velocity ω , its kinetic energy is

$$E = \frac{1}{2}I\omega^2 = \frac{(I\omega)^2}{2I} = \frac{L^2}{2I}$$

where L is the angular momentum. The solution of the Schrödinger equation for this problem leads to quantized energy values given by

$$E_\ell = \frac{\ell(\ell + 1)\hbar^2}{2I}$$

(a) Make an energy-level diagram of these energies, and indicate the transitions that obey the selection rule $\Delta\ell = \pm 1$. (b) Show that the allowed transition energies are $E_1, 2E_1, 3E_1, 4E_1$, etc., where $E_1 = \hbar^2/I$. (c) The moment of inertia of the H_2 molecule is $I = \frac{1}{2}m_p r^2$, where m_p is the mass of the proton and $r \approx 0.074 \text{ nm}$ is the distance between the protons. Find the energy of the first excited state $\ell = 1$ for H_2 , assuming it is a rigid rotor. (d) What is the wavelength of the radiation emitted in the transition $\ell = 1$ to $\ell = 0$ for the H_2 molecule?

7-65. In a Stern-Gerlach experiment hydrogen atoms in their ground state move with speed $v_x = 14.5 \text{ km/s}$. The magnetic field is in the z direction, and its maximum gradient is given by $dB_z/dz = 600 \text{ T/m}$. (a) Find the maximum acceleration of the hydrogen atoms. (b) If the region of the magnetic field extends over a distance $\Delta x = 75 \text{ cm}$ and there is an additional 1.25 m from the edge of the field to the detector, find the maximum distance between the two lines on the detector.

7-66. Find the minimum value of the angle between the angular momentum \mathbf{L} and the z axis for a general value of ℓ , and show that for large values of ℓ , $\theta_{\min} \approx 1/\ell^{1/2}$.

7-67. The wavelengths of the photons emitted by potassium corresponding to transitions from the $4P_{3/2}$ and $4P_{1/2}$ states to the ground state are 766.41 nm and 769.90 nm. (a) Calculate the energies of these photons in electron volts. (b) The difference in energies of these photons equals the difference in energy ΔE between the $4P_{3/2}$ and $4P_{1/2}$ states in potassium. Calculate ΔE . (c) Estimate the magnetic field that the $4p$ electron in potassium experiences.

7-68. The radius of the proton is about $R_0 = 10^{-15}$ m. The probability that the electron is inside the volume occupied by the proton is given by

$$P = \int_0^{R_0} P(r) dr$$

where $P(r)$ is the radial probability density. Compute P for the hydrogen ground state. (*Hint:* Show that $e^{-2r/a_0} \approx 1$ for $r \ll a_0$ is valid for this calculation.)

7-69. (a) Calculate the Landé g factor (Equation 7-74) for the $^2P_{1/2}$ and $^2S_{1/2}$ levels in a one-electron atom and show that there are four different energies for the transition between these levels in a magnetic field. (b) Calculate the Landé g factor for the $^2P_{3/2}$ level and show that there are six different energies for the transition $^2P_{3/2} \rightarrow ^2S_{1/2}$ in a magnetic field.

7-70. (a) Show that the function

$$\psi = A \frac{r}{a_0} e^{-r/2a_0} \cos \theta$$

is a solution of Equation 7-9, where A is a constant and a_0 is the Bohr radius. (b) Find the constant A .

Level III

7-71. Consider a hypothetical hydrogen atom in which the electron is replaced by a K^- particle. The K^- is a meson with spin 0, hence, no intrinsic magnetic moment. The only magnetic moment for this atom is that given by Equation 7-43. If this atom is placed in a magnetic field with $B_z = 1.0$ T, (a) what is the effect on the $1s$ and $2p$ states? (b) Into how many lines does the $2p \rightarrow 1s$ spectral line split? (c) What is the fractional separation $\Delta\lambda/\lambda$ between adjacent lines? (See Problem 7-57.) The mass of the K^- is 493.7 MeV/ c^2 .

7-72. If relativistic effects are ignored, the $n = 3$ level for one-electron atoms consists of the $^3S_{1/2}$, $^3P_{1/2}$, $^3P_{3/2}$, $^3D_{3/2}$, and $^3D_{5/2}$ states. Compute the spin-orbit-effect splittings of $3P$ and $3D$ states for hydrogen.

7-73. In the anomalous Zeeman effect, the external magnetic field is much weaker than the internal field seen by the electron as a result of its orbital motion. In the vector model (Figure 7-30) the vectors \mathbf{L} and \mathbf{S} precess rapidly around \mathbf{J} because of the internal field and \mathbf{J} precesses slowly around the external field. The energy splitting is found by first calculating the component of the magnetic moment μ_J in the direction of \mathbf{J} and then finding the component of μ_z in the direction of \mathbf{B} . (a) Show that $\mu_J = \frac{\mu_B}{\hbar J}$ can be written

$$\mu_J = -\frac{\mu_B}{\hbar J} (L^2 + 2S^2 + 3\mathbf{S} \cdot \mathbf{L})$$

(b) From $J^2 = (\mathbf{L} + \mathbf{S}) \cdot (\mathbf{L} + \mathbf{S})$ show that $\mathbf{S} \cdot \mathbf{L} = \frac{1}{2}(J^2 - L^2 - S^2)$. (c) Substitute your result in part (b) into that of part (a) to obtain

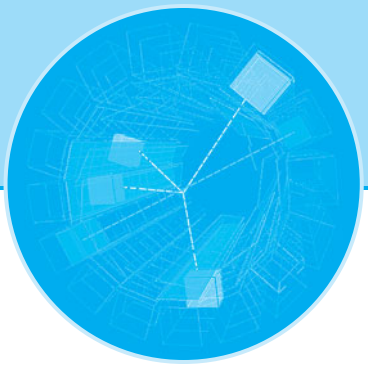
$$\mu_J = -\frac{\mu_B}{2\hbar J} (3J^2 + S^2 - L^2)$$

(d) Multiply your result by J/J to obtain

$$\mu_z = -\mu_B \left(1 + \frac{J^2 + S^2 - L^2}{2J^2} \right) \frac{J_z}{\hbar}$$

7-74. If the angular momentum of the nucleus is \mathbf{I} and that of the atomic electrons is \mathbf{J} , the total angular momentum of the atom is $\mathbf{F} = \mathbf{I} + \mathbf{J}$, and the total angular momentum quantum number f ranges from $I + J$ to $|I - J|$. Show that the number of possible f values is $2I + 1$ if $I < J$ or $2J + 1$ if $J < I$. (If you can't find a general proof, show it for enough special cases to convince yourself of its validity.) (Because of the very small interaction of the nuclear magnetic moment with that of the electrons, a hyperfine splitting of the spectral lines is observed. When $I < J$, the value of I can be determined by counting the number of lines.)

7-75. Because of the spin and magnetic moment of the proton, there is a very small splitting of the ground state of the hydrogen atom called *hyperfine splitting*. The splitting can be thought of as caused by the interaction of the electron magnetic moment with the magnetic field due to the magnetic moment of the proton, or vice versa. The magnetic moment of the proton is parallel to its spin and is about $2.8\mu_N$, where $\mu_N = e\hbar/2m_p$ is called the *nuclear magneton*. (a) The magnetic field at a distance r from a magnetic moment varies with angle, but it is of the order of $B \sim 2k_m\mu/r^3$, where $k_m = 10^{-7}$ in SI units. Find B at $r = a_0$ if $\mu = 2.8\mu_N$. (b) Calculate the order of magnitude of the hyperfine splitting energy $\Delta E \approx 2\mu_B B$, where μ_B is the Bohr magneton and B is your result from part (a). (c) Calculate the order of magnitude of the wavelength of radiation emitted if a hydrogen atom makes a "spin flip" transition between the hyperfine levels of the ground state. [Your result is greater than the actual wavelength of this transition, 21.22 cm, because $\langle r^{-3} \rangle$ is appreciably smaller than a_0^{-3} , making the energy ΔE found in part (b) greater. The detection of this radiation from hydrogen atoms in interstellar space is an important part of radio astronomy.]



Statistical Physics

The physical world that we experience with our senses consists entirely of *macroscopic* objects, i.e., systems that are large compared with atomic dimensions and thus are assembled from very large numbers of atoms. As we proceed to the description of such systems from our starting point of studying single-electron atoms, then multielectron atoms and molecules, we expect to encounter increasing complexity and difficulty in correctly explaining their observed properties. Classically, the behavior of any macroscopic system could, in principle, be predicted in detail from the solution of the equation of motion for each constituent particle, given its state of motion at some particular time; however, the obvious problems with such an approach soon become intractable. For example, consider the difficulties that would accompany the task of accounting for the measured properties of a standard liter of any gas by simultaneously solving the equations of motion for all of the 10^{22} molecules of which the system is composed. Fortunately, we can predict the values of the measurable properties of macroscopic systems without the need to track the motions of each individual particle. This remarkable shortcut is made possible by the fact that we can apply general principles of physics, such as conservation of energy and momentum, to large ensembles of particles, ignoring their individual motions, and determine the *probable* behavior of the system from *statistical* considerations. We then use the fact that there is a relation between the calculated probable behavior and the observed properties of the system. This successful, so-called microscopic approach to explaining the behavior of large systems is called *statistical mechanics*. It depends critically on the system containing a sufficiently large number of particles so that ordinary statistical theory is valid.¹

In this chapter we will investigate how this statistical approach can be applied to predict the way in which a given amount of energy will most likely be distributed among the particles of a system. You may have already encountered kinetic theory, the first successful such microscopic approach, in introductory physics. Since the assumptions, definitions, and basic results of kinetic theory form the foundation of classical statistical physics, we have included a brief review of kinetic theory in the Classical Concept Review. We will see how, in an isolated system of particles in thermal equilibrium, the particles must be able to exchange energy, one result of which is that the energy of any individual particle may sometimes be larger and sometimes smaller than the average value for a particle in the system. Classical statistical mechanics requires

| | | |
|------------|---|------------|
| 8-1 | Classical Statistics: A Review | 316 |
| 8-2 | Quantum Statistics | 328 |
| 8-3 | The Bose-Einstein Condensation | 335 |
| 8-4 | The Photon Gas: An Application of Bose-Einstein Statistics | 344 |
| 8-5 | Properties of a Fermion Gas | 351 |



that the values of the energy taken on by an individual particle over time, or the values of the energy assumed by all of the particles in the system at any particular time, be determined by a specific probability distribution, the *Boltzmann distribution*. In the first section of the chapter we will briefly review the principal concepts of classical statistical physics, noting some of the successful applications and some of the serious failures. We will then see how quantum considerations require modification of the procedures used for classical particles, obtaining in the process the quantum-mechanical *Fermi-Dirac distribution* for particles with antisymmetric wave functions, such as electrons, and the *Bose-Einstein distribution* for particles with symmetric wave functions, such as helium atoms. Finally, we will apply the distributions to several physical systems, comparing our predictions with experimental observations and gaining an understanding of such important phenomena as superfluidity and the specific heat of solids.

8-1 Classical Statistics: A Review

Statistical physics, whether classical or quantum, is concerned with the distribution of a fixed amount of energy among a large number of particles, from which the observable properties of the system may then be deduced. Classically, the system consists of a large ensemble of identical but distinguishable particles. That is, the particles are all exactly alike, but in principle they can be individually tracked during interactions. Boltzmann² derived a distribution relation that made possible prediction of the probable numbers of particles that will occupy each of the available energy states in such a system in thermal equilibrium.

Boltzmann Distribution

The *Boltzmann's distribution* $f_B(E)$ given by Equation 8-1 is the fundamental distribution function of classical statistical physics:

$$f_B(E) = Ae^{-E/kT} \quad \text{8-1}$$

where A is a normalization constant whose value depends on the particular system being considered, $e^{-E/kT}$ is called the *Boltzmann factor*, and k is the *Boltzmann constant*:

$$k = 1.381 \times 10^{-23} \text{ J/K} = 8.617 \times 10^{-5} \text{ eV/K}$$

 Boltzmann's derivation was done to establish the fundamental properties of a distribution function for the velocities of molecules in a gas in thermal equilibrium that had been obtained by Maxwell a few years before and to show that the velocity distribution for a gas that was not in thermal equilibrium would evolve toward Maxwell's distribution over time. Boltzmann's derivation is more complex than is appropriate for our discussions, but in the Classical Concept Review we present a straightforward numerical derivation that results in an approximation of the correct distribution and then show by a simple mathematical argument that the form obtained is exact and is the only one possible. Here we will illustrate application of the Boltzmann distribution with some examples by way of providing a basis for comparing classical and quantum statistical physics later in the chapter.

The number of particles with energy E is given by

$$n(E) = g(E)f_B(E) = A g(E)e^{-E/kT} \quad \text{8-2}$$

where $g(E)$ is the statistical weight (degeneracy) of the state with energy E .

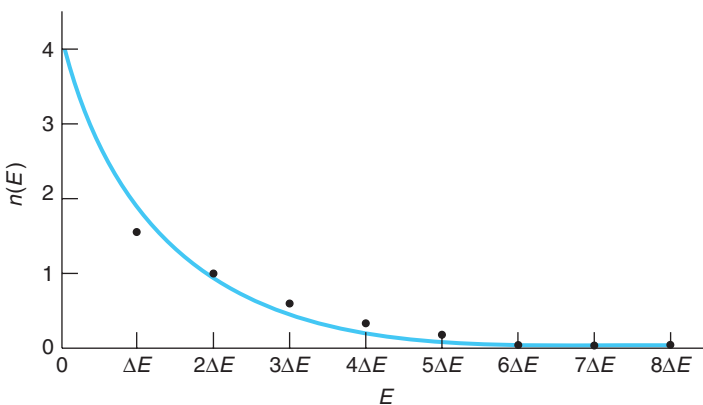


Figure 8-1 $n(E)$ versus E for data from Table 1 in the CCR Boltzmann distribution derivation. The solid curve is the exponential $n(E) = Be^{-E/E_c}$, where the constants B and E_c have been adjusted to give the best fit to the data points.

Classically, the energy E is a continuous function and so is $n(E)$ (Figure 8-1). Consequently, $g(E)$ and $f_B(E)$ are also continuous functions, in which case $g(E)dE$ is the number of states with energy between E and $E+dE$. The next two examples illustrate how to apply the Boltzmann distribution and how the results explain observations of physical systems.

EXAMPLE 8-1 The Law of Atmospheres Consider an ideal gas in a uniform gravitational field. (a) Find how the density of the gas depends upon the height above ground. (b) Assuming that air is an ideal gas with molecular weight 28.6, compute the density of air 1 km above the ground when $T = 300$ K. (The density at the ground is 1.292 kg/m^3 at 300 K.)

SOLUTION

(a) Let the force of gravity be in the negative z direction and consider a column of gas of cross-sectional area A . The energy of a gas molecule is then

$$E = \frac{p_x^2}{2m} + \frac{p_y^2}{2m} + \frac{p_z^2}{2m} + mgz = \frac{p^2}{2m} + mgz$$

where $p^2 = p_x^2 + p_y^2 + p_z^2$ and mgz is the potential energy of a molecule at height z above the ground. The density ρ is proportional to f_B since ρ is proportional to N , the number of molecules in a unit volume at height z , and N is proportional to f_B .

From Equation 8-1 we have

$$f_B = Ae^{-p^2/2mkT}e^{-mgz/kT}$$

Since we are interested only in the dependence on z , we can integrate over the other variables p_x , p_y , and p_z . The integration merely gives a new normalization constant A' ; i.e., the result is equivalent to ignoring these variables. The fraction of the molecules between z and $z + dz$ is then

$$f_B(z) dz = A' e^{-mgz/kT} dz \quad 8-3$$

The constant A' is obtained from the normalization condition $\int_0^\infty f_B(z) dz = 1$. The result is $A' = mg/kT$. The density, therefore, also decreases exponentially with the distance above the ground. Equation 8-3 is known as the *law of atmospheres*.

- (b) The ratio of the density at $z = 1000$ m to that at $z = 0$ m is the same as $f_B(1000)/f_B(0)$, where $f_B(z)$ is given by Equation 8-3. Thus,

$$\frac{\rho(1000)}{\rho(0)} = \frac{f_B(1000)}{f_B(0)} = \frac{e^{-mg(1000)/k(300)}}{e^{-mg(0)/k(300)}} = e^{-mg(1000)/k(300)}$$

Substituting $m = 28.6 \times 1.67 \times 10^{-27}$ kg and $g = 9.8$ m/s² yields

$$\rho(1000) = \rho(0)e^{-0.113} = 1.292 \times 0.893 = 1.154 \text{ kg/m}^3$$

EXAMPLE 8-2 H Atoms in the First Excited State The first excited state E_2 of the hydrogen atom is 10.2 eV above the ground state E_1 . What is the ratio of the number of atoms in the first excited state to the number in the ground state at (a) $T = 300$ K and (b) $T = 5800$ K? The latter is the temperature at the surface of the Sun.

SOLUTION

1. The number of atoms in a state with energy E is given by Equation 8-2:

$$n(E) = g(E)f_B(E) = A g(E)e^{-E/kT}$$

2. The ratio of the number in the first excited state to the number in the ground state is then

$$\frac{n_2}{n_1} = \frac{A g_2 e^{-E_2/kT}}{A g_1 e^{-E_1/kT}} = \frac{g_2}{g_1} e^{-(E_2 - E_1)/kT}$$

3. The statistical weight (= degeneracy) of the ground state g_1 , including spin, is 2; the degeneracy of the first excited state g_2 is 8 (one $\ell = 0$ and three $\ell = 1$ states, each with two spin states). Therefore:

$$\frac{g_2}{g_1} = \frac{8}{2} = 4$$

and

$$\frac{n_2}{n_1} = 4e^{-(E_2 - E_1)/kT}$$

4. For question (a), at $T = 300$ K, $kT \approx 0.026$ eV. Substituting this and $E_2 - E_1 = 10.2$ eV from above gives

$$\frac{n_2}{n_1} = 4e^{-(10.2)/(0.026)} = 4e^{-392} \approx 10^{-171} \approx 0$$

5. For question (b), at the surface of the Sun where $T = 5800$ K, $kT \approx 0.500$. Substituting this and $E_2 - E_1 = 10.2$ eV gives

$$\begin{aligned} \frac{n_2}{n_1} &= 4e^{-(10.2)/(0.500)} = 4e^{-20.4} \\ &\approx e^{-19} \approx 10^{-8} \end{aligned}$$

Remarks: The result in step 4 illustrates that, because of the large energy difference between the two states compared with kT , very few atoms are in the first excited state. Even fewer would be in the higher excited states, which explains why a container of hydrogen sitting undisturbed at room temperature does not spontaneously emit the visible Balmer series. At the surface of the Sun (step 5 above) about 10^{15} atoms of every mole of atomic hydrogen are in the first excited state at any given time.